

**Crosstalk and antibacterial molecules from endophytes  
harbored in *Narcissus tazetta* and *Buxus sinica***

**DISSERTATION**

Submitted for the degree of Dr. rer. nat. (*rerum naturalium*)

to the

Department of Chemistry and Chemical Biology

Technische Universität Dortmund

by

**Wen-Xuan Wang**

**2016**

# **Crosstalk and antibacterial molecules from endophytes**

**harbored in *Narcissus tazetta* and *Buxus sinica***

**APPROVED DISSERTATION**

## **Doctoral Committee**

**Chairman:** Prof. Dr. Daniel Rauh

**Reviewers:**

1. Prof. Dr. Dr.h.c. Michael Spiteller

2. Prof. Dr. Oliver Kayser

**Date of defense examination:**

**Chairman of the examination:**

## Declaration

---

### Declaration

I declare that this thesis is an independent summary of my original research work for my doctoral program, without any inappropriate assistance. All contributions of others are clearly demonstrated, with proper citation to the literature(s), and acknowledgment of collaboration and discussions.

This work was completed under the guidance and supervision of Professor Dr. Dr.h.c. Michael Spiteller and Dr. Souvik Kusari, at the Institute of Environmental Research (INFU) of the Department of Chemistry and Chemical Biology, Chair of Environmental Chemistry and Analytical Chemistry, TU Dortmund, Germany.

Dated:

**Wen-Xuan Wang**

Location: Dortmund, Germany

In my capacity as supervisor of the candidate's thesis, I certify that the above statements are true to the best of my knowledge.

**Prof. Dr. Dr.h.c. Michael Spiteller**

Date:

---

### List of original contributions

Parts of the work reported in this thesis have already been published, presented and/or are intended for publication.

#### Research paper:

1. **Wang W-X**, Kusari S, Kusari P, Kayser O, Spiteller M. An endophytic fungus *Phyllosticta capitalensis* harboring uncultivable endosymbiotic bacterium *Herbaspirillum* sp. produces lactam-fused 4-pyrones. RSC advances, submitted.
2. **Wang W-X**, Kusari S, Laatsch H, Golz C, Kusari P, Strohmann C, Kayser O, Spiteller M. Antibacterial azaphilones from an endophytic fungus *Colletotrichum* sp. BS4. *Journal of Natural products*, **2016**, doi: 10.1021/acs.jnatprod.5b00436.
3. **Wang W-X**, Kusari S, Sezgin S, Lamshöft M, Kusari P, Kayser O, Spiteller M. Hexacyclopeptides secreted by an endophytic fungus *Fusarium solani* N06 act as crosstalk molecules in *Narcissus tazetta*, *Applied Microbiology and Biotechnology*, **2015**, 99, 7651–7662.

#### Book chapter:

**Wang W-X**, Kusari S, Spiteller M. Unraveling the chemical interactions of fungal endophytes for exploitation as microbial factories, in *Fungal Applications in Sustainable Environmental Biotechnology*, Part V: *Future biotechnological potentials and environmental applications*, Springer, Landon, **2016**, in revision.

#### Poster presentation:

**Wang W-X**, Kusari S, Sezgin S, Lamshöft M, Kusari P, Kayser O, Spiteller M. **2015** "Endophytic *Fusarium solani* secretes hexacyclopeptides to communicate with an associated endophytic bacterium", At the 6th Junges Chemie Symposium Ruhr (JCS Ruhr); venue: Universität Essen; dated: 17 September 2015

**Wang W-X**, Kusari S, Sezgin S, Spiteller M. **2014** "Detection and sequencing of traceable new hexacyclopeptides from an endophytic fungus *Fusarium solani* harbored in bulb of *Narcissus tazetta* by MALDI and LC/MS<sup>n</sup>" At the 5th Junges Chemie Symposium Ruhr (JCS Ruhr); venue: Universität Bochum; dated: 9 September 2014

# **ACKNOWLEDGEMENTS**

## Acknowledgement

---

The period of more than 3 years in Germany is one of the toughest experiences in my life, but thanks to God, I have never been alone here. I have to express my gratitude to many mentors and friends, because they generously offered me precious assistance and enable me to fulfill my doctoral program and lead a happy life in an entirely different country.

First of all, I must thank **Prof. Dr. Dr. h.c. Michael Spiteller** (INFU, TU-Dortmund) for offering me this invaluable opportunity to start my doctoral program at INFU and it is also a great honor for me to be his student. As a Chinese old proverb says, he who teaches me for one day is my father for life. He showed me all the excellent qualities as an amazing teacher, and he is as respectful as a father to me. His earnest scientific attitude and profound knowledge have impressed me deeply, and what I have learned under his supervision is the invaluable wealth I have obtained for my entire life. At the beginning of my doctoral study, he enlightened me to start my research in an appropriate direction. When I was faced with difficulties, he always showed me great patience and provided me selfless assistance. More importantly, he is not only a strict advisor, but also a considerate and easy-going friend.

I also have to thank **Dr. Souvik Kusari**. He is one of the most brilliant, creative and energetic scientists I have ever seen. I adore his devotion to science and his ambition to make a breakthrough at the frontier of endophytes study. From the very beginning to now, he has been offering precious assistance upon every detail in my project. I am very grateful to him for having taught me so much from basic experimental skills to scientific strategies. I need to thank him for the help of the microbial identification and bio-assays.

I also appreciate the kind help and advice from **Dr. Sebastian Zühlke**, **Dr. Marc Lamshöft** and **Dr. Ferdinand Talontsi**. Their guidance and discussions in the seminar meeting are very important for me to adopt a correct strategy of research and to solve difficulties I encountered during experiments. I am especially grateful to **Dr. Sebastian Zühlke** for his kind revision of this thesis.

Furthermore, **Professor Dr. Hartmut Laatsch** (Institute for Organic and Biomolecular Chemistry, Georg-August University) used very expensive and high-quality methods to perform the quantum chemical calculation of my compounds to determine their

## **Acknowledgement**

---

structures, and he also provided me many suggestions to improve my work on structure elucidation of bioactive compounds. I am very grateful for his kind help, and it was an amazing learning experience for me to collaborate with him.

I must show my deepest gratitude to **Dr. Parijat Kusari** and **Professor Dr. Oliver Kayser** (Department of Biochemical and Chemical Engineering, TU-Dortmund) for the molecular biological identification of endophytic fungi and bacteria as well as the evaluation of biosynthetic genes. Their high level of scientific skill and knowledge has impressed me deeply.

I would also like to say thanks to **Mr. Christopher Golz** and **Professor Dr. Carsten Strohmann** for their kind help for single crystal X-ray diffraction measurement.

**Mr. Selahaddin Sezgin** was very helpful for me to perform MALDI imaging experiments and had taught me a lot of skills and knowledge, and helped me analyze obtained data. He has also translated the abstract of this thesis from English to German for me. I am very grateful for his kindness and patience. I also appreciate the help of **Mr. Dennis Eckelmann** for LC-MS<sup>n</sup> measurement as well as his kind help for many other things.

I am also appreciate that **Mr Gang Li** and **Mr. James Oppong Kyekyeku** helped me check this thesis and provided me many suggestions to improve it.

The other members in INFU including **Mrs. Anke Bullach**, **Mrs. Gabriele Harges**, **Mrs. Cornelia Stolle**, **Mr. Ulrich Schoppe**, and **Miss. Evelyn Mireku** did me many favors, and because of them, I have never felt lonely here. I would like to say thanks to all of them. And I have to thank the other Chinese friends Nan Cheng, Zongyi Chen, Wei Zhou, Mengyao Zheng, and all the friends in the church, because of their generous assistance.

I must show my sincere gratitude to the **China Scholarship Council (CSC)** for funding me by the Ph.D. student fellowship, as well as **Ministry of Innovation, Science, Research and Technology of the State of North Rhine-Westphalia**, and **Germany and the German Research Foundation (DFG)** for funding the facilities of my projects at INFU, TU-Dortmund.

## **Acknowledgement**

---

Finally, I am also grateful to my family and my friends in China, who always support me whole-heartedly.



## Table of content

		Page
I	Abstract	1
II	Zusammenfassung	3
<b>Chapter 1</b>	<b>INTRODUCTION</b>	<b>5</b>
1.	Introduction	6
1.1	Plants, “bustling” niches of microbes	6
1.2	Why we study endophytes	8
1.3	Natural products, important basis of interactions of endophytic system	13
1.4	Host plant screening	14
<b>Chapter 2</b>	<b>OUTLINE OF LITERATURE</b>	<b>16</b>
1	Overview of host plant	17
1.1	<i>Narcissus tazetta</i>	17
1.2	<i>Buxus sinica</i>	17
2	Overview of endophytes investigated herein	17
2.1	Fungal species <i>Fusarium solani</i>	17
2.2	Bacterial species <i>Achromobacter xylosoxidans</i>	18
2.3	Fungal genus <i>Colletotrichum</i>	19
2.4	Fungal species <i>Phyllosticta capitalensis</i> (teleomorph <i>Guignardia mangiferae</i> )	19
2.5	Bacterial genus <i>Herbaspirillum</i>	20
3	Overview of the microbial secondary metabolites investigated herein	20
3.1	Biosynthetic pathways of nonribosomal peptide synthetase (NRPS) and polyketide synthase (PKS)	20
3.2	Cyclic peptides	23
3.3	Azaphilones	24
3.4	Lactam-fused 4-pyrones	25
4	Technical development of structural elucidation for unknown organic molecules	26
4.1	MS <sup>n</sup> technology for cyclic peptides sequencing	26
4.2	Density functional theory (DFT) gauge-including atomic orbitals (GIAO) <sup>13</sup> C NMR shielding tensor calculation	27
5	Strategies for microbial chemical crosstalk investigation	28
5.1	What is microbial chemical crosstalk	28
5.2	Visualization of chemical crosstalk	29
<b>Chapter 3</b>	<b>RESEARCH OBJECTIVES</b>	<b>32</b>
1	Aim of research	33
1.1	Hexacyclopeptides from endophytic <i>F. solani</i> N06 and their plausible ecological function	33
1.2	Antibacterial azaphilones from endophytic fungus <i>Colletotrichum</i> sp. BS4	34

## Table of content

---

1.3	Lactam-fused 4-pyrone produced by endophytic fungus <i>P. capitalensis</i> BS5 and its endosymbiont	34
<b>Chapter 4</b>	<b>EXPERIMENTAL SECTION</b>	<b>35</b>
1.	General experimental procedures and instruments	36
2.	Isolation and culture of endophytes	37
2.1	Collection and identification of host plants	37
2.2	LC-MS analysis of plant extracts	37
2.3	Isolation of endophytes	38
3.	Identification of isolated fungi and bacteria	38
4.	Secondary metabolites profiling of endophytes	40
4.1	Selection of fermentation conditions	40
4.2	LC-MS analysis of endophytic products	40
5.	Fungal and bacterial material	40
5.1	Endophytic fungus <i>F. solani</i> N06 and endophytic bacterium <i>A. xylosoxidans</i> N12B from bulbs of <i>N. tazetta</i>	40
5.2	Endophytic fungi <i>Colletotrichum</i> sp. BS4 and <i>P. capitalensis</i> BS5 and endosymbiotic bacterium <i>Herbaspirillum</i> sp. BS5B from leaves of <i>B. sinica</i>	41
6	LC-MS <sup>n</sup> analysis of hexacyclopeptides from <i>F. solani</i> N06	41
7.	Purification of target compounds	42
7.1	Azaphilones from <i>Colletotrichum</i> sp. BS4	42
7.2	Lactam-fused 4-pyrone from endosymbiotic community of <i>P. capitalensis</i> BS5 and <i>Herbaspirillum</i> sp.	44
8.	Bioactivity assays for isolated pure compounds	44
8.1	Disc diffusion antibacterial assay	44
8.2	Cytotoxic assay	45
9.	Quantum chemical computation	46
10.	MALDI IMS	47
10.1	Sample preparation	47
10.2	Measurement parameters	48
11.	Synthesis	48
11.1	Synthesis of precursor $\alpha$ -deuterated amino acids	48
11.2	Synthesis of 2,4,4,4-tetradeuterium-threonine	48
11.3	Synthesis of 4-OH-4-deuterium-proline	49
11.4	Semi-synthesis of compound <b>16</b> from compound <b>15</b>	49
12	Detection of fungal and bacterial polyketide synthase (PKS)	50
13	Detection of fungal and bacterial nonribosomal peptide synthetase (NRPS)	50
<b>Chapter 5</b>	<b>RESULTS &amp; DISCUSSION</b>	<b>52</b>
1	Chemical crosstalk between endophytic fungi <i>F. solani</i> N06 and endophytic bacteria via new hexacyclopeptides	53
1.1	Metabolites screening of <i>F. solani</i> N06	53
1.2	Strategy to investigate the new hexacyclopeptides	54
1.3	Visualization of hexacyclopeptides in the dual culture of <i>F. solani</i> N06 and <i>A. xylosoxidans</i> N12B by MALDI IMS	55

## Table of content

---

1.4	Structure elucidation of hexacyclopeptides ( <b>1–9</b> ) by LC-MS <sup>n</sup>	57
1.5	Isotope labeling to verify the biosynthetic origin of hexacyclopeptides	60
1.6	Discussion	63
2	Azaphilones produced by endophytic fungus <i>Colletotrichum</i> sp. BS4 and their anti-bacterial potential	64
2.1	Obtainment of azaphilones ( <b>10–14</b> )	64
2.2	The structural elucidation of compound <b>10</b>	65
2.3	The structural elucidation of compound <b>11</b>	68
2.4	The structural elucidation of compound <b>12</b>	73
2.5	The structural elucidation of compound <b>13</b>	75
2.6	Proposal of biosynthetic pathway of azaphilones ( <b>10–14</b> )	78
2.7	Antibacterial assay of compounds ( <b>10–14</b> ) and cytotoxic assay of compounds ( <b>10–12</b> , and <b>14a</b> )	79
2.8	Visualization of azaphilones in the colony of <i>Colletotrichum</i> sp. BS4 by MALDI IMS	82
2.9	Discussion	83
3	Lactam-fused 4-pyrones producing endosymbiotic community comprising of endophytic fungus <i>P. capitalensis</i> BS5 and its endosymbiotic bacterium <i>Herbaspirillum</i> sp. BS5B	84
3.1	Identification of fungus <i>P. capitalensis</i> BS5 and endosymbiotic bacterium <i>Herbaspirillum</i> sp. BS5B	84
3.2	Structural elucidation of compounds <b>15</b> and <b>16</b>	85
3.3	Biosynthetic pathway of compounds <b>15</b> and <b>16</b>	89
3.4	Discussion	92
<b>Chapter 6</b>	<b>CONCLUSION &amp; OUTLOOK</b>	95
1	Conclusion	96
2	Interspecies chemical crosstalks among endophytic communities	97
3	Endophytes are rich resource of bioactive compounds	99
4	Perspectives for investigating secondary metabolites of endophytes	100
<b>Chapter 7</b>	<b>REFERENCES</b>	102
<b>Chapter 8</b>	<b>SUPPLEMENTAL DATA</b>	118
Appendix A	List of abbreviations	191
	List of figures	193
	List of tables	197
Appendix B	Curriculum vitae	198

### Abstract

Endophytic fungi and bacteria are microorganisms harbored in the plant tissues without causing any disease. They are proven to be a rich source of new anticancer and antimicrobial compounds as well as clinically valuable agents identified from plant materials. However, recent research encounters enormous difficulties, which reveals that endophytic systems are complex ecological communities maintained by inter-species and inter-kingdom interactions, including chemical crosstalk. Consequently, investigating the chemical basis of these interactions is essential to interpret the interaction among endophytes and host plant, and exploit the true potential of endophytes. Based on metabolite screening of endophytes from several Chinese traditional medicinal plants with antibacterial related uses, endophytic fungi and bacteria isolated from two plants *Narcissus tazetta* and *Buxus sinica* were selected for the investigation in this thesis.

From an endophytic fungus, *Fusarium solani* N06, isolated from a bulb of *N. tazetta*, nine new hexacyclopeptides (**1–9**) were discovered as crosstalk molecules between it and another endophytic bacterium, *Achromobacter xylosoxidans* N12B, from the same tissue. In the matrix-assisted laser desorption ionization imaging high-resolution mass spectrometry (MALDI-imaging-HRMS) experiments, the secretion of these compounds from this *F. solani* N06 and the accumulation towards *A. xylosoxidans* N12B was visualized on the border between the fungus and bacterium. From the optimized culture of *F. solani* N06, sufficient extracts of these hexacyclopeptides were analyzed by liquid chromatography-multiple stage mass spectrometry (LC-MS<sup>n</sup>) and their sequence was identified to be cyclo((Hyp or Dhp)-Xle-Xle-(Ala or Val)-Thr-Xle) (Dhp: dehydroproline) based on the characteristic *a*, *b*, or *y* ions in MS<sup>n</sup> spectra. The phenomenon that coexisting endophytes utilize new signal molecules suggests that they have developed communication strategies to survive and function in their distinct ecological niches.

Four new compounds, colletotrichones A–D (**10–13**) and one known compound chermesinone B (**14a**) were isolated from the fermented rice medium of an endophytic fungus *Colletotrichum* sp. BS4, which was isolated from the leaves of *B. sinica*. With comprehensive spectroscopic methods including 1D and 2D NMR, HRMS, ECD spectra, UV, and IR as well as single crystal X-ray diffraction and quantum chemistry calculation, their structures were identified to be azaphilones sharing a 3,6a-dimethyl-9-(2-

## Abstract

---

methylbutanoyl)-9*H*-furo[2,3-*h*]isochromene-6,8-dione core structure. In the antibacterial bioassay against two environmental strains of *Escherichia coli* and *Bacillus subtilis*, as well as two human pathogenic clinical strains *Staphylococcus aureus* and *Pseudomonas aeruginosa*, colletotrichone A (**10**) exhibited extraordinary activity against *E. coli* and *B. subtilis*, with a minimum inhibitory concentration lower than positive controls streptomycin and gentamicin. In the cytotoxic assay, interestingly, compounds **10–12**, and **14a** showed slight cytotoxicity at high concentration (100  $\mu$ M). Furthermore, the spatial distribution and localization of the compounds produced by the endophyte were visualized by MALDI-imaging-HRMS, which revealed their plausible ecological functions.

In the investigation of endophytic fungus *Phyllosticta capitalensis* harbored in the leaves of *B. sinica*, two new lactam-fused 4-pyrones (**15**, **16**) were discovered in static PDB fermentation. Their structures were elucidated by 1D and 2D NMR, LC-MS<sup>n</sup>, DFT <sup>13</sup>C NMR calculation and chemical reaction. By 16S rRNA analyses, an endosymbiotic bacterium *Herbaspirillum* sp. was discovered in the hyphae of *P. capitalensis*, which was not cultivable in ordinary culturing condition. The PKS/NRPS gene cluster analyses showed these two compounds were biosynthesized by fungal PKS and bacterial NRPS. This cross-species cooperation of secondary metabolites production unveiled another level of interaction between the endophytic bacterium and fungus.

### Zusammenfassung

Als endophytische Pilze und Bakterien werden die im Pflanzenkörper eingelagerten Mikroorganismen bezeichnet, welche keine Schäden oder Krankheitssymptome für das sie umgebende Pflanzengewebe hervorrufen. Studien zeigen auf, dass Endophyten eine reiche Quelle für die Gewinnung neuer Verbindungen mit antimikrobiellen Eigenschaften als auch neuer potenziell als Antikrebsmittel in Frage kommenden Verbindungen sind. Einige Verbindungen endophytischen Ursprungs sind bereits klinisch etabliert. Die derzeitige Forschung bezüglich der Endophyten ist allerdings mit erheblichen Schwierigkeiten verbunden, welche den komplexen Charakter endophytischer Gemeinschaften in ihrer ökologischen Umgebung aufzeigen. Die Komplexität wird durch Interaktionen zwischen den unterschiedlichen endophytischen Spezies, deren Umgebungen, einschließlich des chemischen „Crosstalks“ begründet. Daher sind Untersuchungen betreffend der chemischen Natur der Interaktionen von erheblichem Wert, um deren Bedeutung zu interpretieren und somit das gesamte Potenzial der Endophyten erschließen zu können. Basierend auf Screenings von Metaboliten endophytischen Ursprungs, die von mehreren chinesischen Heilkräutern mit traditioneller antibakterieller Verwendung isoliert wurden, fiel die Auswahl auf endophytische Pilze und Bakterien der Strauß-Narzisse (*Narcissus tazetta*) und des chinesischen Buchsbaums (*Buxus sinica*), die in der vorliegenden Arbeit untersucht wurden.

Vom endophytischen Pilz *Fusarium solani* N06, welcher von der Knolle der *N. tazetta* gewonnen wurde, konnten neun neue Hexazyklopeptide (**1–9**) als „Crosstalk“-Moleküle zwischen diesem Organismus und dem endophytischen Bakterium *Achromobacter xylosoxidans* N12B vom selben Gewebe identifiziert werden. Die Sekretion dieser Verbindungen vom *F. solani* N06 konnte mit Hilfe hochaufgelöster bildgebender Matrix-assistierter Laser Desorption/Ionisation (MALDI-imaging-HRMS) Experimente visualisiert werden. Es zeigte sich dabei eine Akkumulation der Stoffe im Grenzbereich zwischen dem sekretierenden Pilz und dem Bakterium *A. xylosoxidans* N12B in Richtung des Bakteriums. Von der optimierten *F. solani* N06 Kultur konnten die Hexazyklopeptide gewonnen und über Flüssigchromatographie Massenspektrometrie (LC-MS<sup>n</sup>) analysiert werden. Ihre Sequenz wurde dabei basierend auf charakteristischen Ionen *a*, *b*, oder *y* in den MS<sup>n</sup> Spektren als zylo((Hyp oder Dhp)-Xle-Xle(Ala or Val)-

## Zusammenfassung

Thr-Xle) (Dhp: Dehydroprolin) identifiziert werden. Diese Erkenntnisse deuten darauf hin, dass koexistierende Endophyten Kommunikationsstrategien entwickelt haben, um in ihren speziellen ökologischen Nischen zu funktionieren und zu überleben.

Vier neue Verbindungen, die Colletotrichone A–D (**10–13**), und eine bekannte Substanz, das Chermisonon B (**14a**), konnten vom fermentierten Reismedium des von den Blättern vom *B. sinica* isolierten endophytischen Pilzes *Colletotrichum* sp. BS4 erhalten werden. Durch Einsatz umfassender spektroskopischer Methoden, u.a. der 1D und 2D NMR, HRMS, ECD, UV und IR Techniken als auch der Einkristallröntgenstrukturanalyse sowie durch quantenchemische Berechnungen konnten ihre Strukturen als Azophilone, die sich ein 3,6a-Dimethyl-9-(2-methylbutanoyl)-9H-furo[2,3-h]isochromen-6,8-dion Kerngerüst teilen, aufgeklärt werden. Durch antibakteriellen Biotests wurde die außergewöhnlich hohe Aktivität des Colletotrichon A (**10**) gegen *E. coli* and *B. subtilis* festgestellt. Verglichen mit den Kontrollsubstanzen Streptomycin und Gentamycin besitzt dieses eine niedrigere minimale Hemm-Konzentration. Darüberhinaus konnte für die Substanzen **10–14** keine signifikante Zytotoxizität festgestellt werden. Selbst bei Applikation hoher Konzentrationen (100 µM) zeigte sich nur eine geringfügige Zytotoxizität. Außerdem wurde die räumliche Verteilung dieser von den Endophyten produzierten Verbindungen mittels bildgebender MALDI-HRMS gezeigt, was Rückschlüsse auf deren ökologischen Funktionen erlaubt.

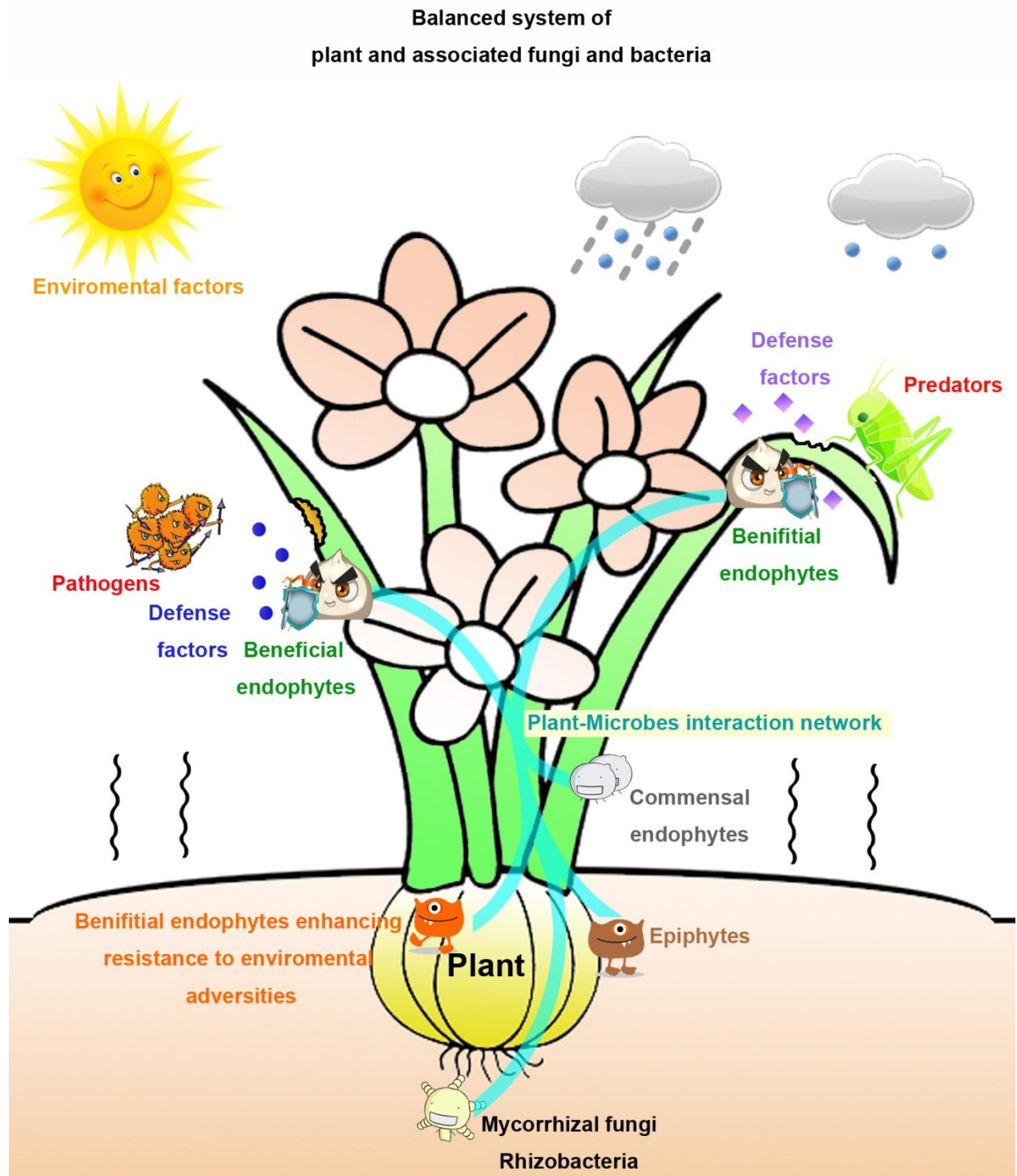
Im Extrakt der statischen PDB Fermentierung vom endophytischen Pilz *Phyllosticta capitalensis*, welche in den Blättern des *B. sinica* zu finden ist, konnten zwei neue Lactam-Einheiten enthaltende 4-Pyrone (**15**, **16**) entdeckt werden. Die Strukturaufklärung erfolgte mit Hilfe der 1D and 2D NMR und LC-MS<sup>n</sup> Techniken und DFT <sup>13</sup>C NMR Berechnungen sowie durch chemische Modifikationen. Durch die 16S rRNA Analyse konnte das endosymbiotische Bakterium *Herbaspirillum* sp. in den Hyphen der *P. capitalensis* aufgefunden werden. Dieses ist jedoch unter gewöhnlichen Kulturbedingungen nicht kultivierbar. Die PKS/NRPS Gen-Clusteranalyse bewies, dass **15** und **16** durch das fungale PKS und bakterielle NRPS biosynthetisiert werden. Diese „Cross Species Cooperation“ zur gemeinsamen Produktion von Sekundärmetaboliten offenbart eine andere, neue Stufe innerhalb möglicher Interaktionen zwischen endophytischen Bakterien und Pilzen.

**Chapter 1**  
**INTRODUCTION**



# 1. Introduction

## 1.1 Plants, “bustling” niches of microbes



## Chapter 1: Introduction

---

Fungi and bacteria used to be well-known as unconscious and selfish decomposers or pathogens leading saprobiontic or parasitic lifestyle, except those photosynthetic bacteria. In the ecological systems, however, fungi and bacteria are actually able to collaborate with other organisms, utilizing highly organized strategies. For example, lichen is a typical symbiotic organism consisting of supporting fungi and photoautotrophic algae or cyanobacteria (or both).<sup>1</sup>

Plants, the major primary producers in most terrestrial ecosystems, are also bustling habitats of microbes. They have probably been colonizing living plants since the appearance of the most primitive plants.<sup>2</sup> Microbes and plants are likely to have been co-evolving for more than 400 million years and generating complex ecological communities.<sup>2-4</sup> Overwhelming evidence shows that microbes could not be only sojourners or parasites associated with plants but also beneficial partners playing essential roles in the ecological systems.<sup>2-4</sup>

The surface of global phyllosphere is more than 1 billion km<sup>2</sup>, and it is not surprising that plants provided vast habitat above the ground for countless epiphytic microbes.<sup>5</sup> Although these microbes are exposed to the atmospheric environment and antimicrobes compounds released by plants, with limited water and nutrients supply,<sup>5,6</sup> they have adapted on the surface of plants with multiple strategies. For example, *Pseudomonas syringae* is capable of producing coronatine<sup>7</sup> or syringolin A<sup>8</sup> to counteract the closure of stomata.<sup>5</sup> And mossed epiphytic bacterium *Methylobacterium funariae* interact with plants by secreting phytohormones.<sup>7</sup>

In the middle of the nineteenth century, scientists had discovered mycorrhizae, which are symbiotic fungi associated with vascular plant roots.<sup>9</sup> Moreover, the investigation of biofertilizers revealed the hidden communities of rhizobacteria,<sup>10</sup> and they are well-known because of forming root nodules in legume crops.<sup>11</sup> These associated microbes help plants overcome biotic or abiotic adversities in the environment, by providing host plants limited nutrients like phosphates and nitrates,<sup>12,13</sup> secreting growth promoting factors.<sup>12,14</sup> enhancing the tolerance to extreme conditions like drought, heat waves, high salinity or ion toxicity,<sup>14</sup> as well as increasing disease resistance of plants.<sup>14,15</sup>

## Chapter 1: Introduction

---

Beside rhizosphere associated microbes, the symbiotic microbes living in the plant tissues have drawn increasing attention, which are named as endophytes (endo means living inside and phyte means plants, in Latin).<sup>16</sup> Endophytes are defined as microorganisms living in plant tissues without causing perceptible pathological symptoms,<sup>17-20</sup> but there is no clear boundary between endophytes and plant pathogens. Many pathogenic species can also be isolated as endophytes from healthy plant tissues.<sup>16,21</sup> On one hand, evidence showed the signaling pathways are essential to maintain the endophytic association, and signaling interference can switch endophytes from mutualism to pathogenesis.<sup>21</sup> On the other hand, the mutation or disruption of certain virulent genes can also change pathogenic fungi into endophytes.<sup>22,23</sup> Therefore, distinguishing the trophic strategy between pathogenic and endophytic life is problematic. It is compelling that the endophytic systems are balanced by the interactions or communications between each individual, which determine the role of associated microbes.

Endophytes are one of the most cryptic community and they have been remained unexploited for decades after the first discovery,<sup>12,18</sup> because they are showing less manifest phenomena than other associated microbes mentioned above. Even in the middle of the 90s the term of “endophyte” was still controversial.<sup>16</sup> Thus far, all plants are proven to harbor endophytes and “endophytism” is a common phenomenon in the plant kingdom.<sup>24</sup>

Most of the endophytes reported till now are fungi or bacteria (including actinomycete),<sup>18</sup> but different types of endophytes are possible to be unveiled in the future because the majority of endophytes are probably uncultivated yet (for example, endophytic virus).<sup>25</sup> Metagenomic research showed that the role of endophytes residing in plants remains largely unclear,<sup>3,26,27</sup> even though there are nearly 10,000 publications on the topic of endophytes according to *Web of Knowledge* search to date.

### 1.2 Why we study endophytes

Comparing to phyllosphere epiphytes or rhizosphere microbes, endophytes are living in the tissue of plants, and have the closest relationship with host plants.<sup>2,17,18,21,28,29</sup> In the endophytic lifestyle, the host defenses are suppressed as well as the growth and

## Chapter 1: Introduction

---

virulence of endophytes, and the micro-ecological systems are regulated in complex and precise manners to allow the co-existence of each other.<sup>18,21</sup> The mechanism to maintain the balance between endophytes, host and other associated microbes is poorly understood to date,<sup>18</sup> which is a fascinating and challenging topic of exploiting endophytes in the fields of biotechnology.

30 years ago in the United State, the fescue toxicosis of livestock caused by feeding tall fescue (*Festuca arundinacea*) drew the attention of scientists.<sup>30</sup> Investigation showed the reason is the toxic peptide and clavinet ergot alkaloids produced by the endophytic fungus *Neotyphodium coenophialum* harbored in tall fescue.<sup>30</sup> Moreover, the endophytic fungi infected grasses were reported to be toxic against insect and other mammalian predators as well.<sup>31</sup> This milestone case inspired scientists that these endophytes harbored in plants are capable of defending hosts against invaders or predators to obtain the competitive advantages.<sup>18</sup> In the later research, it is believed that endophytes are helpful to enhance their hosts tolerance towards diverse ambient stresses.<sup>32</sup> To defend against biotic invaders, endophytes provide not only chemical warfare to inhibit pathogens but also communication interference strategies to attenuate virulence of pathogens (for example, quorum quenching).<sup>33</sup> These ecological traits suggest that the investigation on endophytic chemical basis may lead to the development of novel clinical drugs, to tackle current major problems including bacterial resistance towards antibiotics.<sup>33</sup> Because most endophytes have not been well-investigated yet, the ecologically functional natural products from endophytes were considered as a promising resource of new compounds.<sup>34</sup> A review stated that the possibility to discover unknown bioactive compounds from endophytic fungi was 51%, whereas it is only 38% for soil fungi, according to the survey of published new natural products.<sup>35</sup> With respect to their ecological relevance, natural product research on endophytes has resulted in extraordinary success in the past two decades, with a great number of antimicrobial or anticancer agents discovered,<sup>25,34,35</sup> and the number is keeping increasing. However, most of the compounds were obtained from *in vitro* axenic monocultural fermentation,<sup>19</sup> which led to a debatable question that whether these bioactive compounds are also produced in natural niches of endophytes since most of them were proposed as biofunctional compounds for the fitness of host plants. Connecting these bioactive

## Chapter 1: Introduction

compounds with the function of endophytes in their niches is still a challenging task with current technologies.

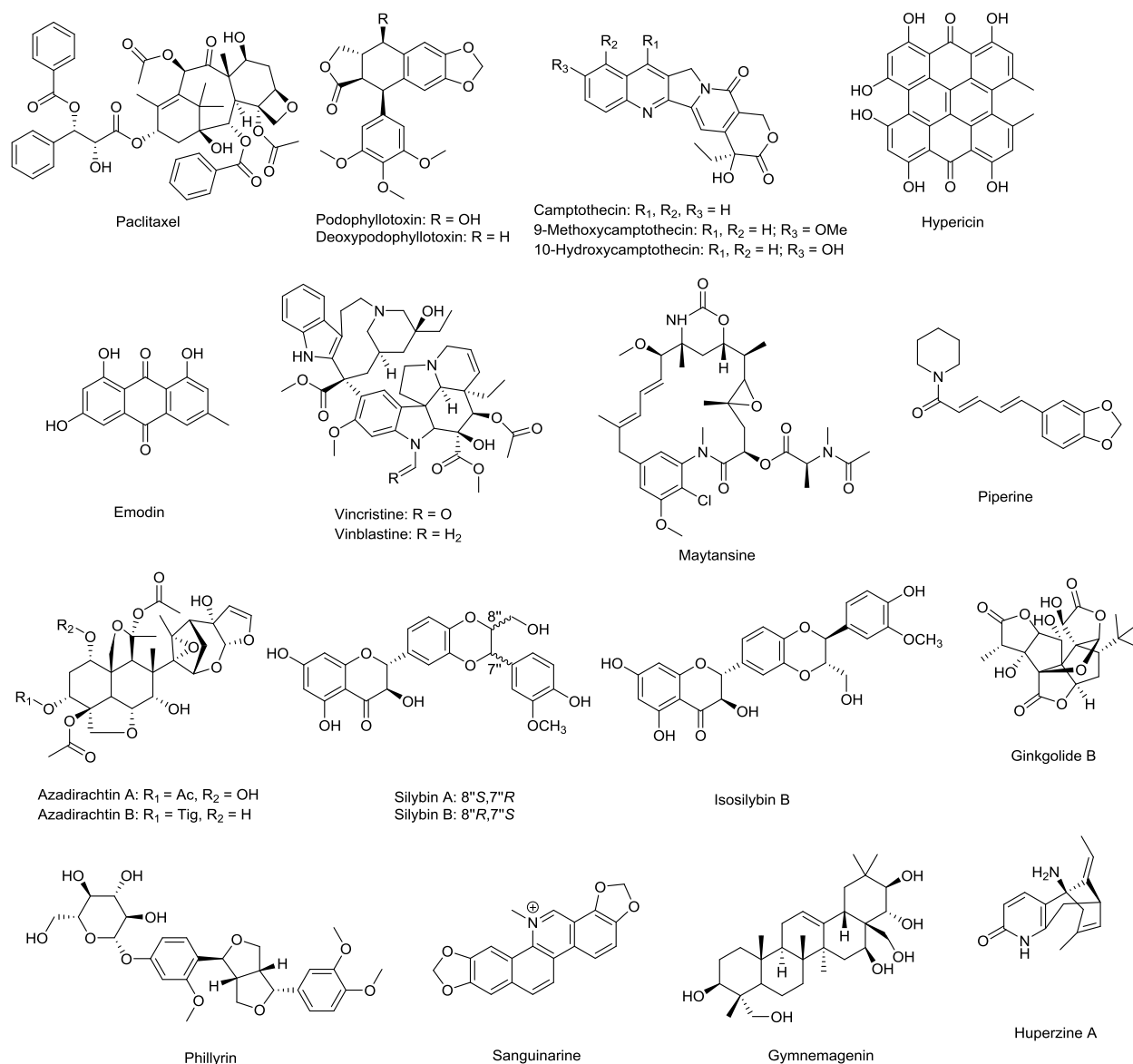


**Figure 1.** Representative plant natural products with alternative endophytic sources

In 1993, another historic discovery was published in *Science* that valuable anti-cancer agent paclitaxel (Taxol<sup>®</sup>) was detected to be produced by an endophytic fungus *Taxomyces andreanae*, which is harbored in the inner bark of pacific yew (*Taxus brevifolia*).<sup>36</sup> Thereafter, many research were focusing on the endophytes which are capable of producing or partially producing bioactive compounds previously thought to be plant-originated.<sup>17–20,25</sup> Some other outstanding examples have also refreshed the

## Chapter 1: Introduction

perspective of us for endophytes and host plants, including podophyllotoxins,<sup>37,38</sup> camptothecins,<sup>39–44</sup> huperzine A,<sup>45–50</sup> hypericin and emodin,<sup>51,52</sup> vinblastine and vincristine,<sup>53</sup> maytansine,<sup>54</sup> piperine,<sup>55</sup> azadirachtin A and B,<sup>56</sup> silybin A and B,<sup>57</sup> isosilybin A,<sup>57</sup> ginkgolide B,<sup>58</sup> phillyrin,<sup>59</sup> sanguinarine,<sup>60</sup> and gymnemagenin<sup>61</sup> (Figure 1 and Table 1).

**Table 1.** Representative plant natural products with alternative endophytic sources

Natural products from plant material	Plant sources	Endophytic producers	References
Paclitaxel	<i>Taxus</i> sps. <i>Corylus avellana</i>	More than 200 fungi and bacteria belonging to more than 40 genera	62,63
Podophyllotoxins	<i>Podophyllum</i> sps. <i>Juniperus</i> sps.	<i>Trametes hirsute</i> <i>Phialocephala fortinii</i> <i>Aspergillus fumigatus</i> Fresenius	37,38,64
Camptothecins	<i>Camptotheca acuminata</i> <i>Nothapodytes</i> sps.	<i>Trichoderma atroviride</i> LY357 <i>Fusarium solani</i> <i>Fomitopsis</i> sp. P. Karst <i>Alternaria alternata</i> (Fr.) Keissl <i>Phomopsis</i> sp. <i>Neurospora</i> sp. <i>Entrophospora infrequens</i>	39–44
Huperzine A	Family Huperziaceae	<i>Paecilomyces tenuis</i> YS-13 <i>Colletotrichum gloeosporioides</i>	45–50
Hypericin and emodin	<i>Hypericum</i> sps.	<i>Chaetomium globosum</i> <i>Thielavia subthermophila</i>	51,52
Vinblastine and vincristine	<i>Catharanthus roseus</i>	<i>Fusarium oxysporum</i>	53
Piperine	<i>Piper longum</i>	<i>Periconia</i> sp.	55
Azadirachtin A and B	<i>Azadirachta indica</i>	<i>Eupenicillium parvum</i>	56
Silybin A, silybin B, and isosilybin A	<i>Silybum marianum</i>	<i>Aspergillus iizukae</i>	57
Ginkgolide B	<i>Ginkgo biloba</i>	<i>Fusarium oxysporum</i>	58
Phillyrin	<i>Forsythia suspensa</i>	<i>Colletotrichum gloeosporioides</i> . (Penz.)	59
Sanguinarine	<i>Macleaya cordata</i>	<i>Fusarium proliferatum</i> BLH51	60
Maytansine	<i>Putterlickia</i> sps. <i>Maytenus</i> sps.	Bacterial community harbored in the host plant	54
Gymnemagenin	<i>Gymnema sylvestre</i>	<i>Penicillium oxalicum</i>	61

Because the controlled microbial fermentation is much more efficient and easier to scale-up for the industry, people have been attempting to utilize endophytes as a sustainable source for precious pharmacy-relevant natural products from limited plant

## Chapter 1: Introduction

---

material.<sup>17</sup> Even though recent development enables the heterologous expression of biosynthetic pathway in other organisms, there are still many technological bottlenecks. As a representative example, the heterologous biosynthesis of final product paclitaxel is still impossible, because of the lack of understanding on several key steps.<sup>65</sup> For instance, when the cP450's (key enzymes for the final biosynthesis of paclitaxel) were expressed in heterologous systems, they presented no functionality because of incorrect folding, translation and insertion to the cell membrane.<sup>66,67</sup> On the contrary, these endophytes are naturally occurred "heterologous host" with biosynthetic capacity of producing plant natural products (PNP), which can be readily obtained without artificially engineering of plant biosynthetic machinery to mimic PNP pathways in microbes.<sup>67,68</sup> However, to date all efforts to maintain the biosynthesis of target compounds in large-scale fermentation do not succeed.<sup>19</sup> It appears that the triggers or other essential factors from the natural niches were lost in the fermentation conditions.<sup>39,67,69</sup> For instance, there are approximately 200 fungi strains belonging to 40 fungal genera capable of producing paclitaxel, but no scale-up fermentation for the industry has been reported yet.<sup>20,67</sup> It is compelling that some biosynthetic genes of endophytes are only expressed in endophytic status, but barely expressed in mycelia status in artificial conditions, which was well exemplified by lolitrems producing fungus *Neotyphodium lolii*.<sup>70</sup> Moreover, given that some unknown compounds might only be produced in natural niches, they could plausibly be missed in the process of conventional approaches. Therefore, new strategies should be developed to unravel these cryptic biofunctional compounds produced by endophytes.

The promising future of the research on endophytes is a consensus of opinion among scientists in biotechnology.<sup>20</sup> However, regardless of searching new compounds from endophytes or fermenting valuable agents discovered from plants, we have to answer many open questions such as: how do the endophytes produce bioactive compounds in plant tissues and avoid disturbing the balance of endophytic systems? How do the interactions happen between endophytes, host plants, and pathogens or predators? What is the chemical basis of communication in endophytic systems? How do the endophytes maintain the production of bioactive compounds in natural niches?

## Chapter 1: Introduction

---

Indeed, chemists and biologists have already made significant progress in the research of endophytes. But there is still a long way to go to fully exploit the potential of endophytes. The realm of endophytes is like a Jigsaw puzzle just at the beginning. To put more small tessellating pieces to the giant picture of endophytes, herein, my work is committed to investigating the secondary metabolites from endophytic fungi and bacteria as well as the crosstalk basis and ecologically relevant bioactivities of them.

### 1.3 Natural products, important basis of interactions of endophytic system

In organic chemistry, natural products are mostly restricted to the secondary metabolites produced by organisms, which are not essential for the survival of producers.<sup>71</sup> Organisms, like microbes, plants, and lower animals, produce bioactive compounds to gain advantages in the process of evolution, although the biosynthesis pathways are energy consuming.<sup>71</sup> Even though the development of synthetic chemistry such as combinatorial chemistry can assess enormous structures with unparalleled efficiency, natural products are still considered as an indispensable resource of bioactivity-related structures, because they have been naturally selected as biofunctional agents in competitive environments for billions of years.<sup>72</sup> Scientists are mostly interested in their potential to be human's arsenal to fight against challenging diseases including infections and cancer. In 2015, *Nobel Prize in Physiology or Medicine* was awarded jointly to Youyou Tu for the discovery of anti-malaria agent artemisinin,<sup>73</sup> and William Cecil Campbell and Ōmura Satoshi for the discovery of anti-parasite agents ivermectin<sup>74</sup> and avermectin,<sup>75</sup> and their great contribution to human health. In recent few years, the number of natural products or natural product scaffold based compounds is expanding in the approved drugs.<sup>76</sup> Particularly, the discovery of bioactive compounds from endophytes will not only enrich the lead compounds in the compound library but also provide us opportunities to understand the ecological functions of endophytes. Thus, all the isolated pure compounds from endophytes herein were evaluated by antibacterial assay, as the contribution to the continuous screening for antibacterial agents.<sup>77-79</sup>

Because of the increasing pharmaceutical demand, the higher bioactivities of natural products demonstrate in the *in vitro* or *in vivo* screening models, the more attention will be paid on them.<sup>72</sup> However, these "less interesting" inactive natural products may be



## Chapter 1: Introduction

---

essential for organisms to adapt to the environment. For example, most pheromones produced by microbes are neither lethal nor toxic to other competitors, but still function for microbes to regulate their social behaviors and obtain competitive advantages.<sup>80</sup> By secreting and sensing these pheromone molecules, microbes are able to communicate with other individuals as well as other inter-kingdom species like plants.<sup>80</sup> Furthermore, even though many microbial antibiotics are generally considered as weapons, they are also signal molecules influencing the colonization, virulence, stress response, motility, and/or biofilm formation of microbes.<sup>81</sup> Therefore, for investigating endophytic systems with complex relationships between microbes and plants, all detectable compounds including inactive compounds in bio-assay could be important.

Herein, the secondary metabolites from endophytes which can be characterized for further investigation are all interesting for my projects. Moreover, MALDI-imaging-HRMS experiments were performed on the bio-samples (colonies of endophytes) to reveal the bio-functions of these metabolites.

### 1.4 Host plant screening

In this research, the main target is seeking the endophytes capable of producing physiologically active compounds, or communicating with other endophytes via signal molecules. I focused on the endophytes harbored in traditional Chinese medicinal (TCM) plants, which has more than 2500 years history of therapeutic application.<sup>82</sup> Based on the accumulated knowledge of TCM, the possibility of discovering bioactive compounds from plants as well as endophytes is plausibly higher than random screening.<sup>83</sup> Two candidate TCM plants, namely *Narcissus tazetta* (for the treatment of parotitis and skin infection), and *Buxus sinica* (for the treatment of furuncle), were selected for first screening because of their recorded medical effects relating to antibacterial activities. After the LC-MS profiling of secondary metabolites from host plants as well as isolated endophytes, endophytes from *N. tazetta* and *B. sinica* (Figure 2) were chosen for further investigation.



**Figure 2.** *N. tazetta* (left) collected from Fujian and *B. sinica* (right) collected from Shanghai

## Chapter 2

# OUTLINE OF LITERATURE

### 1. Overview of host plant

#### 1.1 *Narcissus tazetta*

*N. tazetta*, a species in family Amaryllidaceae, is not only well-known as an ornamental plant in the south of China, but also a traditional medicine for the treatment of mumps, mastitis, carbuncles, and insect bites.<sup>84</sup> The *in vitro* cytotoxicity assay against HepG-2 and HCT116 cell lines revealed that the extracts from the bulbs of *N. tazetta* have even stronger activity than doxorubicin.<sup>85</sup> The previous phytochemical research showed family Amaryllidaceae is a rich resource of alkaloids, which are related to the traditional medical uses.<sup>85</sup> From species *N. tazetta*, bioactive compounds such as flavans,<sup>86</sup> polysaccharide,<sup>87</sup> alkaloids,<sup>88</sup> phenylethanoid and phenylpropanoid glycosides<sup>84</sup> were also identified.

#### 1.2 *Buxus sinica*

*B. sinica*, a species in family Buxaceae, is widely used as evergreen boxwood in China, because of its tolerance against pruning and shearing. This interesting property drew our attention to investigating the endophytes harbored in the leaves and stems, which may provide benefits for host plant against biotic or abiotic stress<sup>18</sup> such as pathogens or harmful substance invading the wounds.<sup>89</sup>

As a traditional medicine, *B. sinica* is applied for the treatment of syphilis, malaria, dermatitis, rheumatism, and rabies.<sup>90</sup> More than 160 compounds were reported from genus *Buxus*, such as alkaloids, triterpenoids, steroids, flavonoids, coumarin, and lignans, with a broad range of bioactivities like cytotoxicity, anticholinesterase, antifungal activity, antibacterial, antileishmanial, phytotoxic, immunosuppressive and anticancer activities.<sup>91</sup>

### 2. Overview of endophytes investigated herein

#### 2.1 Fungal species *Fusarium solani*

*F. solani*, belonging to family Nectriaceae, is a widely distributed pathogenic fungus causing crop loss worldwide.<sup>92</sup> *F. solani* is also reported as an opportunistic pathogen

## Chapter 2: Outline of literature

---

for human, causing high mortality rate infections in immunocompromised patients.<sup>93</sup> However, it was also isolated as endophytes from healthy plant tissues. The *F. solani* strain isolated from the root tissue of tomato is beneficial for the host to suppress foliar and soil pathogens.<sup>94</sup> Furthermore, in a former research at INFU, it was demonstrated that the endophytic strain of *F. solani* collaborates with host plant *Camptotheca acuminata* to biosynthesize anticancer agent camptothecin.<sup>41,95</sup> Another research showed that one strain of *F. solani* as well as two other *Fusarium* species isolated from pigeon pea are capable of producing antioxidant cajanistilbene acid.<sup>96</sup> These reports suggested that the ecological role of species *F. solani* might be variable in different natural niches.

From the genus *Fusarium*, a great number of bioactive compounds have been identified, most of which are polyketides (PK) and nonribosomal peptides (NRP) with high structural diversity.<sup>97</sup> Gene mining for polyketide synthase (PKS) and nonribosomal peptides synthetase (NRPS) revealed many unknown PKS and NRPS genes in the genus *Fusarium*, which suggests this genus is a potential resource for new natural products.<sup>97</sup>

### 2.2 Bacterial species *Achromobacter xylosoxidans*

*A. xylosoxidans* (family Alcaligenaceae) was widely distributed in the aquatic environment including intravenous fluids, well water and water in humidifier.<sup>98–100</sup> However, this species was firstly discovered and named from the patients with chronic purulent otitis media and described as aerobic, non-fermentative, gram-negative rod.<sup>101</sup> The strains of *A. xylosoxidans* showed to a wide range of resistance towards antimicrobial agents and five of the isolates possibly played pathogenic roles in the former research.<sup>102</sup> The full genome sequence of an *A. xylosoxidans* strain from a cystic fibrosis patient was published in 2013.<sup>103</sup>

Interestingly, *A. xylosoxidans* was also isolated as functional endophytic bacterium from the roots of *Phragmites australis* and *Ipomoea aquatic*, which can improve the aromatic pollutants removal rate when it is harbored in host plant *Arabidopsis thaliana*.<sup>104,105</sup>

## Chapter 2: Outline of literature

---

### 2.3 Fungal genus *Colletotrichum*

The genus *Colletotrichum* belongs to family Glomerellaceae and it includes major important plant pathogens causing devastating diseases of many woody and herbaceous plants, such as anthraconose diseases.<sup>106–110</sup> After a short symptomless period in the early stage of *Colletotrichum* infection, the fungi change to a necrotrophic phase and result in significant death of plant tissues and the emergence of pathogenic lesions via host-induced virulence effectors.<sup>110</sup> However, some species were also reported as endophytes causing no symptoms harbored in the leaves,<sup>111–115</sup> fruits,<sup>59,116</sup> branches<sup>117</sup> or stems<sup>55,118</sup> of plants. The investigation on the conversion between pathogenic strain and endophytic strain of *Colletotrichum magna* showed that single mutation or disruption of a pathogenicity gene would transform it from a pathogen to an endophytic mutualist.<sup>22,23</sup>

*Colletotrichum* species are able to produce alkaloids, polyketides, and cyclic peptides with high structural diversity and broad range bioactivities.<sup>109,114,117–124</sup> Moreover, the strain *Colletotrichum gloeosporioides* TA67 isolated from anglojap yew (*Taxus x media*) was reported as a paclitaxel producer.<sup>125</sup> And another strain of *C. gloeosporioides* isolated from *Piper nigrum* is capable of producing piperine, which is a characteristic natural product from the host plant.<sup>55</sup> Furthermore, by screening the endophytic fungi in *Huperzia serrata*, researchers discovered that the isolated strain of *C. gloeosporioides* is a producer of Alzheimer's disease medicine huperzine A, which was supposed to be produced by host plants.<sup>45–48</sup>

Some bioactive compounds from this genus were documented as phytotoxic metabolites playing a significant role in pathogenesis.<sup>109</sup> Other antimicrobial, antioxidant, immunosuppressive or cytotoxic compounds might be beneficial agents for the fitness of host plants against biotic or abiotic stresses.<sup>114,115,118,119,122–124,126</sup>

### 2.4 Fungal species *Phyllosticta capitalensis* (teleomorph *Guignardia mangiferae*)

The genus *Phyllosticta* (family Botryosphaeriaceae) includes many species of plant pathogens and endophytes.<sup>127</sup> *P. capitalensis* is generally considered as endophytic fungus,<sup>127</sup> although it was reported to cause leaf blight of *Elaeocarpus glabripetalus*<sup>128</sup>

and spots on leaves and fruits of mango and guava.<sup>129,130</sup> Comparing to the closely related pathogenic species *G. citricarpa*, *P. capitalensis* produces a significantly smaller amount of amylases, endoglucanases and pectinases, which might be the keys for virulent species to cause citrus black spots on plants.<sup>127</sup> For the secondary metabolites, *P. capitalensis* was able to produce meroterpenes with toll-like receptor 3 regulating activity.<sup>131–133</sup>

### 2.5 Bacterial genus *Herbaspirillum*

Genus *Herbaspirillum* (family Oxalobacteraceae), a group of gram-negative diazotrophic bacteria, belongs to betaproteobacteria which includes a great number of plant-associated bacteria.<sup>134</sup> It used to be considered as a new *Azospirillum* species, because of its cell appearance, growth behavior and habitat in grass roots.<sup>134</sup> *Herbaspirillum* species aggressively colonize the whole plant not only in the cortex and vascular tissues but also intercellular spaces as endophytes,<sup>134</sup> and some species were even detected in intact root cells.<sup>135</sup> Most species in this genus are harmless endophytes, while few species cause diseases including red stripe on some sorghums and mottled stripe disease on sugarcane.<sup>136</sup> The significance of this genus is the nitrogen fixing capacity, which provides substantial nitrogen source and promotes the growth of host plants (especially for the economical crops like sorghum, sugar cane, rice, and maize).<sup>136</sup> Although *Herbaspirillum* species are not known as human pathogens, they were also isolated from 28 patients with cystic fibrosis as reported previously.<sup>134</sup>

## 3. Overview of the microbial secondary metabolites investigated herein

### 3.1 Biosynthetic pathways of nonribosomal peptide synthetase (NRPS) and polyketide synthase (PKS)

NRPSs and PKSs are two essential secondary metabolic pathways of organisms especially microbes, the products of which represent a huge family of bio-functional natural products including siderophores, toxins, antibiotics, pigments, immunosuppressants, and cytostatics.<sup>137–139</sup> The enzyme complexes of these two pathways synthesize secondary metabolites by conserved thiotemplate mechanism,

## Chapter 2: Outline of literature

providing unparalleled structural diversity for drug development. Many clinically applied drugs including vancomycin, erythromycin, cyclosporine, rapamycin, bleomycin, and epothilone are derived from NRPS or PKS pathways.<sup>137–139</sup> The microbial products investigated in this thesis are all biosynthesized by these two pathways or their hybrid pathways.

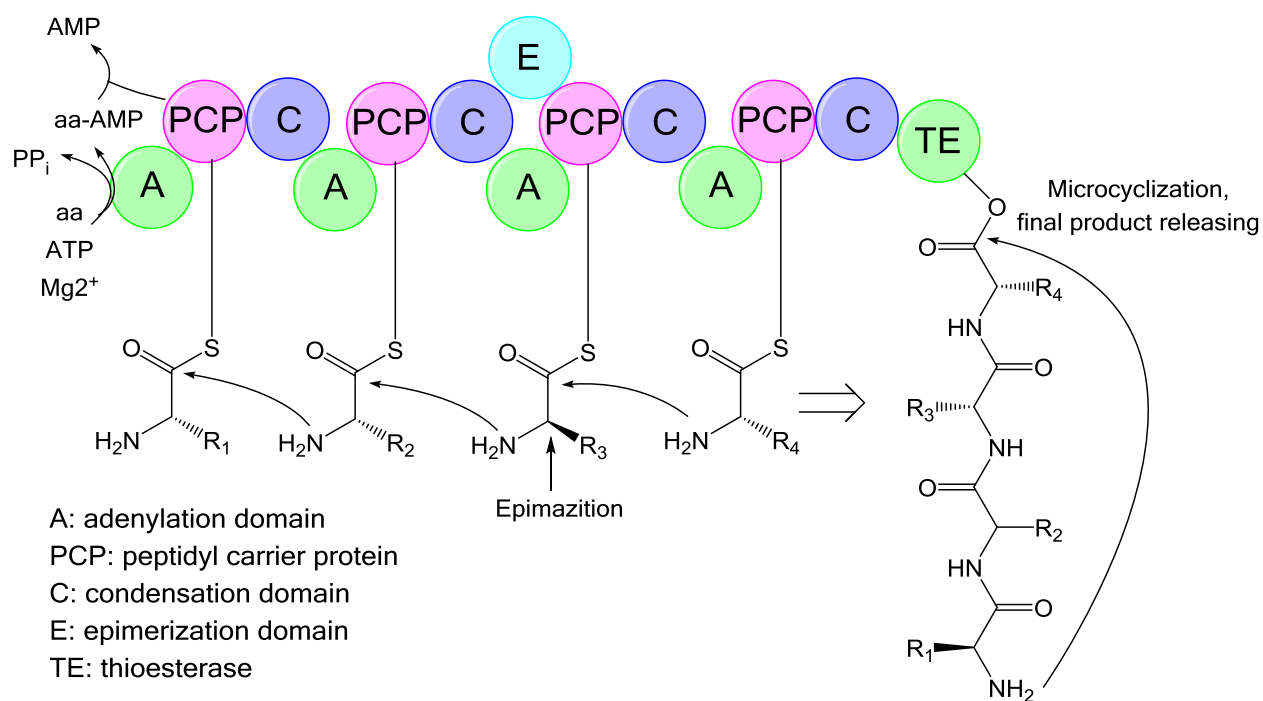


**Figure 3.** The chain elongation of NRPS biosynthesis pathway

Unlike ribosomal peptides synthesis, nonribosomal peptides (NRPs) are a group of peptides synthesized by multimodular nonribosomal peptide synthetases enzyme clusters (NRPS) independent of mRNA and tRNA.<sup>140</sup> Remarkably, the building blocks of NRPs are not confined to 20 proteinogenic amino acids. Reported NRPs present more than 500 different monomers including nonproteinogenic amino acids and fatty acids.<sup>140</sup> The selectivity of these enzymes for specific amino acid is still ambiguous.<sup>141</sup> Moreover, D-amino acids are also present in NRPs because of the epimerization-domain (E) in NRPS modules.<sup>142</sup> This property enables the high structural diversity of NRPS products with broad range of bioactivities.<sup>140</sup> NRPSs consist of an array of enzyme modular sections (Figure 3), in which each section is responsible for incorporating each monomer into the growing NRP chains.<sup>140</sup> Beside E domains, three domains, namely adenylation



## Chapter 2: Outline of literature

---

domain (A), thiolation or peptidyl carrier protein domains (PCP) and condensation domain (C), are essential for peptide elongation and ubiquitous in NRPSs.<sup>140</sup> Typically, at the end of the assembly lines of NRPSs as well as PKSs, thioesterase domains (TE) is responsible for the macrocyclization and final product release.<sup>143</sup>

PKSs are multienzyme systems with large molecular weight from  $M_r$  100 to 10,000 KDa, which synthesize extraordinarily complex polyketides stepwise from simple building blocks like acetyl-CoA, propionyl-CoA, butyryl-CoA or their other derivatives.<sup>144</sup> The reaction of linking the chain-building blocks is decarboxylative condensation, which is an analogue of the chain elongation step of primary metabolic fatty acid biosynthesis.<sup>144</sup> The genetic, protein-structural and mechanistic analyses reveal astonishing similarity between PKSs and fatty acid synthases.<sup>144–149</sup> However, the elongation of PKSs lacks one or multiple steps of consequent keto-reduction, dehydration, and enoyl reduction in the chain extension of fatty acid biosynthesis, resulting in remaining functional groups (hydroxyl, double bond, ketone groups, etc) on the aliphatic chain which is feasible for numerous reactions such as cyclization, oxidation, acylation or other modifications.<sup>144–149</sup> This remarkable character leads to high level of structural diversity and versatility of final PKS products.<sup>146</sup>

To date, PKSs are known to have majorly three types (type I–III).<sup>146</sup> Type I PKSs are large multidomain enzyme modules carrying all the active sites for polyketide biosynthesis, and each module has a set of distinct, catalyzing one cycle of polyketide chain elongation non-iteratively (the function domain of each module are different) (Figure 4A).<sup>144–149</sup> This type of PKS is similar to vertebrate fatty acid synthases, and the typical compounds are erythromycins.<sup>148</sup> In contrast, type II PKSs comprise several iterative modules (typically monofunctional) (Figure 4B), which is similar to the bacterial fatty acid synthases,<sup>144–149</sup> as exemplified by biosynthesis of doxorubicin<sup>150</sup> and actinorhodin.<sup>151</sup> Unlike type I and II PKSs, type III PKSs have no ACP and catalyze elongation reaction directly on the acyl-CoA substrates (Figure 4C),<sup>144–149</sup> as exemplified by biosynthesis of flavolin.<sup>152</sup>

Because of the similarity of these two pathways, notably, PKSs and NRPSs are able to fuse hybrid pathways utilizing both PKS and NRPS building blocks. For example,

## Chapter 2: Outline of literature

compounds bleomycin,<sup>153</sup> yersiniabactin,<sup>154</sup> epothilone,<sup>155</sup> and rapamycin<sup>156</sup> are polyketide-amino acid hybrid molecules synthesized by hybrid PKS and NRPS pathways. This flexible combination expands the capacity of NRPS/PKS to produce compounds with surprising structures.<sup>141</sup> Insights into the molecular mechanism of biosynthesis pathway offer us the opportunity to explain the ecological role of natural products as well as their microbial producers.<sup>141</sup> Furthermore, the engineering of NRPS/PKS might enable us to synthesize new chemicals which are difficult to obtain via conventional synthetic methods.<sup>141</sup>

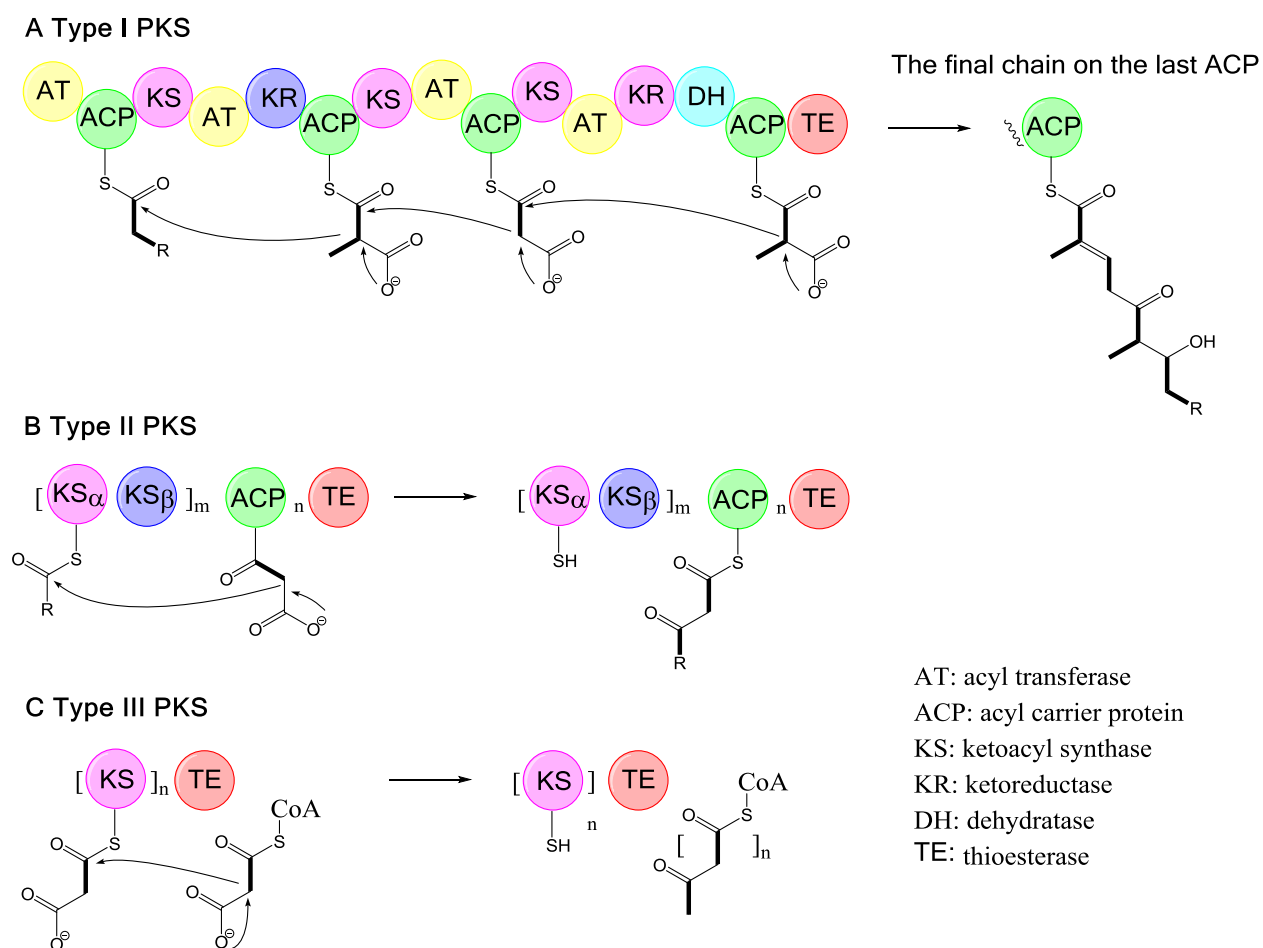


**Figure 4.** The chain elongation of type I–III PKS biosynthesis pathways

### 3.2 Cyclic peptides

Cyclic peptides are polypeptide chains synthesized via NRPS pathway without free N- and C- terminal because of the cyclization from head to tail.<sup>157</sup> The linking bonds of ring system are not limited to peptide bond, and other stable bonds such as lactone, ether,

## Chapter 2: Outline of literature

---

disulfide, thioether are also very common in the main scaffold.<sup>157</sup> On one hand, this property leads to much higher tolerance towards degradation in organisms or in the environment than the linear peptides.<sup>157</sup> On the other hand, the ring systems have rigid conformation, which may result in reinforced binding of molecules towards target receptors.<sup>157</sup> Many cyclic peptides have strong bio-activities and ecological functions, which can be exemplified by natural toxins amanitins<sup>158</sup> and microcystin.<sup>159</sup> Several of them are applied clinically as well. For example, antibiotics such as vancomycin,<sup>160</sup> gramicidin,<sup>161</sup> daptomycin,<sup>162</sup> and tyrocidine<sup>163</sup> are typical cyclic peptides.

### 3.3 Azaphilones

Azaphilones have a common isochromene core structure (Figure 5), belonging to the group of polyketides biosynthesized by PKS pathways.<sup>164</sup> Some of them are substituted by halogen on the olefinic carbons (most commonly chlorine substitution at position 5). They are mostly produced by numerous species of basidiomyceteous and ascomyceteous fungi, including genera *Chaetomium*, *Aspergillus*, *Penicillium*, *Pestalotiopsis*, *Phomopsis*, *Talaromyces*, *Emericella*, *Monascus*, *Epicoccum*, and *Hypoxyton*.<sup>164</sup> Some azaphilones are characteristic metabolites of certain species, which can be utilized as important chemotaxonomical markers.<sup>165–167</sup>

Azaphilones are not only pigments produced by fungi but also molecules with a significantly wide range of biological effects, including antimicrobial, cytotoxic, antiviral, anti-inflammatory and anticancer activities.<sup>164</sup> Several azaphilones are reported to be inhibitors of gp120-CD4 binding (anti-HIV related assay),<sup>168</sup> Grb2-SH2 interaction (anticancer related assay),<sup>169</sup> MDM2-p53 interaction (anticancer related assay),<sup>170</sup> and heat shock protein 90 (Hsp90, anticancer related assay).<sup>171</sup>

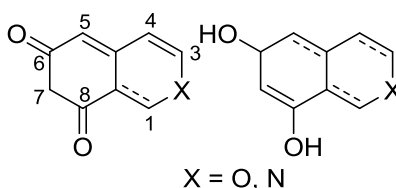
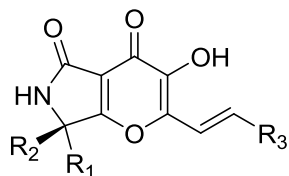
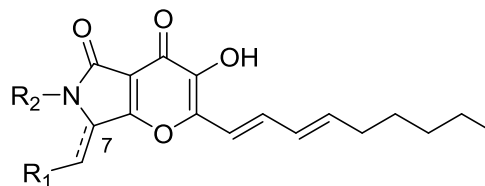


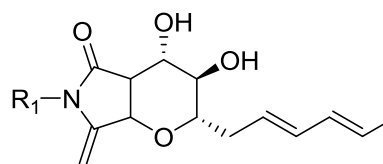
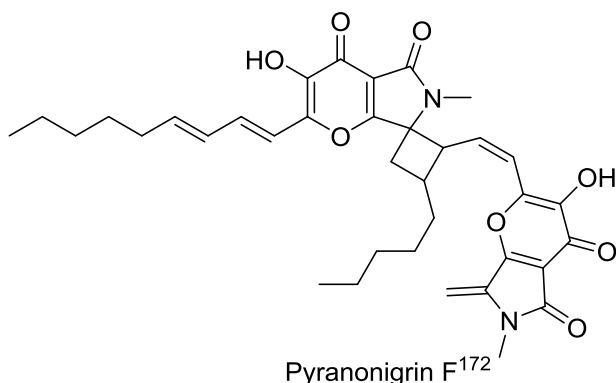
**Figure 5.** Basic azaphilone scaffold



Pyranonigrin A,  $R_1 = H, R_2 = OH, R_3 = Me$   
 Pyranonigrin S,  $R_1 = R_2 = H, R_3 = Me$   
 Pyranonigrin E,<sup>167</sup>  $R_1 = H, R_2 = Me, R_3 = Me$   
 Cordylactam,  $R_1 = H, R_2 = Me, R_3 = n\text{-propyl}$   
 Pyranonigrin F,<sup>173</sup>  $R_1 = H, R_2 = OH, R_3 = n\text{-propyl}$



Pyranonigrin E,<sup>174</sup>  $\Delta^7$ ,  $R_1 = H, R_2 = Me$   
 Pyranonigrin G,  $R_1 = H, R_2 = Me$   
 Pyranonigrin H,  $R_1 = OH, R_2 = H$



Curvupallide B,  $R_1 = OCH_3$   
 Curvupallide C,  $R_1 = H$

**Figure 6.** Reported lactam-fused 4-pyrone

### 3.4 Lactam-fused 4-pyrone

Lactam-fused 4-pyrone are biosynthesized via hybrid PKS/NRPS pathway, with pyrano[2,3-c]pyrrole basic scaffold (Figure 6).<sup>172</sup> In the former investigation, these compounds were isolated from *Cordyceps* sp.,<sup>173</sup> *Curvularia pallescens*,<sup>174</sup> and *Aspergillus niger*.<sup>172,175–179</sup> The compounds pyranonigrin E and F have confusing common names of nomenclature, with one name assigned to two different compounds respectively. Pyranonigrin A and F<sup>178</sup> showed potent antimicrobial activities against a broad spectrum of human, aquatic, and plant pathogens.<sup>178</sup>

## 4. Technical development of structural elucidation for unknown organic molecules

### 4.1 MS<sup>n</sup> technology for cyclic peptides sequencing

Tandem mass spectrometry (MS/MS) or multiple stage mass spectrometry (MS<sup>n</sup>) consist of two or more stages of MS, associated with the dissociation of certain mass weights between each stage. With low energy dissociation method, peptides most frequently cleavage at peptide bonding to generate b or y ions (Figure 7).<sup>180</sup> The b ions can further lose a CO group to generate a ions (Figure 7),<sup>180</sup> which is a major difference between b or y ions. Because most building blocks of peptides, namely amino acids, have different molecular weights (except some isomers like leucine and isoleucine), MS/MS becomes an efficient tool for peptides and even protein analysis and sequencing, due to its efficiency, robustness, sensitivity, and versatility.<sup>181</sup> For the linear peptides, the well-defined N- and C- terminal can be the unambiguous anchors to assign the sequence of amino acids in a certain order in MS/MS,<sup>182–184</sup> and the automatic analysis by software is also well established.<sup>185,186</sup>

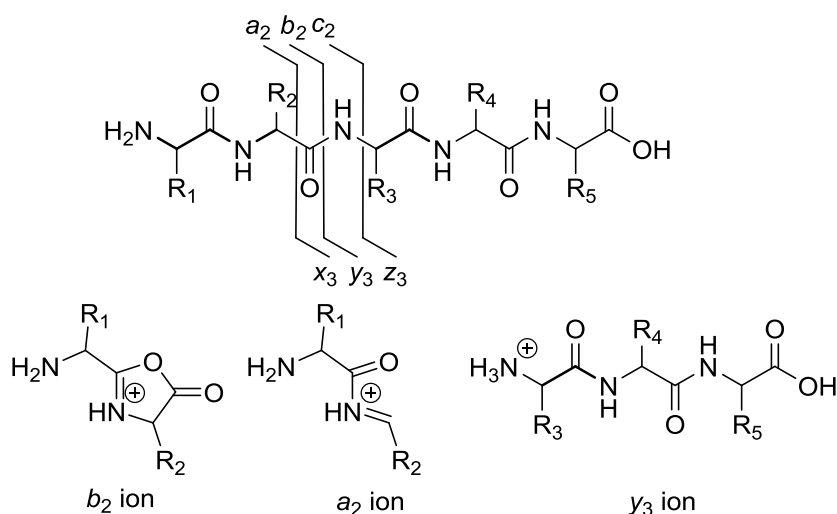


**Figure 7.** Representative a, b, c, x, y, and z ion pattern of linear peptides

For cyclic peptides, however, the sequencing is much more challenging, because of the absence of terminal amino acid.<sup>187</sup> Unlike linear peptides, the mass loss of amino acids in cyclic peptides results from cleavage of at least two bonds in the ring system, which

## Chapter 2: Outline of literature

---

can randomly occur at several backbone positions.<sup>187</sup> Without the reference of terminal amino acid, the fragments of cyclic peptides in MS/MS have many overlapping units and cannot be organized in an orderly fashion.<sup>187</sup>

After the development of MS<sup>n</sup> technologies, multistep fragmentation enables the analysis of amino acid sequence of each fragment obtained from the MS<sup>2</sup> of cyclic peptides, associated with low energy dissociation method (collisionally activated dissociation, CAD; also known as collision-induced dissociation, CID).<sup>187–191</sup>

### 4.2 Density functional theory (DFT) gauge-including atomic orbitals (GIAO) <sup>13</sup>C NMR shielding tensor calculation

Although the developments such as nuclear magnetic resonance (NMR) and MS technologies have been unprecedentedly promoting the structure elucidation of organic compounds, in some cases these technologies cannot always work out with satisfactory results.<sup>192,193</sup> Consequently, structures of some reported natural products including the molecules with interesting bioactivities are incorrectly assigned in the literature,<sup>192,193</sup> and the work of total synthesis or further biological investigation will take the risk of wasting enormous time, money and efforts.<sup>194</sup>

The shielding tensor of NMR spectroscopy is one of the most important atomic properties. As the successful progress made by DFT, the accurate GIAO shielding tensor DFT calculation was also proposed and practically applied by Schreckenbach *et al.*<sup>195</sup> and Cheeseman *et al.*<sup>196</sup> Barone *et al.* had done pioneering work that they employed GIAO <sup>13</sup>C NMR calculations to revise the misassigned structures and assigned the relative configurations of several natural products, which showed us the GIAO <sup>13</sup>C NMR calculation can be a powerful tool to solve the problematic structural assignment and secure the structure elucidation by NMR assignment.<sup>197,198</sup> Notably, for the famous complex compound maitotoxin, O. Frederick *et al.* utilized GIAO <sup>13</sup>C NMR calculation to verify the controversial sub-structure.<sup>199</sup> In many cases, the GIAO <sup>13</sup>C NMR calculation showed astonishing accuracy and reliability and was successfully applied in the structure elucidation.<sup>200–206</sup> Smith *et al.* adopted a multiple standard method (MTSD) using benzene (for *sp*<sup>2</sup> and *sp* carbon) and methanol (for *sp*<sup>3</sup> carbon) as references, which showed improved accuracy in the benchmark of different organic

compounds.<sup>207</sup> With the hybrid functional mPW1PW91 and small basis set 6-31G(d), the averaged MAD and RMS for the test sets is only 2.1 ppm and 4.9 ppm respectively.<sup>207</sup> Based on the efficiency and accuracy of GIAO <sup>13</sup>C NMR calculation, Sarotti *et al.* combined geometry optimization with computationally inexpensive approaches like MM+, AM1 or HF/3-21G and NMR shielding constants calculation on mPW1PW91/6-31G(d) level of theory, into a new strategy for simple and rapid identification of proposed structures.<sup>194</sup> This strategy of GIAO <sup>13</sup>C NMR calculation is helpful for preventing the publication of wrong structures and the consequences of these mistakes.<sup>194</sup>

## 5. Strategies for microbial chemical crosstalk investigation

### 5.1 What is microbial chemical crosstalk

In natural niches, microbes face myriad environmental factors and they adopt internal species or species to species communication as an essential strategy to survive. Since the end of 1970s the investigation on mechanisms of controlling bacterial bioluminescence opened a gate to reveal that bacteria are not unconscious organisms but social individuals, which are capable of achieving group behaviors and accomplishing complex tasks via cell to cell communication.<sup>208–215</sup> Hereafter, since the beginning of 1980s, N-Acyl homoserine lactones (AHL) and autoinducers 2 (AI-2) were discovered as corresponding signaling molecules, of which the concentration is correlated to the population density and utilized by bacteria to control social behavior by altering gene expression.<sup>209</sup> Therefore, the term quorum sensing was proposed and stupendous progress was accomplished upon the mechanism of the cascade signaling pathways.<sup>208–215</sup>

However, more and more phenomena exhibit so-called quorum sensing molecules do not only function for “quorum sensing (QS)”, but also for different functions including regulating virulence factor production, formation of inner-species or inter-species biofilm, dormancy, and competence.<sup>208–215</sup> These so-called QS molecules are also able to influence the functions of other eukaryotic species such as fungi, plants or even mammals, which is known as inter-kingdom communication.<sup>214,216</sup> Moreover, chemical communication behaviors were observed in the investigations on fungi as well, which shared homologous characters as bacterial quorum sensing molecules.<sup>12,212,217</sup> The

## Chapter 2: Outline of literature

chemical language spoken in microbes implicates the sophisticated social networks connecting them, their neighbors, or their host, and the extensive influence is far beyond the initial definition of “quorum sensing”.<sup>214,218</sup> Therefore, chemical crosstalk, which is a vivid description of the dialogue-like chemical communication or interaction between microbes, is suitable not only for bacteria but also other microbes.

### 5.2 Visualization of chemical crosstalk

As the general procedure of microbial natural product investigation, strains are firstly purified and then subjected to large-scale fermentation to obtain sufficient quantity of pure compounds for further investigation. However, microorganisms are living in complex niches consisting of many different other individuals, which results in the difficulties for investigating the ecological roles of bioactive compounds by conventional strategies. For uncultivable microbes, which are the remaining untapped sources of new biofunctional compounds, the research on secondary metabolites requires complex *in situ* approaches.<sup>219,220</sup>

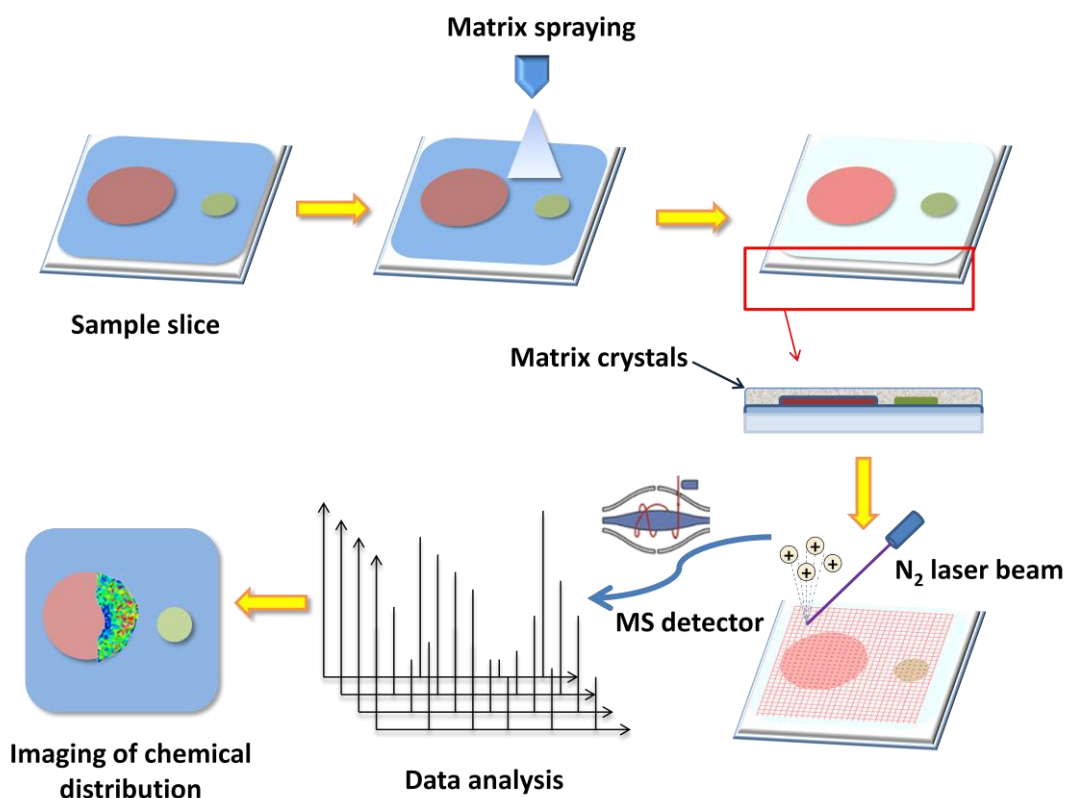


**Figure 8.** The flow chart of MALDI IMS measurement



## Chapter 2: Outline of literature

---

Thus, scientists have been developing experimental techniques to resolve these challenges, resulting in the invention of many novel technologies including the imaging mass spectrometry (IMS) for the visualization of chemical maps in complex biological samples.<sup>221–224</sup> As one of the extraordinary examples, MALDI ion source was initially developed to analyze high polar, ionic, and high molecular mass compounds, and it could also be applied to samples without complex pre-treatment for MS measurement.<sup>225–227</sup> The specific matrix consists of small organic compounds with strong resonance absorption to laser with certain wavelength.<sup>225</sup> Matrix can transfer controllable energy to the matrix-analyte mixture in a manner of uniform and soft desorption, as well as promote the ionization of analytes by chemical reactions or charge transfer.<sup>225</sup> It showed outstanding advantages on intact cell metabolites profiling, which allow us to measure a small location on the surface of samples without disturbing other parts, and organize the MS information of each location as pixel to obtain chemical maps on the samples (Figure 8).<sup>221–224</sup> This method comprises five main steps, namely sample preparation, matrix application, dehydration of samples, data acquisition, and data processing.<sup>228</sup> Although the MALDI IMS analysis is rapid and simple because it only needs mixing the matrix with the analytes, the sample preparation is still challenging.<sup>228</sup> Those samples, which are difficult to yield flat and stable surfaces, are not suitable for MALDI IMS measurement.<sup>228</sup>

Some similar methods like desorption/ionization on silicon mass spectrometry (DIOS MS) are able to analyze small natural products without the interference of matrix signals.<sup>228</sup> In addition, there are also some ion source of IMS requiring no sample pre-treatment, such as desorption electrospray ionization (DESI) and nanospray DESI, which allows us to profile the metabolites directly under ambient conditions.<sup>229</sup> Notably, the technology of liquid micro-junction surface sampling probe (LMJ-SSP), using micro tube extract system with solvent flow, are also capable of producing IMS of living organisms.<sup>230</sup>

The application of IMS on microbial crosstalk successfully brought the interaction of the microbial world to light in the recent decade, and provided us insights to the microbial interaction.<sup>228</sup> For example, *Bacillus subtilis* is mostly investigated bacterium by IMS, which secretes several secondary metabolites to compete or communicate with other species, including subtilin, subtilosin, surfactins, plipastatins and bacillaene.<sup>228</sup> IMS was

## Chapter 2: Outline of literature

---

used to search for the cannibalistic toxins produced by *B. subtilis*, track the metabolites exchanged between it and *Streptomyces sp.* Mg1, as well as observe the chemicals produced in the microbial assemblage comprising *B. subtilis* SIO-1 and *Promicromonosporaceae* strain SIO-11.<sup>228</sup> Moreover, IMS is also an important tool for the investigation of endophytic microbes. Especially for the investigation of endophytes in their natural niches, IMS technology presented unmatched ascendancy that was exemplified by the visualization of maytansine production of endophytic microbial community in *Putterlickia* roots.<sup>54</sup>

## Chapter 3

# RESEARCH OBJECTIVES

### 1 Aim of research

The aim of this research was to search bioactive or biofunctional secondary metabolites from endophytic fungi and bacteria harbored in traditional Chinese medicinal plants. After pre-screening the endophytes isolated from several collected plant materials, the subjects were determined to be the endophytic fungi and bacteria isolated from plant *N. tazetta* and *B. sinica*.

The general workflow of this research is showed as follow:

Collecting plant samples of *N. tazetta* and *B. sinica* from different location of China and measuring the LC-MS chromatograms of the extracts from plant samples as metabolites fingerprints data.

Isolating, purifying and identifying endophytic fungi and bacteria from plant tissues. Analyzing the metabolites produced by obtained endophytes in many different fermentation conditions by LC-MS<sup>n</sup>. Targeting these secondary metabolites having sufficient amount for further research, as well as having novel fragmentation pattern in MS<sup>n</sup> spectra.

Accumulating enough amount of compounds for structural identification and bioassay by large-scale fermentation.

Proposing possible bio-functions of these compounds based on the identified structures. Designing proper experiments to check whether these compounds have bioactivities or biofunctions by IMS and bio-assay.

#### 1.1 Hexacyclopeptides from endophytic *F. solani* N06 and their plausible ecological function

Investigating on the hexacyclopeptides produced by *F. solani* N06 in stationary condition including structure elucidation via MS<sup>n</sup>, and stable isotope labeling to verify the original producer.

## Chapter 3: Research objectives

---

Investigating the plausible ecological functions of these hexacyclopeptides as well as the interaction between isolated endophytes from the same plant tissue including endophytic *F. solani* N06 and bacterium *A. xylosoxidans* N12B.

### 1.2 Antibacterial azaphilones from endophytic fungus *Colletotrichum* sp. BS4

Optimizing the fermentation condition for the strain *Colletotrichum* sp. BS4 to obtain enough amount of azaphilone type compounds. Purifying targeted new azaphilones from the crude extracts of fermented biomass by extensive chromatographic techniques. Elucidating the structure of these compounds via spectroscopic technologies including 1D, 2D NMR and MS, X-ray diffraction as well as the quantum chemistry calculation of ECD and NMR properties.

Evaluating the antibacterial activities as well as the cytotoxicity of these compounds to examine the potential for further antibiotic development. Visualization of these compounds in the fungal colony to propose the possible bio-functions.

### 1.3 Lactam-fused 4-pyrones produced by endophytic fungus *P. capitalensis* BS5 and its endosymbiont.

Optimizing the fermentation condition for the endosymbiotic system to yield sufficient amount of lactam-fused 4-pyrones for further investigation. Elucidating the structures of these new compounds via diverse spectroscopic method and *ab initio* DFT NMR calculations.

Based on the structure, proposing the possible biosynthesis pathway and then analyzing the corresponding biosynthetic genes to verify the original producer(s) in this endosymbiotic system.

**Chapter 4**  
**EXPERIMENTAL SECTION**

### 1. General experimental procedures and instruments

A. KRÜSS Optronic polarimeter P8000-T was used for optical rotation measurement, and ECD were recorded by a Jasco J-715 spectrometer.<sup>231</sup> IR spectrum measurements were performed on a Bruker IR spectrometer TENSOR27.<sup>231</sup> NMR spectra were measured by a Bruker DRX-500 spectrometer with frequency 500 (<sup>1</sup>H) and 125 (<sup>13</sup>C) MHz using TMS as reference standard.<sup>231</sup> HRMS and HRMS<sup>n</sup> experiments were performed using a LTQ-Orbitrap spectrometer (Thermo Fisher, USA) equipped with an HESI-II ion source.<sup>231</sup> The LC system for LC-MS is Agilent 1200 HPLC system consisting of pump, PDA detector, column oven (30 °C), and autosampler (injection volume 5 µL for every sample).<sup>231</sup> The LC column was NUCLEODUR<sup>®</sup> C<sub>18</sub> Gravity, 1.8 µm, 2 mm × 30 mm. Ion source parameters: heater temperature: 400 °C; sheath gas flow rate: 60 a.u., gas flow rate 12 a.u.; sweep gas flow rate 0 a.u.; spray voltage 4.60 kV, capillary temperature: 350 °C; capillary voltage 25 V, tube lens voltage: 65 V.<sup>231</sup> Full scan MS parameters: mass range: 190–1000, resolution: 60,000 (*m/z* 400), polarity mode: positive, lock masses *m/z* 214.0896 and 231.1161 ([M+H]<sup>+</sup> and [M+NH<sub>4</sub>]<sup>+</sup> adducts of N-butylbenzenesulfonamide, C<sub>10</sub>H<sub>15</sub>NO<sub>2</sub>S, respectively).<sup>69</sup> Semi-preparative HPLC consists of a Gynkotek pump, a Dionex DG-1210 degasser, a Dionex UVD 340S detector, and a Dionex Gina 50 autosampler with Venusil XBP (2) C<sub>18</sub> column (10 × 250 mm).<sup>231</sup> Column chromatography was using silica gel 60 (70-230 mesh; AppliChem, GmbH, Darmstadt, Germany) as stationary phase.<sup>231</sup> Solid phase extraction (SPE) Columns BAKERBOND spe<sup>™</sup> C<sub>18</sub> polar plus were purchased from J.T.Baker, Avantor Performance Materials B. V., Deventer Netherlands.<sup>130</sup> Thin-layer chromatography (TLC) was performed with pre-coated silica gel 60 plates (0.25 mm; Merck, Darmstadt, Germany). Spots were visualized by UV light at 254 nm and 365 nm, and by spraying with 10 % H<sub>2</sub>SO<sub>4</sub> (v/v) EtOH solution followed by heating at 120 °C.<sup>231</sup>

$\alpha$ -Cyano-4-hydroxycinnamic acid (HCCA; >99.0 %) was purchased from Sigma-Aldrich life Science, USA. Ethyl acetate (EtOAc), MeOH, CH<sub>2</sub>Cl<sub>2</sub> and acetonitrile were HPLC grade from J. T. Baker, Avantor Performance Materials B. V., Deventer Netherlands.<sup>69</sup> Mobile phase water was double distilled deionized water.<sup>69</sup> Analytical-grade amino acids were provided by AppliChem, Darmstadt, Germany. Triethylamine (>99.5%), chemical-

## Chapter 4: Experimental section

---

grade acetaldehyde (99%), trifluoroacetic acid (TFA; 99 %), N-Boc-4-oxo-L-proline methyl ester, NaBD<sub>4</sub> and Dowex™ 50WX8-100 resin were purchased from Sigma-Aldrich, Steinheim, Germany.<sup>69</sup>

All the commercial media for microbes were purchased from Sigma-Aldrich. Constitution of media: Potato dextrose broth (PDB), potato extracts 4 g, dextrose 20 g, in 1 L; potato dextrose agar (PDA), potato extracts 4 g, dextrose 20 g, agar 15 g, in 1 L; Sabouraud dextrose agar (SDA), mycological peptone 10 g, dextrose 40 g, agar 15 g, in 1 L; nutrient agar (NA), meat extract 1 g, peptone 5 g, sodium chloride 5 g, yeast extract 2 g, agar 15 g, in 1 L; nutrient broth (NB), meat extract 1 g, peptone 5 g, sodium chloride 5 g, yeast extract 2 g, in 1 L; solid rice medium consisted of 1 : 1 (w/v) rice and water, which had been sterilized at 120 °C in autoclave; rice agar (RA), 20 g rice flour, 15 g agar, in 1 L. Petri-dishes were purchased from TPP, Trasadingen, Switzerland. And the 6 mm sterile diffuse assay paper disks were provided by Schleicher & Schuell GmbH, Dassel, Germany.<sup>69</sup>

## 2. Isolation and culture of endophytes

### 2.1 Collection and identification of host plants

Each tissue was recorded by photography and then carefully cut from host plants. The wounds of tissues were covered by Parafilm® to prevent water loss. Then they were transported in sealed plastic bags and preserved at 4 °C within 48 h of collection before processing. *N. tazetta* was collected from Zhangzhou, Fujian Province, People's Republic of China, in November 2012, which was identified by Shanghai Botanical Garden.<sup>69</sup> *B. sinica* was collected from Guangzhou, Guangdong Province, People's Republic of China, in November 2013, which was identified by South China Botanical Garden.<sup>130,231</sup>

### 2.2 LC-MS analysis of plant extracts

A part of collected tissues (about 2–10 g) was dried and crushed in liquid N<sub>2</sub>, and then extracted by CH<sub>2</sub>Cl<sub>2</sub> : MeOH (1 : 1, v/v) (for low polar compounds) and MeOH (for high polar compounds) successively. The extraction solution was concentrated under vacuum in 40 °C water bath. All the crude extracts were weighted and prepared into 1



## Chapter 4: Experimental section

---

mg/mL MeOH solution for LC-MS/MS<sup>n</sup> measurement. The LC condition was used acetonitrile: water system with 0.1 % formic acid. The general gradient was set to be: 0-2 min, 0% acetonitrile; 2 min-30 min, 0%-100% acetonitrile; 30-34 min, 100% acetonitrile; 34-35 min, 100-0% acetonitrile. The column was NUCLEODUR<sup>®</sup> C18 gravity (1.8  $\mu$ m 2 mm $\times$ 30 mm) and flow rate was 0.4 mL/min, and the column oven temperature was 30 °C.<sup>69</sup> Parameters of FTMS<sup>n</sup>: polarity: positive, isolation width:  $m/z$  2 amu, CID energy: 35 eV, act. Q.: 0.25 and act time: 30 ms.<sup>69</sup>

### 2.3 Isolation of endophytes

The plants were washed thoroughly in running tap water followed by sterilized water to clean all dirt and mud sticking to them.<sup>39,96</sup> The healthy tissues were slit into approximately 10  $\times$  5 mm pieces by flame-sterilized razor blades.<sup>39,96</sup> Then, the small fragments were surface-sterilized by successive immersion in 70% ethanol for 1 min, 1.3 M sodium hypochlorite (3–5% available chlorine) for 3 min, and 70% ethanol for 30 s.<sup>39,96</sup> Finally, these surface-sterilized tissue pieces were rinsed in sterilized water for 1 min and wrapped by sterilized paper to remove excess water.<sup>39,96</sup> Obtained surface sterilized tissues were evenly placed on water agar medium in Petri-dishes, then sealed with Parafilm<sup>®</sup> and incubated at 28  $\pm$  2 °C in an incubator until microbial growth started.<sup>39,96</sup> The procedure of isolation was similar to the experiment reported in literature.<sup>39,96</sup> To eliminate microbial contaminants from surface and ensure the sterilization was completed, the sterilized water used to wash sterilized tissues was subcultured on PDA in parallel. The cultures were monitored every day to check the outgrowth of endophytic fungal mycelia or bacterial colonies from plant tissue, after one week.<sup>39,96</sup> Then the growing endophytic fungi and bacteria were isolated and subcultured onto SDA medium and NA medium respectively, and brought into pure culture by successive purification if it was necessary.<sup>39,96</sup> These isolates were coded with abbreviation of plant name and numbers, and then preserved in 20% glycerol solution at -80 °C in the microbial library at INFU, TU Dortmund, Germany.<sup>69</sup>

## 3. Identification of isolated fungi and bacteria

By strictly following the manufacturer's guidelines, the fungal total genomic DNA (gDNA) was extracted from the *in vitro* cultures using peqGOLD fungal DNA mini kit (cat. no. 12-

## Chapter 4: Experimental section

---

3490-02, Peqlab Biotechnologie GmbH, Erlangen, Germany). The DNA was then PCR amplified by primers ITS4 and ITS5 according to the literature.<sup>130,232</sup> The amplified fragment included ITS1, 5.8S and ITS2 regions of the rDNA.<sup>69,130</sup> The PCR reacted in 50  $\mu\text{L}$  reaction mixture consisting of 1  $\mu\text{L}$  dNTPs (10 mM), 0.5  $\mu\text{L}$  forward primer (100  $\mu\text{M}$ ), 10  $\mu\text{L}$  Phusion HF buffer (5X), 3  $\mu\text{L}$  of template DNA, 0.5  $\mu\text{L}$  reverse primer (100  $\mu\text{M}$ ), and 1  $\mu\text{L}$  of Phusion polymerase (2U  $\mu\text{L}^{-1}$ ), and 34  $\mu\text{L}$  of sterile double-distilled water.<sup>69,130</sup> The PCR cycling setting included an initial denaturation at 98°C for 3 min, 30 cycles of denaturation, annealing, and elongation at 98°C for 10 s, 58°C for 30 s and 72°C for 45 s.<sup>69,130</sup> This was followed by a final elongation step of 72°C for 10 min.<sup>69,130</sup> Sterile double-distilled water was used as a negative control.<sup>69,130</sup> The PCR amplification products were checked by gel electrophoresis spanning approximately 500-600 bp (base pairs).<sup>69,130</sup> According to the manufacturer's instructions, the PCR products were further purified using peqGOLD micro spin cycle pure kit (cat. no. 12-6293-01, Peqlab Biotechnologie GmbH, Erlangen, Germany).<sup>69,130</sup> The amplified products were then sequenced from both sides at GATC Biotech (Cologne, Germany).<sup>69,130</sup>

The 16S rRNA analysis of bacteria was following the procedures reported in the literature.<sup>54</sup> The genomic DNA was extracted from the *in vitro* cultures using peqGold bacterial DNA kit (Peqlab Biotechnologie GmbH, Germany), then subjected to PCR amplification using the primers 27f and 1492r.<sup>233</sup> The PCR amplification was performed in a 50  $\mu\text{L}$  reaction mixture with 45  $\mu\text{L}$  Red Taq DNA Polymerase Master Mix (1.1x), 0.5  $\mu\text{L}$  reverse primer (100  $\mu\text{M}$ ), 0.5  $\mu\text{L}$  forward primer (100  $\mu\text{M}$ ), 3  $\mu\text{L}$  template DNA, and 1  $\mu\text{L}$  of sterile double-distilled water.<sup>54</sup> The PCR cycling comprised an initial denaturation at 95 °C for 2 min, 30 cycles of denaturation, annealing and elongation at 95 °C for 30 s, 60 °C for 40 s and 72 °C for 30 s.<sup>54</sup> Then a final elongation step was performed at 72 °C for 5 min.<sup>54</sup> The sterile double-distilled water was used as negative control. The PCR amplified products spanning around 1500 bp were checked by agarose gel electrophoresis.<sup>54</sup> The PCR products were further purified using GFX™ PCR DNA and Gel Band Purification kit (GE Healthcare life Sciences, Germany) following manufacturer's instructions.<sup>54</sup> The amplified products were then sequenced from both directions using primers 27f and 1492r at GATC biotech (Cologne, Germany).<sup>54</sup>

### 4. Secondary metabolites profiling of endophytes

#### 4.1 Selection of fermentation conditions

3 standard pre-screening fermentation conditions were used for secondary metabolites screening, namely PDB shaking condition (150 mL broth in 250 mL Erlenmeyer flask, 150 rpm, 28 °C, 14 days), PDB stationary condition (100 mL broth in 250 mL Erlenmeyer flask, 25 ± 2 °C, 16 days), rice medium (solid medium, 10 g rice in 50 mL flask, 25 ± 2°C, 30 days).

#### 4.2 LC-MS analysis of endophytic products

For broth media, the biomass was extracted by equal volume AcOEt for 24 h at room temperature, and the organic layers were separated and concentrated under vacuum in 40 °C water bath. For the solid media, the biomass was broken by knife and extracted by 200 mL AcOEt. Then the AcOEt solution was filtered and concentrated as described above.

The crude extracts were dissolved in 1 mL HPLC grade MeOH, and then diluted for 1000 times for LC-MS measurement. The solvent system was the same as plant fingerprint assay described above. The general gradient was: 0-2 min, 20% acetonitrile; 2 min-25 min, 20%-80% acetonitrile; 25-27 min, 80-100% acetonitrile; 27-28 min, 100% acetonitrile; 28-30 min 100-20% acetonitrile. The MS and MS<sup>n</sup> settings were the same as plant fingerprint assay.

### 5. Fungal and bacterial material

#### 5.1 Endophytic fungus *F. solani* N06 and endophytic bacterium *A. xylooxidans* N12B from bulbs of *N. tazetta*

After approximately 2 weeks, some visible hyphae tips started to emerge from the plant tissues, which were then subcultured and purified on SDA. Endophytic bacterial could be seen emerging as oil-drop-like colony from the edge of tissues, which were subcultured and purified on NA. The isolated pure colonies of endophytic fungus and bacterium were assigned strain codes N06 and N12B respectively. The endophytic fungus *F. solani* N06

## Chapter 4: Experimental section

---

has also been submitted to the Leibniz Institute DSMZ – German Collection of Microorganisms and Cell Cultures, Braunschweig, Germany, with accession number DSM 29858.<sup>69</sup> The ITS sequence of *F. solani* N06 has been deposited at the EMBL-Bank (accession number LN624513) and the 16s rDNA sequence of *A. xylooxidans* N12B has also been deposited at the EMBL-Bank (accession number LN810108).<sup>69</sup> The fermentation of *F. solani* N06 was in 100 mL stationary PDB broth at 25 °C, in 250 mL Erlenmeyer flask.<sup>69</sup>

### 5.2 Endophytic fungi *Colletotrichum* sp. BS4 and *P. capitalensis* BS5 and endosymbiotic bacterium *Herbaspirillum* sp. BS5B from leaves of *B. sinica*

By the established methods, fungi *Colletotrichum* sp. BS4 and *P. capitalensis* BS5 were isolated from the leaves of *B. sinica*, and the endophytic bacterium *Herbaspirillum* sp. BS5B was identified to be an endo hyphal microorganism in *P. capitalensis* BS5.<sup>130,231</sup> Pure colonies of these two endophytic fungi were preserved in 20% glycerol at -80 °C in the internal culture library with assigned strain codes BS4 and BS5 respectively.<sup>130,231</sup> The ITS sequence of the identified endophytic fungus *Colletotrichum* sp. BS4 and *P. capitalensis* BS5 have been deposited at the EMBL-Bank (accession number LN552210 and LN828209).<sup>130,231</sup> The 16S RNA sequence of *Herbaspirillum* sp. BS5B has been deposited at the EMBL-Bank with accession number LN864763.<sup>130</sup> Following the reported isolation procedures for the endosymbiotic bacterium,<sup>234</sup> however, no free living bacterial colony of *Herbaspirillum* sp. was observed. For *Colletotrichum* sp. BS4, rice medium was used as fermentation medium, at 25 °C, and for *P. capitalensis* BS5, the fermentation condition was the same as strain *F. solani* N06 mentioned before.<sup>130,231</sup>

## 6. LC-MS<sup>n</sup> analysis of hexacyclopeptides from *F. solani* N06

The 100 mL fermentation broth was extracted 3 times with 300 mL EtOAc at room temperature, and the organic layer was evaporated under vacuum in a water bath (40 °C) to yield 4 mg semi-dry dark red residues.<sup>69</sup> This residue was then re-dissolved in 500 µL MeOH for LC-HRMS measurement.<sup>69</sup> The auto sampler temperature was 10 °C and the drawing and ejecting speed were both set to be 200 µL/min.<sup>69</sup> For the optimized LC condition, 30%–40% gradient acetonitrile aqueous solution with 0.1% formic acid was used as mobile phase (linear gradient program: 0–1 min, 30%; 1–26 min,

30%–40%; 26–27 min, 40%–100%; 27–30 min, 100%; 30–31 min, 100%–30%; 31–32 min, 30%).<sup>69</sup> Parameters of ion trap MS<sup>n</sup>: positive mode, isolation width:  $m/z$  2 amu, CID energy: 35 eV, act. Q.: 0.25 and act time: 30 ms.<sup>69</sup> From the MS<sup>3</sup> in FTMS mode, I did not obtain enough ion abundance for some peaks, but the MS<sup>2</sup> spectra in FTMS mode is attached in Chapter 8, Figure S10.<sup>69</sup>

## 7. Purification of target compounds

### 7.1 Azaphilones from *Colletotrichum* sp. BS4

The large-scale fermentation was performed on solid rice medium (80 g rice, 100 mL water, in each 1000 mL flask) at 25 °C with PDB culture as seed broth. After 30 days, the culture (1.6 kg) was extracted with 4 L EtOAc at room temperature 3 times to yield 33 g brown residue after removing the solvent under vacuum.<sup>231</sup> This extract was subjected to a silica gel column (2 × 10) cm, and eluted by a stepwise cyclohexane/EtOAc gradient from ratio 1:0 to 0:1 into 4 fractions (Fr. 1–Fr. 4).<sup>231</sup> Fr. 3 was eluted on a silica gel column with CH<sub>2</sub>Cl<sub>2</sub>/EtOAc (3:1) to obtain two subfractions (Fr 3a, 3b).<sup>231</sup> Successive purification of Fr. 3a by semi-preparative HPLC (UV detection at 355 nm, flow rate 3 mL/min, mobile phase MeCN and H<sub>2</sub>O (0.1% formic acid) yielded 5 mg colletotrichone A (**10**), (33% MeCN,  $R_t$ : 31.8 min), 10 mg colletotrichone B (**11a**) (45% MeCN,  $R_t$ : 27.6 min), 2 mg colletotrichone C (**12**) (55% MeCN,  $R_t$ : 25.0 min), 2 mg colletotrichone D (60% MeCN,  $R_t$ : 21.5 min) and 8 mg chermesinone B (**14a**) (45% MeCN,  $R_t$ : 32 min).<sup>231</sup>

*Colletotrichone A (10)*: Colorless amorphous powder;  $[\alpha]_D^{20}$  +340.4 (c 0.05, MeOH); LC-UV [(acetonitrile in H<sub>2</sub>O/0.1% FA)]  $\lambda_{max}$  222, 340 nm; IR (film)  $\nu_{max}$  3368, 2917, 2849, 1741, 1653, 1612, 1081, 1060 cm<sup>-1</sup>; CD spectrum (0.1 mg/mL, MeOH), 200 ( $\Delta\epsilon$  -1.85), 213 ( $\Delta\epsilon$  +0.66), 256 ( $\Delta\epsilon$  -8.23), 326 nm ( $\Delta\epsilon$  +10.21); <sup>1</sup>H NMR (CD<sub>3</sub>OD, 500 MHz) and <sup>13</sup>C NMR (CD<sub>3</sub>OD, 125 MHz), see Table 3 and 4. ESI-HRMS  $m/z$ : 349.1280, [M+H]<sup>+</sup> (calcd for C<sub>18</sub>H<sub>21</sub>O<sub>7</sub>, 349.1282,  $\Delta$  -0.5108 ppm), 366.1547, [M+NH<sub>4</sub>]<sup>+</sup> (calcd for C<sub>18</sub>H<sub>24</sub>O<sub>7</sub>N, 366.1547,  $\Delta$  -0.0934 ppm).<sup>231</sup>

X-ray crystallographic analysis of *colletotrichone A (10)*: Diffraction experiment was performed on an Oxford Diffraction Xcalibur S diffractometer with graphite

## Chapter 4: Experimental section

---

monochromated Mo-K $\alpha$  radiation ( $\lambda = 0.71073 \text{ \AA}$ ).<sup>231</sup> The crystal structures were solved with direct methods (SHELXS97) and refined against  $F^2$  with the full-matrix least-squares method (SHELXL97).<sup>231,235</sup> A multi-scan absorption correction using the CrysAlis RED program (Oxford Diffraction, 2006) was employed.<sup>231</sup> The non-hydrogen atoms were placed in geometrically calculated positions and each was assigned a fixed isotropic displacement parameter based on a riding-model.<sup>231</sup>

A colorless crystal was obtained from a solution of EtOAc: MeOH (1:1, v/v), orthorhombic crystal system; space group  $P2_12_12_1$ ;  $a = 15.0896(7) \text{ \AA}$ ,  $b = 15.6838(7) \text{ \AA}$ ,  $c = 7.1843(3) \text{ \AA}$ ,  $\alpha = \beta = \gamma = 90^\circ$ ,  $V = 1700.25(13) \text{ \AA}^3$ ;  $Z = 4$ ,  $d = 1.361 \text{ g/cm}^3$ ; crystal dimensions  $0.12 \times 0.09 \times 0.04 \text{ mm}$ ; the final indices were  $R_1 = 0.0346$ ,  $wR_2 = 0.0796$ .<sup>231</sup> Crystallographic data of colletotrichone A (**1**) was deposited in the Cambridge Crystallographic Data Centre with supplementary publication number CCDC 1013027. Copies of the data can be obtained, free of charge, on application to the Director, 12 Union Road, Cambridge CB2 1EZ, UK (fax: +44(0)1223 336033 or by e-mail: deposit@ccdc.cam.ac.uk).<sup>231</sup>

*Colletotrichone B (11a)*: Yellowish oil;  $[\alpha]_D^{20} +81.0$  ( $c$  1.29,  $\text{CHCl}_3$ ); LC-UV [(acetonitrile in  $\text{H}_2\text{O}/0.1\% \text{ FA}$ )]  $\lambda_{\text{max}}$  222, 366 nm; IR (film)  $\nu_{\text{max}}$  3453, 2968, 2929, 1773, 1623, 1550, 1088  $\text{cm}^{-1}$ ; CD spectrum (0.1 mg/mL, MeOH), 209 nm ( $\Delta\epsilon$  -1.63), 254 ( $\Delta\epsilon$  +1.89), 327 ( $\Delta\epsilon$  +8.19), 361 ( $\Delta\epsilon$  -4.81), 373 nm ( $\Delta\epsilon$  -4.86);  $^1\text{H}$  NMR ( $\text{CDCl}_3$ , 500 MHz) and  $^{13}\text{C}$  NMR ( $\text{CDCl}_3$ , 125 MHz), see Table 3 and 4;  $^1\text{H}$  NMR (acetone- $d_6$ , 500 MHz) and  $^{13}\text{C}$  NMR (acetone- $d_6$ , 125 MHz), see Table 5. ESI-HRMS  $m/z$ : 317.1385,  $[\text{M}+\text{H}]^+$  (calcd for  $\text{C}_{18}\text{H}_{21}\text{O}_5$ , 317.1384,  $\Delta$  0.3609 ppm).<sup>231</sup>

*Colletotrichone C (12)*: Colorless amorphous powder;  $[\alpha]_D^{20} +124.2$  ( $c$  0.07,  $\text{CHCl}_3$ ); LC-UV [(acetonitrile in  $\text{H}_2\text{O}/0.1\% \text{ FA}$ )]  $\lambda_{\text{max}}$  214, 332 nm; IR (film)  $\nu_{\text{max}}$  2971, 2933, 1779, 1711, 1612, 1219, 1105, 1029  $\text{cm}^{-1}$ ; CD spectrum (0.1 mg/mL, MeOH), 202 ( $\Delta\epsilon$  +2.45), 224 ( $\Delta\epsilon$  -0.26), 250 ( $\Delta\epsilon$  +2.28), 286 ( $\Delta\epsilon$  -0.67), 344 nm ( $\Delta\epsilon$  +3.64);  $^1\text{H}$  NMR ( $\text{CDCl}_3$ , 500 MHz) and  $^{13}\text{C}$  NMR ( $\text{CDCl}_3$ , 125 MHz), see Table 3 and 4. ESI-HRMS  $m/z$ : 319.1542,  $[\text{M}+\text{H}]^+$  (calcd for  $\text{C}_{18}\text{H}_{23}\text{O}_5$ , 319.1540,  $\Delta$  0.7083 ppm), 341.1361,  $[\text{M}+\text{Na}]^+$  (calcd for  $\text{C}_{18}\text{H}_{22}\text{O}_5\text{Na}$ , 341.1359,  $\Delta$  -0.5143 ppm), 659.2836,  $[\text{2M}+\text{Na}]^+$  (calcd for  $\text{C}_{36}\text{H}_{44}\text{O}_{10}\text{Na}$ , 659.2827,  $\Delta$  1.4080 ppm).<sup>231</sup>

## Chapter 4: Experimental section

---

*Colletotrichone D (13)*: Colorless amorphous powder;  $[\alpha]_D^{20} +139.58$  (c 0.14, CHCl<sub>3</sub>); LC-UV [(acetonitrile in H<sub>2</sub>O/0.1% FA)]  $\lambda_{\max}$  226, 344 nm; IR (film)  $\nu_{\max}$  3394, 2966, 2934, 1718, 1646, 1268, 1241, 1113 cm<sup>-1</sup>; CD spectrum (0.1 mg/mL, MeOH), 200 ( $\Delta\epsilon$  +2.59), 237 ( $\Delta\epsilon$  -1.89), 326 ( $\Delta\epsilon$  +4.67); <sup>1</sup>H NMR (CDCl<sub>3</sub>, 500 MHz) and <sup>13</sup>C NMR (CDCl<sub>3</sub>, 125 MHz), see Table 7. ESI-HRMS  $m/z$ : 363.1439, [M+H]<sup>+</sup> (calcd for C<sub>19</sub>H<sub>23</sub>O<sub>7</sub>, 363.1438,  $\Delta$  0.2490 ppm), 380.1699, [M+NH<sub>4</sub>]<sup>+</sup> (calcd for C<sub>19</sub>H<sub>26</sub>O<sub>7</sub>N, 380.1704,  $\Delta$  -1.2060 ppm).<sup>231</sup>

7.2 Lactam-fused 4-pyrones from endosymbiotic community of *P. capitalensis* BS5 and *Herbaspirillum* sp.

The large-scale fermentation was performed in 10 L static PDB medium at 25 °C. After 60 days, the broth and mycelium was extracted with 10 L EtOAc at room temperature 3 times.<sup>130</sup> The EtOAc solution was evaporated under vacuum to yield 930 mg dark brown residue.<sup>130</sup> The residue was dissolved in 70% MeOH and washed by n-hexane.<sup>130</sup> The 70% MeOH layer was concentrated and subjected to C<sub>18</sub> SPE column then eluted by water, 60% MeOH, and 100% MeOH successively.<sup>130</sup> The 60% MeOH eluates were collected and evaporated to yield 229 mg residues (Fr. B).<sup>130</sup> From Fr. B, 10 mg phyllostictalactam A (**15**) was purified on HPLC system with mobile phase 55% MeOH and 3 mL/min flow rate ( $R_t$ : 25.0 min).<sup>130</sup>

*Phyllostictalactam A (15)*: Colorless amorphous powder;  $[\alpha]_D^{20} \approx 0$  (c 0.117, MeOH); LC-UV [(acetonitrile in H<sub>2</sub>O/0.1% FA)]  $\lambda_{\max}$  218, 314 nm; IR (film)  $\nu_{\max}$  3284, 2925, 2839, 1709, 1646, 1565, 1081, 675 cm<sup>-1</sup>; CD spectrum (0.1 mg/mL, MeOH), no Cotton effect observed; <sup>1</sup>H NMR (acetone-*d*<sub>6</sub>, 500 MHz) and <sup>13</sup>C NMR (acetone-*d*<sub>6</sub>, 125 MHz), see Table 10. ESI-HRMS  $m/z$ : 266.1024, [M+H]<sup>+</sup> (calcd for C<sub>13</sub>H<sub>16</sub>O<sub>5</sub>N, 266.1023,  $\Delta$  0.4431 ppm), 283.1290, [M+NH<sub>4</sub>]<sup>+</sup> (calcd for C<sub>13</sub>H<sub>19</sub>O<sub>5</sub>N<sub>2</sub>, 283.1288,  $\Delta$  0.6363 ppm).<sup>130</sup>

## 8. Bioactivity assays for isolated pure compounds

### 8.1 Disc diffusion antibacterial assay

This part of work was performed based on the established methods reported in the literature.<sup>78</sup> The agar plates were prepared with 90 mm diameter Petri-dishes and approximately 22 mL melted NA solution.<sup>78</sup> The assay strains of bacteria were

## Chapter 4: Experimental section

---

inoculated in NB medium for 24 h at 37 °C with shaking speed 150 rpm.<sup>78</sup> Then 200 µL bacterial suspensions were spread on each agar plates evenly.<sup>78</sup> Parallely, 40 µL MeOH solution of each candidate compound was dropped on paper dishes and then dried in the clean bench under the laminar airflow hood, to avoid airborne contamination.<sup>78</sup> The paper dishes were placed on the inoculated agar plates with sufficient distance, and on each agar plates, there were three duplicates of each concentration of compounds.<sup>78</sup> Then the agar plates were stored at 4 °C for 2 h to enable the compounds to diffuse on the agar surface before the bacteria started to grow.<sup>78</sup> Afterward, the agar plates were incubated at 37 °C for 24 h.<sup>78</sup> The blank control was pure MeOH and the positive control was streptomycin and gentamicin.<sup>78</sup> The inhibitory activity of candidate compounds was determined by observable inhibitory zone surrounding paper dishes.<sup>78</sup>

### 8.2 Cytotoxic assay

A 50 mM stock solution was prepared for each compound (**10**, **11a**, **12** and **14a**) in DMSO and filter-sterilized through 0.2 µm filter under vacuum.<sup>51</sup> From the stock solution, working concentrations were prepared with a dilution factor (DF) of 3 to reach a maximum concentration of 100 µM.<sup>51</sup> The *in vitro* cytotoxicity of each compound against the human cancer cell line THP-1 was determined (48 h exposure) using 96-well flat bottom tissue culture plates (black) using two established methods<sup>51</sup> in parallel using a VICTOR multilabel plate reader (PerkinElmer Life And Analytical Sciences, Inc., Boston, MA).<sup>51</sup> The first method consisted of quantification using resazurin (Sigma-Aldrich Chemie GmbH), to measure the mitochondrial activity.<sup>51</sup> The second method consisted of quantification using ATPlite (PerkinElmer Life and Analytical Sciences, Inc.), to measure the available ATP concentration.<sup>51</sup> The final relative viabilities were calculated and represented in percent fractional survival (FS).<sup>51</sup>

Culturing of the THP-1 Cell Line. The human acute monocytic leukemia cell line (THP-1), with DSMZ number ACC 16, was used.<sup>51</sup> The THP-1 cells were grown in tissue culture flasks in complete growth medium in an atmosphere of 5% CO<sub>2</sub> and 90% relative humidity in a carbon dioxide incubator.<sup>51</sup> The complete growth medium was prepared by using RPMI-1640 supplemented with 2 mM L-glutamine, 10% FBS, and penicillin (100



## Chapter 4: Experimental section

---

IU mL<sup>-1</sup>, just before use) in double-distilled water.<sup>51</sup> The pH of the medium was adjusted to 7.2, and the medium was sterilized by filtering through 0.2 µm filters in a laminar air flow hood under aseptic conditions.<sup>51</sup>

Subculturing of the THP-1 Cell Line. For subculturing, the medium of the flask having subconfluent growth was changed 1 day in advance. The entire medium from the flask was taken out and discarded. Cells were washed with PBS.<sup>51</sup> Thereafter, 0.5 mL of Trypsin-EDTA in PBS (pre-warmed at 37 °C) was added to make a thin layer on the monolayer of the THP-1 cells.<sup>51</sup> The flask was incubated for approximately 5 min at 37 °C and observed under a microscope.<sup>51</sup> If the cells were found to be detached, complete growth medium (1 mL, pre-warmed at 37 °C) was added to make the cell suspension. An aliquot was taken out and cells were counted and checked for viability with Trypan blue.<sup>51</sup> Cell stock of more than 98% cell viability was accepted for determination of the *in vitro* cytotoxicity.<sup>51</sup> The cell density was adjusted to  $7.5 \times 10^4$  cells mL<sup>-1</sup> by addition of a complete growth medium.<sup>51</sup>

## 9. Quantum chemical computation

For the azaphilones (**10–12**, **14**) isolated from Fungus *Colletotrichum* sp. BS4:

The conformer candidates were searched with the MMFF force field routine of Spartan'14 (Wavefunction, Inc.: Irvine, CA, 2014).<sup>236</sup> The geometries of all obtained conformers within 25 kJ/mol above the global minimum were optimized on wB97X-D/6-31+G(d) level of theory. The resulted geometries were directly used for NMR spectra calculation with EDF2/6-31G\*; the final Boltzmann factors were obtained with wB97X-D/6-311+G(2df,2p), using Gaussian g09.<sup>231,237</sup> The NMR shifts of all remaining conformers were averaged with respect to their final Boltzmann factors. ECD calculation was performed on wB97X-D/6-311G(d,p) based on the optimized geometries and the Boltzmann factors. The ORD spectrum was calculated on wB97X-D/6-311G(d,p) level of theory.

For Colletotrichone D (**13**) isolated from Fungus *Colletotrichum* sp. BS4

Frog2 online version was used for conformational searches with 50 kcal/mol energy window, 1000 maximum steps and 100 kcal/mol maximum energy.<sup>238</sup> The optimization

## Chapter 4: Experimental section

---

and frequency calculations of all obtained conformers were performed with GAMESS 2014 R1<sup>239</sup> on B3PW91-D3/6-31G(d)<sup>240,241</sup> level of theory with C-PCM solvent model. <sup>13</sup>C NMR GIAO shielding constants calculation on mPW1PW91/6-31+G(d) level of theory and ECD calculation on mPW1PW91/pcSeg-1<sup>242</sup> level of theory were performed on Dalton 2015,<sup>243</sup> with IEF-PCM solvent model.<sup>244</sup> ECD curves were simulated by Gaussian function according to formula 8d in literature.<sup>245</sup>

For the lactam-fused 4-pyrones from Fungus *Phyllosticta capitalensis* BS5 and endosymbiotic bacterium *Herbaspirillum* sp. BS5B:

Frog2 online version was used for conformational searches with 100 kcal/mol energy window, 1000 maximum steps and 100 kcal/mol maximum energy.<sup>130,238</sup> The optimization and frequency calculations of all obtained conformers were performed with GAMESS 2014 R1<sup>239</sup> on B3PW91-D3/6-311G(d,p)<sup>240,241</sup> level of theory with C-PCM solvent model.<sup>130</sup> <sup>13</sup>C NMR GIAO shielding constants calculation was performed on Dalton 2015 on mPW1PW91/6-31+G(d) level of theory,<sup>243</sup> with IEF-PCM solvent model.<sup>130,244</sup>

## 10. MALDI IMS

### 10.1 Sample preparation

All samples were growing colony cut from agar medium. 18 × 18 × 1 mm glass plates were used as sample holder for the measurement.<sup>69</sup> After the detection areas were placed on the glass plates, the agar layers were dried by oil pump at room temperature slowly.<sup>69</sup> The matrix solution used was HCCA (7 mg/mL) in acetonitrile : water 1 : 1 (v/v) with additional 0.2% organic acid (TFA for the experiment of *F. solani* and *A. xylooxidans*, and FA for the experiment of *Colletotrichum* sp. BS4).<sup>69</sup> The matrix solution was sprayed with the following parameters: 50 rpm sample plate revolution speed, 4.5 L/min gas (N<sub>2</sub>) flow rate, 10 μL/min matrix flow rate, and 3 × 10 min spray cycle and duration.<sup>69</sup> The sample glass plates were recorded by microscope before and after spray application, and the regions for measurement were marked for locating the measured areas.<sup>246</sup>

### 9.2 Measurement parameters

Scan resolution was adjusted to 60  $\mu\text{m}$ , the scan was taken from a rectangular region via full scan in the positive ion mode with internal lock mass correction (mass:  $m/z$  379.09246  $[\text{2M}+\text{H}]^+$ , HCCA).<sup>69</sup> Mass range was  $m/z$  300–800 for the experiment of hexacyclopeptides, and was  $m/z$  100–800 for the experiment of azaphilones. The resolution of mass spectra was adjusted to be 140,000 @  $m/z$  200.<sup>69</sup> And the S-lens level was set to be 65 with a spray voltage of 2.0 kV and injection time of 200 ms. Laser beam attenuator value was 20°.<sup>69</sup> The software package for data processing and generation of ion density images was ImageQuest v. 1.1.0 (Thermo Fisher Scientific).<sup>69,246</sup>

## 11. Synthesis

### 11.1 Synthesis of precursor $\alpha$ -deuterated amino acids

This part of the experiment was applied for amino acid leucine, isoleucine, valine, alanine, and proline, with more than 90% deuterium purity for  $\alpha$ -position (checked by  $^1\text{H}$  NMR and MS). 0.1 mM amino acid, 3  $\mu\text{L}$  anisaldehyde were dissolved in 1 mL AcOD. Then the solution was stirred and heated in 95  $^\circ\text{C}$  oil bath for 3 h before concentrated under vacuum.<sup>247</sup> Then the residue was dissolved in water and washed by EtOAc. The water layer was evaporated under vacuum to yield  $\alpha$ -deuterated amino acids.

### 11.2 Synthesis of 2,4,4,4-tetradeuterium-threonine

Anhydrous  $\text{CuCl}_2$  was prepared by dehydration of 34 mg  $\text{CuCl}_2 \cdot 2\text{H}_2\text{O}$  in 110  $^\circ\text{C}$  oven for 1 h, and then sealed and cooled down to r. t. and then dissolved in 1 mL  $\text{D}_2\text{O}$ .<sup>69</sup> Thereby, 20 mg glycine and 100  $\mu\text{L}$  triethylamine were added into this solution, which was stirred at 50  $^\circ\text{C}$  for 2 h.<sup>69</sup> After the solution was cooled down at 0  $^\circ\text{C}$ , 112  $\mu\text{L}$  acetaldehyde was added and it was stirred for 3 h more and then temperature was increased to r. t. for another 14 h.<sup>69</sup> Afterwards, the solution was concentrated under vacuum and then subjected on 0.5 cm  $\times$  2 cm Dowex<sup>TM</sup> 50WX8-100 CC ion-exchange resin column, and washed by deionized water and 2.5%  $\text{NH}_3 \cdot \text{H}_2\text{O}$  solution 15 mL successively.<sup>69</sup> The eluate of  $\text{NH}_3 \cdot \text{H}_2\text{O}$  solution was collected and concentrated under vacuum and then washed by EtOH to yield 11 mg 2,4,4,4-tetradeuterium-threonine (35% yield).<sup>69</sup>

## Chapter 4: Experimental section

---

### 11.3 Synthesis of 4-OH-4-deuterium-proline

A 0.3 mM N-Boc-4-oxo-L-proline methyl ester was dissolved in 3 mL MeOH, and the solution was cooled down at 0 °C. After 0.6 mM NaBD<sub>4</sub> was added, the solution was stirred for 3 h and then stirred for 24 h at r. t. Afterwards, the solution was evaporated under vacuum, and the residue was dissolved in saturated NH<sub>4</sub>Cl and extracted by AcOEt. The AcOEt layer was separated and washed by brine and dried by anhydrous MgSO<sub>4</sub>. Then AcOEt was removed under vacuum to yield 60 mg N-Boc-4-OH-4-deuterium-L-proline methyl ester (81% yield).<sup>248</sup> 0.24 mM N-Boc-4-OH-4-deuterium-L-proline methyl ester was dissolved in 2 mL 6 M HCl solution, and stirred for 2 h at r. t. Then the solution was evaporated under vacuum and re-dissolved in 1 mL de-ionized water. The water solution was subjected on 0.5 cm × 2 cm Dowex<sup>TM</sup> 50WX8-100 CC ion-exchange resin column, and washed by water and 2.5% NH<sub>4</sub>OH solution successively. The 2.5% NH<sub>4</sub>OH solution eluate was collected and concentrated under vacuum to yield 25 mg 4-OH-4-deuterium-proline (80% yield).<sup>248</sup>

### 11.4 Semi-synthesis of compound **16** from compound **15**

5 mg compound **15** was dissolved in 600 µL CF<sub>3</sub>COOH / AcOEt (1 : 4, v/v) and stirred for 24 h at r. t.<sup>130</sup> And then the brown reacted solution was evaporated under vacuum in 40 °C water bath, yielding approximately 5 mg brown gum (90% yield, checked by LC-MS), then it was measured by <sup>1</sup>H NMR and LC-MS<sup>n</sup>, and the product had identical retention time, UV spectrum and MS<sup>2</sup> spectrum with compound **16** in crude extraction of fungus *Phyllosticta capitalensis* BS5 and endosymbiotic bacterium *Herbaspirillum* sp. BS5B in stationary PDB medium.<sup>130</sup> LC-UV [(acetonitrile in H<sub>2</sub>O/0.1% FA)] λ<sub>max</sub> 218, 260, 300, 338 nm; <sup>1</sup>H NMR (acetone-*d*<sub>6</sub>, 500 MHz): 6.77 (1H, dd, *J* = 16.1, 7.5, H-9), 6.66 (1H, d, *J* = 16.1, H-10), 5.55 (1H, br s, H<sub>a</sub>-8), 5.27 (1H, br s, H<sub>b</sub>-8), 2.34 (2H, dt, *J* = 7.4, 7.4, CH<sub>2</sub>-11), 1.57 (2H, tq, *J* = 7.4, 7.4, CH<sub>2</sub>-12), 0.99 (3H, t, *J* = 7.4, CH<sub>3</sub>-13). ESI-HRMS *m/z*: 248.0917, [M+H]<sup>+</sup> (calcd for C<sub>13</sub>H<sub>14</sub>O<sub>4</sub>N, 248.0917, Δ -0.3319 ppm), 265.1182, [M+NH<sub>4</sub>]<sup>+</sup> (calcd for C<sub>13</sub>H<sub>17</sub>O<sub>4</sub>N<sub>2</sub>, 265.1183, Δ -0.3354 ppm).<sup>130</sup>

### **12. Detection of fungal and bacterial polyketide synthase (PKS)**

The total genomic DNA (gDNA) was subjected to PCR amplification of genes encoding the ketoacyl synthase (KS) domain essential for fungal and bacterial polyketide synthesis using previously established primers.<sup>249–251</sup> The PCR reaction was performed in 50 µL reaction mixture containing 45 µL Red Taq DNA Polymerase Master Mix (1.1x), 0.5 µL forward primer (100 µM), 0.5 µL reverse primer (100 µM), 3 µL template DNA and 1 µL of sterile double-distilled water.<sup>130</sup> The PCR cycling protocol consisted of an initial denaturation at 95 °C for 2 min, 30 cycles of denaturation at 95 °C for 30 s, annealing at 44 °C (for fungal PKS) and 59 °C (bacterial PKS) for 40 s and elongation at 72 °C for 30 s.<sup>130</sup> This was followed by a final elongation step at 72 °C for 5 min.<sup>130</sup> As a negative control, the template DNA was replaced by sterile double distilled water.<sup>130</sup> As a positive control, the genomic DNA of *Bacillus subtilis* (DSM 1088) and *Aspergillus versicolor* (Isolate A12; EMBL accession number HE962600)<sup>252</sup> was used.<sup>130</sup> The PCR amplified product spanning approximately 700 bp for both fungal and bacterial PKS were checked by gel electrophoresis and purified using GFX™ PCR DNA and Gel Band Purification kit (GE Healthcare Life Sciences, Germany) following manufacturer's instructions.<sup>130</sup> The amplified products of positive sequences were then sequenced from both directions at SeqLab Sequence Laboratories (Göttingen, Germany).<sup>130</sup>

### **13. Detection of fungal and bacterial nonribosomal peptide synthetase (NRPS)**

The total genomic DNA (gDNA) was subjected to PCR amplification of genes encoding the adenylation domain (A domain) domain essential for fungal and bacterial nonribosomal peptide synthesis using previously established primers.<sup>251,253,254</sup> The PCR reaction was performed in 50 µL reaction mixture containing 45 µL Red Taq DNA Polymerase Master Mix (1.1x), 0.5 µL forward primer (100 µM), 0.5 µL reverse primer (100 µM), 3 µL template DNA and 1 µL of sterile double-distilled water.<sup>130</sup> The PCR cycling protocol consisted of an initial denaturation at 95 °C for 2 min, 30 cycles of denaturation at 95 °C for 30 s, annealing at 44 °C (for fungal NRPS) and 46 °C (bacterial

## Chapter 4: Experimental section

---

NRPS) for 40 s and elongation at 72 °C for 30 s.<sup>130</sup> This was followed by a final elongation step at 72 °C for 5 min.<sup>130</sup> As a negative control, the template DNA was replaced by sterile double distilled water.<sup>130</sup> As a positive control, the genomic DNA of *Bacillus subtilis* (DSM 1088) and *Aspergillus versicolor* (Isolate A12; EMBL accession number HE962600) was used.<sup>252</sup> The PCR amplified product spanning approximately 300 bp for fungal and 1000 bp for bacterial NRPS were checked by gel electrophoresis and purified using GFX<sup>TM</sup> PCR DNA and Gel Band Purification kit (GE Healthcare Life Sciences, Germany) following manufacturer's instructions.<sup>130</sup> The amplified products of positive sequences were then sequenced from both directions at SeqLab Sequence Laboratories (Göttingen, Germany).<sup>130</sup>

# Chapter 5

# **RESULTS & DISCUSSION**

# 1. Chemical crosstalk between endophytic fungi *F. solani* N06 and endophytic bacteria via new hexacyclopeptides

## 1.1 Metabolites screening of *F. solani* N06

Based on the “OSMAC” (One Strain Many Compounds) strategy,<sup>255</sup> the endophytic strain *F. solani* N06 was cultured in different conditions, which were combined by several viable parameters, such as different media with diverse carbon/nitrogen sources including liquid media (PDB, SDB) and solid rice medium, different shaking condition like stationary state or rotating state with speed 150 rpm, and different temperature (25 °C or 29 °C). This screening step was also the routine approach for other strains mentioned herein. In the stationary PDB broth and PDA agar medium, a series of hexacyclopeptides were detected by LC-MS measurements (Table 2, Figure 9).<sup>69</sup> These hexacyclopeptides could also be produced in stationary SDB medium with smaller amount.

**Table 2.** Retention time and adducts ion intensity of compounds 1–9 ( $\Delta < 2$  ppm)

Compound	r. t. (min)	<i>m/z</i> of adducts (Maximum intensity)					
		[M+H-2H <sub>2</sub> O] <sup>+</sup>	[M+H-H <sub>2</sub> O] <sup>+</sup>	[M+H] <sup>+</sup>	[M+NH <sub>4</sub> ] <sup>+</sup>	[M+Na] <sup>+</sup>	[M+K] <sup>+</sup>
<b>1</b>	4.46	589.3708	607.3814	625.3919	n. d.	647.3739	663.3478
C <sub>30</sub> H <sub>52</sub> O <sub>8</sub> N <sub>6</sub>		(6.69E4)	(2.50E6)	(6.15E5)		(1.37E6)	(2.53E5)
<b>2</b>	8.20	589.3708	607.3814	625.3919	n. d.	647.3739	663.3478
C <sub>30</sub> H <sub>52</sub> O <sub>8</sub> N <sub>6</sub>		(3.89E5)	(1.80E5)	(5.28E3)		(3.89E5)	(3.31E4)
<b>3</b>	9.89	589.3708	607.3814	625.3919	n. d.	647.3739	663.3478
C <sub>30</sub> H <sub>52</sub> O <sub>8</sub> N <sub>6</sub>		(4.14E6)	(2.03E6)	(9.71E3)		(2.52E4)	(2.54E3)
<b>4</b>	11.24	589.3708	607.3814	625.3919	n. d.	647.3739	n. d.
C <sub>30</sub> H <sub>52</sub> O <sub>8</sub> N <sub>6</sub>		(1.98E6)	(1.16E6)	(2.50E3)		(1.27E4)	
<b>5</b>	13.42	n. d.	589.3708	607.3814	624.4079	629.3633	645.3372
C <sub>30</sub> H <sub>50</sub> O <sub>7</sub> N <sub>6</sub>			(1.16E5)	(3.22E6)	(3.42E5)	(1.06E6)	(1.42E5)
<b>6</b>	10.43	617.4021	635.4127	653.4232	670.4498	675.4052	691.3791
C <sub>32</sub> H <sub>56</sub> O <sub>8</sub> N <sub>6</sub>		(2.14E4)	(9.25E5)	(3.47E5)	(6.85E3)	(5.88E5)	(7.61E4)
<b>7</b>	18.49	617.4021	635.4127	653.4232	n. d.	675.4052	n. d.
C <sub>32</sub> H <sub>56</sub> O <sub>8</sub> N <sub>6</sub>		(4.04E6)	(1.68E6)	(4.98E3)		(7.61E3)	
<b>8</b>	19.01	617.4021	635.4127	653.4232	n. d.	675.4052	n. d.
C <sub>32</sub> H <sub>56</sub> O <sub>8</sub> N <sub>6</sub>		(1.73E6)	(8.98E5)	(3.27E3)		(4.66E3)	
<b>9</b>	22.07	n. d.	617.4021	635.4127	652.4392	657.3946	673.3686
C <sub>32</sub> H <sub>54</sub> O <sub>7</sub> N <sub>6</sub>			(1.02E5)	(1.87E6)	(1.74E5)	(5.65E5)	(7.72E4)

<sup>a</sup> n. d., not detected



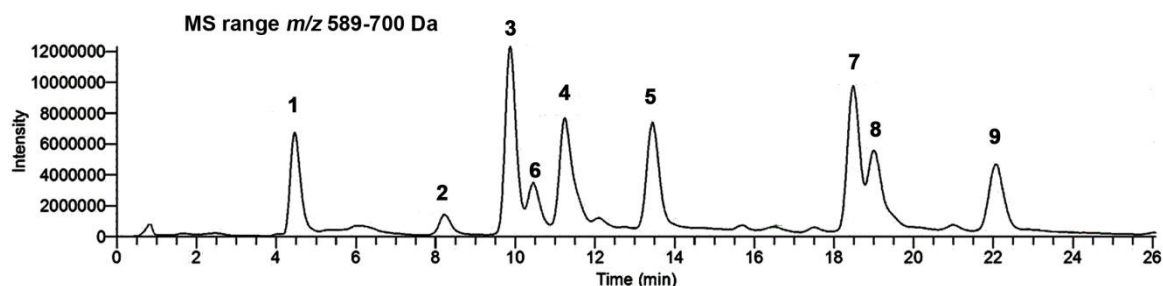


**Figure 9.** LC-MS positive full scan chromatogram of hexacyclopeptides (1–9) from *F. solani* in static PDB medium<sup>69</sup>

### 1.2 Strategy to investigate the new hexacyclopeptides

Significant degeneration of the production of these hexacyclopeptides was observed during sub-culture or even growth process of this strain, which caused that the large scale fermentation for these compounds was not possible.<sup>69</sup> This biosynthetic attenuation could not be restored either by co-culturing it with other endophytes (including the endophytic bacterium *A. xylooxidans* N12B isolated from the same bulb tissue), or by addition of plant extracts or amino acid precursors into the culture media, or by other modifications of fermentation conditions.<sup>69</sup> Thus far, accumulation of more compounds could not be achieved *in vitro* just by tweaking the culture conditions or increasing the volume of media, thereby preventing us from purifying them by chromatography and identifying them by established structure elucidation techniques such as 1D and 2D NMR.<sup>69</sup> For the currently available techniques for natural products discovery, the lower limit is around 10  $\mu\text{g}$ ,<sup>256,257</sup> which is, in fact, a barrier keeping us from elucidating trace compounds produced by endophytes.<sup>69</sup>

In this case, therefore, a “location dictates function” strategy was adopted to utilize MALDI-imaging-HRMS and LC-HRMS<sup>n</sup> to elucidate our target functional molecules and investigate their structural information.<sup>69</sup> On MALDI plates (18 × 18 × 1 mm), endophytes can grow into visible colonies suitable for detection in 1 or 2 days, which enables us to study the production and temporal release of our target compounds produced by endophytes from the time after their isolation up to 48 h (before some plausible biological changes occurred in laboratory conditions).<sup>69</sup> The spatial and temporal distribution of potential biofunctional compounds provided by MALDI-imaging-HRMS helped us to efficiently target specific compounds.<sup>69</sup> And the structure elucidation

## Chapter 5: Results & discussion

of hexacyclopeptides can be achieved by LC-MS<sup>n</sup> technique, which requires only small quantity of compounds.<sup>69</sup>

### 1.3 Visualization of hexacyclopeptides in the dual culture of *F. solani* N06 and *A. xylooxidans* N12B by MALDI IMS

We used the MALDI-imaging-HRMS to investigate the small molecular metabolites produced by endophytic *F. solani* N06 and their spatial as well as temporal distribution up to 48 h, and attempted to reveal the chemical crosstalk between this fungus and other endophytic microorganisms harbored the same bulb tissue.<sup>69</sup> MALDI imaging with lateral resolution of 60  $\mu\text{m}$  enabled us to assemble the chemical information in subtle parts of the endophytic microorganism's colony over a period of 2 days.<sup>69</sup>

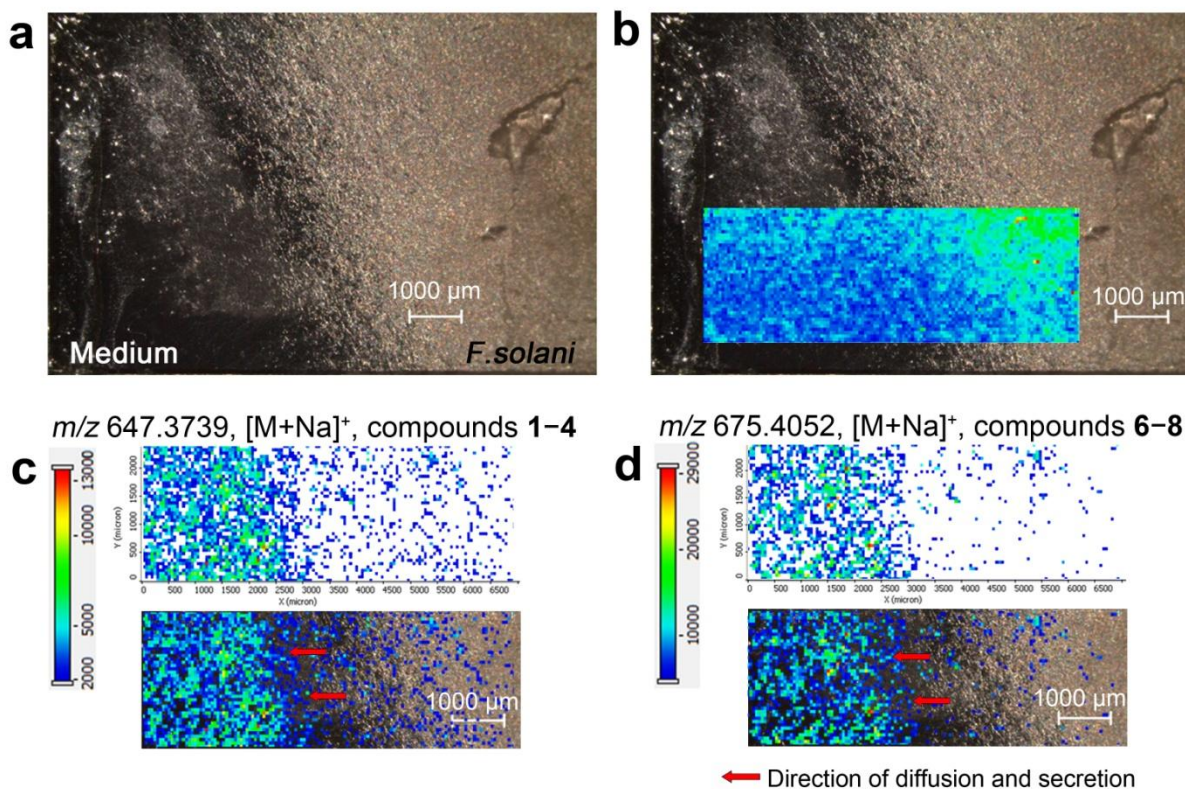


**Figure 10.** Distribution visualization of hexacyclopeptides (1-9) by MALDI IMS after 48 h. **a** Optical image of *F. solani* N06. **b** TIC ( $m/z$  300-800) of detected area. **c** Ion intensity map of  $\text{C}_{30}\text{H}_{52}\text{O}_8\text{N}_6\text{Na}$ . **d** Ion intensity map of  $\text{C}_{32}\text{H}_{56}\text{O}_8\text{N}_6\text{Na}$ <sup>69</sup>

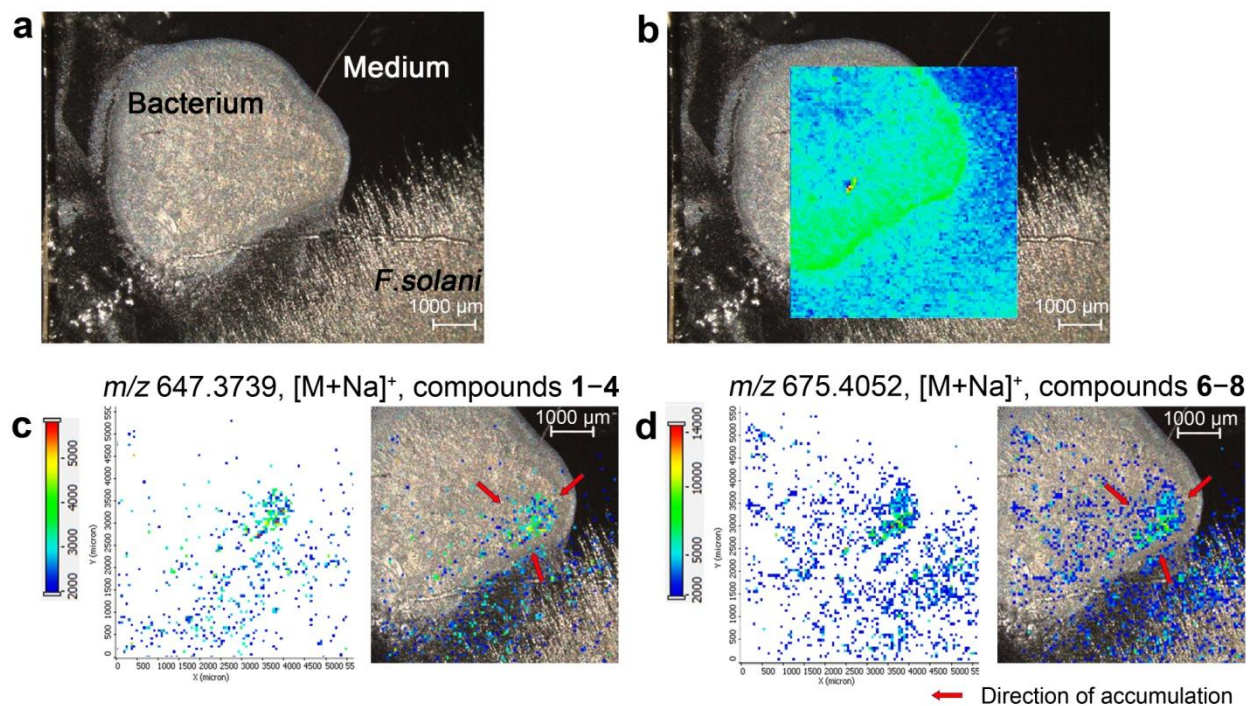


**Figure 11.** Distribution visualization of hexacyclopeptides detected in MALDI-imaging-HRMS scan of the endophytic fungus *F. solani* and another endophytic bacterium *A. xylosoxidans* isolated from the same plant tissue after 48 h. **a** Optical image of the boundary area between *F. solani* and bacterium *A. xylosoxidans*. **b** TIC ( $m/z$  300–800) of detected area. **c** Ion intensity map of  $C_{30}H_{52}O_8N_6Na$ . **d** Ion intensity map of  $C_{32}H_{56}O_8N_6Na$ <sup>69</sup>

We measured the strain *F. solani* N06 alone (Figure 10) and *F. solani* co-cultured with the endophytic bacterium *A. xylosoxidans* N12B from the same tissue on PDA (Figure 10).<sup>69</sup> In our preliminary study, a group of interesting compounds was observed to be gradually secreted from the fungal colony to surrounding media. Moreover, they were accumulated by a specific part of the bacterial colony closest to fungal mycelia, while the intensity of the nearby region was much lower than the region without bacterium (see Figure 10 and 11 for measurements done after 48 h).<sup>69</sup> It was particularly interesting to note that the endophytic bacterium could selectively accumulate the hexacyclopeptides produced and secreted by the endophytic fungus into the agar (Figure 10c,d).<sup>69</sup> At regions where the bacterium was absent, the hexacyclopeptides secreted by the endophytic fungus diffused uniformly into the agar (Figure 10c,d).<sup>69</sup> However, the bacterium can expediently accumulate the hexacyclopeptides from its vicinity (see the

## Chapter 5: Results & discussion

---

agar without hexacyclopeptides diffused into it nearby the bacterial colony in Figure 11c,d).<sup>69</sup> Furthermore, the intensity of bacterium-accumulated hexacyclopeptides was lower than what was observed in the agar without bacterium (free diffusion), corroborating the notion of signal elimination that occurs during 'neighbor communication' between cells.<sup>69,258</sup>

To exclude the interference from any experimental material, I checked the mass of targeted molecules in unseeded agar plates sprayed with matrix solution. For mass  $m/z$  675.4052, there were few interfering signals in blank matrix or blank agar.<sup>69</sup> However, mass  $m/z$  647.3739 was also found in blank agar with relatively lower intensity (Chapter 8, Figure S12).<sup>69</sup> Therefore, I increased the lower limit of the intensity scale during data processing of the ion density images in order to reduce the background signal.<sup>69</sup> The EtOAc extracts of blank agar medium and the agar medium with the fungus *F. solani* were measured with LC-HRMS/MS, and I excluded the existence of these hexacyclopeptides in blank agar and proved that the target compounds were identical with those detected in static PDB medium.<sup>69</sup> It was notable that the hexacyclopeptides were released by the cultured endophytic fungus into the agar in line with what was observed (visualized) in our MALDI-imaging-HRMS experiments (see Figure 10 and 11).<sup>69</sup>

### 1.4 Structure elucidation of hexacyclopeptides (1–9) by LC-MS<sup>n</sup>

In MALDI-imaging-HRMS, the ions of one pixel were collected from a small area on the surface of the sample,<sup>228,259</sup> which led to having their intensity very low.<sup>69</sup> Therefore, I decided to investigate enriched samples from higher amount of biomass to discover smaller amount of isomers or other derivatives by LC-HRMS<sup>n</sup>.<sup>69</sup> Moreover, the interference of compounds with the same molecular weight from blank medium could also be avoided by LC separation.<sup>69</sup>

After screening several media compositions, along with fermentation parameters such as temperature and shaking conditions, I found that static fermentation in PDB medium was optimal for culturing *F. solani* N06 for maximum production of our target compounds.<sup>69</sup> With the same PDB medium, notably, our target compounds could not be produced at all (< LOD) under shaking condition (150 rpm).<sup>69</sup> Using an optimized



## Chapter 5: Results & discussion

chromatographic condition on LC-HRMS with C<sub>18</sub> column, hexacyclopeptides could be well-separated into nine peaks (compounds **1–9**) (Figure 9).<sup>69</sup> I detected four compounds with formula C<sub>30</sub>H<sub>52</sub>O<sub>8</sub>N<sub>6</sub> (**1–4**) and a dehydrated product with formula C<sub>30</sub>H<sub>50</sub>O<sub>7</sub>N<sub>6</sub> (**5**), as well as three compounds with formula C<sub>32</sub>H<sub>56</sub>O<sub>8</sub>N<sub>6</sub> (**6–8**) and a relevant dehydrated product C<sub>32</sub>H<sub>54</sub>O<sub>7</sub>N<sub>6</sub> (**9**) (Table 2).<sup>69</sup> Both for compounds **1–4** and **6–8**, [M+H-H<sub>2</sub>O]<sup>+</sup> and [M+H-2H<sub>2</sub>O]<sup>+</sup> were observed by full scan MS, while compounds **5** and **9** showed only [M+H-H<sub>2</sub>O]<sup>+</sup>, which indicated two hydroxyl-group-containing amino acid residues in compounds **1–4** and **6–8**, and one in compounds **5** and **9**.<sup>69</sup>

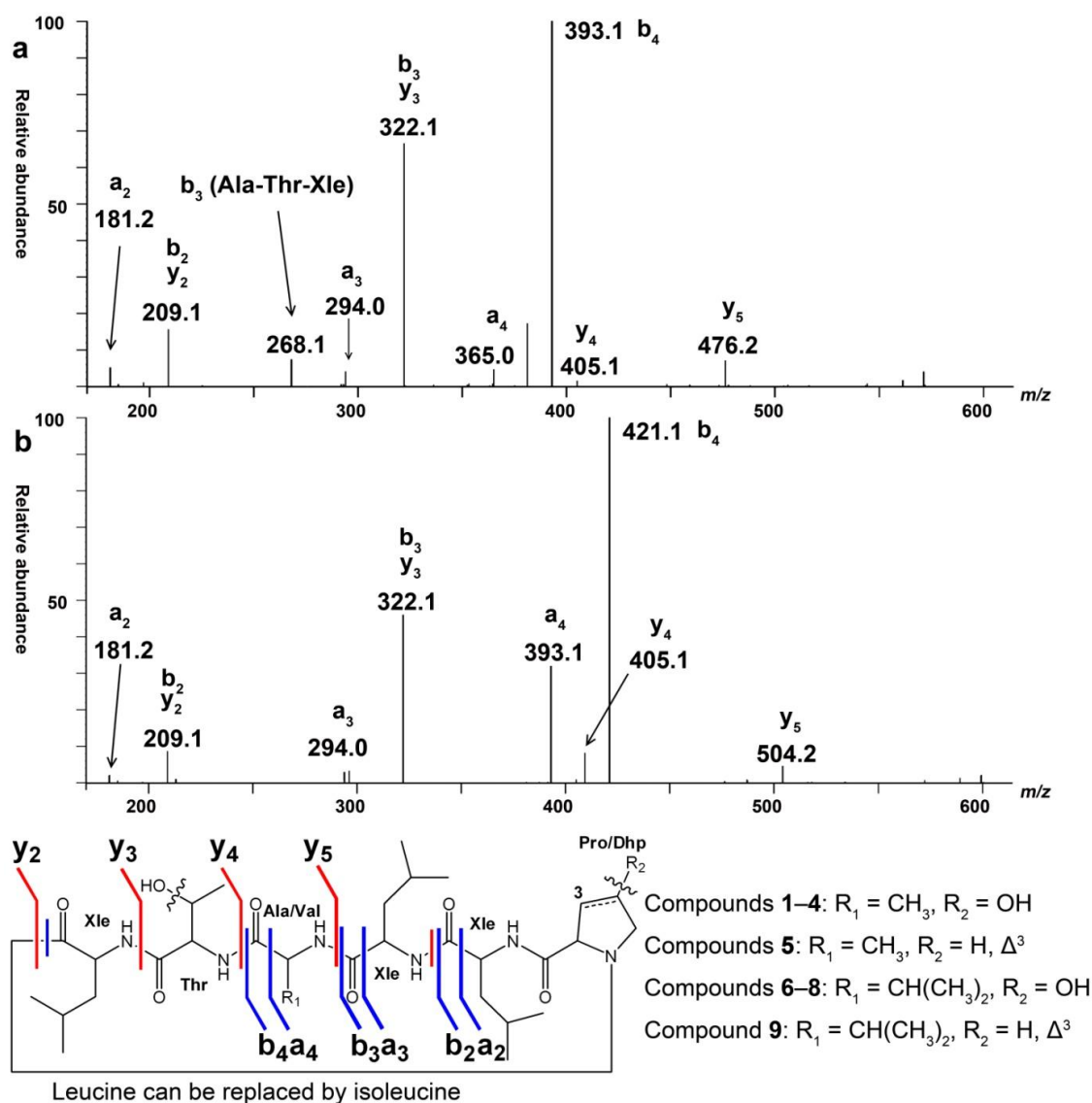


**Figure 12.** MS<sup>2</sup> fragments of compounds **1–9** with CID (35 eV). **a** MS<sup>2</sup> of [M+H-2H<sub>2</sub>O]<sup>+</sup>, *m/z* 589.4 (compounds **1–4**) and [M+H-H<sub>2</sub>O]<sup>+</sup>, *m/z* 589.4 (compound **5**). **b** MS<sup>2</sup> of [M+H-2H<sub>2</sub>O]<sup>+</sup>, *m/z* 617.4 (compounds **6–8**) and [M+H-H<sub>2</sub>O]<sup>+</sup>, *m/z* 617.4 (compound **9**)<sup>69</sup>

In ITMS mode, [M+H-2H<sub>2</sub>O]<sup>+</sup> of compounds **1–4** and **6–8**, and [M+H-H<sub>2</sub>O]<sup>+</sup> of compound **5** and compound **9** were selected for MS<sup>2</sup> with CID (35 eV), and they showed typical *a*, *b* and *y* ions (Figure 12).<sup>69,187</sup> Two different patterns of fragmentation were confirmed by further collision of *y*<sub>5</sub> and *a*<sub>2</sub> fragments in MS<sup>3</sup> experiments (Figure 13).<sup>69</sup> For compounds **5** and **9**, the dehydrated amino acid was confirmed to be Dhp residue, because I observed a loss of Thr-Xle fragment from parent mass to *b*<sub>4</sub> ion and the *y*<sub>5</sub> ion with an intact threonine residue, when I selected [M+H]<sup>+</sup> as parent mass for MS<sup>2</sup> measurement (Chapter 8, Figure S10).<sup>69</sup> Therefore, the nine hexacyclopeptides were identified to be cyclo(Hyp-Xle-Xle-Ala-Thr-Xle) (**1–4**), cyclo(Dhp-Xle-Xle-Ala-Thr-Xle) (**5**), cyclo(Hyp-Xle-Xle-Val-Thr-Xle) (**6–8**) and cyclo(Dhp-Xle-Xle-Val-Thr-Xle) (**9**) (Figure 12).<sup>69</sup>

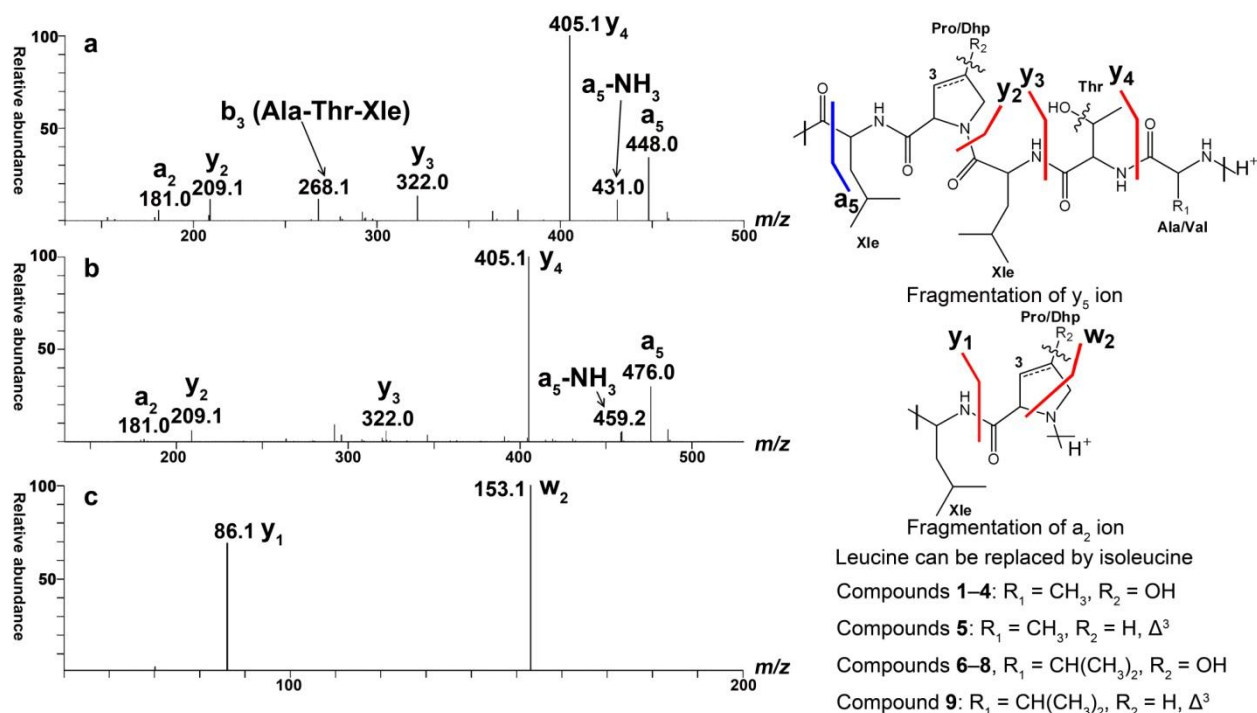


**Figure 13.** MS<sup>3</sup> of *y*<sub>5</sub> ions and *a*<sub>2</sub> ions of compounds **1–9**. **a** *y*<sub>5</sub> ion (*m/z* 476.2) of compounds **1–5**. **b** *y*<sub>5</sub> ion (*m/z* 504.2) of compounds **6–9**. **c** *a*<sub>2</sub> ion (*m/z* 181.2) of compounds **1–9**<sup>69</sup>

## Chapter 5: Results & discussion

---

The difference between the compounds sharing the same formula (**1–4** or **6–8**) is the number of leucine and isoleucine which do not differ by molecular weight.<sup>69</sup> In the case of compounds with a sum formula  $C_{30}H_{52}O_8N_6$ , a maximum of eight peaks can be expected.<sup>69</sup> However, I could detect merely four peaks.<sup>69</sup> Similarly, in the case of compounds with sum formula  $C_{32}H_{56}O_8N_6$ , even though a maximum of eight peaks can be expected, I could detect only three peaks (see Table 2).<sup>69</sup> To assign the Leu/Ile residue, I have tried the method described by Armirotti *et al.* to observe the characteristic 69 Da fragment of isoleucine.<sup>260</sup> However, I failed to collect enough ions after choosing Leu/Ile containing fragment for secondary collision in MS<sup>5</sup> or MS<sup>6</sup>.<sup>69</sup> Compared to the 500 fmol/ $\mu$ L sample concentration and direct infusion analysis at 5  $\mu$ L/min flow rate as reported in the literature, I could obtain far less ion abundance for target molecules after LC separation.<sup>69</sup> In contrast to this, I also measured the MS<sup>3</sup> spectrum of a standard isoleucine sample, wherein I observed the 69 Da fragment that I assigned to  $C_5H_9^+$  (69.0701, calcd. 69.0699,  $\Delta$  3.4351 ppm) (Chapter 8, Figure S13).<sup>69</sup>

### 1.5 Isotope labeling to verify the biosynthetic origin of hexacyclopeptides

In order to exclude the possibility that the hexacyclopeptides were introduced or assimilated from host plant or artificial environment (media contaminants, etc.), I performed an isotope labeling experiment to verify the biosynthesis of these compounds by the endophytic fungus.<sup>69</sup>

First of all, I adopted deuterium exchange reaction to prepare labeled amino acids. The racemization reaction of amino acids catalyzed by aromatic aldehydes in deuterated acetic acid will readily produce 2-deuterium-amino acids, according to the mechanism.<sup>247</sup> For the aliphatic amino acids such as Leu, Ile, Pro, Ala, and Val, 2-deuterium amino acids were prepared with high percentages of deuterium and decent yields. However, threonine was not stable in the racemization condition and no product was obtained in this reaction. 10 mg of each yielded precursor amino acid was then injected into the medium through 0.22  $\mu$ m sterile MILLEX<sup>®</sup>-GP filter on the fourth day of fermentation (final concentration: 100 mg/L). The feeding experiment of 2-deuterated Leu, Ile, Pro, Ala and Val didn't introduce deuterium in the final hexacyclopeptide

## Chapter 5: Results & discussion

products. The reason is probably the transaminase in the fungal cells, which removed the 2-deuterium in the fed amino acids.<sup>261</sup>

Therefore, I designed other reactions to label amino acids other than  $\alpha$  position. The 2,4,4,4-tetradeuterium-threonine (Chapter 8, Figure S6 and S7) was synthesized with a method similar to the one described in the literature (Figure 14).<sup>262</sup> However, I avoided the active proton containing reagents and instead used  $D_2O$  to exchange the  $\alpha$ -protons of acetaldehyde and glycine, and the base was changed from NaOH to TEA.<sup>69</sup> After feeding 10 mg obtained 2,4,4,4-tetradeuterium-threonine as described above, the LC-HRMS analysis of the broth showed labeled threonine was incorporated in these hexacyclopeptides (Figure 16).<sup>69</sup> However, one of the deuterium label was almost lost, which confirmed that the deuterium at 2-position can be removed by transaminases.<sup>261</sup> The label of threonine verified that these hexacyclopeptides were indeed synthesized by the endophytic fungus *F. solani* N06.<sup>69</sup>

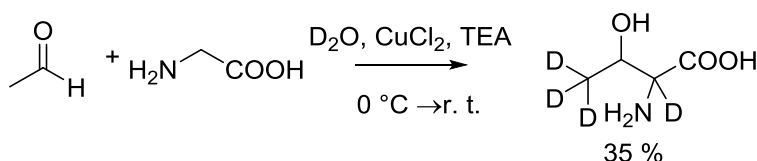


**Figure 14.** Synthesis of 2,4,4,4-tetradeuterium-threonine<sup>69</sup>

4-OH-4-deuterium-proline was synthesized by reduction of N-Boc-4-Oxo-L-proline methyl ester with  $NaBD_4$  followed by hydrolysis (Figure 15). Notably, the fed 4-OH-4-deuterium-proline could not be detected in the hexacyclopeptides, which suggests that 4-OH-4-deuterium-proline is not the building block in the NRPS bio-synthesis. The 4-OH proline residue in hexacyclopeptides was probably modified after NRPS biosynthesis or the OH-proline residue is 3-OH-proline (uncommon in natural products).

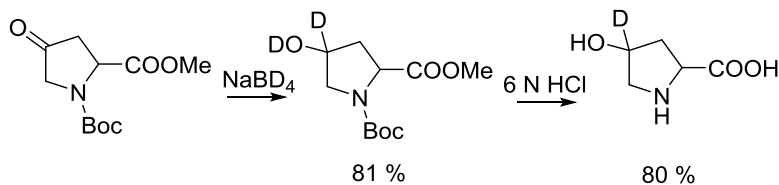


**Figure 15.** Synthesis of 4-OH-4-deuterium-proline



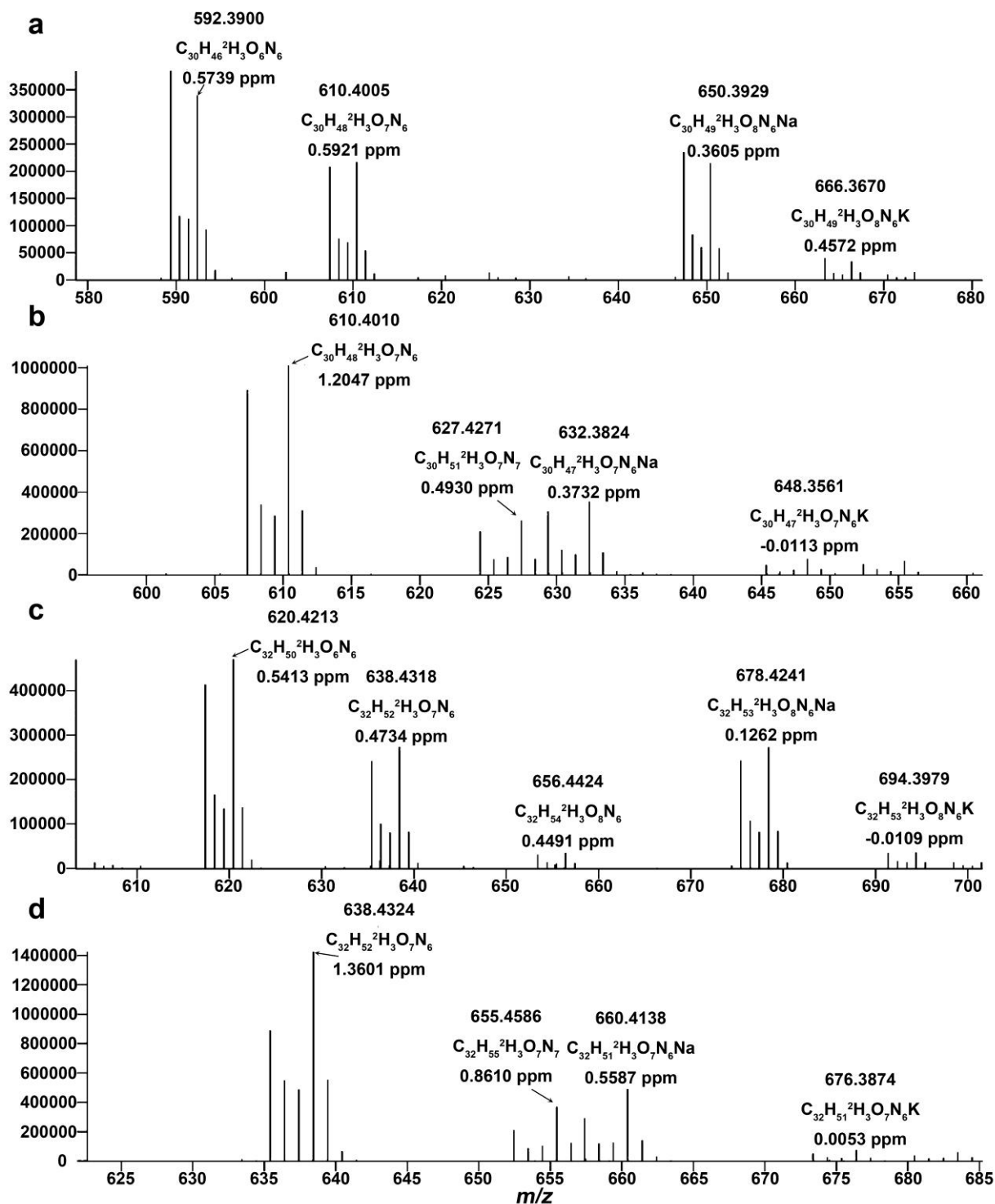


**Figure 16.** The MS of labeled hexacyclopeptides in feeding experiment with 2,4,4,4-tetradeuterium-threonine. **a** Labeled compounds 1–4. **b** Labeled compound 5. **c** Labeled compounds 6–8. **d** Labeled compound 9<sup>69</sup>

## Chapter 5: Results & discussion

---

Further labeling experiment was not continued because the stock in -80 °C storage of the first generation fungus was limited. The effort to isolate the same fungus from plant tissue will be included in future research.

### 1.6 Discussion

The novel behavior of the hexacyclopeptides reported in this manuscript between endophytic *F. solani* and the endophytic bacterium *A. xylosoxidans* N12B harbored in the same host plant tissue demonstrates a proof-of-concept of endophyte-endophyte interspecies neighbor communication.<sup>18,69</sup> This interesting phenomenon upholds the analogous behaviors of other signal molecules reported earlier such as AI-2<sup>215</sup> and  $\alpha$ -factor,<sup>258</sup> which can be taken up and/or eliminated from extracellular environment by sensing cells in the crosstalk with each other.<sup>69,263</sup> Remarkably, strains of *A. xylosoxidans* are well known as exhibiting various microbial crosstalk strategies including the ability to form biofilms, be motile and produce a plethora of virulence factors.<sup>69,264</sup> Incidentally, in an earlier study, a strain of *A. xylosoxidans* F3B, was not only shown to be endophyte in *Arabidopsis thaliana*, but also to tolerate selected pollutants and aid in phytoremediation.<sup>69,105</sup> Thus far, within the contexts of plant-microbe and microbe-microbe interactions (including endophytes), our results add further novel insights to the plethora of mutualistic, defensive and synergistic functionalities of plant and microbial peptides reported in the last decade.<sup>69,265,266</sup> During the process of evolution, endophytes generally establish one or more communication strategies with their host plant as well as with other coexisting endophytes to survive and function in their distinct ecological niches.<sup>54,69</sup> These strategies often include triggers or inducers to initiate the pathway(s) of certain metabolites.<sup>18,69</sup> In the present case, the production of target hexacyclopeptides diminished gradually after the endophytic *F. solani* was separated from its 'natural' ambient within the host plant tissue.<sup>69</sup> Surprisingly, albeit in line with several former investigations, the trigger could not be transferred to in vitro conditions only by adding extracts from the host plant or tweaking the fermentation media or conditions.<sup>69</sup>

To reveal the 'cryptic' natural products that cannot be produced under artificial conditions, genome-based natural product discovery is developing rapidly, wherein

numerous compounds are being discovered that remained unexploited earlier.<sup>69,267–269</sup> However, complete or, at least, partial sequencing of the target microorganism is an integral prerequisite for gene analyses and prediction of the biosynthetic products.<sup>69,267–269</sup> On one hand, MALDI-imaging-HRMS not only revealed the spatial and temporal distribution of functional molecules but also showed an unparalleled advantage in the investigation of interspecies interaction.<sup>69</sup> On the other hand, LC-HRMS<sup>n</sup> enabled us to analyze relatively concentrated samples and gather the information of fragments to identify unknown compounds.<sup>69</sup> The combination of the two tools can be a supplementary approach to discover new functional natural products from endophytes and ascertain their plausible functions in their natural habitats.<sup>69</sup>

## **2. Azaphilones produced by endophytic fungus *Colletotrichum* sp. BS4 and their anti-bacterial potential**

### 2.1 Obtainment of azaphilones (**10–14**)

Based on the pre-screened fermentation of strain *Colletotrichum* sp. BS4, it was fermented on rice medium and the biomass was extracted by EtOAc. By successive chromatographic and extensive spectroscopic methods as well as X-ray diffraction, four new compounds were isolated and identified, namely colletotrichones A–D (**10–13**), along with one known compound chermesinone B (**14a**)<sup>270</sup> (Figure 17) (The detailed isolation procedure, see Chapter 4, 7.1).<sup>231</sup>

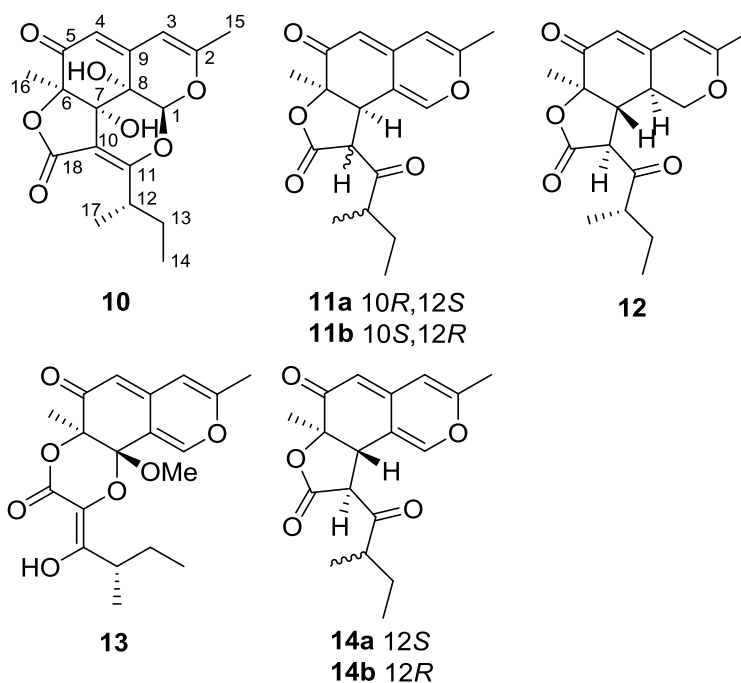


**Figure 17.** Structures of compounds **10–14**

## 2.2 The structural elucidation of compound **10**

Compound **10** was a colorless amorphous powder with the formula  $C_{18}H_{20}O_7$  determined by ESI-HRMS, which showed 9 double bond equivalents (DBEs).<sup>231</sup> In the  $^1H$  NMR spectrum, four methyl groups,  $\delta_H$  0.69 (3H, t,  $J = 7.5$ , Me-14), 2.09 (3H, s, Me-15), 1.65 (3H, s, Me-16) and 1.15 (3H, d,  $J = 7.0$ , Me-17), two olefinic protons  $\delta_H$  5.82 (2H, s, H-3 and H-4), one acetal proton,  $\delta_H$  5.90, (1H, s, H-1) (identified by HSQC), and three further alkyl protons at  $\delta_H$  3.39 (1H, m, H-12), and 1.41 (2H, m,  $CH_2$ -13) were observed (Table 3), which suggested two active protons exchanged by deuterium of NMR solvent.<sup>231</sup> The signals of four methyl carbons, four downfield  $sp^3$  oxygen connected carbons, eight  $sp^2$  carbons including two carbonyl groups, one  $sp^3$  methylene, and one  $sp^3$  methine carbon were observed in the  $^{13}C$  NMR (Table 4) and HSQC experiments.<sup>231</sup>  $^1H$ ,  $^1H$  COSY showed a spin-spin coupling system comprising Me-14 /  $CH_2$ -13 / CH-12 / Me-17 (Figure 18).<sup>231</sup> The key heteronuclear correlations between carbons and protons ( $J_{2,3}$ ) in HMBC confirmed a dimethyl isochromene structure and a *sec*-butyl group (Figure 18).<sup>231</sup> Since the 5 double bonds and two identified rings contribute only 7 DBEs, the remaining 2 DBEs were assigned to two further rings, as no additional  $sp^2$  signals were visible.<sup>231</sup> However, the information above was not sufficient

## Chapter 5: Results & discussion

to connect these moieties, because of the lack of protons at positions 6 to 11 for 2D NMR interpretations.<sup>231</sup> To determine the correct structure of compound **10**, a single crystal from ethyl acetate and methanol (1 : 1) was subjected to X-ray crystallography to analyze the structure (Figure 18).<sup>231</sup> The crystal structure showed an isochromene group *cis*-fused with a furan ring and a pyran ring, which formed a unique stereo structure with a rigid and nearly rectangular bent core skeleton.<sup>231</sup>

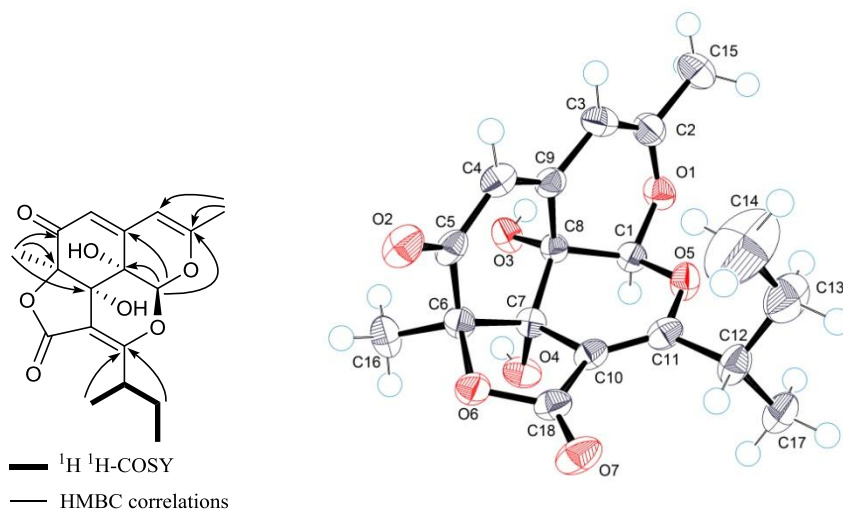


**Figure 18.**  $^1\text{H}$ ,  $^1\text{H}$  COSY, key HMBC correlations and X-ray diffraction crystal structure (ORTEP drawing) of colletotrichone A (**10**)<sup>231</sup>

**Table 3.**  $^1\text{H}$  NMR Spectroscopic Data of **10–12** at 500 MHz<sup>231</sup>

Position	<b>10</b> <sup>a</sup>	<b>11a</b> <sup>b</sup>	<b>12</b> <sup>b</sup>
1	5.90, 1H, s	7.30, 1H, s	3.95, 1H, dd (11.5, 5.4) 3.84, 1H, dd (13.5, 11.5)
3	5.82, 1H, s	6.00, 1H, s	5.48, 1H, br s
4	5.82, 1H, s	5.36, 1H, br s	5.62, 1H, br s
7	-	3.89, 1H, br s	3.10, 1H, dd (12.5, 11.5)
8	-	-	2.74, 1H, dddd (13.5, 11.5, 5.4, 1.5)
10	-	3.89, 1H, br s	3.93, 1H, d (12.5)
12	3.39, 1H, m	3.10, 1H, m	3.07, 1H, m
13	1.41, 2H, m	1.60, 1H, m 1.37, 1H, m	1.79, 1H, m 1.42, 1H, m
14	0.69, 3H, t (7.5)	0.81, 3H, t (7.4)	0.90, 3H, t (7.5)
15	2.09, 3H, s	2.14, 3H, s	1.95, 3H, s
16	1.65, 3H, s	1.57, 3H, s	1.50, 3H, s
17	1.15, 3H, d (7.0)	1.09, 3H, d (6.5)	1.19, 3H, d (7.2)

<sup>a</sup> Measured in  $\text{CD}_3\text{OD}$ , <sup>b</sup> measured in  $\text{CDCl}_3$

**Table 4.**  $^{13}\text{C}$  NMR Spectroscopic Data of **10–12** at 125 MHz<sup>231</sup>

Position	<b>10</b> <sup>a</sup>	<b>11a</b> <sup>b</sup>	<b>12</b> <sup>b</sup>
1	97.2	147.2	69.0
2	159.5	159.4	163.9 <sup>c</sup>
3	101.2	107.3	101.1
4	118.9	105.8 <sup>c</sup>	115.0
5	194.9	191.5	192.5
6	85.8	83.2 <sup>c</sup>	83.4
7	73.7	43.0	44.5
8	63.4	114.6	35.6
9	149.2	144.5	153.0
10	103.2	55.7	52.6
11	168.2	206.3	206.2
12	35.1	46.6	47.8
13	27.0	26.2	24.5
14	11.0	11.1	11.5
15	19.4	19.5	20.6
16	17.1	23.2	18.8
17	17.0	14.1	16.7
18	168.4	168.6	168.8 <sup>c</sup>

<sup>a</sup> Measured in CD<sub>3</sub>OD, <sup>b</sup> measured in CDCl<sub>3</sub>, <sup>c</sup> assigned by HMBC

As the relative configuration was unequivocally defined by X-ray diffraction, the absolute configuration must be identical with that depicted in the structure of **10**, or with the mirror image thereof.<sup>231</sup> The determination was made by calculation of the ECD and ORD data and by comparison of these data with the experimental values. Molecular mechanics calculations (SPARTAN'14, MMFF<sup>236</sup>) for **10** in a systematic approach resulted in the lowest energy 18 conformers in an energy range of 45 kJ/mol above the global minimum.<sup>231</sup> By *ab initio* calculations using SPARTAN'14<sup>236</sup> and Gaussian g09<sup>237</sup> [finally with the wB97X-D functional and the 6-311++G(2df,2p) basis set], 11 conformers within a range of 16 kJ/mol (Gibbs free energy) above the global minimum were selected for further DFT calculations of the ECD and ORD data as described previously.<sup>78,231</sup> As all conformers had positive OR values, the optical rotation Boltzmann-weighted from all conformers was positive (calcd. molar rotation = +396°/specific rotation +11.4°), and an experimental value of 340.4° was found for **10**.<sup>231</sup> As the enantiomer *ent*-**10** would give a negative optical rotation and a mirror-imaged ECD spectrum with respect to Figure 19, the high similarity of experimental and calculated ECD and OR data unambiguously confirmed the absolute (1*S*,6*R*,7*S*,8*S*,12*S*)-configuration of **10**, as depicted in the structure.<sup>231</sup>

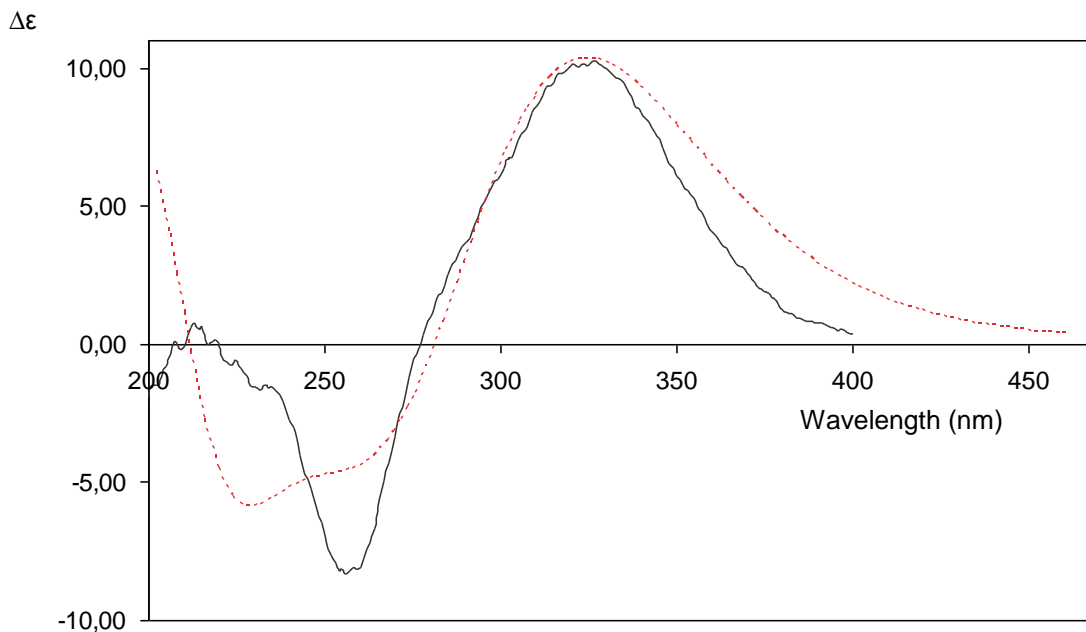


**Figure 19.** Experimental (continuous line) and calculated (dashed curve) ECD spectra (in MeOH) of colletotrichone A (**10**)<sup>231</sup>

### 2.3 The structural elucidation of compound **11**

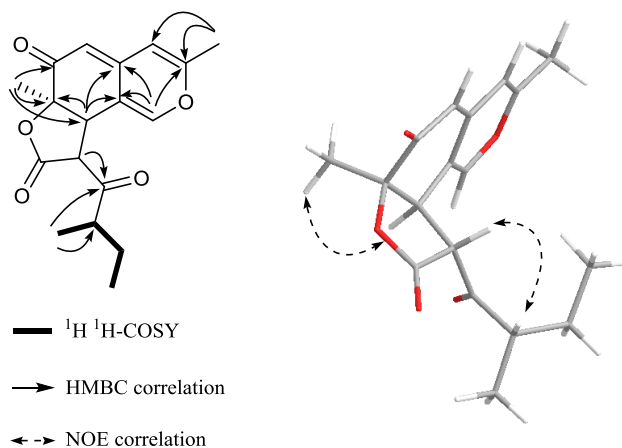


**Figure 20.** <sup>1</sup>H, <sup>1</sup>H COSY, key HMBC and NOESY correlations of colletotrichone B (**11a**); 3D structure is the conformer with the lowest energy<sup>231</sup>

Compound **11a** was isolated as yellowish oil with the formula C<sub>18</sub>H<sub>20</sub>O<sub>5</sub>, determined by ESI-HRMS.<sup>231</sup> The <sup>1</sup>H NMR, <sup>13</sup>C NMR and HSQC data of **11a** indicated the same pattern of *sp*<sup>2</sup> and *sp*<sup>3</sup> carbons as the known compound **14a** isolated here as well, while the signals of CH-1, CH-10, Me-16 and Me-17 were quite different.<sup>231</sup> HMBC and <sup>1</sup>H, <sup>1</sup>H

## Chapter 5: Results & discussion

COSY experiments (Figure 20) revealed the same planar structure as for **14a** and **14b**.<sup>231</sup> In 2D NOESY experiments (in acetone-*d*<sub>6</sub>, see Chapter 8, Figure S30), nuclear Overhauser effects (NOE) were clearly observed between Me-16 and H-7 (H-7 and H-10 have different chemical shifts in acetone-*d*<sub>6</sub>, Table 5), which indicated that the lactone ring is *cis* fused (Figure 20).<sup>231</sup> Although there was a NOE cross peak between H-7 and H-10, it didn't determine that H-7 and H-10 are on the same side of lactone ring, because even though they are on the different sides of the ring, the distance between them is still close enough to show NOE.<sup>231</sup> For example, the NOE correlation between H-7 and H-10 appeared also in the NOESY spectrum of chermesinone B (in which H-7 and H-10 have different orientations).<sup>231,270</sup> Moreover, no unambiguous NOE was observed between H-10 and Me-16 even in 1D NOESY experiment with sufficient scan times (Chapter 8, Figure S31).<sup>231</sup> Therefore, the configuration of H-10 related to Me-16 and H-7 was not certain in the interpretation of NOESY experiments.<sup>231</sup> For the relative configuration of H-12/Me-17, the NOE correlation was only observed between H-10 and H-12.<sup>231</sup>

**Table 5.** <sup>13</sup>C NMR (125 MHz) and <sup>1</sup>H NMR (500 MHz) data of compound **11a** in acetone-*d*<sub>6</sub>.<sup>231</sup>

Position	<b>11a</b> (acetone- <i>d</i> <sub>6</sub> )	
	$\delta_C$	$\delta_H$ mult. (J in Hz)
1	146.9	7.38, 1H, s
2	159.1	
3	106.8	6.25, 1H, s
4	105.3	5.28, 1H, br s
5	190.6	
6	82.7	
7	43.4	3.93, 1H, d (12.0)
8	114.5	
9	144.0	
10	55.6	4.36, 1H, d (12.0)
11	206.5	
12	46.7	3.05, 1H, m
13	25.4	1.67, 1H, m 1.36, 1H, m
14	10.5	0.83, 3H, t (7.4)
15	18.3	2.17, 3H, s
16	22.4	1.51, 3H, s
17	13.5	1.07, 3H, d (6.7)
18	169.5	



## Chapter 5: Results & discussion

**Table 6.** Boltzmann averaged distances from H-10 to Me-17 and from H-10 to H-12 of four diastereomers of compound **11a** (6*R*,7*R*,10*R*,12*R* (**11c**); 6*R*,7*R*,10*R*,12*S* (**11a**); 6*R*,7*R*,10*S*,12*S* (**11d**); 6*R*,7*R*,10*S*,12*R* (**11b**))<sup>a</sup>, calculated on wB97XD/6-311+G(2df,2p) level of theory<sup>231</sup>

6 <i>R</i> ,7 <i>R</i> ,10 <i>R</i> ,12 <i>R</i>			Distance (Å)	
Conformer	$\Delta G$ (Hartree)	B-Factor	H-10 to Me-17	H-10 to H-12
1	0.00145	0.060484	2.505	2.585
2	0	0.278278	2.417	2.605
3	0.002852	0.01581	2.343	3.342
6	5.9E-05	0.261522	2.824	2.514
8	0.002454	0.024037	2.335	3.334
10	0.001427	0.061966	2.5	2.589
15	3.8E-05	0.267367	2.757	2.515
20	0.00142	0.062425	2.497	2.588
Weighted average			2.620	2.58372903

6 <i>R</i> ,7 <i>R</i> ,10 <i>R</i> ,12 <i>S</i>			Distance (Å)	
Conformer	$\Delta G$ (Hartree)	B-Factor	H-10 to Me-17	H-10 to H-12
1	0	0.325127	4.258	2.462
2	0.001332	0.080012	4.516	3.006
3	0.002346	0.027519	4.482	2.585
4	0.002216	0.031554	4.099	2.634
6	0.00235	0.027403	4.483	2.589
13	0.000114	0.288364	4.254	2.462
17	0.000373	0.219555	4.255	2.464
Weighted average			4.284	2.518

6 <i>R</i> ,7 <i>R</i> ,10 <i>S</i> ,12 <i>S</i>			Distance (Å)	
Conformer	$\Delta G$ (Hartree)	B-Factor	H-10 to Me-17	H-10 to H-12
1	0.003284	0.014895	2.887	2.559
3	0.003339	0.014058	4.258	2.358
9	0.001525	0.094874	3.025	3.604
10	0	0.472355	3.473	3.636
12	0.002321	0.041046	3.379	3.617
13	0.000312	0.340129	3.467	3.640
Weighted average			3.426	3.599

6 <i>R</i> ,7 <i>R</i> ,10 <i>S</i> ,12 <i>R</i>			Distance (Å)	
Conformer	$\Delta G$ (Hartree)	B-Factor	H-10 to Me-17	H-10 to H-12
1	0.002892	0.04132	2.454	2.348
2	0.003739	0.016942	4.37	2.363
3	0.003056	0.034769	4.087	2.35
4	0.004156	0.010923	2.593	2.429
9	0	0.86733	4.831	3.633
10	0.003904	0.014241	4.775	3.462
Weighted average			4.711	3.525

## Chapter 5: Results & discussion

---

The H-10 / H-12 and H-10 / Me-17 distances of optimized preferential conformers (Boltzmann factor > 0.01; Table 6) were calculated to figure out the possible configurations.<sup>231</sup> In Table 6, I presumed that the configuration of C-6 is *R*, and the discussion showed below is useful for the assignment of relative configurations at position C-10 and C-12 of compound **11a**.<sup>231</sup>

For a flexible structure, the distance of each contributing conformer will result in dynamic averaged NOEs, if the interconversion between conformers is rapid enough on the NMR time-scale.<sup>231,271,272</sup> Therefore, I can use Boltzmann averaged distance to describe the spatial relationship of atoms in compound **11a** for NOESY analysis.<sup>231</sup>

The relationship of interproton distance ( $r_{IS}$ ) and normalized NOE intensity ( $\eta_{IS}$ ) can be described by formulae:<sup>231,271,272</sup>

$$\eta_{IS} = \sigma_{IS} \tau_m \quad \sigma_{IS} = k r_{IS}^{-6} \quad k = \left( \frac{\mu_0}{4\pi} \right) \frac{\hbar^2 \gamma^4}{10} \left( \frac{6\tau_c}{1 + 4\omega^2 \tau_c^2} - \tau_c \right)$$

When the NOESY measurement was performed within one experiment, the  $k$  and  $\tau_m$  value can be considered to be constant for each spin pair.<sup>231,271,272</sup>

Thus far, the distance and NOE intensity can be described in a proportional relationship showed below:<sup>231,271,272</sup>

$$\frac{\eta_{I1S}}{\eta_{I2S}} = \frac{r_{I1S}^{-6}}{r_{I2S}^{-6}}$$

Therefore, I can conclude which pair of protons has closer distance by comparing the NOE intensities.<sup>231</sup>

From the 2D NOESY spectrum, I can clearly see that there is a cross peak between H-10 and H-12, while no cross peak is observed between H-10 and Me-17, which suggests that the averaged distance of H-10 and H-12 is smaller than H-10 and Me-17.<sup>231</sup> Moreover, the absence of cross peak between H-10 and Me-17 indicates the distance between them is larger than the detection limit.<sup>231</sup>

## Chapter 5: Results & discussion

---

For *6R,7R,10R,12R* (**11c**) configuration, the distance from Me-17 to H-10 and the distance from H-10 to H-12 are similar (the difference is only 0.036 Å), and are both smaller than 3 Å, where the NOE can be detected.<sup>231,273</sup> For *6R,7R,10S,12S* (**11d**) configuration, however, the distances between H-10 and Me-17 is smaller than H-10 and H-12.<sup>231</sup>

It is worth to mention here that the earlier reported compound chermesinone C has *7S,10S,12S* configuration (which is also the same relative configuration to *7R,10R,12R*), and its H-10 and Me-17 as well as H-10 and H-12 have cross peaks in NOESY spectrum.<sup>231,270</sup>

Therefore, the two possibilities for compound **11a** are *6R,7R,10R,12S* and *6R,7R,10S,12R* (less likely) (or their enantiomers).<sup>231</sup>

To distinguish between both diastereomers, I compared *ab initio*-calculated and experimental NMR data. Huang *et al.*<sup>231,270</sup> solved the relative configuration of H-12/Me-17 in the same way for two further diastereomers of **11a**, namely the *trans*-lactones chermesinone B (**14a**) and monochaetin (**14b**).<sup>231,270,274</sup> In accordance with the comparison of experimental NMR data and calculations (see Chapter 8, Tables S41 and S42), the chemical shift of Me-17 ( $\delta_{C17} = 14.1$ ,  $\delta_{H17} = 1.09$ ; calcd. 15.4 (err. 1.06) for (*6R,6R,10R,12S*)-**11a**) suggested that H-10 and Me-17 have the same relative orientation as in monochaetin (**14b**) (Me-17,  $\delta_{C17} = 14.4$ ,  $\delta_{H17} = 1.11$ ).<sup>231,246</sup> For all other (*6R,7R,10 $\xi$ ,12 $\xi$* ) diastereomers **11c**, **d**, higher shifts were calculated (see Chapter 8, Table S1), as exemplified experimentally for chermesinone B (**14a**: Me-17,  $\delta_{C17} = 17.1$ ,  $\delta_{H17} = 1.24$ ).<sup>231,270</sup>

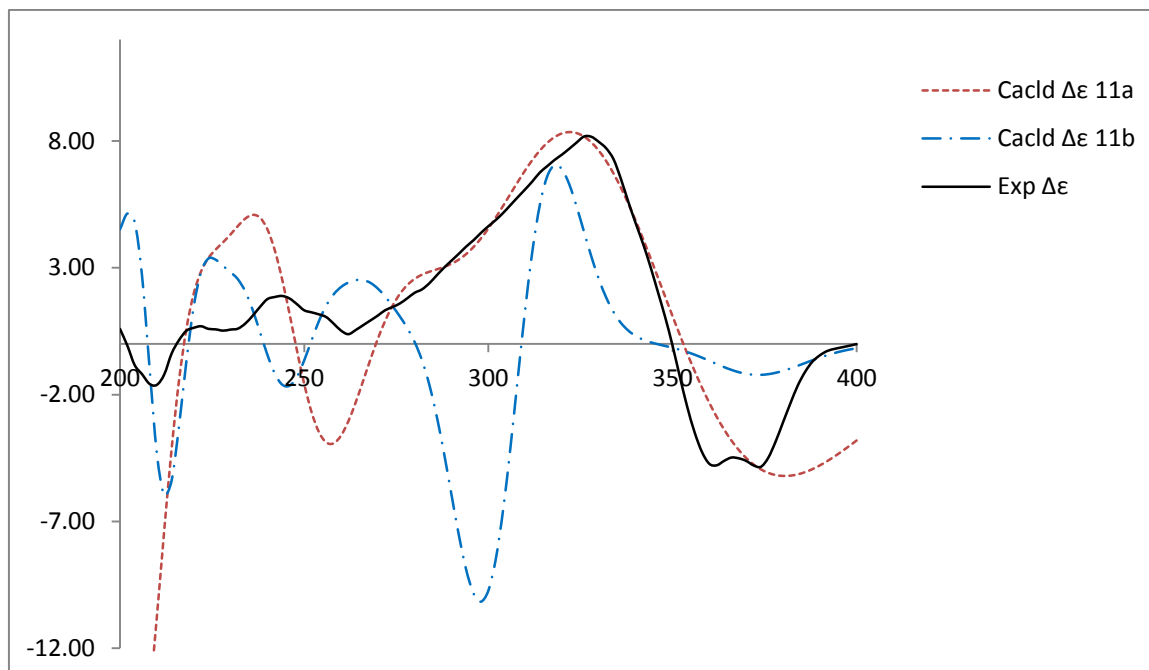


**Figure 21.** Experimental CD data in MeOH (black continuous line) and calculated ECD spectra of colletotrichone B (**11a**; red, dashed curve) and 10*S*,12*R*-*epi*-colletotrichone B (**11b**; blue dashed curve)<sup>231</sup>

To further differentiate between the structures **11a** and **11b**, *ab initio* ECD calculations were performed.<sup>231</sup> The calculated ECD curve of **11a** showed the Cotton effect coincided with the experimental ECD spectrum (Figure 21).<sup>231</sup> In contrast to this, the major negative Cotton effect at 290 nm in the calculated ECD value of **11b** could not be explained by the experimental data.<sup>231</sup> Therefore, the structure of colletotrichone B was determined to be **11a**, and the absolute configuration was consequently determined to be 6*R*,7*R*,10*R*,12*S*.<sup>231</sup> Notably, the assignment of the 6*R*,12*S* configuration could also be explained in view of its proposed biosynthetic pathway.<sup>231</sup>

#### 2.4 The structural elucidation of compound **12**

Colletotrichone C (**12**) was obtained as a colorless amorphous powder showing a pseudomolecular  $[M+H]^+$  ion, according to the formula  $C_{18}H_{22}O_5$ .<sup>231</sup> In comparison with **11a** and **14a**, the  $^1H$  NMR data (Table 3) of **12** displayed three further peaks at  $\delta_H$  2.74, 3.95 and 3.84, and the absence of the  $sp^2$  CH signal of H-1 in compounds **11a** ( $\delta_H$  7.30) as well as **14a** ( $\delta_H$  6.83).<sup>231</sup>  $^{13}C$  NMR (Table 4), HMBC and  $^1H$ ,  $^1H$  COSY data (Figure 22)

## Chapter 5: Results & discussion

suggested that the pyran ring was hydrogenated at positions 1 and 8.<sup>231</sup> The coupling constants of H-7 ( $\delta_{\text{H}}$  3.10, 1H, dd, 12.5, 11.5), H-8 ( $\delta_{\text{H}}$  2.74, 1H, dddd, 13.5, 11.5, 5.4, 1.5) and H-10 ( $\delta_{\text{H}}$  3.93, 1H, d, 12.5) indicated that these three methine protons are at axial positions, which was further confirmed by NOESY experiments (Figure 22).<sup>231</sup> To determine the absolute configuration, ECD spectra were calculated by the method described above.<sup>231</sup> The experimental spectrum was in agreement with the expected (6*R*,7*R*,8*S*,10*S*)-configuration of **12** (Figure 23).<sup>231</sup> The configuration of C-12 was assigned as (*S*), based on the Me-17 shift ( $\delta_{\text{C}}$  16.7,  $\delta_{\text{H}}$  1.19) of **12**, in comparison with the NMR data of compounds **11a** and **14a**.<sup>231</sup>

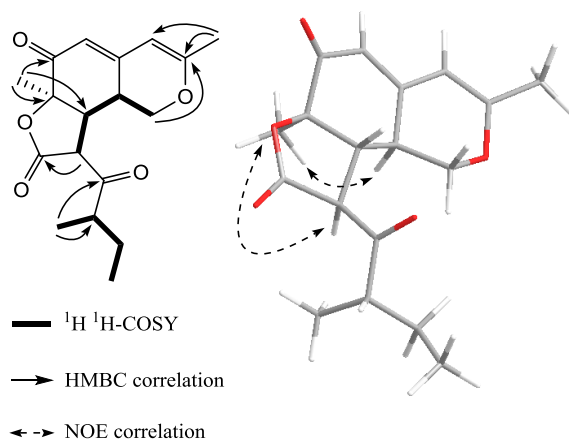


**Figure 22.**  $^1\text{H}$ ,  $^1\text{H}$  COSY, key HMBC and NOESY correlation of colletotrichone C (**12**)<sup>231</sup>

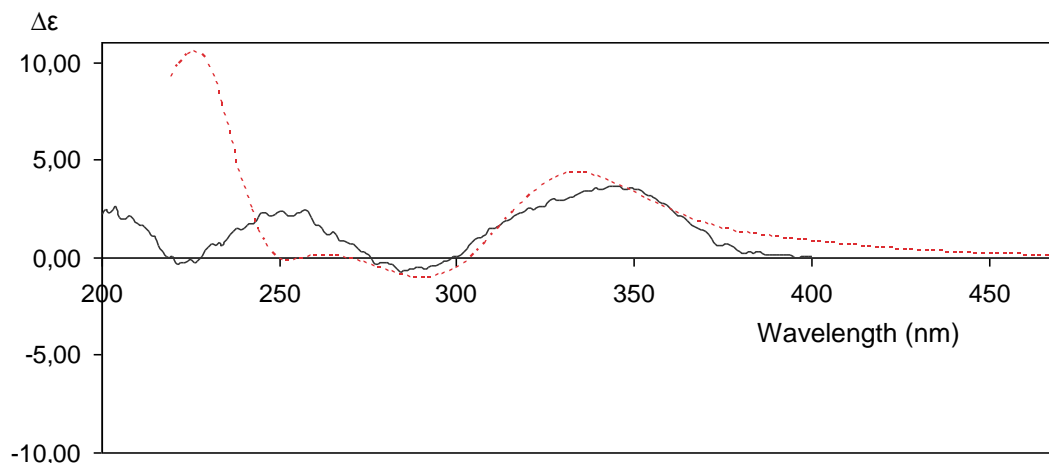


**Figure 23.** Experimental (continuous line) and calculated (dashed curve) ECD spectra (in MeOH) of colletotrichone C (**12**)<sup>231</sup>

## Chapter 5: Results & discussion

### 2.5 The structural elucidation of compound **13**

Compound **13** was isolated as a colorless amorphous powder, whose formula was determined by ESI-HRMS to be  $C_{19}H_{22}O_7$ . Its  $^1H$  NMR spectrum (Table 7) showed similar signals like compound **14**, such as  $\delta$  7.38 (1H, s, H-1), 6.01 (1H, s, H-3) and 5.30 (1H, br s, H-4), and four methyl peaks  $\delta$  2.17 (3H, s, Me-15), 1.49 (3H, s, Me-16), 1.18 (3H, d, 6.9, Me-17) and  $\delta$  0.94 (3H, t, 6.8, Me-14), but it had one more methyl group at  $\delta$  3.09 (3H, s, OMe-7), and a deuterium hydrogen exchangeable signal at  $\delta$  11.64 (1H, br s, OH-11). In  $^{13}C$  NMR spectrum (Table 7), compound **13** showed only one ketone carbonyl at  $\delta$  190.6 (C-5), eight other  $sp^2$  carbons at  $\delta$  146.2, 158.9, 105.8, 107.7, 114.2, 142.0, 116.4 and 170.0, and two down field  $sp^3$  carbons connected with oxygen at  $\delta$  83.4 and 96.5. In HMBC experiment (Table 7), key correlations were observed, including Me-15 ( $\delta$  2.17, 3H, s) between C-2 ( $\delta$  158.9) and C-3 ( $\delta$  107.7); Me-16 ( $\delta$  1.49, 3H, s) between C-5 ( $\delta$  190.6), C-6 ( $\delta$  83.4) and C-7 ( $\delta$  96.5); Me-17 ( $\delta$  1.18, 3H, d, 6.9) between C-11 ( $\delta$  170.0) and C-12 ( $\delta$  35.2); 11-OH ( $\delta$  11.64, 1H, br s) between C-10 ( $\delta$  116.4) and C-12 ( $\delta$  35.2); and OMe-7 ( $\delta$  3.09, 3H, s) between C-7 ( $\delta$  96.5). By  $^1H$ ,  $^1H$ -COSY technology, moreover, the fragment of *sec*-butyl side chain was clearly confirmed. After assigning all these proton and carbon signals, there were two  $sp^3$  quaternary carbons connected with oxygen, namely C-6 ( $\delta$  83.4) and C-7 ( $\delta$  96.5), while there were three unassigned oxygen atoms according to the formula  $C_{19}H_{22}O_7$ . The C-7 ( $\delta$  96.5) with significant deshielding effect suggested the bond between C-17 and the methyl group ( $\delta$  3.09, 3H, s) is a ketal group connected with OMe-7 and another oxygen atom between C-7 and C-11. In 1D NOESY, OMe-7 and Me-16 showed no correlation, which suggested the OMe-7 group and Me-16 are on the different sides.

**Table 7.**  $^1H$  NMR (500 MHz) and  $^{13}C$  NMR (125 MHz) spectroscopic data for compound **13** at 500 MHz

Position	$^1H$ NMR ( <i>J</i> in Hz)	$^{13}C$ NMR	HMBC
1	7.38, 1H, s	146.2	C-2, C-8, C-9
2		158.9	
3	6.01, 1H, s	107.7	C-2, C-4, C-8
4	5.30, 1H, br s	105.8	C-3, C-6, C-8
5		190.6	
6		83.4	
7		96.5	
8		114.2	

## Chapter 5: Results & discussion

9		142.0	
10		116.4	
11		170.0	
12	2.88, 1H, m	35.2	
13	1.69, 1H, m	27.6	C-12, C-14, C-11, C-17
	1.59, 1H, m		
14	0.94, 3H, t (6.8)	12.5	C-12, C-13
15	2.17, 3H, s	19.9	C-2, C-3
16	1.49, 3H, s	21.9	C-5, C-6, C-7
17	1.18, 3H, d (6.9)	17.6	C-11, C-12, C-13
18		165.2	
11-OH	11.64, 1H, br s		C-10, C-11, C-12
7-OMe	3.09, 3H, s	50.3	C-7

<sup>a</sup> Assigned by HSQC because of overlapping

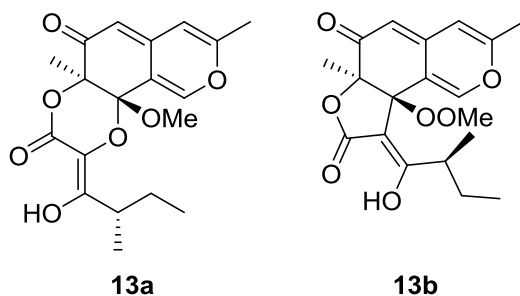


**Figure 24.** Two possible structures of compound **13**

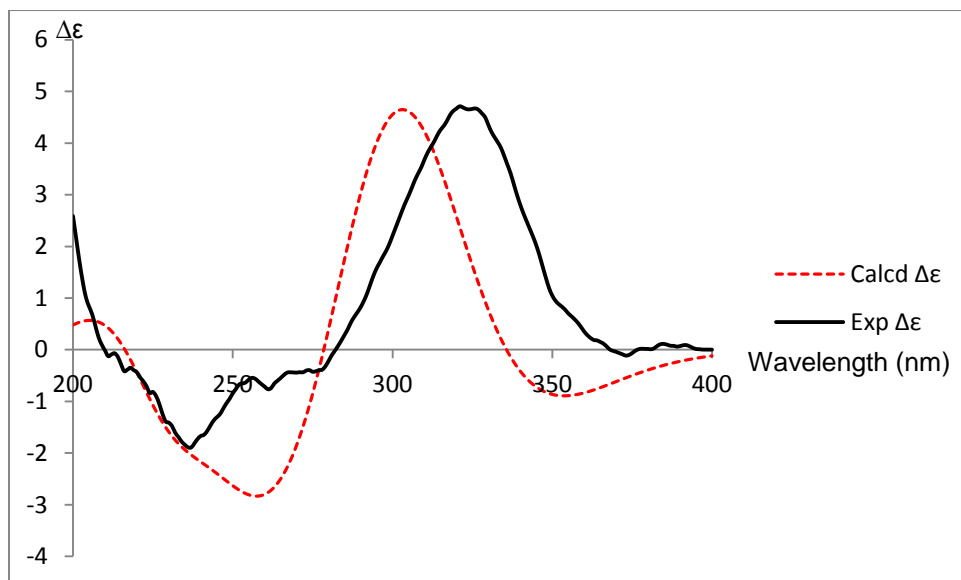


**Figure 25.** Experimental (continuous line) and calculated (dashed curve) ECD spectra (in MeOH) of colletotrichone C (**13**)

**Table 8.** Calculated  $^{13}\text{C}$  NMR of structure **13a** and **13b**

Position	Exp. $^{13}\text{C}$ NMR	<b>13a</b>	Abs. error	<b>13b</b>	Abs. error
1	146.2	148.6	2.4	148.0	1.8
2	158.9	161.1	2.2	160.2	1.3
3	107.7	109.7	2.0	110.0	2.3
4	105.8	106.6	0.8	108.4	2.6
5	190.6	187.9	2.7	191.7	1.1
6	83.4	81.5	1.9	86.6	3.2
7	96.5	94.6	1.9	89.3	7.2
8	114.2	116.1	1.9	118.8	4.6
9	142.0	142.6	0.6	145.4	3.4
10	116.4	117.5	1.1	97.0	19.4
11	170.0	171.4	1.4	186.1	16.1
12	35.2	36.1	0.9	41.4	6.2
13	27.6	29.4	1.8	27.0	0.6
14	12.5	13.3	0.8	13.4	0.9
15	19.9	19.8	0.1	19.2	0.7
16	21.9	22.1	0.2	27.2	5.3
17	17.6	18.6	1.0	20.5	2.9
18	165.2	164.6	0.6	175.1	9.9
OMe	50.3	47.7	2.6	60.9	10.6
		<b>MAE</b>	1.4	<b>MAE</b>	5.3

\*MAE is an abbreviation of mean absolute error

However, there is another possibility that C-7 and C-11 have a direct bonding and C-7 is connected to a methyl group by a peroxide bond (Figure 24). Therefore, GIAO DFT  $^{13}\text{C}$  NMR calculations of these two structures were performed (Table 8). The calculated data of proposed structure **13a** showed high agreement with the experimental  $^{13}\text{C}$  NMR, which revealed that the correct structure is **13a** as proposed.

The absolute configuration of **13a** was determined by ECD calculation similar to the methods described for compounds (**10–12**) (by different software and level of theory, see Chapter 4, section 8). The Boltzmann averaged calculated ECD curve of structure **13a** matched the experimental data well (Figure 25). Therefore, the absolute configuration of compound **13a** was assigned to be 6*S*,7*S*,12*S*.



2.6 Proposal of biosynthetic pathway of azaphilones (**10–14**)

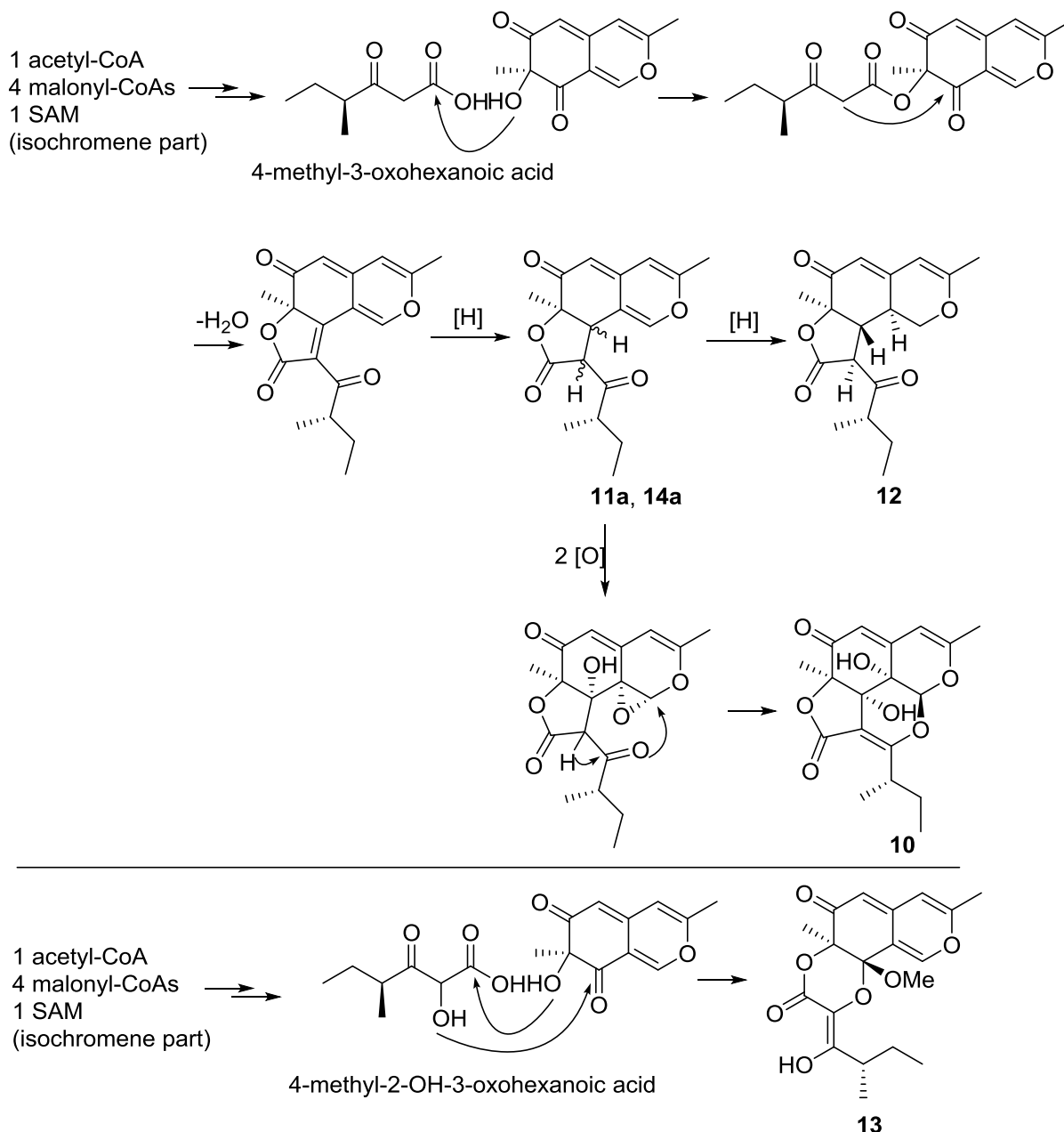


**Figure 26.** Proposed biosynthetic pathway of compounds **10–14**<sup>231</sup>

The compounds **10–14** are typical polyketides, whose biosyntheses have been comprehensively investigated in numerous studies.<sup>231,164</sup> Interestingly, for the *sec*-butyl substructure, a condensation product originating from two different polyketides, but not from a single octaketide chain was proposed.<sup>164,231,274</sup> With respect to their structures, the biosynthesis of compounds **10–14** might proceed from a pentaketide via an

## Chapter 5: Results & discussion

---

isochromene analogue, which is first acylated and then condensed with a 4-methyl-3-oxohexanoic acid or 4-methyl-2-OH-3-oxohexanoic acid, and further modified by oxidation or hydrogenation, according to the proposed biosynthesis of other azaphilones (Figure 26).<sup>164,231,275</sup> Borges *et al.* proposed a pathway of cyclization of chaetoviridin I, whose essential steps were an epoxidation at double bond  $\Delta^7$  and subsequent hydrolysis.<sup>231,276</sup> Considering the  $S_N2$  mechanism or steric effects, however, the hydrolysis at the epoxy group is more likely to generate two *trans*-hydroxy groups.<sup>231</sup> Therefore, I proposed an aforementioned biosynthetic pathway to explain the formation of the ring system and configurations of compound **10** and **13** (Figure 26).<sup>231</sup>

### 2.7 Antibacterial assay of compounds (**10–14**) and cytotoxic assay of compounds (**10–12**, and **14a**)

It is well-known that azaphilones have a broad range of biological activities including antimicrobial, cytotoxic, anticancer, antiviral and anti-inflammatory properties.<sup>164,231</sup> In an earlier investigation on azaphilones from stromata of Xylariaceae, Hellwig *et al.* suggested that they are maintained in the course of their co-evolution with angiosperm hosts and involved in a kind of chemical defense reaction to keep the fitness of their producers.<sup>231,277</sup> Moreover, some azaphilones with similar lactone substructures were reported to have antibacterial activities. For instance, deflectin B-2a showed a minimum inhibitory concentration (MIC) of 5  $\mu\text{g}/\text{mL}$  against *Bacillus. brevis* and *B. subtilis* ATCC 6633 on a complex medium.<sup>231,278</sup> Moreover, sassafrins A–C showed moderate antibacterial activities against *Staphylococcus aureus*, *Pseudomonas aeruginosa*, *Klebsiella pneumonia*, and *Escherichia coli*. In another study, multiformins A–D were shown to have moderate to strong activity against *S. aureus*, *P. aeruginosa*, *K. pneumonia*, *E. coli* and *Salmonella enteritidis*.<sup>231,279</sup>

Therefore, given the potent antibacterial efficacies of azaphilones, we evaluated the antibacterial effectiveness of our isolated compounds against two widely distributed environmental strains of *E. coli* (Gram-negative) and *B. subtilis* (Gram-positive), as well as against two human pathogenic bacterial strains of *S. aureus* (Gram-positive) and *P. aeruginosa* (Gram-negative).<sup>78,231</sup> Compound **10** showed pronounced efficacies particularly against both the tested environmental strains comparable to the standard

## Chapter 5: Results & discussion

antibiotics (Table 9).<sup>231</sup> Additionally, compound **12** was quite active against the environmental strain of *E. coli*.<sup>231</sup> Furthermore, compound **11a** exhibited the same efficacy as streptomycin against clinically relevant, risk-group 2 (RG2) bacterium *S. aureus*.<sup>231</sup> Since the endophytic fungus was isolated from the leaves of *B. sinica*, it is compelling that it provides some form of azaphilone-mediated chemical defense to the host plant against invading specialist and generalist bacteria.<sup>231</sup> In order to discern the antibacterial selectivity of the compounds, their cytotoxicity against human acute monocytic leukemia cells (THP-1) was evaluated not only using a resazurin-based assay to measure the THP-1 mitochondrial metabolic inhibition but also an ATPlite assay to measure the THP-1 cytoplasmic ATP depletion.<sup>231</sup>

**Table 9.** Minimum inhibitory concentrations (MIC) of the compounds **10–14** against Gram-positive and Gram-negative bacteria compared to standard references<sup>231</sup> (streptomycin and gentamicin)<sup>a</sup>

Organism (DSMZ no.)	<b>10</b>	<b>11a</b>	<b>12</b>	<b>13</b>	<b>14a</b>	streptomycin	gentamicin
<i>Staphylococcus aureus</i> (DSM 799)	>10	5.0	>10	>10	>10	5.0	1.0
<i>Escherichia coli</i> (DSM 1116)	1.0	>10	5.0	>10	>10	1.0	1.0
<i>Bacillus subtilis</i> (DSM 1088)	0.1	>10	>10	>10	>10	5.0	1.0
<i>Pseudomonas aeruginosa</i> (DSM 22644)	>10	>10	>10	>10	>10	10.0	1.0

<sup>a</sup>All values are in  $\mu\text{g/mL}$  and derived from experiments in triplicate.

None of the tested compounds (**10**, **11a**, **12** and **14a**) demonstrated potential cytotoxic effects against THP-1 cells at low concentrations (Figure 27) while they inhibited the growth of tested microorganisms in the antibacterial assay (Table 9). Although compounds **12** and **14a** showed moderate cytotoxic efficacies at higher concentrations ( $\geq 10 \mu\text{M}$ ), these could be considered potentially insignificant.<sup>231</sup>

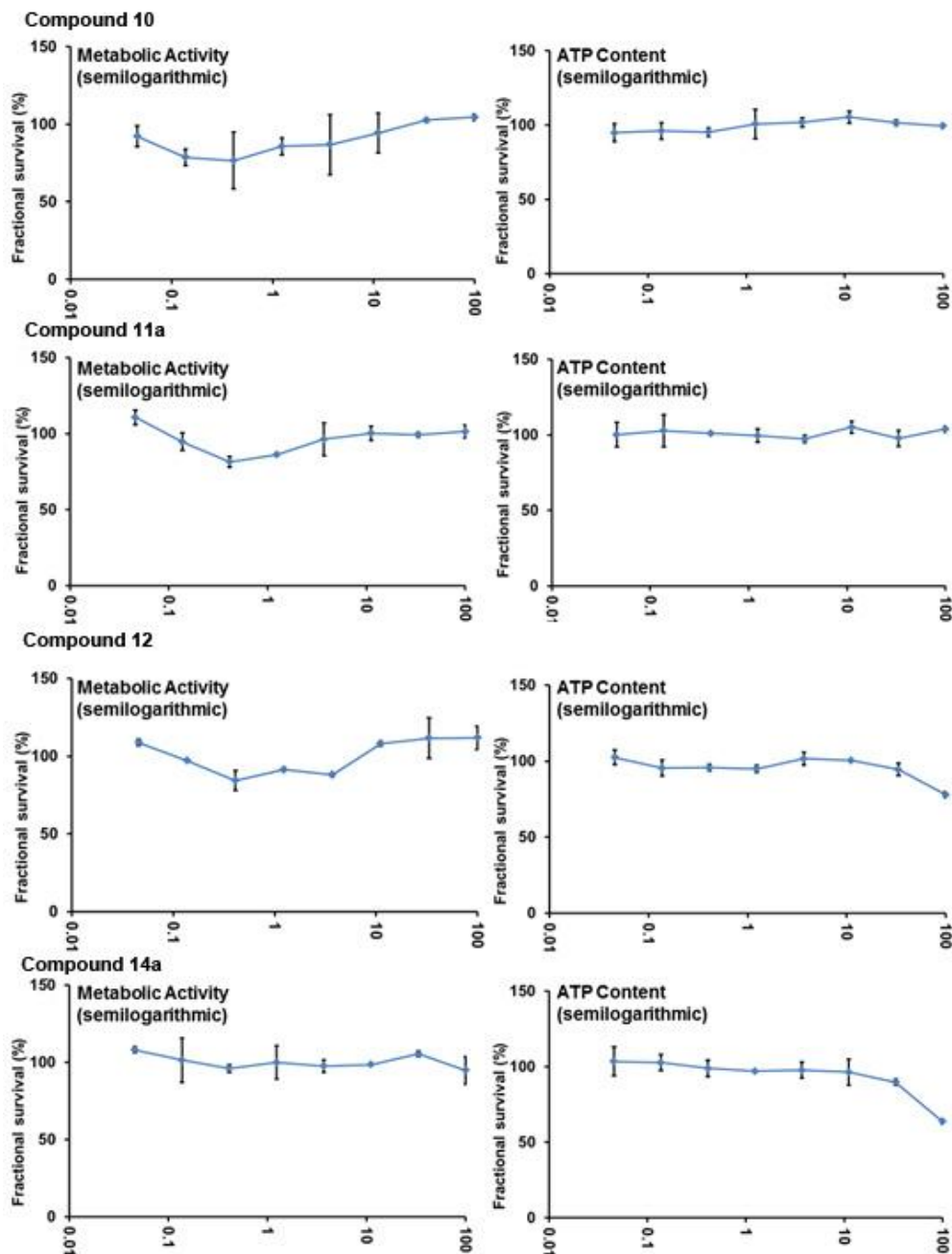


**Figure 27.** *In vitro* cytotoxic assays of compounds **10**, **11a**, **12** and **14a** against THP-1 cells using a resazurin-based assay (to measure metabolic activity) as well as an ATPlite assay (to measure ATP content). Semilogarithmic representation of the fractional survival (FS in %) of THP-1 cells as a function of concentration is provided<sup>231</sup>

## Chapter 5: Results & discussion

### 2.8 Visualization of azaphilones in the colony of *Colletotrichum* sp. BS4 by MALDI IMS

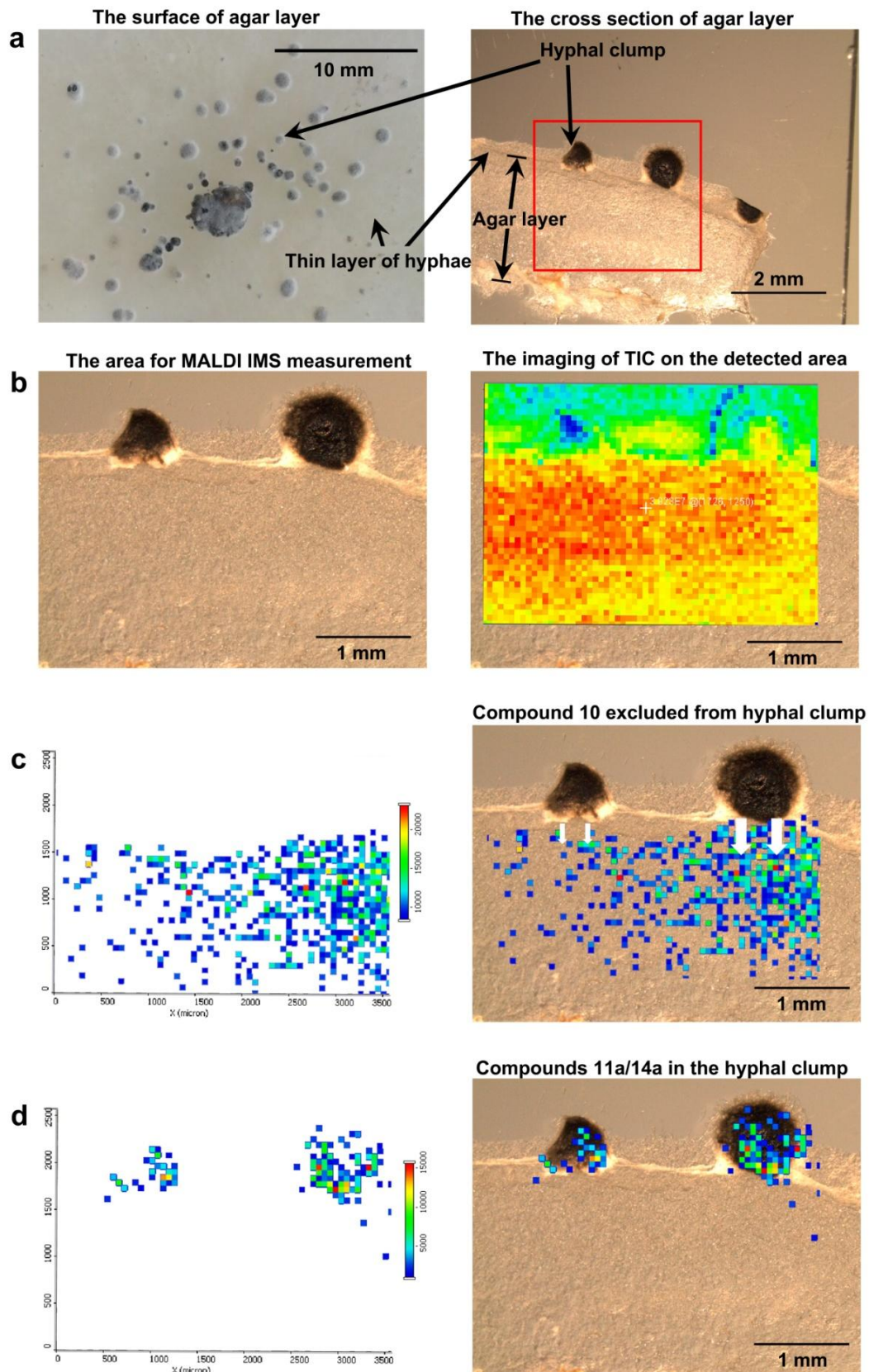


**Figure 28.** Spatial distribution of compound **10** and compound **11a/14a** produced by endophytic *Colletotrichum* sp. BS4 on rice agar after 16 days. **a** Optical image of colony and the cross section of agar layer on glass slide. **b** Detected area for MALDI IMS. **c** Spatial distribution of compound **10** ( $[M+K]^+$ ,  $m/z$  387.0841). **d** Spatial distribution of compound **11a** and/or **14a** ( $[M+K]^+$ ,  $m/z$  355.0942)<sup>67</sup>

Matrix-assisted laser desorption ionization imaging high-resolution mass spectrometry (MALDI-imaging-HRMS) experiments were performed to visualize the endophytic production and spatial distribution of compounds **10–14** over 16 days in an attempt to understand the plausible ecological relevance (Figure 28).<sup>67</sup> *Colletotrichum* sp. BS4 revealed some typical morphological features of the genus<sup>110,280,281</sup> such as the dark-colored, thick-walled hyphal clumps (setae) (Figure 28a), which was the primary site of production of compound **10** as well as compound **11a** and/or **14a** within only a few days of culturing on rice agar.<sup>67</sup> However, it was interesting to note that compound **10** was secreted into agar after production, while compound **11a/14a** was localized at the site of production at or around the hyphal clumps (Figure 28c, d).<sup>67</sup> From the ecological point of view, some interesting connotations could be made.<sup>67</sup> Plant-associated *Colletotrichum* species are known to utilize setae (or associated appressoria) for attachment to host surface for penetration into the host tissue.<sup>67,281</sup> Concomitantly, it was noteworthy that the bioactive compound **10** diffused away from the site of production (hyphal clump) by the endophyte while retaining the less active compound **11a/14a** (Table 9) at the hyphal clumps where they were produced.<sup>67</sup> It might be plausible that compound **10** is removed from the site of production by the endophyte, which is also the possible site of its association with the host plant, in order to avoid activation of the plant immune signals and/or to prevent it from interfering with the endophyte-mediated ecological balance in plant tissues.<sup>67,282</sup> This is further coincident with its proposed biosynthetic pathway (Figure 26) that **14a** is the lesser-active precursor of the potent bioactive compound **10**.

### 2.9 Discussion

Endophytic fungi are considered as a rich source of functional metabolites, owing to their specialized niches.<sup>34,35</sup> Given that endophytic fungi can increase the ecological adaptability of host plants,<sup>34,35</sup> these endophytic fungi are supposed to be relevant to the

tolerance of *B. sinica* towards biotic or abiotic stresses. *B. sinica* is widely used as boxwood and cut into different shapes. These anti-bacterial azaphilones may help the host plant to defend against the pathogens invading from wounds, which has proven that we can discover new bioactive compounds based on proposed ecological functions of endophytes. Most importantly, since the most active compound **10** showed insignificant cytotoxicity towards a human cell line, it has the potential to be an anti-bacterial lead compound to develop new antibiotics in further investigation.

### **3. Lactam-fused 4-pyrones producing endosymbiotic community comprising of endophytic fungus *P. capitalensis* BS5 and its endosymbiotic bacterium *Herbaspirillum* sp. BS5B**

#### 3.1 Identification of fungus *P. capitalensis* BS5 and endosymbiotic bacterium *Herbaspirillum* sp. BS5B

In the research of endophytes harbored in traditional Chinese medicinal plant *Buxus sinica*, endophytic fungus BS5 was isolated from healthy leaves on water agar. This fungus was identified and characterized to be *Phyllosticta capitalensis* BS5 (teleomorph *Guignardia mangiferae*) harboring an endosymbiotic bacterium *Herbaspirillum* sp. BS5B, based on ITS and 16S rRNA analysis of the total genomic DNA of fungal culture following previously established methods.<sup>54,130,252</sup> Briefly, the sequences were matched against the nucleotide database of the US National Centre for Biotechnology Information (NCBI) using the Basic Local Alignment Search Tool (BLASTn) and aligned using the EMBOSS-Pairwise Sequence Alignment of the EMBL Nucleotide Database.<sup>130</sup> The ITS and 16S rRNA sequences have been deposited at the EMBL Bank (accession numbers LN828209 and LN864763, respectively).<sup>130</sup> The presence of endosymbiotic bacterium *Herbaspirillum* sp. BS5B within fungal mycelia was confirmed by the amplification of highly conserved 16S rRNA region<sup>283</sup> using fungal DNA as template.<sup>130</sup> As a negative control template DNA was replaced with sterile double distilled water.<sup>130</sup> Amplification of 1500 bp (base pairs) fragment in endophytic fungal isolate BS5 and its absence in negative control confirmed the presence of endosymbiotic bacterium within fungal

## Chapter 5: Results & discussion

---

mycelia (Figure 29).<sup>130</sup> In this case, however, free living endosymbiotic bacterium is not yet isolated in the laboratory conditions. Moreover, it was observed that the amplification of 16S rRNA from the fungal metagenome was related to the subculture generation of fungus.<sup>130</sup> The positive band was amplified only when PCR analysis was performed using template DNA of first generation fungal isolate (mother plate).<sup>130</sup> Repeated subculturing resulted in loss of the desired fragment (data not shown), which pointed towards the loss of endosymbiotic bacterium, when culturing the fungus under *in vitro* conditions different to that of its ecological niche.<sup>130</sup>

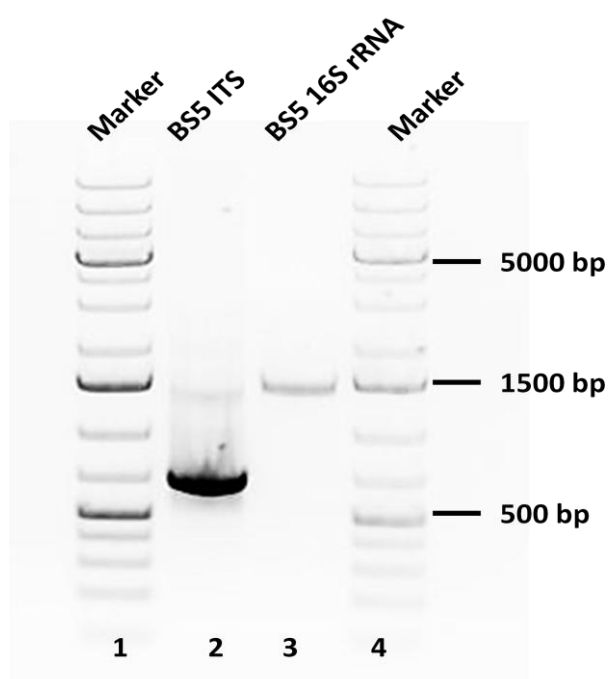


**Figure 29.** Stained agarose gels of purified PCR products of ITS and 16S rRNA sequences of total genomic DNA of endophytic fungal isolate BS5 harbored in *Buxus sinica*. An approximately 600 bp (sample 2) and 1500 bp (sample 3) band obtained for fungal isolate BS5 and its bacterial endosymbiont

### 3.2 Structural elucidation of compounds **15** and **16**

As the OSMAC (One Strain Many Compounds) approach<sup>255</sup> utilized in our former investigation on endophytes,<sup>69,78</sup> different media and conditions were screened for the fermentation of this fungus. In static PDB, two new compounds phyllostictalactam A and



## Chapter 5: Results & discussion

B (**15** and **16**) (Figure 30) was detected in the ethyl acetate (EtOAc) extracts of both mycelia and broth by LC-HRMS.<sup>130</sup>

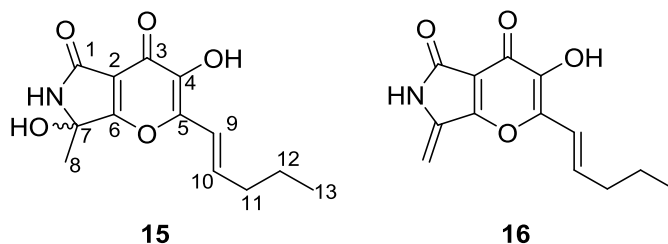


**Figure 30.** The structures of compound **15** and **16**

Compound **15** was purified as a colorless powder from by C<sub>18</sub> column on semi-preparative HPLC from large scale fermentation media.<sup>130</sup> The formula C<sub>13</sub>H<sub>15</sub>O<sub>5</sub>N of compound **15** was determined by ESI-HRMS.<sup>130</sup> The <sup>1</sup>H NMR spectrum showed a typical n-propyl group consisting of δ<sub>H</sub> 2.07 (2H, dt, *J* = 7.4, 6.0 Hz), 1.57 (2H, dq, *J* = 7.4, 7.4 Hz) and 0.99 (3H, t, *J* = 7.4 Hz), two *trans* double bond protons δ<sub>H</sub> 6.62 (1H, d, *J* = 16.0 Hz) and 6.66 (1H, d, *J* = 16.0, 6.0, Hz), one singlet of methyl group at δ<sub>H</sub> 1.78 (3H, s) and one deuterium exchangeable proton at δ<sub>H</sub> 7.76 (1H, br s) (Table 10).<sup>130</sup>

**Table 10.** <sup>1</sup>H and experimental <sup>13</sup>C NMR, and HMBC correlations of compound **15** (acetone-*d*<sub>6</sub>)<sup>130</sup>

Position	<sup>1</sup> H NMR ( <i>J</i> in Hz)	Exp. <sup>13</sup> C NMR	HMBC correlations
1	-	164.0	
2	-	110.5	
3	-	176.3	
4	-	82.9	
5	-	169.2	
6	-	142.5	
7	-	145.5	
8	1.78, 3H, s	23.3	C-3, C-4
9	6.62, 1H, d, <i>J</i> = 16.0	118.0	C-7
10	6.66, 1H, d, <i>J</i> = 16.0, 6.0	137.1	C-7, C-9, C-11, C-12
11	2.07, 2H, dt, <i>J</i> = 7.4, 6.0	35.4	C-7, C-9, C-10, C-12, C-13
12	1.57, 2H, dq, <i>J</i> = 7.4, 7.4	22.2	C-10, C-11, C-13
13	0.99, 3H, t, <i>J</i> = 7.4	13.5	C-11, C-12
HN	7.76, 1H, br s	-	C-1, C-2, C-3, C-4, C-5,

The <sup>13</sup>C NMR and HSQC spectra displayed thirteen carbons including two methyl groups, two methylene groups, two olefinic methine groups and other seven quaternary

## Chapter 5: Results & discussion

---

carbons (Table 10), suggesting two more deuterium exchangeable protons which were not observed in  $^1\text{H}$  NMR spectrum.<sup>130</sup> In the HMBC experiment (Table 10), the lack of available protons around the core structure caused difficulties for determining the planar structure and only the side chain namely 1-pentene substructure can be confirmed by 2D NMR.<sup>130</sup>

Herein, the 1D and 2D NMR technologies can hardly resolve this structure elucidation of compound **15**. Unfortunately, to date all efforts to culture the single crystal of compound **15** proved futile, and consequently X-ray diffraction experiment was not feasible either. The chemical shifts of C-1, C-3 and C-5 showed they are carbonyl groups or  $\beta$  position of unsaturated ketone. Therefore, there are only dozens of structures possible and GIAO DFT  $^{13}\text{C}$  NMR calculation can be applied to verify those proposed structures. The GIAO shielding constants were calculated on mPW1PW91/6-31+G(d) level of theory,<sup>284</sup> using MeOH and benzene as references for  $sp^3$  and  $sp^2$  hybridized carbons respectively.<sup>207</sup> To increase the efficiency, the maximum gradient of geometry optimization for candidate structures was set to threshold 0.001 (default value is 0.0001) and only their global minimum conformers (calculated by semi-empirical PM3 method) were calculated. After the first screen, only the structure **15** as depicted in Figure 30 has maximum absolute deviation within 10 ppm. Then geometry optimization and frequency calculations were further performed for all the conformers of structure **15**, and the calculated  $^{13}\text{C}$  NMR data of them were Boltzmann averaged according to Gibbs free energy (Table 11).<sup>130</sup> Owing to the energy barrier, some conformers are not able to interchange freely.<sup>130</sup> The detected  $^{13}\text{C}$  NMR signals may not be the dynamically averaged value of all conformers in some cases, and the Boltzmann averaged data are not always better than the global minimum conformer.<sup>130,207</sup> Therefore, the data of global minimum conformer and averaged data of different sets of conformers were all considered in order to confirm the proposed structure (Table 11).<sup>130</sup> According to the reported standard and many applied cases,<sup>197,202–206</sup> the MAE showed high agreement between experimental data and calculated data.<sup>130</sup> Compared to the reported compound cordylactam, the  $^{13}\text{C}$  NMR data are similar except the significant difference at position 4 (cordylactam,  $\delta_{\text{C}}$  50.3; compound **15**,  $\delta_{\text{C}}$  82.9) and Me-8 (cordylactam,  $\delta_{\text{C}}$  17.8; compound **15**,  $\delta_{\text{C}}$  23.3).<sup>173</sup> Thus, the planar structure of compound **15** can be determined affirmatively. The optical

## Chapter 5: Results & discussion

rotation and CD effect of compound **15** can be barely detected, which revealed it is a mixture of enantiomers.<sup>130</sup>

**Table 11.** Experimental <sup>13</sup>C NMR, calculated <sup>13</sup>C NMR data of global minimum conformer (G. M.), and Boltzmann averaged data of *s-trans*, *s-cis* and all conformers

Position	Exp. data	G. M.		S- <i>trans</i> (64.48%)		S- <i>cis</i> (35.52%)		All conformers	
		Data	Error	Data	Error	Data	Error	Data	Error
1	164.0	163.2	-0.8	163.3	-0.7	163.4	-0.6	163.3	-0.7
2	110.5	110.8	0.3	110.8	0.3	110.2	-0.3	110.6	0.1
3	176.3	177.3	1.0	177.3	1.0	177.0	0.7	177.2	0.9
4	82.9	80.8	-2.1	80.8	-2.1	81.0	-1.9	80.9	-2.0
5	169.2	165.9	-3.3	165.9	-3.3	165.5	-3.7	165.8	-3.4
6	142.5	143.4	0.9	143.5	1.0	145.5	3.0	144.2	1.7
7	145.5	145.8	0.3	145.9	0.4	146.8	1.3	146.2	0.7
8	23.3	23.0	-0.3	23.0	-0.3	22.7	-0.6	22.9	-0.4
9	118.0	119.5	1.5	119.2	1.2	122.7	4.7	120.5	2.5
10	137.1	142.7	5.6	142.2	5.1	149.1	12.0	144.6	7.5
11	35.4	36.0	0.6	36.0	0.6	37.0	1.6	36.4	1.0
12	22.2	22.4	0.2	23.4	1.2	23.1	0.9	23.3	1.1
13	13.5	12.6	-0.9	12.5	-1.0	12.3	-1.2	12.4	-1.1
		<b>MAE</b>	1.4	<b>MAE</b>	1.4	<b>MAE</b>	2.5	<b>MAE</b>	1.8

\*MAE is an abbreviation of mean absolute error

Compound **16** was detected by LC-ESI-HRMS with formula C<sub>13</sub>H<sub>13</sub>O<sub>4</sub>N determined, which has one less H<sub>2</sub>O than compound **15**.<sup>130</sup> However, I failed to use conventional chromatographic methods to purify it, because of its poor stability and insufficient quantity during the process of purification.<sup>130</sup> By the dehydration reaction of compound **15** (Figure 31),<sup>285</sup> I confirmed the product is exactly compound **16** with the same retention time and MS<sup>2</sup> fragmentation in LC-MS<sup>n</sup> measurement (Chapter 8, Figure S56 and S57).<sup>130</sup>

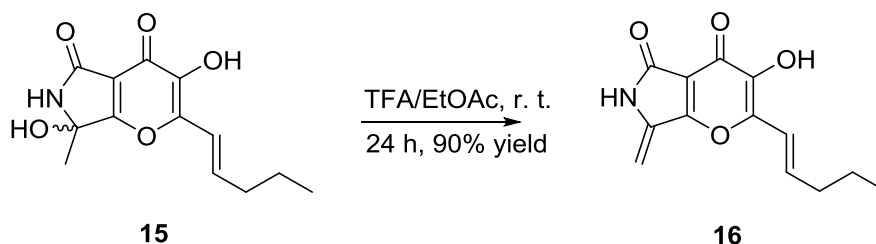


**Figure 31.** Semi-synthesis of compound **16**<sup>130</sup>

### 3.3 Biosynthetic pathway of compounds **15** and **16**

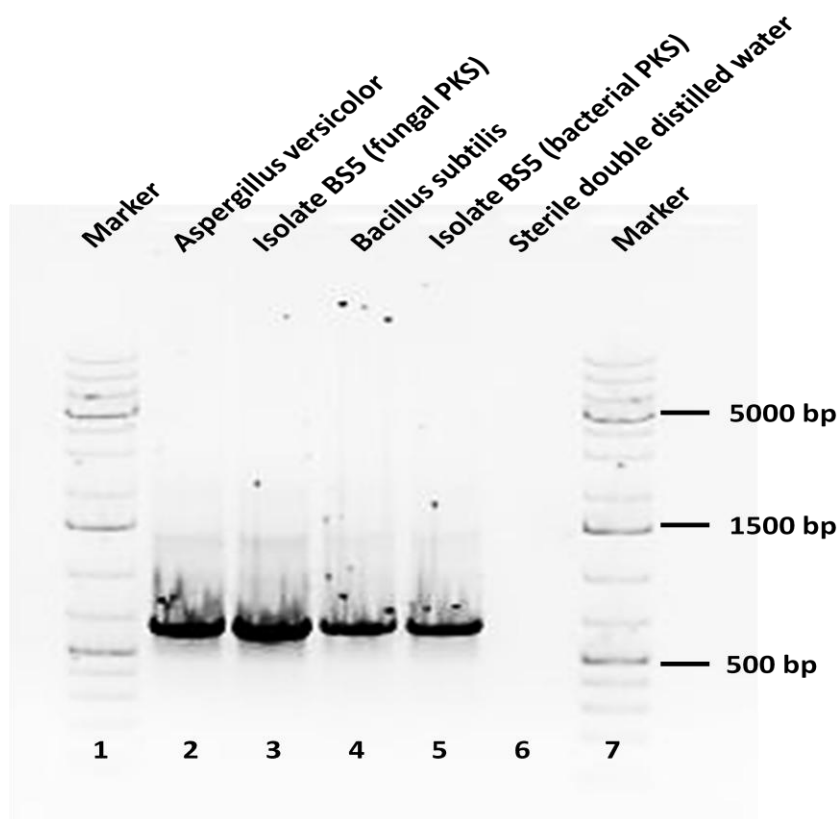


**Figure 32.** Stained agarose gels of purified PCR products of polyketide synthase genes (PKS; spanning around 700 bp) of endophytic isolate BS5 (harboring bacterial endosymbiont). An approximately 700 bp PKS band amplified for isolate BS5 using both bacterial and fungal PKS degenerate primers (sample 3 and 5), although both PKS bands encode for fungal polyketide. *Aspergillus versicolor* (isolate A12)<sup>252</sup> (sample 2) and *Bacillus subtilis* (DSM 1088) (sample 4) are the positive controls and sterile double distilled water is the negative control (sample 6)<sup>130</sup>

Similar compounds such as cordylactam,<sup>173</sup> and pyranonigrin A, E, F, G, H, and S<sup>172,175–179</sup> were isolated from *Cordyceps* sp. and *Aspergillus niger*.<sup>130</sup> The isotope labeling experiment<sup>172</sup> and gene mining<sup>179</sup> showed that these compounds are biosynthesized via hybrid PKS/NRPS pathways.<sup>130</sup> Considering the case that endosymbiotic *Burkholderia* bacteria was unveiled to be the hidden producers of

## Chapter 5: Results & discussion

fungal phytotoxin,<sup>234,286,287</sup> we evaluated the fungal and bacterial PKS and NRPS to assign the production of compounds **15** and **16**.<sup>130</sup>

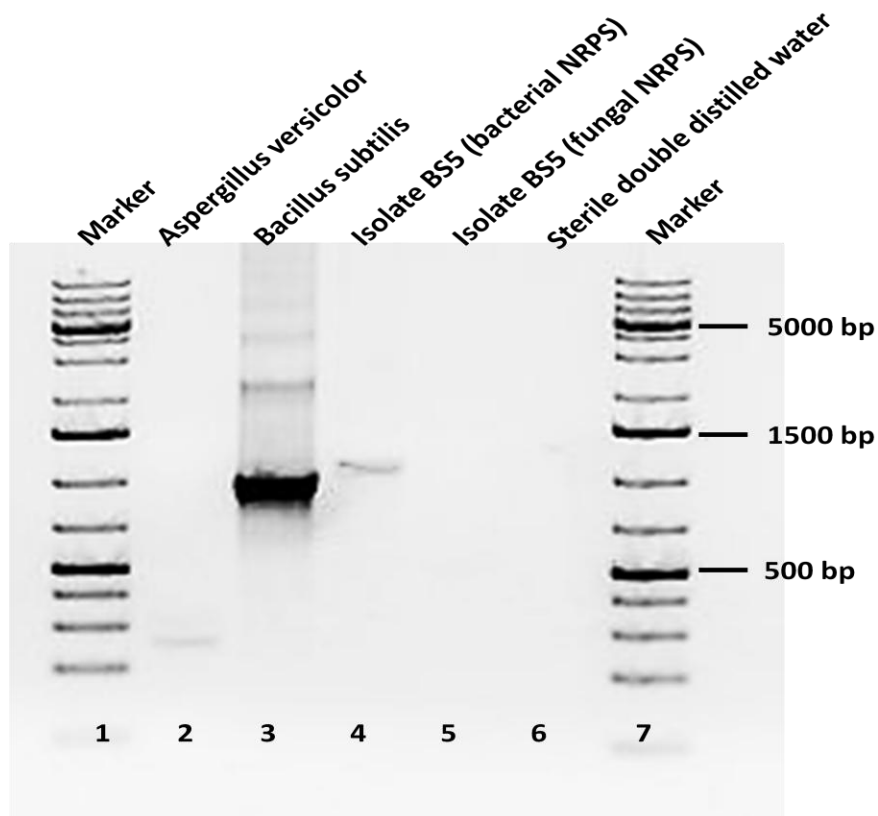


**Figure 33.** Stained agarose gels of purified PCR products of nonribosomal peptide synthetase (NRPS; spanning around 300 bp for fungus and 1000 bp for bacterium) of endophytic isolate BS5 (harboring bacterial endosymbiont). No NRPS band present in fungal isolate BS5 (sample 5), but an approximately 1000 bp NRPS band amplified for bacterial endosymbiont of isolate BS5 (sample 4). *Aspergillus versicolor* (isolate A12)<sup>252</sup> (sample 2) and *Bacillus subtilis* (DSM 1088) (sample 3) are the positive controls and sterile double distilled water is the negative control (sample 6)<sup>130</sup>

Production of secondary metabolites usually comprises of a combination of PKS and NRPS,<sup>253,288</sup> that often forms PKS-NRPS hybrids determining the structure and biological activity of resulting natural products.<sup>130</sup> For the identification of PKS, degenerate primers were designed based on genes encoding the highly

## Chapter 5: Results & discussion

---

conserved KS domain of fungal and bacterial isolates as described in literature.<sup>130,249–251</sup> As expected, the degenerate primers amplified the desired 700 bp fragments in positive controls *Bacillus subtilis* and *Aspergillus versicolor* under optimized PCR cycling conditions.<sup>130</sup> The amplified fragments were sequenced, translated into respective protein sequences and matched using UniProtKB showing homology to polyketide synthases (M4KVE6 and W5S7R8) of positive controls.<sup>130</sup>

Thereafter, the template DNA of fungal endophyte harboring bacterial endosymbiont was subjected to PCR amplification with same degenerate primers.<sup>130</sup> This resulted in amplification of 700 bp fragment with fungal and bacterial PKS primers (Figure 32).<sup>130</sup> The obtained positive sequences were purified, sequenced and matched using the Basic Local Alignment Search Tool (BLASTn) of NCBI.<sup>130</sup> Even though both degenerate primers amplified the desired positive fragments, the amplified fragments showed 95% identity only with polyketide synthase gene of *Guignardia* sp. (JX144685.1) (teleomorph of genus *Phyllosticta*), which is a fungal polyketide synthase gene.<sup>130</sup> The sequences were further translated to respective protein sequences using UniProtKB showing 76.6% identity with fungal polyketide synthase (V5FKW9).<sup>130</sup> Thus this proved that the PKS originated from the endophytic fungus BS5 and not the endosymbiotic bacterium.<sup>130</sup>

For the identification of NRPS, degenerate primers were designed based on genes encoding the conserved adenylation domain (A) of fungal and bacterial isolates as described in literature.<sup>130,251,253,254</sup> As expected, the degenerate primers amplified the desired 1000 bp fragment in positive control *Bacillus subtilis* and 300 bp fragment in positive control *Aspergillus versicolor* under optimized PCR cycling conditions.<sup>130</sup> The amplified fragments were sequenced, translated into respective protein sequences and matched using UniProtKB showing homology to nonribosomal peptides of positive controls.<sup>130</sup> Henceforth, the template DNA of fungal endophyte harboring bacterial endosymbiont was subjected to PCR amplification with same degenerate primers.<sup>130</sup> This resulted in amplification of 1000 bp fragment of bacterial NRPS (Figure 33).<sup>130</sup> No

## Chapter 5: Results & discussion

amplification of fungal NRPS was observed.<sup>130</sup> The positive sequence thus obtained was purified and sequenced.<sup>130</sup> Unfortunately, the fragment did not yield any sequencing results.<sup>130</sup> On rechecking the purified fragment by agarose gel electrophoresis, it was found that the single band was separating into two bands; one at 1000 bp and another at 700 bp (fragment size similar to fungal PKS).<sup>130</sup> On repeating the purification and separation steps, similar result was always obtained (Figure 34).<sup>130</sup> It pointed towards the fact that there might be presence of PKS-NRPS hybrid in endophytic fungus BS4 harboring the endosymbiotic bacterium which could not be separated from the fungal PKS by general PCR amplification methods using degenerate primers.<sup>130</sup>



**Figure 34.** Stained agarose gels of separating the purified 1000 bp fragment of bacterial NRPS resulting in 1000 bp fragment and 700 bp fragment (similar to fungal PKS).<sup>130</sup>

### 3.4 Discussion

In the previous research, Kusari *et al.* demonstrated that the cross-species biosynthesis pathway of camptothecin consists of endophytic precursor biosynthesis and the final condensation of host plant,<sup>39,95,130</sup> and also elaborated that endophytic bacteria harboured in the roots of *Putterlickia verrucosa* and *P. retrospinosa* are the producer(s) of maytansine.<sup>54,130</sup> Furthermore, the investigation of the biosynthesis of rhizoxin showed that the bacterial

## Chapter 5: Results & discussion

endosymbiont produced the basic scaffold and the host fungus involved in core structure tailoring.<sup>130,289</sup> To our best knowledge, however, the cross-species collaboration of hybrid PK/NRP backbone biosynthesis is firstly reported in fungus-bacterium endosymbiotic system in this article (Figure 35).<sup>130</sup>

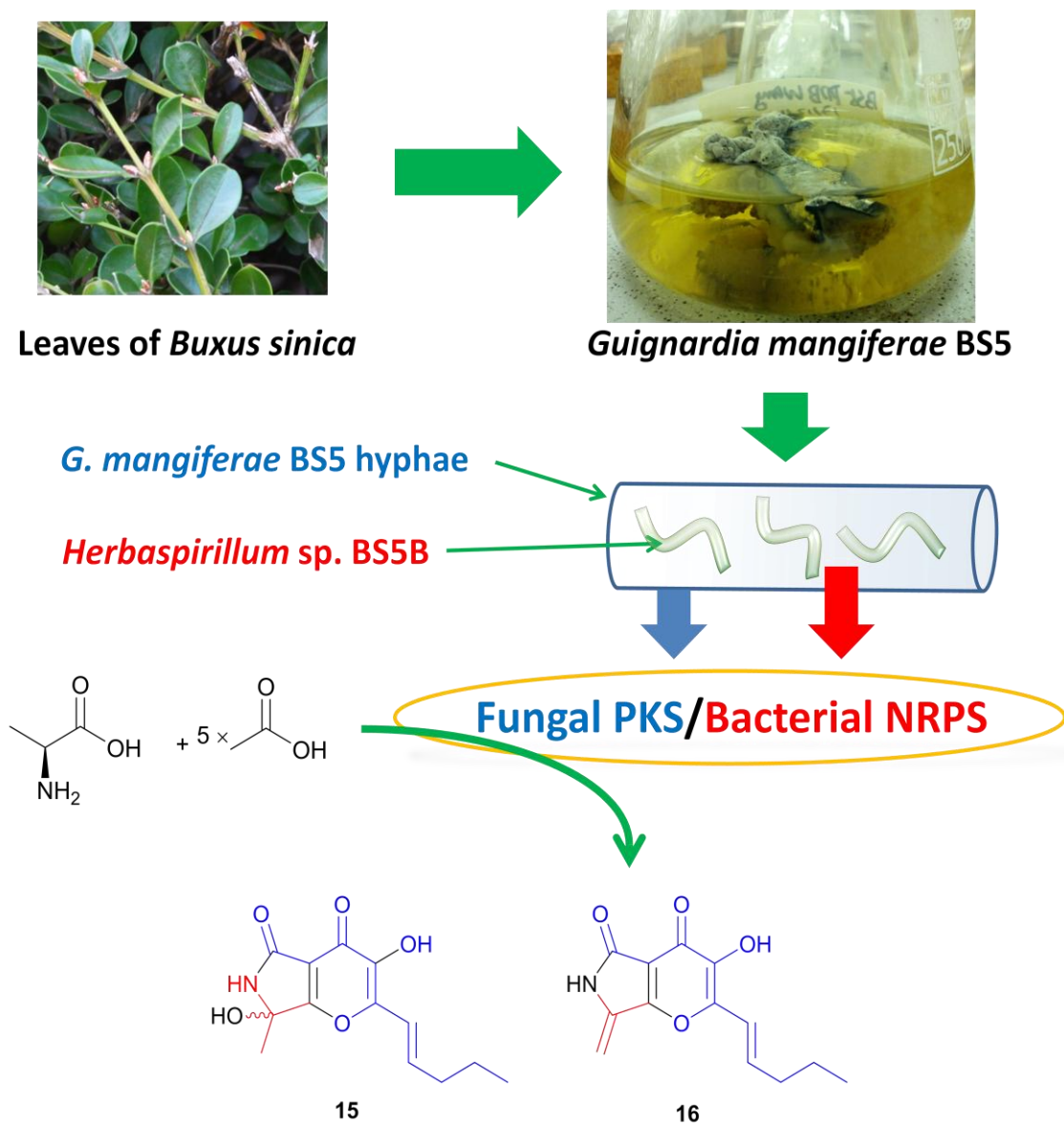


**Figure 35.** Biosynthetic pathway of compounds **15** and **16**<sup>130</sup>

Endophytic communities consisting of host plants and endophytes are complex ecological systems. In previous reports, a number of “plant” natural products could be actually produced or partially biosynthesized by associated endophytes.<sup>18,130</sup> The



## Chapter 5: Results & discussion

---

endosymbiotic scenarios of endophytes, furthermore, lead to probably a higher level of complexity of endophytic interactions,<sup>18,130</sup> which could be another challenge for the future investigation. These hidden endosymbiotic endophytes and their corresponding functions are likely essential parts of the whole interaction network of the endophytic system.<sup>130</sup>

**Chapter 6**  
**CONCLUSION & OUTLOOK**

### 1. Conclusion

In this work, the discovery of these cryptic hexacyclopeptides showed that the standard procedure herein is robust and efficient to investigate secondary metabolites produced by endophytes including the compounds with only physiological concentration. The structures of hexacyclopeptides were elucidated by LC-MS<sup>n</sup>, with the information of their building blocks determined. Considering the D-amino acids could also be building blocks in cyclopeptides (because of the E domain of NRPS pathways), however, the relative configurations cannot be assigned. Although the  $\alpha$ -deuterated amino acids of all building blocks were successfully obtained, it still did not work following the reported methods of absolute configuration assignment for cyclopeptides,<sup>261</sup> because of the transaminase in the fungal cells. In the literature, they knocked out corresponding genes of transaminases in the host bacteria.<sup>261</sup> The same strategy could also be applied on the strain *F. solani* N06. Whereas, the corresponding genes in eukaryotes are different from prokaryotes, whose structures and functions should be investigated in future work. Herein, the deuterium labeling experiment is a very important method to determine whether the natural products are produced by this fungus. Moreover, by labeled Leu/Ile precursors and proline derivatives the planar structure of each compound (**1–9**) could also be determined. The bottleneck, however, is the lack of available fungal materials of this strain because of the degeneration of the production of these hexacyclopeptides, which hampered further labeling experiments. The visualization of the chemical crosstalk between the two endophytes unambiguously supported the hypothesis of signaling interactions among endophytic niches. This case also exemplified the idea of “distribution represents functions”, which could be developed as a routine method for future research of secondary metabolites from endophytes. However, beside the accumulation and degradation behavior of the neighbor bacterium, no in-depth function can be deciphered for now, which could be a blind spot of current methods. In the future, the investigation on the possible cascade pathway of this signaling system should be emphasized, because it could lead to the interpretation of many functions of the endophytic system in their host plants.

From the endophytic *Colletotrichum* sp. BS4 harbored in the leaves of *B. sinica*, azaphilones were purified and elucidated by extensive spectroscopic methods, X-ray

diffraction as well as quantum chemical calculations. Notably, compound **10** exhibited even higher activities against *E. coli* and *B. subtilis* than selected antibiotics in the antibacterial assay. Considering they didn't show significant cytotoxicity towards the human cancer cell line, they could have the potential to be developed as a group of antibiotics with different core structure from the known antibacterial drugs. This case also exemplified that promising microbial sources of natural products could be isolated from the niches with evolutionary traits corresponding to bioactivities. For the next research, *in vivo* experiments including bioassay on animal models are necessary for us to determine whether they can be applied as efficiently and safely as antibiotics.

The endophytic fungus *P. capitalensis* BS5 was isolated from the leaves of *B. sinica*, with a cryptic endosymbiotic bacterium *Herbaspirillum* sp. BS5B detected by 16S rRNA analysis. This fungus produced lactam-fused 4-pyrones (**15** and **16**) in static PDB medium. To determine their producer(s), metagenome evaluation towards PKS and NRPS was performed, revealing the PKS gene was from this fungus while NRPS gene was from the endosymbiotic bacterium. However, the bacterial NRPS was not successfully sequenced. The further studies including full gene sequence of both microorganisms along these lines will be underway. To my best knowledge, this is the first report of cooperation of PKS/NRPS biosynthesis for endophytes. In the view of co-evolution, these compounds are supposed to have one or more ecological functions regarding endosymbiotic relationship. So far, however, no bioactivity of these compounds was detected within current bioassay or co-culture experiments. The mutants of this fungus with defection of biosynthesis or the endosymbiont-free strain of this fungus could be important negative controls to unveil the true biofunctions of these compounds, which may be obtained in future research.

## **2. Interspecies chemical crosstalks among endophytic communities**

The association of microbes with higher plants or animals is a common phenomenon in nature. Recently, Wada-Katsumata *et al.* demonstrated that the gut microbial community is responsible for the production of aggregation pheromones for the host German cockroach.<sup>67,290</sup> Moreover, Santhanam *et al.* reported that root-associated bacterial

## Chapter 6: Conclusion & Outlook

---

community of tobacco plants (*Nicotiana attenuata*) in their native habitat increased the resistance and survivability of host plant towards sudden tissue collapse and black roots significantly.<sup>67,291</sup> The consortium of bacteria rather than any single member in the bacterial community provides protection for the host plant, which revealed that prokaryotes and plants have developed opportunistic mutualisms by co-evolution.<sup>67,291</sup> It is widely accepted that, in most ecological niches comprising of multiple members including endophytic systems, organisms are not simply living together but maintaining complex relationships encompassing each member.<sup>67</sup>

Co-evolving for millions of years, endophytes and plants have already developed many strategies to survive with the presence of each other and change their living status to adapt towards coexistence. For example, Lahrmann *et al.* reported how endophytic fungus *Piriformospora indica* evades the defense of host plants like *Arabidopsis* by establishing a biotrophic interaction.<sup>67,292</sup> At the early stage of colonization, *P. indica* interferes with the plant hormone level and secretes fungal lectins and small proteins to suppress host defenses.<sup>67,292</sup> Then, *P. indica* grows in moribund host cells and secretes hydrolytic enzymes to digest proteins.<sup>67,292</sup> However, the invasion does not cause massive host cell death as other necrotrophic or hemibiotrophic fungi, but benefit the host plant by providing it tolerance to biotic and abiotic adversities.<sup>67,292</sup> Moreover, the colonization of endophytes can also influence the gene expression of both endophytic fungi and host plants. Bailey *et al.* reported that when bio-control endophytic *Trichoderma* species colonize into host plant (*Theobroma cacao*), a number of genes of both fungal and plant are induced or repressed.<sup>67,293</sup> The switch-on/off of genes reveals that fungal endophytes and their hosts have established a genetic crosstalk system during the endophytic association.<sup>67,293</sup> Therefore, separating endophytic fungi from their habitat (host plant tissue) will probably alter their genotypic as well as phenotypic characteristics, including the biosynthetic genes responsible for producing certain secondary metabolites.<sup>67</sup> Some metabolites or pathways are only necessary for microbes in the endophytic life cycles, and they will shut them down in the environments without association with plants.<sup>67</sup> This may be the reason why *F. solani* N06 stopped producing these crosstalk molecules in laboratory conditions.

It is also worth to note that the crosstalk hexacyclopeptides are structurally different from previously reported microbial signal molecules, including acyl-homoserine lactones (AHLs), AI-2, CAI-1 related  $\alpha$ -hydroxy ketones (AHKs), ComX pheromones, diffusible signal factors (DSFs), diffusible extracellular factor (DF), and *Phytophthora* mating hormones.<sup>80</sup> There are many coexisting micro- and macro-organisms including cells of host plant, other endophytes as well as their endosymbiotic bacteria in the natural niches of endophytes. Because of unique adaptive traits and natural selection, endophytes may develop specialized signaling systems, which are independent on the ones of other microbes including invading pathogens. Kusari *et al.* reported that endophytic bacteria employ quorum quenching strategy to defend host plant against virulent microbes.<sup>246</sup> Given that these endophytic bacteria are not influenced by quorum quenching strategy, their quorum sensing systems are likely different from common ones including AHLs systems. Therefore, utilizing unique crosstalk molecules can provide endophytic system advantages to keep balance and to prevent external interferences.

Nevertheless, similar to the multiple functions of other signaling systems,<sup>80</sup> the endophytic signaling systems may also have extensive functions including awareness of population density, regulating secondary metabolites production, the formation of inner-species or inter-species biofilm, dormancy, and competence as well as influencing the behavior of host plants. Comprehending these functions is crucial for us to exploit the potential of endophytes and reveal their ecological roles.

### 3. Endophytes are rich resource of bioactive compounds

Scientists have been aware of that endophytes are a bonanza of bioactive compounds for pharmaceutical development in the recent two decades, because many endophytes benefit host plant by producing bioactive secondary metabolites.<sup>35</sup> Every year, there are many bioactive natural products reported from different microorganisms.<sup>294</sup> Because of toxicity or non-selectivity, however, many bio-active compounds cannot be applied as clinical medicines. Whereas, these antibacterial azaphilones from *Colletotrichum* sp. BS4 showed ignorable cytotoxicity towards human cell line at the same order of magnitude of active concentration towards tested environmental bacteria, which could be interesting for further pharmaceutical investigation. This discovery also provides us

insights to consider the strategy of endophytes to produce bioactive compounds. In a balanced endophytic system, the defending factors produced by endophytes ought to be less toxic towards host plant cells and other endophytes than pathogens or predators. These special selective stress may be the driving force for endophytes to produce selective defending secondary metabolites, from which the possibility to discover promising drug lead might be higher than from other origins. For example, cytotoxic and antimicrobial maytansine was determined to be produced by the endophytic bacterial community harbored in the roots of *Putterlickia* plants, which obviously has an impact on other coexisting organisms.<sup>54,67</sup> However, host plant cells and the endophytic bacterial community of the plant are immune to the toxicity of maytansine over an evolutionary period.<sup>54</sup>

### **4. Perspectives for investigating secondary metabolites of endophytes**

There are many well-established chemical or biological techniques in recent years, including genome mining and genetic modification, biosynthetic pathways engineering in heterologous organisms, and direct utilization of enzymes to synthesize target compounds.<sup>67</sup> However, many bottlenecks still need to be overcome to investigate endophytes comprehensively. For example, the relevant biosynthetic pathway of paclitaxel has not been successfully constructed correctly in heterologous hosts, because the mechanism of several key biosynthetic steps is still not clear.<sup>63</sup>

Moreover, discerning fermentation methods employing strategies like OSMAC,<sup>255</sup> dual and multiple/mixed cultures<sup>295</sup> can hardly introduce the natural triggers into artificial conditions or mimic the natural endophytic environment.<sup>67</sup> The reason is that the endophytic communities consist of many other cryptic microorganisms (including endophytes besides bacteria and fungi, for example, endophytic viruses) that are influenced by an enormous number of ambient factors.<sup>67,296</sup>

Presently, the *in situ* approaches used to investigate uncultured microorganisms may provide useful clues to reconstruct the natural conditions for endophytes in the laboratory,<sup>67,219</sup> which might enable us to figure out the reason why some endophytes

## Chapter 6: Conclusion & Outlook

---

stop producing these interesting compounds. Furthermore, in this case, the application of IMS exemplified a strategy to visualize, both spatially and temporally, the chemical communication between endophytes (fungi and bacteria), and discover important secondary metabolites at low physiological concentrations and in a short available window (because of gradual degeneration of endophytes in artificial conditions). IMS technology also allows us to visualize the functional compounds produced by endophytes in plant tissues directly.<sup>54</sup> With these approaches, future investigation of natural products ought to connect bioactive compounds with their ecological functions, rather than only document their structures and bioactivities.

Despite the high sensitivity of MS technology for detecting microbial secondary metabolites, the structures of complex compounds with many isomers cannot be satisfactorily elucidated merely by MS or MS<sup>n</sup>. To elucidate natural products besides peptides, such as terpenoids and polyketides, conventional purification and characterization by other technologies (including 1D and 2D NMR, X-ray diffraction) are indispensable. Therefore, these unknown compounds with only traceable amount (insufficient for NMR or X-ray diffraction analysis) can barely be fully elucidated by current technologies.

With sufficient pure compounds, however, wrong structural assignments of natural products are still very common,<sup>192,193</sup> even though scientists had X-ray diffraction data in some cases.<sup>297–299</sup> In the structure elucidation of compounds **11**, **13** and **15**, different quantum chemical methods including ECD, structural geometry, and NMR property calculations were employed to assign the relative configuration or the planar structure, which is difficult to be solved by other conventional technologies. As many other cases reported in literature,<sup>300–303</sup> it is compelling that the combination of many other innovative technologies will be routine strategy for structural elucidation.



# Chapter 7

# REFERENCES

## Chapter 7: References

---

- (1) Divakar, P. K.; Crespo, A.; Wedin, M.; Leavitt, S. D.; Hawksworth, D. L.; Myllys, L.; McCune, B.; Randlane, T.; Bjerke, J. W.; Ohmura, Y.; Schmitt, I.; Boluda, C. G.; Alors, D.; Roca-Valiente, B.; Del-Prado, R.; Ruibal, C.; Buaruang, K.; Núñez-Zapata, J.; Amo de Paz, G.; Rico, V. J.; Molina, M. C.; Elix, J. A.; Esslinger, T. L.; Tronstad, I. K. K.; Lindgren, H.; Ertz, D.; Gueidan, C.; Saag, L.; Mark, K.; Singh, G.; Dal Grande, F.; Parnmen, S.; Beck, A.; Benatti, M. N.; Blanchon, D.; Candan, M.; Clerc, P.; Goward, T.; Grube, M.; Hodkinson, B. P.; Hur, J.-S.; Kantvilas, G.; Kirika, P. M.; Lendemer, J.; Mattsson, J.-E.; Messuti, M. I.; Miadlikowska, J.; Nelsen, M.; Ohlson, J. I.; Pérez-Ortega, S.; Saag, A.; Sipman, H. J. M.; Sohrabi, M.; Thell, A.; Thor, G.; Truong, C.; Yahr, R.; Upreti, D. K.; Cubas, P.; Lumbsch, H. T. *New Phytol.* **2015**, *208* (4), 1217–1226.
- (2) Goh, C.-H.; Vallejos, D. F. V.; Nicotra, A. B.; Mathesius, U. *J. Chem. Ecol.* **2013**, *39* (7), 826–839.
- (3) Christian, N.; Whitaker, B. K.; Clay, K. *Front. Microbiol.* **2015**, *6*, 1–15.
- (4) Partida-Martínez, L. P.; Heil, M. *Front. Plant Sci.* **2011**, *2*, 100.
- (5) Vorholt, J. A. *Nat. Rev. Microbiol.* **2012**, *10* (12), 828–840.
- (6) Ryffel, F.; Helfrich, E. J.; Kiefer, P.; Peyriga, L.; Portais, J.; Piel, J.; Vorholt, J. A. *ISME J.* **2016**, *10* (3), 632–643.
- (7) Schauer, S.; Kutschera, U. *Plant Signal. Behav.* **2011**, *6* (4), 510–515.
- (8) Schellenberg, B.; Ramel, C.; Dudler, R. *Mol. Plant-Microbe Interact.* **2010**, *23* (10), 1287–1293.
- (9) Denison, R. F.; Kiers, E. T. *Microbes Infect.* **2004**, *6* (13), 1235–1239.
- (10) Vessey, J. K. *Plant Soil* **2003**, *255* (2), 571–586.
- (11) Nelson, M. S.; Sadowsky, M. J. *Front. Plant Sci.* **2015**, *6*, 491.
- (12) Spiteller, P. *Nat. Prod. Rep.* **2015**, *32* (7), 971–993.
- (13) van der Heijden, M. G. A.; Martin, F. M.; Selosse, M.-A.; Sanders, I. R. *New Phytol.* **2015**, *205* (4), 1406–1423.
- (14) Nadeem, S. M.; Ahmad, M.; Zahir, Z. A.; Javaid, A.; Ashraf, M. *Biotechnol. Adv.* **2014**, *32* (2), 429–448.
- (15) Liu, X.-M.; Zhang, H. *Front. Plant Sci.* **2015**, *6*, 774.
- (16) Wilson, D. *Oikos* **1995**, *73* (2), 274–276.
- (17) Kusari, S.; Spiteller, M. *Nat. Prod. Rep.* **2011**, *28* (7), 1203–1207.
- (18) Kusari, S.; Hertweck, C.; Spiteller, M. *Chem. Biol.* **2012**, *19* (7), 792–798.
- (19) Kusari, S.; Singh, S.; Jayabaskaran, C. *Trends Biotechnol.* **2014**, *32* (6), 297–303.
- (20) Kusari, S.; Singh, S.; Jayabaskaran, C. *Trends Biotechnol.* **2014**, *32* (6), 304–311.
- (21) Eaton, C. J.; Cox, M. P.; Scott, B. *Plant Sci.* **2011**, *180* (2), 190–195.
- (22) Freeman, S.; Rodriguez, R. J. *Science* **1993**, *260* (5104), 75–78.

## Chapter 7: References

---

- (23) Redman, R. S.; Ranson, J. C.; Rodriguez, R. J. *Mol. Plant Microbe Interact.* **1999**, *12* (11), 969–975.
- (24) Saunders, M.; Glenn, A. E.; Kohn, L. M. *Evol. Appl.* **2010**, *3* (5-6), 525–537.
- (25) Newman, D. J.; Cragg, G. M. *Front. Chem.* **2015**, *3*, 34.
- (26) Hardoim, P. R.; Overbeek, L. S. Van; Berg, G.; Maria, A. *Microbiol. Mol. Biol. Rev.* **2015**, *79* (3), 293–320.
- (27) Sessitsch, A.; Hardoim, P.; Döring, J.; Weilharter, A.; Krause, A.; Woyke, T.; Mitter, B.; Hauberg-Lotte, L.; Friedrich, F.; Rahalkar, M.; Hurek, T.; Sarkar, A.; Bodrossy, L.; van Overbeek, L.; Brar, D.; van Elsas, J. D.; Reinhold-Hurek, B. *Mol. Plant Microbe Interact.* **2012**, *25* (1), 28–36.
- (28) Montesinos, E. *Int. Microbiol.* **2003**, *6* (4), 221–223.
- (29) Romero, A.; Carrion, G.; Rico-Gray, V. *Fungal Divers.* **2001**, *7*, 81–87.
- (30) Lyons, P.; Plattner, R.; Bacon, C. *Science* **1986**, *232* (4749), 487–489.
- (31) Clay, K.; Cheplick, G. P. *J. Chem. Ecol.* **1989**, *15* (1), 169–182.
- (32) Nisa, H.; Kamili, A. N.; Nawchoo, I. A.; Shafi, S.; Shameem, N.; Bandh, S. A. *Microb. Pathog.* **2015**, *82*, 50–59.
- (33) Kusari, P.; Kusari, S.; Spiteller, M.; Kayser, O. *Appl. Microbiol. Biotechnol.* **2015**, *99* (13), 5383–5390.
- (34) Tan, R. X.; Zou, W. X. *Nat. Prod. Rep.* **2001**, *18* (4), 448–459.
- (35) Kharwar, R. N.; Mishra, A.; Gond, S. K.; Stierle, A.; Stierle, D. *Nat. Prod. Rep.* **2011**, *28* (7), 1208.
- (36) Stierle, A.; Strobel, G.; Stierle, D. *Science* **1993**, *260* (5105), 214–216.
- (37) Eyberger, A. L.; Dondapati, R.; Porter, J. R. *J. Nat. Prod.* **2006**, *69* (8), 1121–1124.
- (38) Kusari, S.; Lamshöft, M.; Spiteller, M. *J. Appl. Microbiol.* **2009**, *107* (3), 1019–1030.
- (39) Kusari, S.; Zühlke, S.; Spiteller, M. *J. Nat. Prod.* **2011**, *74* (4), 764–775.
- (40) Puri, S. G.; Verma, V.; Amna, T.; Qazi, G. N.; Spiteller, M. *J. Nat. Prod.* **2005**, *68* (12), 1717–1719.
- (41) Kusari, S.; Zühlke, S.; Spiteller, M. *J. Nat. Prod.* **2009**, *72* (1), 2–7.
- (42) Pu, X.; Qu, X.; Chen, F.; Bao, J.; Zhang, G.; Luo, Y. *Appl. Microbiol. Biotechnol.* **2013**, *97* (21), 9365–9375.
- (43) Shweta, S.; Gurusurthy, B. R.; Ravikanth, G.; Ramanan, U. S.; Shivanna, M. B. *Phytomedicine* **2013**, *20* (3-4), 337–342.
- (44) Rehman, S.; Shawl, A. S.; Verma, V.; Kour, A.; Athar, M.; Andrabi, R.; Sultan, P.; Qazi, G. N. *Prikl. Biokhim. Mikrobiol.* **44** (2), 225–231.
- (45) Zhang, G.; Wang, W.; Zhang, X.; Xia, Q.; Zhao, X.; Ahn, Y.; Ahmed, N.; Cosoveanu, A.; Wang, M.; Wang, J.; Shu, S. *PLoS One* **2015**, *10* (3), e0120809.

## Chapter 7: References

---

- (46) Shu, S.; Zhao, X.; Wang, W.; Zhang, G.; Cosoveanu, A.; Ahn, Y.; Wang, M. *World J. Microbiol. Biotechnol.* **2014**, *30* (12), 3101–3109.
- (47) Zhao, X.-M.; Wang, Z.-Q.; Shu, S.-H.; Wang, W.-J.; Xu, H.-J.; Ahn, Y.-J.; Wang, M.; Hu, X. *PLoS One* **2013**, *8* (4), e61777.
- (48) Wang, Y.; Zeng, Q. G.; Zhang, Z. Bin; Yan, R. M.; Wang, L. Y.; Zhu, D. *J. Ind. Microbiol. Biotechnol.* **2011**, *38* (9), 1267–1278.
- (49) Dong, L.-H.; Fan, S.-W.; Ling, Q.-Z.; Huang, B.-B.; Wei, Z.-J. *World J. Microbiol. Biotechnol.* **2014**, *30* (3), 1011–1017.
- (50) Su, J.; Yang, M. *Nat. Prod. Res.* **2015**, *29* (11), 1035–1041.
- (51) Kusari, S.; Zühlke, S.; Košuth, J.; Čellárová, E.; Spiteller, M. *J. Nat. Prod.* **2009**, *72* (10), 1825–1835.
- (52) Kusari, S.; Lamshöft, M.; Zühlke, S.; Spiteller, M. *J. Nat. Prod.* **2008**, *71* (2), 159–162.
- (53) Kumar, A.; Patil, D.; Rajamohanan, P. R.; Ahmad, A. *PLoS One* **2013**, *8* (9), e71805.
- (54) Kusari, S.; Lamshöft, M.; Kusari, P.; Gottfried, S.; Zühlke, S.; Louven, K.; Hentschel, U.; Kayser, O.; Spiteller, M. *J. Nat. Prod.* **2014**, *77* (12), 2577–2584.
- (55) Chithra, S.; Jasim, B.; Sachidanandan, P.; Jyothis, M.; Radhakrishnan, E. K. *Phytomedicine* **2014**, *21* (4), 534–540.
- (56) Kusari, S.; Verma, V. C.; Lamshöft, M.; Spiteller, M. *World J. Microbiol. Biotechnol.* **2012**, *28* (3), 1287–1294.
- (57) El-Elimat, T.; Raja, H. A.; Graf, T. N.; Faeth, S. H.; Cech, N. B.; Oberlies, N. H. *J. Nat. Prod.* **2014**, *77* (2), 193–199.
- (58) Cui, Y.; Yi, D.; Bai, X.; Sun, B.; Zhao, Y.; Zhang, Y. *Fitoterapia* **2012**, *83* (5), 913–920.
- (59) Zhang, Q.; Wei, X.; Wang, J. *Fitoterapia* **2012**, *83* (8), 1500–1505.
- (60) Wang, X.-J.; Min, C.-L.; Ge, M.; Zuo, R.-H. *Curr. Microbiol.* **2014**, *68* (3), 336–341.
- (61) Parthasarathy, R.; Sathiyabama, M. *Appl. Biochem. Biotechnol.* **2014**, *172* (6), 3141–3152.
- (62) Hao, X.; Pan, J.; Zhu, X. In *Natural Products*; Springer Berlin Heidelberg: Berlin, Heidelberg, 2013; Vol. 188, pp 2797–2812.
- (63) Flores-Bustamante, Z. R.; Rivera-Orduña, F. N.; Martínez-Cárdenas, A.; Flores-Cotera, L. B. *J. Antibiot.* **2010**, *63* (8), 460–467.
- (64) Puri, S. C.; Nazir, A.; Chawla, R.; Arora, R.; Riyaz-UI-Hasan, S.; Amna, T.; Ahmed, B.; Verma, V.; Singh, S.; Sagar, R.; Sharma, A.; Kumar, R.; Sharma, R. K.; Qazi, G. N. *J. Biotechnol.* **2006**, *122* (4), 494–510.
- (65) Luo, Y.; Li, B.-Z.; Liu, D.; Zhang, L.; Chen, Y.; Jia, B.; Zeng, B.-X.; Zhao, H.; Yuan, Y.-J. *Chem. Soc. Rev.* **2015**, *44* (15), 5265–5290.

## Chapter 7: References

---

- (66) Howat, S.; Park, B.; Oh, I. S.; Jin, Y.-W.; Lee, E.-K.; Loake, G. J. *N. Biotechnol.* **2014**, *31* (3), 242–245.
- (67) Wang, W.-X.; Kusari, S.; Spiteller, M. Unraveling the chemical interactions of fungal endophytes for exploitation as microbial factories, in *Fungal Applications in Sustainable Environmental Biotechnology, Part V: Future biotechnological potentials and environmental applications*. Springer (Landon), In revision.
- (68) Staniek, A.; Bouwmeester, H.; Fraser, P. D.; Kayser, O.; Martens, S.; Tissier, A.; van der Krol, S.; Wessjohann, L.; Warzecha, H. *Biotechnol. J.* **2014**, *9* (3), 326–336.
- (69) Wang, W.-X.; Kusari, S.; Sezgin, S.; Lamshöft, M.; Kusari, P.; Kayser, O.; Spiteller, M. *Appl. Microbiol. Biotechnol.* **2015**, *99* (18), 7651–7662.
- (70) Young, C. A.; Felitti, S.; Shields, K.; Spangenberg, G.; Johnson, R. D.; Bryan, G. T.; Saikia, S.; Scott, B. *Fungal Genet. Biol.* **2006**, *43* (10), 679–693.
- (71) Maplestone, R. A.; Stone, M. J.; Williams, D. H. *Gene* **1992**, *115* (1-2), 151–157.
- (72) Hunter, P. *EMBO Rep.* **2008**, *9* (9), 838–840.
- (73) Tu, Y.; Ni, M.; Zhong, Y.; Li, L.; Cui, S.; Zhang, M.; Wang, X.; Zheng, J.; Liang, X. *Planta Med.* **1982**, *44*, 143–145.
- (74) Pariser, D. M.; Meinking, T. L.; Bell, M.; Ryan, W. G. *N. Engl. J. Med.* **2012**, *367* (18), 1687–1693.
- (75) Pitterna, T.; Cassayre, J.; Hüter, O. F.; Jung, P. M. J.; Maienfisch, P.; Kessabi, F. M.; Quaranta, L.; Tobler, H. *Bioorg. Med. Chem.* **2009**, *17* (12), 4085–4095.
- (76) Newman, D. J.; Cragg, G. M. *J. Nat. Prod.* **2012**, *75* (3), 311–335.
- (77) Jouda, J.-B.; Kusari, S.; Lamshöft, M.; Talontsi, F. M.; Meli, C. D.; Wandji, J.; Spiteller, M. *Fitoterapia* **2014**, *98*, 209–214.
- (78) Li, G.; Kusari, S.; Lamshöft, M.; Schüffler, A.; Laatsch, H.; Spiteller, M. *J. Nat. Prod.* **2014**, *77* (11), 2335–2341.
- (79) Li, G.; Kusari, S.; Kusari, P.; Kayser, O.; Spiteller, M. *J. Nat. Prod.* **2015**, *78* (8), 2128–2132.
- (80) Yajima, A. *Tetrahedron Lett.* **2014**, *55* (17), 2773–2780.
- (81) Romero, D.; Traxler, M. F.; López, D.; Kolter, R. *Chem. Rev.* **2011**, *111* (9), 5492–5505.
- (82) Cheung, F. *Nature* **2011**, *480* (7378), S82–S83.
- (83) Tang, C.; Ye, Y.; Feng, Y.; Quinn, R. J. *Nat. Prod. Rep.* **2016**, *33* (1), 6–25.
- (84) Morikawa, T.; Ninomiya, K.; Kuramoto, H.; Kamei, I.; Yoshikawa, M.; Muraoka, O. *J. Nat. Med.* **2016**, *70* (1), 89–101.
- (85) Shawky, E.; Abou-Donia, A. H.; Darwish, F. A.; Toaima, S. M.; Takla, S. S.; Asaar, M. M. Al. *Nat. Prod. Res.* **2015**, *29* (4), 363–365.

## Chapter 7: References

---

- (86) Fu, K.-L.; Shen, Y.-H.; Lu, L.; Li, B.; He, Y.-R.; Li, B.; Yang, X.-W.; Su, J.; Liu, R.-H.; Zhang, W.-D. *Helv. Chim. Acta* **2013**, *96* (2), 338–344.
- (87) Tomoda, M.; Yokoi, M.; Torigoe, A.; Maru, K. *Chem. Pharm. Bull.* **1980**, *28* (11), 3251–3257.
- (88) Ma, G.-E.; Li, H.-Y.; Lu, C.-E.; Yang, X.-M.; Hong, S.-H. *Heterocycles* **1986**, *24* (8), 2089–2092.
- (89) Savatin, D. V.; Gramegna, G.; Modesti, V.; Cervone, F. *Front. Plant Sci.* **2014**, *5*, 470.
- (90) Lin, Y.-L.; Qiu, M.-H.; Li, Z.-R.; Zhou, L.; Liu, J.-Q. *Acta Bot. Yunnanica* **2006**, *28*, 429–432.
- (91) Zhang, J.; Qin, X.-Y.; Zhang, S.-D.; Xu, X.-S.; Pei, J.-P.; Fu, J.-J. *Chem. Biodivers.* **2015**, *12* (9), 1289–1306.
- (92) Coleman, J. J. *Mol. Plant Pathol.* **2016**, *17* (2), 146–158.
- (93) Dabas, Y.; Bakhshi, S.; Xess, I. *Mycopathologia* **2015**, 1–6.
- (94) Kavroulakis, N.; Ntougias, S.; Zervakis, G. I.; Ehaliotis, C.; Haralampidis, K.; Papadopoulou, K. K. *J. Exp. Bot.* **2007**, *58* (14), 3853–3864.
- (95) Kusari, S.; Zühlke, S.; Spiteller, M. *Fitoterapia* **2011**, *82* (3), 497–507.
- (96) Zhao, J.; Fu, Y.; Luo, M.; Zu, Y.; Wang, W.; Zhao, C.; Gu, C. *J. Agric. Food Chem.* **2012**, *60* (17), 4314–4319.
- (97) Hansen, F. T.; Gardiner, D. M.; Lysøe, E.; Fuertes, P. R.; Tudzynski, B.; Wiemann, P.; Sondergaard, T. E.; Giese, H.; Brodersen, D. E.; Sørensen, J. L. *Fungal Genet. Biol.* **2015**, *75* (1), 20–29.
- (98) Duggan, J. M.; Goldstein, S. J.; Chenoweth, C. E.; Kauffman, C. A.; Bradley, S. F. *Clin. Infect. Dis.* **1996**, *23* (3), 569–576.
- (99) Igra-Siegman, Y.; Chmel, H.; Cobbs, C. *J. Clin. Microbiol.* **1980**, *11* (2), 141–145.
- (100) Spear, J. B.; Fuhrer, J.; Kirby, B. D. *J. Clin. Microbiol.* **1988**, *26* (3), 598–599.
- (101) Yabuuchi, E.; Ohyama, A. *Jpn. J. Microbiol.* **1971**, *15* (5), 477–481.
- (102) Holmes, B.; Snell, J. J. S.; Lapage, S. P. *J. Clin. Pathol.* **1977**, *30* (7), 595–601.
- (103) Jakobsen, T. H.; Hansen, M. A.; Jensen, P. Ø.; Hansen, L.; Riber, L.; Cockburn, A.; Kolpen, M.; Hansen, C. R.; Ridderberg, W.; Eickhardt, S.; Hansen, M.; Kerpedjiev, P.; Alhede, M.; Qvortrup, K.; Burmølle, M.; Moser, C.; Köhl, M.; Ciofu, O.; Givskov, M.; Sørensen, S. J.; Høiby, N.; Bjarnsholt, T. *PLoS One* **2013**, *8* (7), e68484.
- (104) Ho, Y.-N.; Hsieh, J.-L.; Huang, C.-C. *Bioresour. Technol.* **2013**, *145*, 43–47.
- (105) Ho, Y.-N.; Mathew, D. C.; Hsiao, S.-C.; Shih, C.-H.; Chien, M.-F.; Chiang, H.-M.; Huang, C.-C. *J. Hazard. Mater.* **2012**, *219-220*, 43–49.
- (106) Cai, L.; Hyde, K. D.; Taylor, P. W. J.; Weir, B. S.; Waller, J. M.; Abang, M. M.;

## Chapter 7: References

---

- Zhang, J. Z.; Yang, Y. L.; Phoulivong, S.; Liu, Z. Y.; Prihastuti, H.; Shivas, R. G.; McKenzie, E. H. C.; Johnston, P. R. *Fungal Divers.* **2009**, *39*, 183–204.
- (107) Damm, U.; Cannon, P. F.; Woudenberg, J. H. C.; Johnston, P. R.; Weir, B. S.; Tan, Y. P.; Shivas, R. G.; Crous, P. W. *Stud. Mycol.* **2012**, *73*, 1–36.
- (108) Damm, U.; Baroncelli, R.; Cai, L.; Kubo, Y.; O'Connell, R.; Weir, B.; Yoshino, K.; Cannon, P. F. *IMA Fungus* **2010**, *1* (2), 161–165.
- (109) García-Pajón, C. M.; Collado, I. G. *Nat. Prod. Rep.* **2003**, *20* (4), 426–431.
- (110) Cannon, P. F.; Damm, U.; Johnston, P. R.; Weir, B. S. *Stud. Mycol.* **2012**, *73*, 181–213.
- (111) Lu, G.; Cannon, P. F.; Reid, A.; Simmons, C. M. *Mycol. Res.* **2004**, *108* (1), 53–63.
- (112) Joshee, S.; Paulus, B. C.; Park, D.; Johnston, P. R. *Mycol. Res.* **2009**, *113* (9), 1003–1015.
- (113) Rojas, E. I.; Rehner, S. A.; Samuels, G. J.; Van Bael, S. A.; Herre, E. A.; Cannon, P.; Chen, R.; Pang, J.; Wang, R.; Zhang, Y.; Peng, Y.-Q.; Sha, T. *Mycologia* **2010**, *102* (6), 1318–1338.
- (114) Rabha, A. J.; Naglot, A.; Sharma, G. D.; Gogoi, H. K.; Veer, V. *Indian J. Microbiol.* **2014**, *54* (3), 302–309.
- (115) Kumar, S.; Kaushik, N. *PLoS One* **2013**, *8* (2), e56202.
- (116) Paul, N.; Lee, H.; Lee, J.; Shin, K.; Ryu, T.; Kwon, H.; Kim, Y.; Youn, Y.; Yu, S. *Int. J. Mol. Sci.* **2014**, *15* (9), 15272–15286.
- (117) Lu, X.; Chen, G.; Hua, H.; Dai, H.; Mei, W.; Xu, Y.; Pei, Y. *Fitoterapia* **2012**, *83* (4), 737–741.
- (118) Zou, W. X.; Meng, J. C.; Lu, H.; Chen, G. X.; Shi, G. X.; Zhang, T. Y.; Tan, R. X. *J. Nat. Prod.* **2000**, *63* (11), 1529–1530.
- (119) Chapla, V.; Zeraik, M.; Leptokarydis, I.; Silva, G.; Bolzani, V.; Young, M.; Pfenning, L.; Araújo, A. *Molecules* **2014**, *19* (11), 19243–19252.
- (120) Hsiao, Y.; Cheng, M.-J.; Chang, H.-S.; Wu, M.-D.; Hsieh, S.-Y.; Liu, T.-W.; Lin, C.-H.; Yuan, G.-F.; Chen, I.-S. *Nat. Prod. Res.* **2016**, *30* (3), 251–258.
- (121) Chen, G.; Dai, H.-F.; Sha, Y.; Pei, Y.-H. *J. Asian Nat. Prod. Res.* **2011**, *13* (11), 1042–1046.
- (122) Arivudainambi, U. S. E.; Anand, T. D.; Shanmugaiyah, V.; Karunakaran, C.; Rajendran, A. *FEMS Immunol. Med. Microbiol.* **2011**, *61* (3), 340–345.
- (123) Tianpanich, K.; Prachya, S.; Wiyakrutta, S.; Mahidol, C.; Ruchirawat, S.; Kittakoop, P. *J. Nat. Prod.* **2011**, *74* (1), 79–81.
- (124) Ren, Y.; Strobel, G. A.; Graff, J. C.; Jutila, M.; Park, S. G.; Gosh, S.; Teplow, D.; Condrón, M.; Pang, E.; Hess, W. M.; Moore, E. *Microbiology* **2008**, *154* (7), 1973–1979.
- (125) Xiong, Z.-Q.; Yang, Y.-Y.; Zhao, N.; Wang, Y. *BMC Microbiol.* **2013**, *13* (1), 71.

## Chapter 7: References

---

- (126) Dey, P.; R. Kamdar, M.; M. Mandal, S.; K. Maiti, M. *Protein Pept. Lett.* **2012**, *20* (2), 173–179.
- (127) Romão, A. S.; Spósito, M. B.; Andreote, F. D.; Azevedo, J. L.; Araújo, W. L. *Genet. Mol. Res.* **2011**, *10* (1), 243–252.
- (128) Lou, X.-M.; Xu, Y.-D.; Sun, C.; Lou, B.-G. *Mycosystema* **2014**, *33* (1), 138–142.
- (129) Wickert, E.; Lemos, E. G. D. M.; Kishi, L. T.; de Souza, A.; de Goes, A. *Sci. World J.* **2012**, *2012*, 125654.
- (130) Wang, W.-X.; Kusari, S.; Kusari, P.; Kayser, O.; Spiteller, M. *RSC Adv.* submitted.
- (131) Han, W. B.; Dou, H.; Yuan, W. H.; Gong, W.; Hou, Y. Y.; Ng, S. W.; Tan, R. X. *Planta Med.* **2015**, *81* (2), 145–151.
- (132) Guimarães, D. O.; Lopes, N. P.; Pupo, M. T. *Phytochem. Lett.* **2012**, *5* (3), 519–523.
- (133) Yuan, W. H.; Liu, M.; Jiang, N.; Guo, Z. K.; Ma, J.; Zhang, J.; Song, Y. C.; Tan, R. X. *European J. Org. Chem.* **2010**, *2010* (33), 6348–6353.
- (134) Spilker, T.; Uluer, A. Z.; Marty, F. M.; Yeh, W. W.; Levison, J. H.; Vandamme, P.; LiPuma, J. J. *J. Clin. Microbiol.* **2008**, *46* (8), 2774–2777.
- (135) Olivares, F. L.; James, E. K.; Baldani, J. I.; Döbereiner, J. *New Phytol.* **1997**, *135* (4), 723–737.
- (136) Straub, D.; Rothballer, M.; Hartmann, A.; Ludewig, U. *Front. Microbiol.* **2013**, *4*, 168.
- (137) Wang, H.; Fewer, D. P.; Holm, L.; Rouhiainen, L.; Sivonen, K. *Proc. Natl. Acad. Sci.* **2014**, *111* (25), 9259–9264.
- (138) Shen, B.; Du, L.; Sanchez, C.; Edwards, D. J.; Chen, M.; Murrell, J. M. *J. Ind. Microbiol. Biotechnol.* **2001**, *27* (6), 378–385.
- (139) Zhang, Y.; Zhang, K.; Fang, A.; Han, Y.; Yang, J.; Xue, M.; Bao, J.; Hu, D.; Zhou, B.; Sun, X.; Li, S.; Wen, M.; Yao, N.; Ma, L.-J.; Liu, Y.; Zhang, M.; Huang, F.; Luo, C.; Zhou, L.; Li, J.; Chen, Z.; Miao, J.; Wang, S.; Lai, J.; Xu, J.-R.; Hsiang, T.; Peng, Y.-L.; Sun, W. *Nat. Commun.* **2014**, *5*, 3849.
- (140) Strieker, M.; Tanović, A.; Marahiel, M. A. *Curr. Opin. Struct. Biol.* **2010**, *20* (2), 234–240.
- (141) Boettger, D.; Hertweck, C. *ChemBioChem* **2013**, *14* (1), 28–42.
- (142) Stachelhaus, T.; Walsh, C. T. *Biochemistry* **2000**, *39* (19), 5775–5787.
- (143) Du, L.; Lou, L. *Nat. Prod. Rep.* **2010**, *27* (2), 255–278.
- (144) Khosla, C.; Gokhale, R. S.; Jacobsen, J. R.; Cane, D. E. *Annu. Rev. Biochem.* **1999**, *68* (1), 219–253.
- (145) Chan, Y. A.; Podevels, A. M.; Kevany, B. M.; Thomas, M. G. *Nat. Prod. Rep.* **2009**, *26* (1), 90–114.



## Chapter 7: References

---

- (146) Shen, B. *Curr. Opin. Chem. Biol.* **2003**, 7 (2), 285–295.
- (147) Thattai, M.; Burak, Y.; Shraiman, B. I. *PLoS Comput. Biol.* **2007**, 3 (9), e186.
- (148) Staunton, J.; Weissman, K. J. *Nat. Prod. Rep.* **2001**, 18 (4), 380–416.
- (149) Jenke-Kodama, H.; Sandmann, A.; Müller, R.; Dittmann, E. *Mol. Biol. Evol.* **2005**, 22 (10), 2027–2039.
- (150) Grimm, A.; Madduri, K.; Ali, A.; Hutchinson, C. R. *Gene* **1994**, 151 (1-2), 1–10.
- (151) Fernández-Moreno, M. A.; Martínez, E.; Boto, L.; Hopwood, D. A.; Malpartida, F. *J. Biol. Chem.* **1992**, 267 (27), 19278–19290.
- (152) Moore, B. S.; Hopke, J. N. *ChemBioChem* **2001**, 2 (1), 35–38.
- (153) Du, L.; Sánchez, C.; Chen, M.; Edwards, D. J.; Shen, B. *Chem. Biol.* **2000**, 7 (8), 623–642.
- (154) Pelludat, C.; Rakin, A.; Jacobi, C. A.; Schubert, S.; Heesemann, J. *J. Bacteriol.* **1998**, 180 (3), 538–546.
- (155) Tang, L. *Science* **2000**, 287 (5453), 640–642.
- (156) Aparicio, J. F.; Molnár, I.; Schwecke, T.; König, A.; Haydock, S. F.; Ee Khaw, L.; Staunton, J.; Leadlay, P. F. *Gene* **1996**, 169 (1), 9–16.
- (157) Joo, S. H. *Biomol. Ther.* **2012**, 20 (1), 19–26.
- (158) Litten, W. *Sci. Am.* **1975**, 232 (3), 90–101.
- (159) Agha, R.; Cirés, S.; Wörmer, L.; Quesada, A. *Toxins (Basel)*. **2013**, 5 (6), 1089–1104.
- (160) Levine, D. P. *Clin. Infect. Dis.* **2006**, 42 (Supplement 1), S5–S12.
- (161) Urry, D. W. *Proc. Natl. Acad. Sci.* **1971**, 68 (3), 672–676.
- (162) Tally, F. P.; DeBruin, M. F. *J. Antimicrob. Chemother.* **2000**, 46 (4), 523–526.
- (163) Kohli, R. M.; Walsh, C. T.; Burkart, M. D. *Nature* **2002**, 418 (6898), 658–661.
- (164) Gao, J.; Yang, S.; Qin, J. *Chem. Rev.* **2013**, 113 (7), 4755–4811.
- (165) Stadler, M.; Fournier, J. *Rev. Iberoam. Micol.* **2006**, 23 (3), 160–170.
- (166) Stadler, M.; Ju, Y.-M.; Rogers, J. D. *Mycol. Res.* **2004**, 108 (Pt 3), 239–256.
- (167) Frisvad, J. C.; Andersen, B.; Thrane, U. *Mycol. Res.* **2008**, 112 (2), 231–240.
- (168) Matsuzaki, K.; Tahara, H.; Inokoshi, J.; Tanaka, H.; Masuma, R.; Omura, S. *J. Antibiot. (Tokyo)*. **1998**, 51 (11), 1004–1011.
- (169) Nam, J. Y.; Kim, H. K.; Kwon, J. Y.; Han, M. Y.; Son, K. H.; Lee, U. C.; Choi, J. D.; Kwon, B. M. *J. Nat. Prod.* **2000**, 63 (9), 1303–1305.
- (170) Clark, R. C.; Lee, S. Y.; Searcey, M.; Boger, D. L. *Nat. Prod. Rep.* **2009**, 26 (4), 465–477.
- (171) Musso, L.; Dallavalle, S.; Merlini, L.; Bava, A.; Nasini, G.; Penco, S.; Giannini, G.;

## Chapter 7: References

---

- Giommarelli, C.; De Cesare, A.; Zuco, V.; Vesci, L.; Pisano, C.; Dal Piaz, F.; De Tommasi, N.; Zunino, F. *Bioorg. Med. Chem.* **2010**, *18* (16), 6031–6043.
- (172) Riko, R.; Nakamura, H.; Shindo, K. *J. Antibiot. (Tokyo)*. **2013**, *67* (2), 179–181.
- (173) Isaka, M.; Chinthanom, P.; Rachtawee, P.; Somyong, W.; Luangsa-ard, J. J.; Hywel-Jones, N. L. *Phytochem. Lett.* **2013**, *6* (2), 162–164.
- (174) Abraham, W.; Meyer, H.; Abate, D. *Tetrahedron* **1995**, *51* (17), 4947–4952.
- (175) Hiort, J.; Maksimenka, K.; Reichert, M.; Perović-Ottstadt, S.; Lin, W. H.; Wray, V.; Steube, K.; Schaumann, K.; Weber, H.; Proksch, P.; Ebel, R.; Müller, W. E. G.; Bringmann, G. *J. Nat. Prod.* **2004**, *67* (9), 1532–1543.
- (176) Schlingmann, G.; Taniguchi, T.; He, H.; Bigelis, R.; Yang, H. Y.; Koehn, F. E.; Carter, G. T.; Berova, N. *J. Nat. Prod.* **2007**, *70* (7), 1180–1187.
- (177) Yamamoto, T.; Tsunematsu, Y.; Noguchi, H.; Hotta, K.; Watanabe, K. *Org. Lett.* **2015**, *17* (20), 4992–4995.
- (178) Meng, L.-H.; Li, X.-M.; Liu, Y.; Wang, B.-G. *Chinese Chem. Lett.* **2015**, *26* (5), 610–612.
- (179) Awakawa, T.; Yang, X.-L.; Wakimoto, T.; Abe, I. *ChemBioChem* **2013**, *14* (16), 2095–2099.
- (180) Wysocki, V. H.; Resing, K. A.; Zhang, Q.; Cheng, G. *Methods* **2005**, *35* (3), 211–222.
- (181) Zhang, G.; Annan, R. S.; Carr, S. A.; Neubert, T. A. In *Current Protocols in Protein Science*; John Wiley & Sons, Inc.: Hoboken, NJ, USA, 2010.
- (182) Dančik, V.; Addona, T. A.; Clauser, K. R.; Vath, J. E.; Pevzner, P. A. *J. Comput. Biol.* **1999**, *6* (3-4), 327–342.
- (183) Fälth, M.; Svensson, M.; Nilsson, A.; Sköld, K.; Fenyö, D.; Andren, P. E. *J. Proteome Res.* **2008**, *7* (7), 3049–3053.
- (184) Zhao, Y.; Lin, Y.-H. *Genomics. Proteomics Bioinformatics* **2010**, *8* (1), 33–41.
- (185) Ma, B.; Zhang, K.; Hendrie, C.; Liang, C.; Li, M.; Doherty-Kirby, A.; Lajoie, G. *Rapid Commun. Mass Spectrom.* **2003**, *17* (20), 2337–2342.
- (186) Sadygov, R. G.; Cociorva, D.; Yates, J. R. *Nat. Methods* **2004**, *1* (3), 195–202.
- (187) Williams, S. M.; Brodbelt, J. S. *J. Am. Soc. Mass Spectrom.* **2004**, *15* (7), 1039–1054.
- (188) Stokvis, E.; Rosing, H.; López-Lázaro, L.; Rodriguez, I.; Jimeno, J. M.; Supko, J. G.; Schellens, J. H. M.; Beijnen, J. H. *J. Mass Spectrom.* **2002**, *37* (9), 992–1000.
- (189) Cavelier, F.; Enjalbal, C.; Martinez, J.; Roque, M.; Sanchez, P.; Aubagnac, J.-L. *Rapid Commun. Mass Spectrom.* **1999**, *13* (10), 880–885.
- (190) Yin, J.; Aviles, P.; Lee, W.; Ly, C.; Floriano, P.; Ignacio, M.; Faircloth, G. *Rapid Commun. Mass Spectrom.* **2003**, *17* (16), 1909–1914.

## Chapter 7: References

---

- (191) Ngoka, L. C. M.; Gross, M. L. *J. Am. Soc. Mass Spectrom.* **1999**, *10* (8), 732–746.
- (192) Suyama, T. L.; Gerwick, W. H.; McPhail, K. L. *Bioorg. Med. Chem.* **2011**, *19* (22), 6675–6701.
- (193) Nicolaou, K. C.; Snyder, S. A. *Angew. Chemie Int. Ed.* **2005**, *44* (7), 1012–1044.
- (194) Sarotti, A. M. *Org. Biomol. Chem.* **2013**, *11* (29), 4847–4859.
- (195) Schreckenbach, G.; Ziegler, T. *J. Phys. Chem.* **1995**, *99* (2), 606–611.
- (196) Cheeseman, J. R.; Trucks, G. W.; Keith, T. A.; Frisch, M. J. *J. Chem. Phys.* **1996**, *104* (14), 5497–5509.
- (197) Barone, G.; Gomez-Paloma, L.; Duca, D.; Silvestri, A.; Riccio, R.; Bifulco, G. *Chem. Eur. J.* **2002**, *8* (14), 3233.
- (198) Barone, G.; Duca, D.; Silvestri, A.; Gomez-Paloma, L.; Riccio, R.; Bifulco, G. *Chemistry* **2002**, *8* (14), 3240–3245.
- (199) Nicolaou, K. C.; Frederick, M. O. *Angew. Chemie Int. Ed.* **2007**, *46* (28), 5278–5282.
- (200) Fedorov, S. V.; Rusakov, Y. Y.; Krivdin, L. B. *Russ. J. Org. Chem.* **2014**, *50* (2), 160–164.
- (201) Flaig, D.; Maurer, M.; Hanni, M.; Braunger, K.; Kick, L.; Thubauville, M.; Ochsenfeld, C. *J. Chem. Theory Comput.* **2014**, *10* (2), 572–578.
- (202) Timmons, C.; Wipf, P. *J. Org. Chem.* **2008**, *73* (22), 9168–9170.
- (203) Watts, H. D.; Mohamed, M. N. A.; Kubicki, J. D. *J. Phys. Chem. B* **2011**, *115* (9), 1958–1970.
- (204) Liu, X.; Yang, J.; Wang, W.-G.; Li, Y.; Wu, J.-Z.; Pu, J.-X.; Sun, H.-D. *J. Nat. Prod.* **2015**, *78* (2), 196–201.
- (205) Rychnovsky, S. D. *Org. Lett.* **2006**, *8* (13), 2895–2898.
- (206) Smith, S. G.; Goodman, J. M. *J. Org. Chem.* **2009**, *74* (12), 4597–4607.
- (207) Sarotti, A. M.; Pellegrinet, S. C. *J. Org. Chem.* **2009**, *74* (19), 7254–7260.
- (208) Nealson, K. H.; Hastings, J. W. *Microbiol. Rev.* **1979**, *43* (4), 496–518.
- (209) Schuster, M.; Joseph Sexton, D.; Diggie, S. P.; Peter Greenberg, E. *Annu. Rev. Microbiol.* **2013**, *67* (1), 43–63.
- (210) Hayes, C. S.; Low, D. A. *Curr. Opin. Microbiol.* **2009**, *12* (6), 667–673.
- (211) Taillefumier, T.; Wingreen, N. S. *PLOS Comput. Biol.* **2015**, *11* (5), e1004238.
- (212) Albuquerque, P.; Casadevall, A. *Med. Mycol.* **2012**, *50* (4), 337–345.
- (213) Deng, Y.; Wu, J.; Tao, F.; Zhang, L.-H. *Chem. Rev.* **2011**, *111* (1), 160–173.
- (214) Pacheco, A. R.; Sperandio, V. *Curr. Opin. Microbiol.* **2009**, *12* (2), 192–198.
- (215) Frederix, M.; Downie, J. A. In *Advances in Microbial Physiology*; Elsevier Ltd.,

## Chapter 7: References

---

- 2011; Vol. 58, pp 23–80.
- (216) Atkinson, S.; Williams, P. *J. R. Soc. Interface* **2009**, *6* (40), 959–978.
- (217) Boon, C.; Deng, Y.; Wang, L.-H.; He, Y.; Xu, J.-L.; Fan, Y.; Pan, S. Q.; Zhang, L.-H. *ISME J.* **2008**, *2* (1), 27–36.
- (218) Holm, A.; Vikström, E. *Front. Plant Sci.* **2014**, *5*, 309.
- (219) Ling, L. L.; Schneider, T.; Peoples, A. J.; Spoering, A. L.; Engels, I.; Conlon, B. P.; Mueller, A.; Schäberle, T. F.; Hughes, D. E.; Epstein, S.; Jones, M.; Lazarides, L.; Steadman, V. A.; Cohen, D. R.; Felix, C. R.; Fetterman, K. A.; Millett, W. P.; Nitti, A. G.; Zullo, A. M.; Chen, C.; Lewis, K. *Nature* **2015**, *517* (7535), 455–459.
- (220) Nichols, D.; Cahoon, N.; Trakhtenberg, E. M.; Pham, L.; Mehta, A.; Belanger, A.; Kanigan, T.; Lewis, K.; Epstein, S. S. *Appl. Environ. Microbiol.* **2010**, *76* (8), 2445–2450.
- (221) Sica, V. P.; Raja, H. A.; El-Elimat, T.; Kertesz, V.; Van Berkel, G. J.; Pearce, C. J.; Oberlies, N. H. *J. Nat. Prod.* **2015**, *78* (8), 1926–1936.
- (222) Yang, Y.-L.; Xu, Y.; Straight, P.; Dorrestein, P. C. *Nat. Chem. Biol.* **2009**, *5* (12), 885–887.
- (223) Yang, Y.-L.; Xu, Y.; Kersten, R. D.; Liu, W.-T.; Meehan, M. J.; Moore, B. S.; Bandeira, N.; Dorrestein, P. C. *Angew. Chemie Int. Ed.* **2011**, *50* (26), 5839–5842.
- (224) Sica, V. P.; Raja, H. A.; El-Elimat, T.; Oberlies, N. H. *RSC Adv.* **2014**, *4* (108), 63221–63227.
- (225) Karas, M.; Krüger, R. *Chem. Rev.* **2003**, *103* (2), 427–439.
- (226) Karas, M.; Bachmann, D.; Bahr, U.; Hillenkamp, F. *Int. J. Mass Spectrom. Ion Process.* **1987**, *78*, 53–68.
- (227) Holland, R. D.; Wilkes, J. G.; Ruff, F.; Sutherland, J. B.; Persons, C. C.; Voorhees, K. J.; Lay, Jr, J. O. *Rapid Commun. Mass Spectrom.* **1996**, *10* (10), 1227–1232.
- (228) Shih, C.-J.; Chen, P.-Y.; Liaw, C.-C.; Lai, Y.-M.; Yang, Y.-L. *Nat. Prod. Rep.* **2014**, *31* (6), 739–755.
- (229) Takats, Z.; Wiseman, J. M.; Gologan, B.; Cooks, R. G. *Science* **2004**, *306* (5695), 471–473.
- (230) Hsu, C.-C.; ElNaggar, M. S.; Peng, Y.; Fang, J.; Sanchez, L. M.; Mascuch, S. J.; Møller, K. a.; Alazzeah, E. K.; Pikula, J.; Quinn, R. a.; Zeng, Y.; Wolfe, B. E.; Dutton, R. J.; Gerwick, L.; Zhang, L.; Liu, X.; Månsson, M.; Dorrestein, P. C. *Anal. Chem.* **2013**, *85* (15), 7014–7018.
- (231) Wang, W.-X.; Kusari, S.; Laatsch, H.; Golz, C.; Kusari, P.; Strohmam, C.; Kayser, O.; Spiteller, M. *J. Nat. Prod.* **2016**, 10.1021/acs.jnatprod.5b00436.
- (232) White, T. J.; Bruns, T.; Lee, S.; Taylor, J. *PCR Protoc. A Guid. to Methods Appl.* **1990**, 315–322.
- (233) Schumann, P. *J. Basic Microbiol.* **1991**, *31* (6), 479–480.

## Chapter 7: References

---

- (234) Partida-Martinez, L. P.; Hertweck, C. *Nature* **2005**, *437* (7060), 884–888.
- (235) Sheldrick, G. M. *Acta Crystallogr. Sect. A Found. Crystallogr.* **2008**, *64* (1), 112–122.
- (236) Shao, Y.; Molnar, L. F.; Jung, Y.; Kussmann, J.; Ochsenfeld, C.; Brown, S. T.; Gilbert, A. T. B.; Slipchenko, L. V.; Levchenko, S. V.; O'Neill, D. P.; DiStasio Jr, R. a.; Lochan, R. C.; Wang, T.; Beran, G. J. O.; Besley, N. a.; Herbert, J. M.; Yeh Lin, C.; Van Voorhis, T.; Hung Chien, S.; Sodt, A.; Steele, R. P.; Rassolov, V. a.; Maslen, P. E.; Korambath, P. P.; Adamson, R. D.; Austin, B.; Baker, J.; Byrd, E. F. C.; Dachsel, H.; Doerksen, R. J.; Dreuw, A.; Dunietz, B. D.; Dutoi, A. D.; Furlani, T. R.; Gwaltney, S. R.; Heyden, A.; Hirata, S.; Hsu, C.-P.; Kedziora, G.; Khalliulin, R. Z.; Klunzinger, P.; Lee, A. M.; Lee, M. S.; Liang, W.; Lotan, I.; Nair, N.; Peters, B.; Proynov, E. I.; Pieniazek, P. A.; Min Rhee, Y.; Ritchie, J.; Rosta, E.; David Sherrill, C.; Simmonett, A. C.; Subotnik, J. E.; Woodcock III, L. H.; Zhang, W.; Bell, A. T.; Chakraborty, A. K.; Chipman, D. M.; Keil, F. J.; Warshel, A.; Hehre, W. J.; Schaefer III, H. F.; Kong, J.; Krylov, A. I.; Gill, P. M. W.; Head-Gordon, M. *Phys. Chem. Chem. Phys.* **2006**, *8* (27), 3172–3191.
- (237) Frisch, M. J.; Trucks, G. W.; Schlegel, H. B.; Scuseria, G. E.; Robb, M. A.; Cheeseman, J. R.; Scalmani, G.; Barone, V.; Mennucci, B.; Petersson, G. A.; Nakatsuji, H.; Caricato, M.; Li, X.; Hratchian, H. P.; Izmaylov, A. F.; Bloino, J.; Zheng, G.; Sonnenb, D. J. *Gaussian 09W, Version 7.0; Gaussian: Wallingford, CT*; 2009.
- (238) Miteva, M. A.; Guyon, F.; Tufféry, P. *Nucleic Acids Res.* **2010**, *38* (Web Server), W622–W627.
- (239) Schmidt, M. W.; Baldridge, K. K.; Boatz, J. A.; Elbert, S. T.; Gordon, M. S.; Jensen, J. H.; Koseki, S.; Matsunaga, N.; Nguyen, K. A.; Su, S.; Windus, T. L.; Dupuis, M.; Montgomery, J. A. J. *J. Comput. Chem.* **1993**, *14* (11), 1347–1363.
- (240) Becke, A. D. *J. Chem. Phys.* **1993**, *98* (7), 5648–5652.
- (241) Goerigk, L.; Grimme, S. *Phys. Chem. Chem. Phys.* **2011**, *13* (14), 6670–6688.
- (242) Jensen, F. *J. Chem. Theory Comput.* **2014**, *10* (3), 1074–1085.
- (243) Aidas, K.; Angeli, C.; Bak, K. L.; Bakken, V.; Bast, R.; Boman, L.; Christiansen, O.; Cimiraglia, R.; Coriani, S.; Dahle, P.; Dalskov, E. K.; Ekström, U.; Enevoldsen, T.; Eriksen, J. J.; Ettenhuber, P.; Fernández, B.; Ferrighi, L.; Fliegl, H.; Frediani, L.; Hald, K.; Halkier, A.; Hättig, C.; Heiberg, H.; Helgaker, T.; Hennum, A. C.; Hettema, H.; Hjertenaes, E.; Høst, S.; Høyvik, I.-M.; Iozzi, M. F.; Jansík, B.; Jensen, H. J. A.; Jonsson, D.; Jørgensen, P.; Kauczor, J.; Kirpekar, S.; Kjaergaard, T.; Klopper, W.; Knecht, S.; Kobayashi, R.; Koch, H.; Kongsted, J.; Krapp, A.; Kristensen, K.; Ligabue, A.; Lutnaes, O. B.; Melo, J. I.; Mikkelsen, K. V.; Myhre, R. H.; Neiss, C.; Nielsen, C. B.; Norman, P.; Olsen, J.; Olsen, J. M. H.; Osted, A.; Packer, M. J.; Pawłowski, F.; Pedersen, T. B.; Provasi, P. F.; Reine, S.; Rinkevicius, Z.; Ruden, T. A.; Ruud, K.; Rybkin, V. V.; Sałek, P.; Samson, C. C. M.; de Merás, A. S.; Saue, T.; Sauer, S. P. A.; Schimmelpfennig, B.; Sneskov, K.; Steindal, A. H.; Sylvester-Hvid, K. O.; Taylor, P. R.; Teale, A. M.; Tellgren, E. I.; Tew, D. P.; Thorvaldsen, A. J.; Thøgersen, L.; Vahtras, O.; Watson, M. A.; Wilson, D. J. D.; Ziolkowski, M.;

## Chapter 7: References

---

- Ågren, H. *Wiley Interdiscip. Rev. Comput. Mol. Sci.* **2014**, 4 (3), 269–284.
- (244) Ferrighi, L.; Frediani, L.; Ruud, K. *J. Phys. Chem. B* **2007**, 111 (30), 8965–8973.
- (245) Stephens, P. J.; Harada, N. *Chirality* **2009**, 22 (10), 229–233.
- (246) Kusari, P.; Kusari, S.; Lamshöft, M.; Sezgin, S.; Spiteller, M.; Kayser, O. *Appl. Microbiol. Biotechnol.* **2014**, 98 (16), 7173–7183.
- (247) Yamada, S.; Hongo, C.; Yoshioka, R.; Chibata, I. *J. Org. Chem.* **1983**, 83 (4), 843–846.
- (248) Barraclough, P.; Spray, C. A.; Young, D. W. *Tetrahedron Lett.* **2005**, 46 (27), 4653–4655.
- (249) Zhou, K.; Zhang, X.; Zhang, F.; Li, Z. *Microb. Ecol.* **2011**, 62 (3), 644–654.
- (250) Kaliuzhnaia, O. V.; Kulakova, N. V.; Itskovich, V. B. *Mol. Biol.* **2012**, 46 (6), 790–795.
- (251) Miller, K. I.; Qing, C.; Sze, D. M.-Y.; Roufogalis, B. D.; Neilan, B. A. *Microb. Ecol.* **2012**, 64 (2), 431–449.
- (252) Kusari, P.; Kusari, S.; Spiteller, M.; Kayser, O. *Fungal Divers.* **2013**, 60 (1), 137–151.
- (253) Keller, N. P.; Turner, G.; Bennett, J. W. *Nat. Rev. Microbiol.* **2005**, 3 (12), 937–947.
- (254) Zhang, W.; Li, Z.; Miao, X.; Zhang, F. *Mar. Biotechnol. (NY)*. **2009**, 11 (3), 346–355.
- (255) Bode, H. B.; Bethe, B.; Höfs, R.; Zeeck, A. *Chembiochem* **2002**, 3 (7), 619–627.
- (256) Molinski, T. F. *Curr. Opin. Biotechnol.* **2010**, 21 (6), 819–826.
- (257) Donia, M. S.; Ruffner, D. E.; Cao, S.; Schmidt, E. W. *ChemBioChem* **2011**, 12 (8), 1230–1236.
- (258) Youk, H.; Lim, W. A. *Science* **2014**, 343 (6171), 1242782.
- (259) Esquenazi, E.; Yang, Y.-L.; Watrous, J.; Gerwick, W. H.; Dorrestein, P. C. *Nat. Prod. Rep.* **2009**, 26 (12), 1521–1534.
- (260) Armirotti, A.; Millo, E.; Damonte, G. *J. Am. Soc. Mass Spectrom.* **2007**, 18 (1), 57–63.
- (261) Bode, H. B.; Reimer, D.; Fuchs, S. W.; Kirchner, F.; Dauth, C.; Kegler, C.; Lorenzen, W.; Brachmann, A. O.; Grün, P. *Chem. Eur. J.* **2012**, 18 (8), 2342–2348.
- (262) Feng, M.; Kang, H.; Liu, H.; Zhai, C. *J. Hebei Univ. Sci. Technol.* **2001**, 22 (2), 22–24.
- (263) Taga, M. E.; Semmelhack, J. L.; Bassler, B. L. *Mol. Microbiol.* **2001**, 42 (3), 777–793.
- (264) Trancassini, M.; Iebba, V.; Citerà, N.; Tuccio, V.; Magni, A.; Varesi, P.; De Biase, R. V.; Totino, V.; Santangelo, F.; Gagliardi, A.; Schippa, S. *Front. Microbiol.* **2014**, 5, 138.

## Chapter 7: References

---

- (265) Tan, N.-H.; Zhou, J. *Chem. Rev.* **2006**, *106* (3), 840–895.
- (266) Abdalla, M. A.; Matasyoh, J. C. *Nat. Products Bioprospect.* **2014**, *4* (5), 257–270.
- (267) Zerikly, M.; Challis, G. L. *ChemBioChem* **2009**, *10* (4), 625–633.
- (268) Bachmann, B. O.; Van Lanen, S. G.; Baltz, R. H. *J. Ind. Microbiol. Biotechnol.* **2014**, *41* (2), 175–184.
- (269) Helfrich, E. J. N.; Reiter, S.; Piel, J. *Curr. Opin. Biotechnol.* **2014**, *29* (1), 107–115.
- (270) Huang, H.; Feng, X.; Xiao, Z.; Liu, L.; Li, H.; Ma, L.; Lu, Y.; Ju, J.; She, Z.; Lin, Y. *J. Nat. Prod.* **2011**, *74* (5), 997–1002.
- (271) Butts, C. P.; Jones, C. R.; Towers, E. C.; Flynn, J. L.; Appleby, L.; Barron, N. J. *Org. Biomol. Chem.* **2011**, *9* (1), 177–184.
- (272) Jones, C. R.; Butts, C. P.; Harvey, J. N. *Beilstein J. Org. Chem.* **2011**, *7*, 145–150.
- (273) Yen, W.-H.; Hu, L.-C.; Su, J.-H.; Lu, M.-C.; Twan, W.-H.; Yang, S.-Y.; Kuo, Y.-C.; Weng, C.-F.; Lee, C.-H.; Kuo, Y.-H.; Sung, P.-J. *Molecules* **2012**, *17* (12), 14058–14066.
- (274) Steyn, P. S.; Vlegaar, R. *J. Chem. Soc. Perkin Trans. 1* **1986**, *29* (3), 1975–1976.
- (275) Balakrishnan, B.; Chen, C.-C.; Pan, T.-M.; Kwon, H.-J. *Tetrahedron Lett.* **2014**, *55* (9), 1640–1643.
- (276) Borges, W. S.; Mancilla, G.; Guimarães, D. O.; Durán-Patrón, R.; Collado, I. G.; Pupo, M. T. *J. Nat. Prod.* **2011**, *74*, 1182–1187.
- (277) Hellwig, V.; Ju, Y.-M.; Rogers, J. D.; Fournier, J.; Stadler, M. *Mycol. Prog.* **2005**, *4* (1), 39–54.
- (278) Anke, H.; Kemmer, T.; Höfle, G. *J. Antibiot.* **1981**, *34* (8), 923–928.
- (279) Quang, D. N.; Hashimoto, T.; Stadler, M.; Radulović, N.; Asakawa, Y. *Planta Med.* **2005**, *71* (11), 1058–1062.
- (280) Photita, W.; Taylor, P. W. J.; Ford, R.; Hyde, K. D.; Lumyong, S. *Fungal Divers.* **2005**, *18*, 117–133.
- (281) Cano, J.; Guarro, J.; Gené, J. *J. Clin. Microbiol.* **2004**, *42* (6), 2450–2454.
- (282) Kogel, K.-H.; Franken, P.; Hückelhoven, R. *Curr. Opin. Plant Biol.* **2006**, *9* (4), 358–363.
- (283) Hoffman, M. T.; Gunatilaka, M. K.; Wijeratne, K.; Gunatilaka, L.; Arnold, A. E. *PLoS One* **2013**, *8* (9), 31–33.
- (284) Adamo, C.; Barone, V. *J. Chem. Phys.* **1998**, *108* (2), 664–675.
- (285) Snider, B. B.; Neubert, B. J. *J. Org. Chem.* **2004**, *69* (25), 8952–8955.
- (286) Scherlach, K.; Graupner, K.; Hertweck, C. *Annu. Rev. Microbiol.* **2013**, *67* (June), 375–397.
- (287) Leone, M. R.; Lackner, G.; Silipo, A.; Lanzetta, R.; Molinaro, A.; Hertweck, C.

## Chapter 7: References

---

- Angew. Chemie Int. Ed.* **2010**, *49* (41), 7476–7480.
- (288) Walsh, C. T. *Nat. Prod. Rep.* **2016**, *33* (2), 127–135.
- (289) Scherlach, K.; Busch, B.; Lackner, G.; Paszkowski, U.; Hertweck, C. *Angew. Chemie Int. Ed.* **2012**, *51* (38), 9615–9618.
- (290) Wada-Katsumata, A.; Zurek, L.; Nalyanya, G.; Roelofs, W. L.; Zhang, A.; Schal, C. *Proc. Natl. Acad. Sci.* **2015**, *112* (51), 15678–15683.
- (291) Santhanam, R.; Luu, V. T.; Weinhold, A.; Goldberg, J.; Oh, Y.; Baldwin, I. T. *Proc. Natl. Acad. Sci.* **2015**, *112* (36), E5013–E5020.
- (292) Lahrmann, U.; Zuccaro, A. *Mol. Plant. Microbe. Interact.* **2012**, *25* (6), 727–737.
- (293) Bailey, B. A.; Bae, H.; Strem, M. D.; Roberts, D. P.; Thomas, S. E.; Crozier, J.; Samuels, G. J.; Choi, I.-Y.; Holmes, K. A. *Planta* **2006**, *224* (6), 1449–1464.
- (294) Walsh, C. T.; Fischbach, M. A. *J. Am. Chem. Soc.* **2010**, *132* (8), 2469–2493.
- (295) Jansen, J. J.; Blanchet, L.; Buydens, L. M. C.; Bertrand, S.; Wolfender, J.-L. *Metabolomics* **2015**, *11* (4), 908–919.
- (296) Suryanarayanan, T. S. *Fungal Ecol.* **2013**, *6* (6), 561–568.
- (297) Aldemir, H.; Kohlhepp, S. V.; Gulder, T.; Gulder, T. A. M. *J. Nat. Prod.* **2014**, *77* (11), 2331–2334.
- (298) Ayoup, M. S.; Cordes, D. B.; Slawin, A. M. Z.; O’Hagan, D. *J. Nat. Prod.* **2014**, *77* (6), 1249–1251.
- (299) Jaivel, N.; Uvarani, C.; Rajesh, R.; Velmurugan, D.; Marimuthu, P. *J. Nat. Prod.* **2014**, *77* (1), 2–8.
- (300) Fattorusso, E.; Luciano, P.; Romano, A.; Tagliatela-Scafati, O.; Appendino, G.; Borriello, M.; Fattorusso, C. *J. Nat. Prod.* **2008**, *71* (12), 1988–1992.
- (301) Wang, B.; Dossey, A. T.; Walse, S. S.; Edison, A. S.; Merz, K. M. *J. Nat. Prod.* **2009**, *72* (4), 709–713.
- (302) Nothias-Scaglia, L.-F.; Gallard, J.-F.; Dumontet, V.; Roussi, F.; Costa, J.; Iorga, B. I.; Paolini, J.; Litaudon, M. *J. Nat. Prod.* **2015**, *78* (10), 2423–2431.
- (303) Larionova, M.; Spengler, I.; Nogueiras, C.; Quijano, L.; Ramírez-Gualito, K.; Cortés-Guzmán, F.; Cuevas, G.; Calderón, J. S. *J. Nat. Prod.* **2010**, *73* (10), 1623–1627.

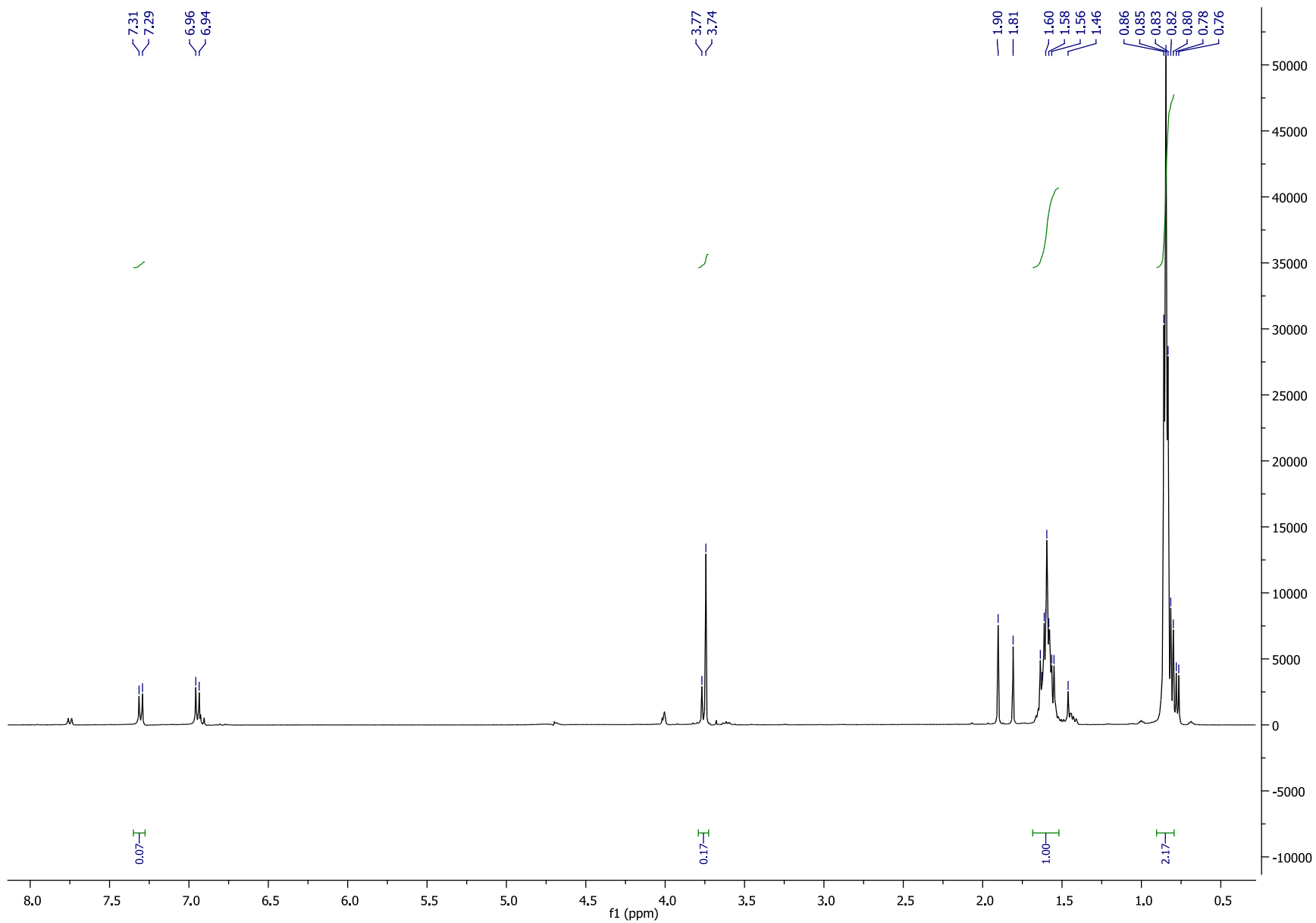


## Chapter 8

# SUPPLEMENTAL DATA

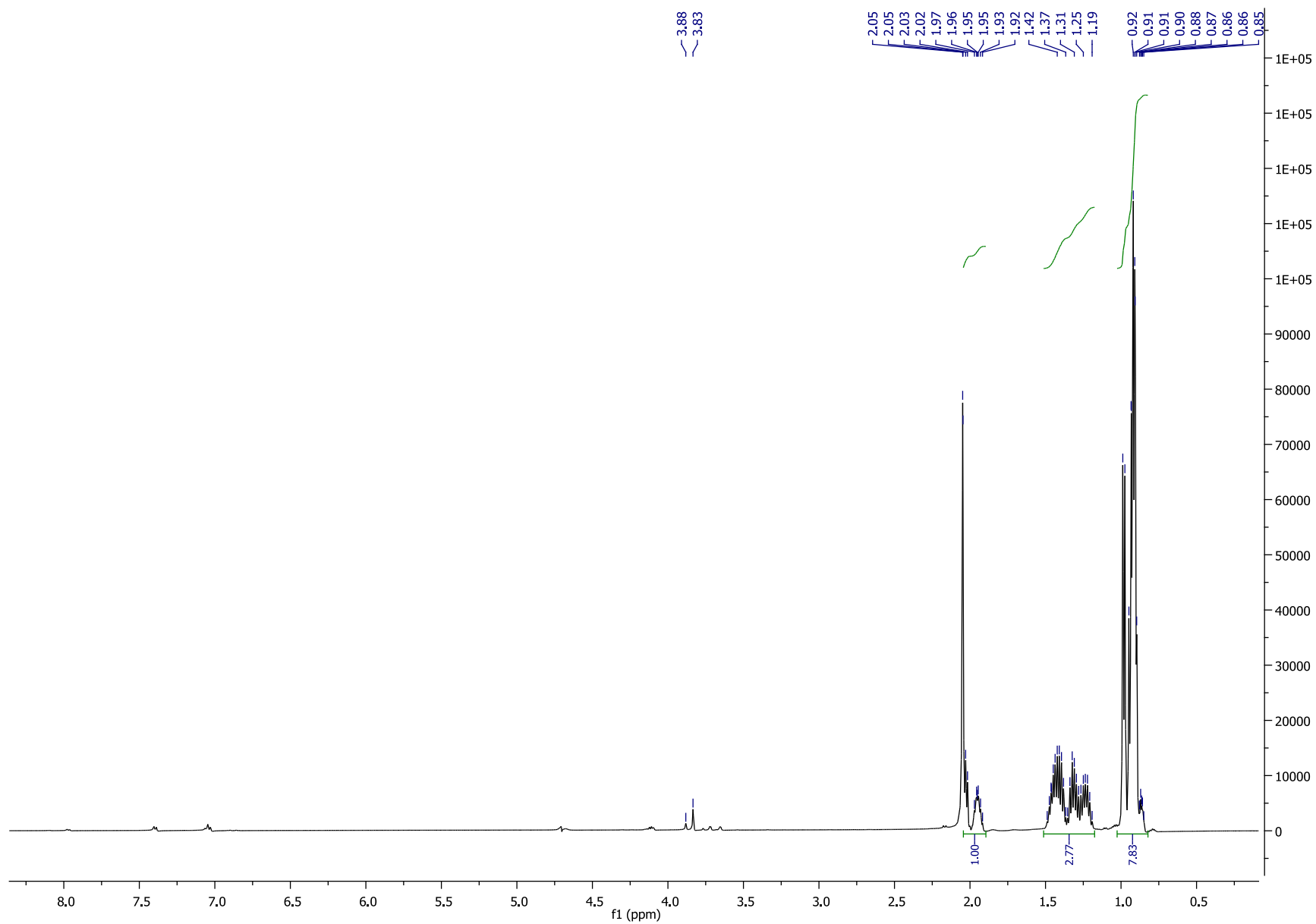
## Chapter 8: Supplemental data

Figure S1  $^1\text{H}$  NMR (500 MHz,  $\text{D}_2\text{O}$ ) of  $\alpha$ -deuterium-leucine



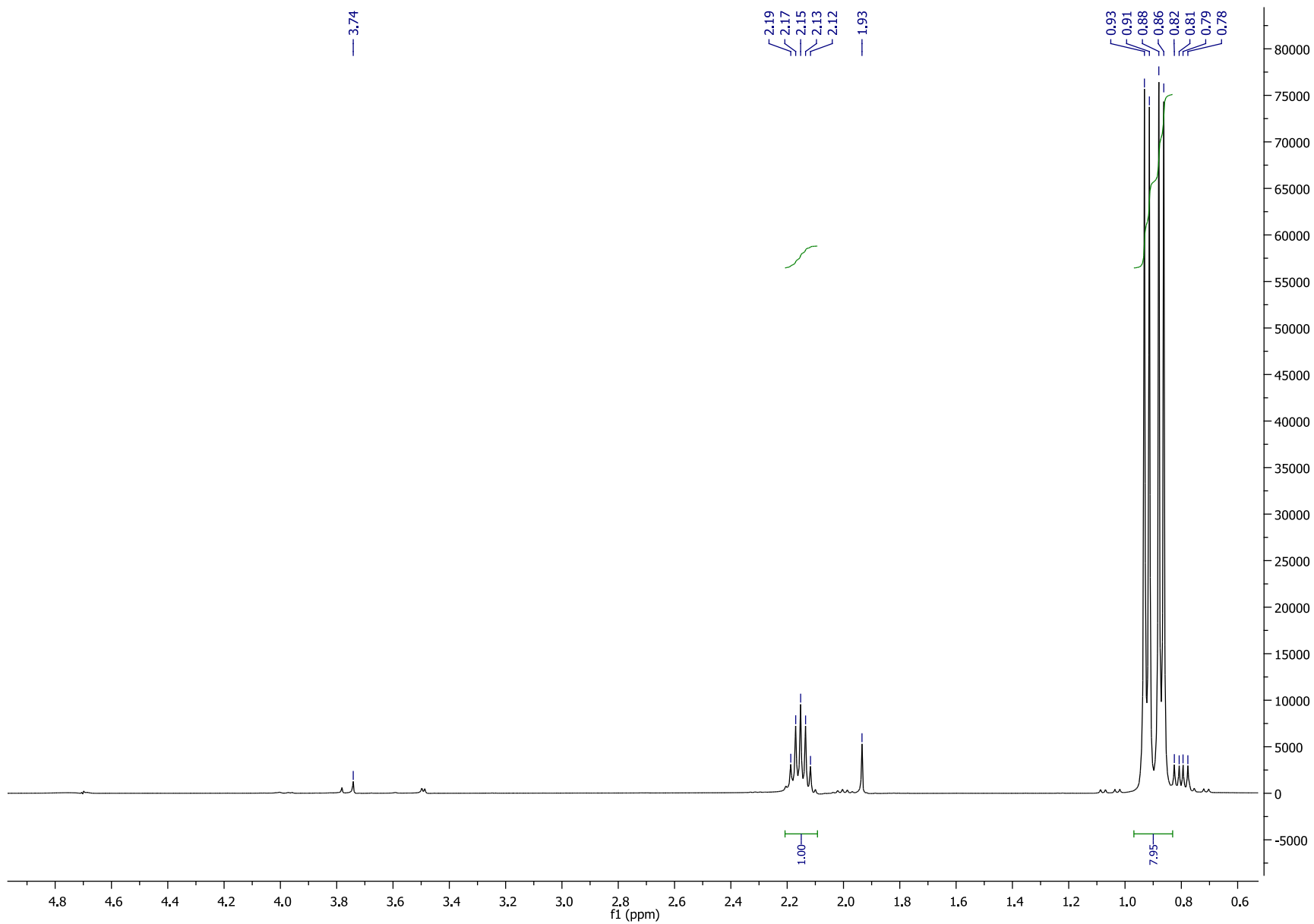
## Chapter 8: Supplemental data

Figure S2  $^1\text{H}$  NMR (500 MHz,  $\text{D}_2\text{O}$ ) of  $\alpha$ -deuterium-isoleucine



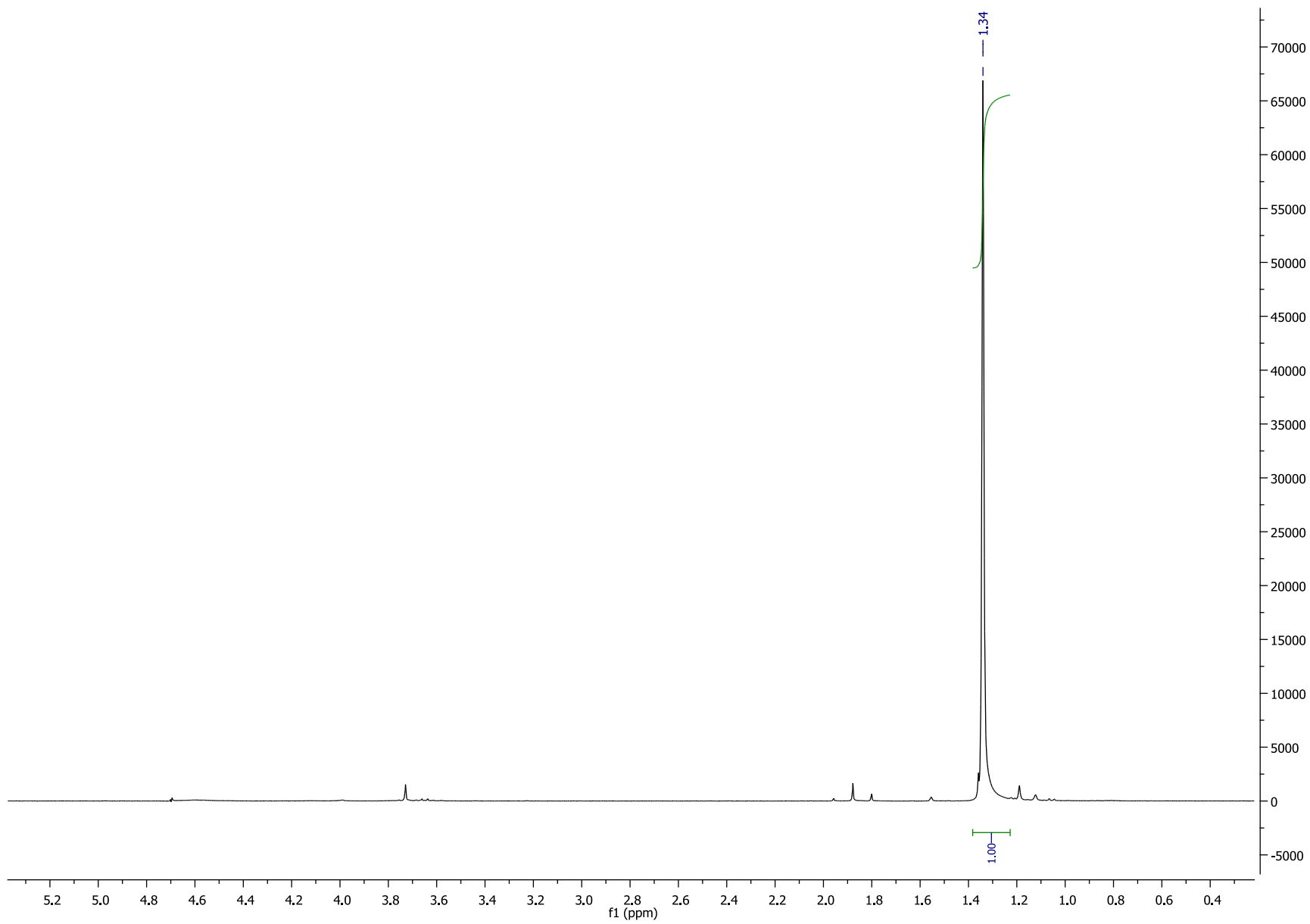
## Chapter 8: Supplemental data

Figure S3  $^1\text{H}$  NMR (500 MHz,  $\text{D}_2\text{O}$ ) of  $\alpha$ -deuterium-valine



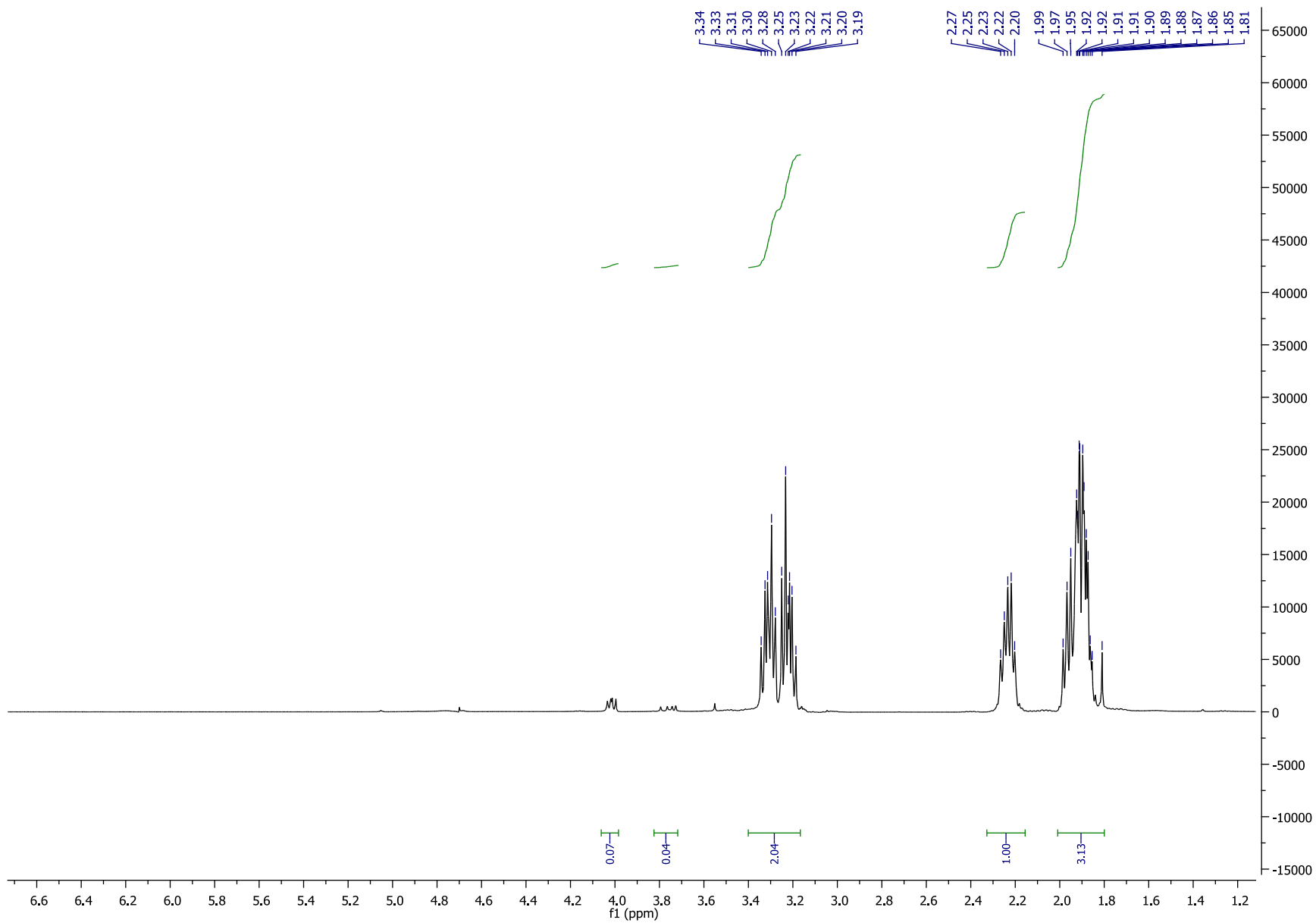
## Chapter 8: Supplemental data

Figure S4  $^1\text{H}$  NMR (500 MHz,  $\text{D}_2\text{O}$ ) of  $\alpha$ -deuterium-alanine



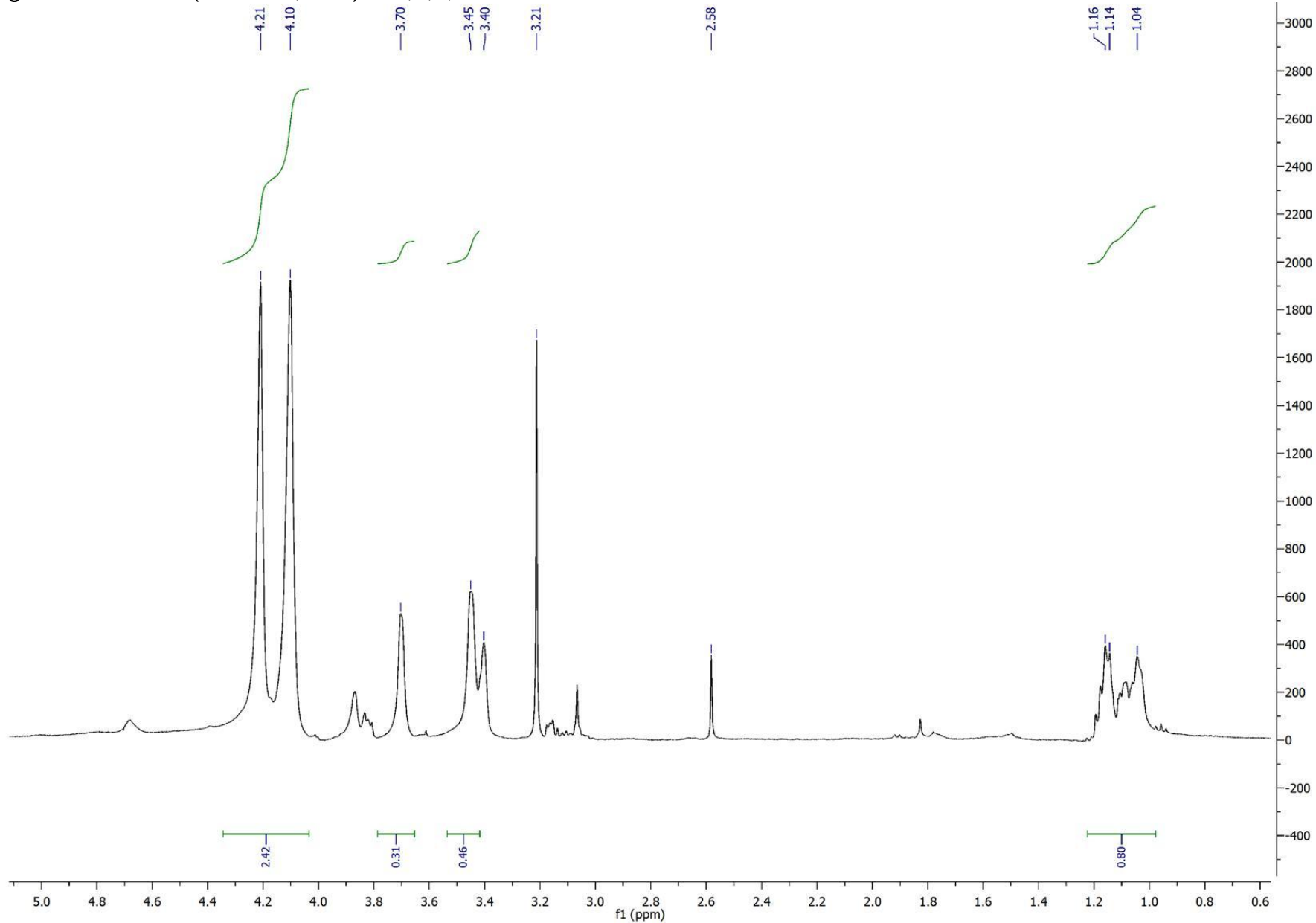
## Chapter 8: Supplemental data

Figure S5  $^1\text{H}$  NMR (500 MHz,  $\text{D}_2\text{O}$ ) of  $\alpha$ -deuterium-proline



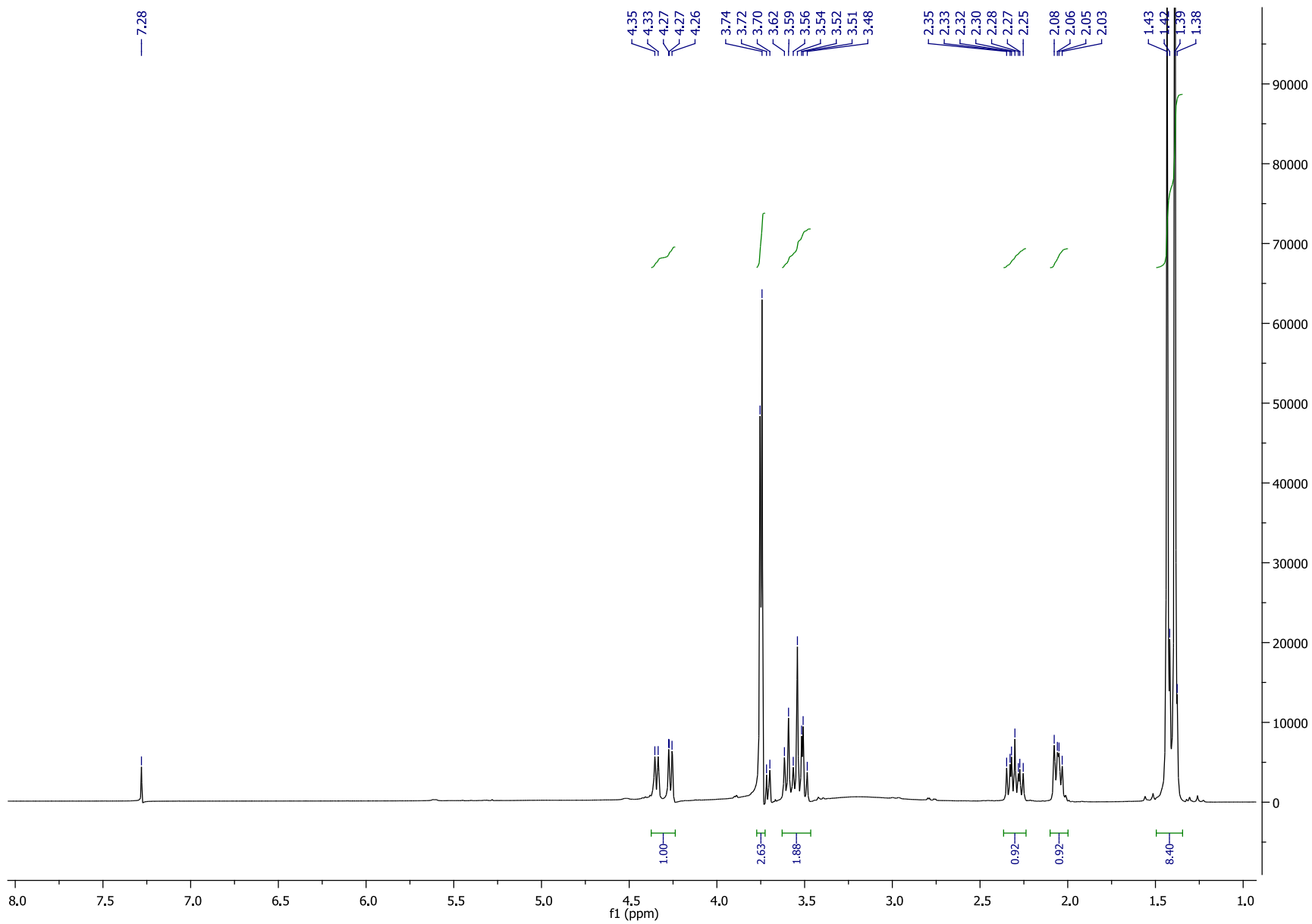
## Chapter 8: Supplemental data

Figure S6  $^1\text{H}$  NMR (500 MHz,  $\text{D}_2\text{O}$ ) of 2,4,4,4-tetradeuterium-threonine



## Chapter 8: Supplemental data

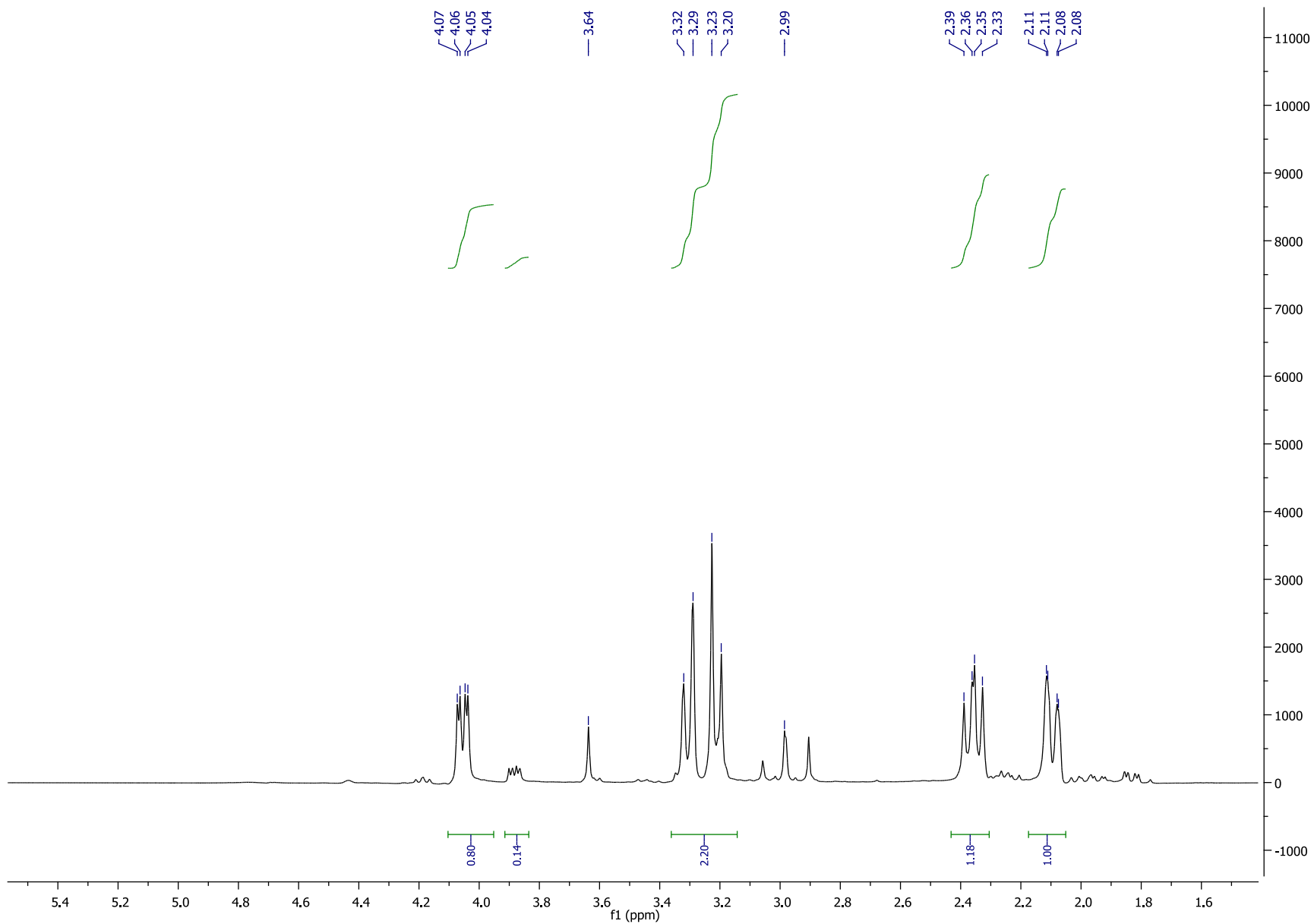
Figure S7  $^1\text{H}$  NMR (500 MHz,  $\text{CDCl}_3$ ) of N-Boc-4-OH-4-deuterium-L-proline methyl ester





## Chapter 8: Supplemental data

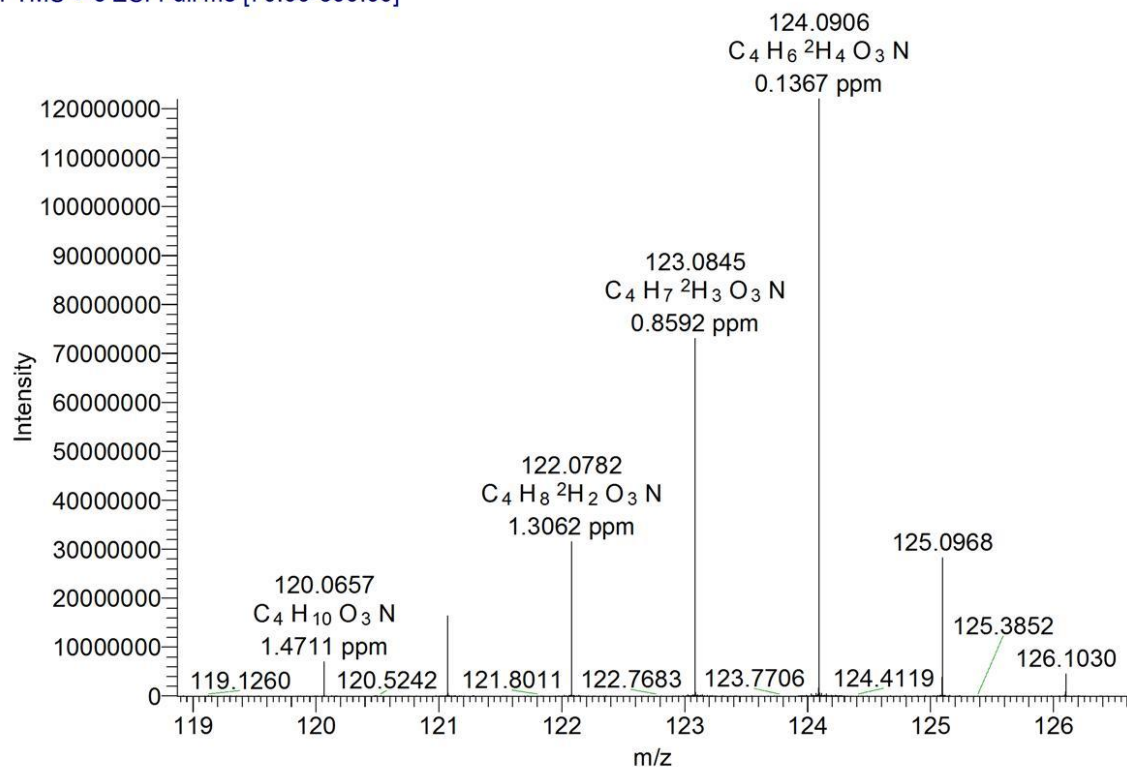
Figure S8  $^1\text{H}$  NMR (500 MHz,  $\text{D}_2\text{O}$ ) of 4-OH-4-deuterium-L-proline methyl ester



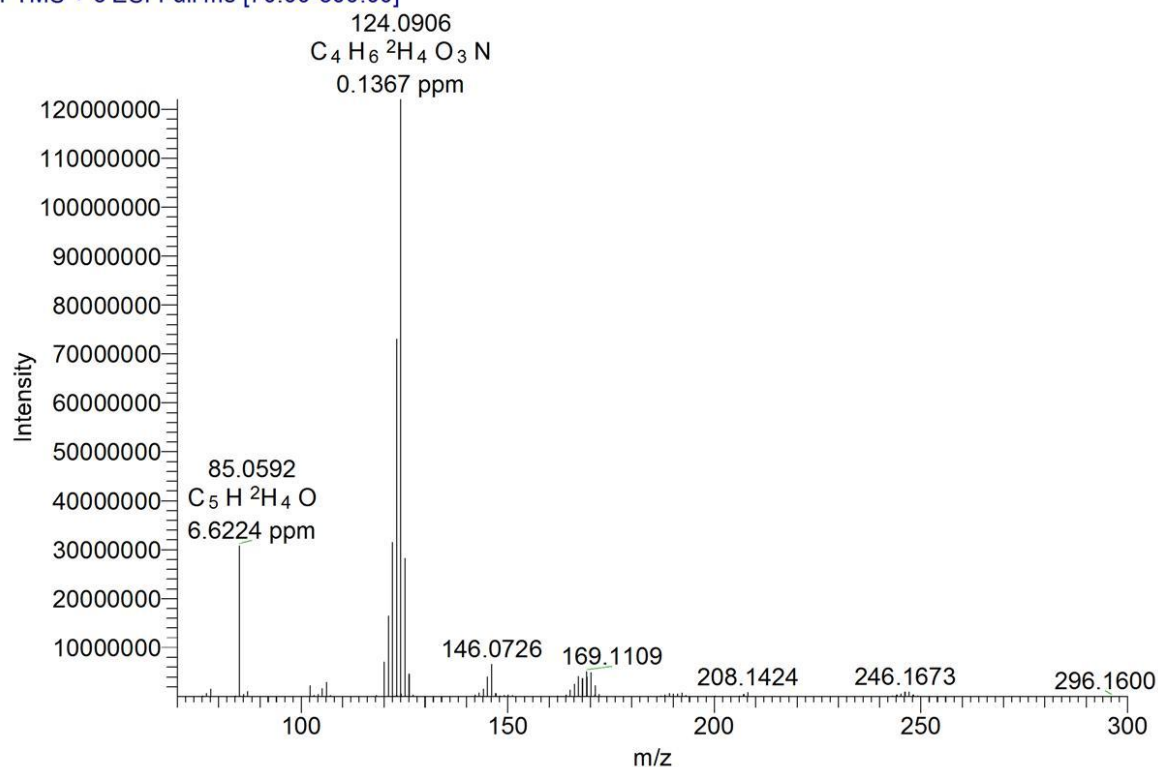
## Chapter 8: Supplemental data

Figure S9 The ESI-HRMS (positive) of 2,4,4,4-tetradeuterium-threonine

THR1408 #28-49 RT: 0.44-0.79 AV: 22 NL: 1.22E8  
T: FTMS + c ESI Full ms [70.00-300.00]



THR1408 #28-49 RT: 0.44-0.79 AV: 22 NL: 1.22E8  
T: FTMS + c ESI Full ms [70.00-300.00]



## Chapter 8: Supplemental data

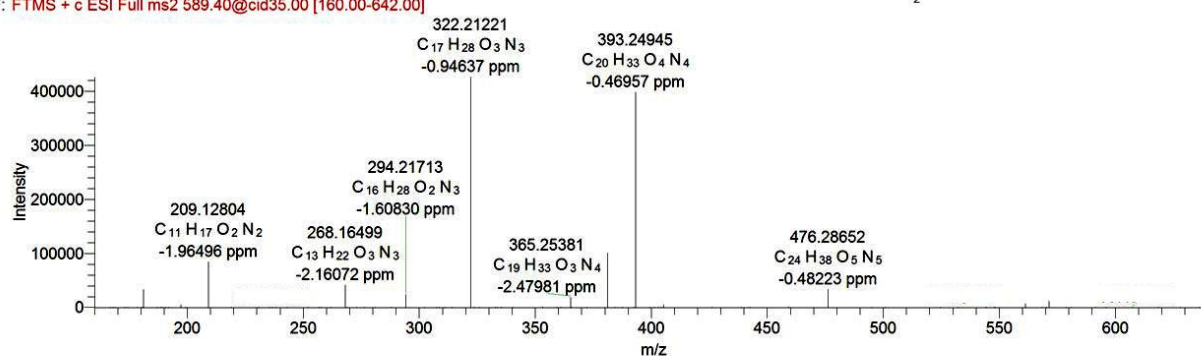
Figure S10 MS<sup>2</sup> (positive) of compounds 1–9 in FTMS mode (CID 35 eV)

C:\Users\...\N06-pdb-s\N06-pdb-s-ms2-589

5/30/2013 5:11:50 PM

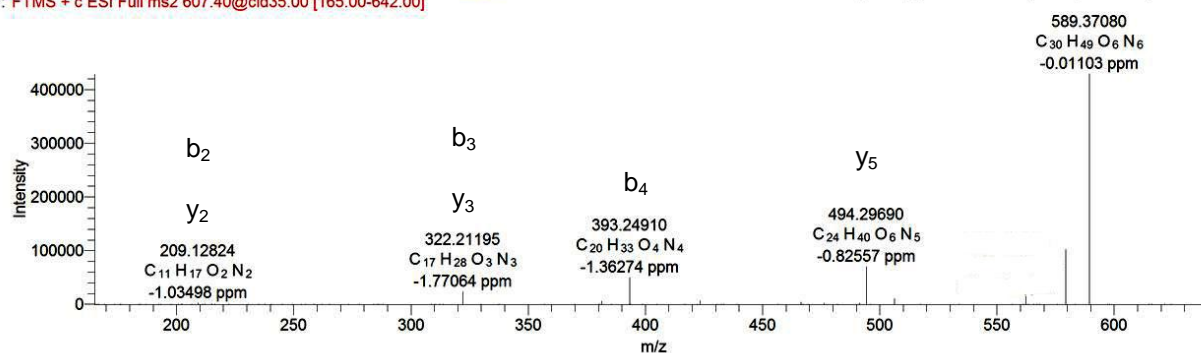
N06-pdb-s-ms2-589 #1090-1097 RT: 10.25-10.32 AV: 8 NL: 4.25E5  
F: FTMS + c ESI Full ms2 589.40@cid35.00 [160.00-642.00]

Parent ion: [M-2H<sub>2</sub>O+H]<sup>+</sup>, m/z 589.4 (compounds 1–4)



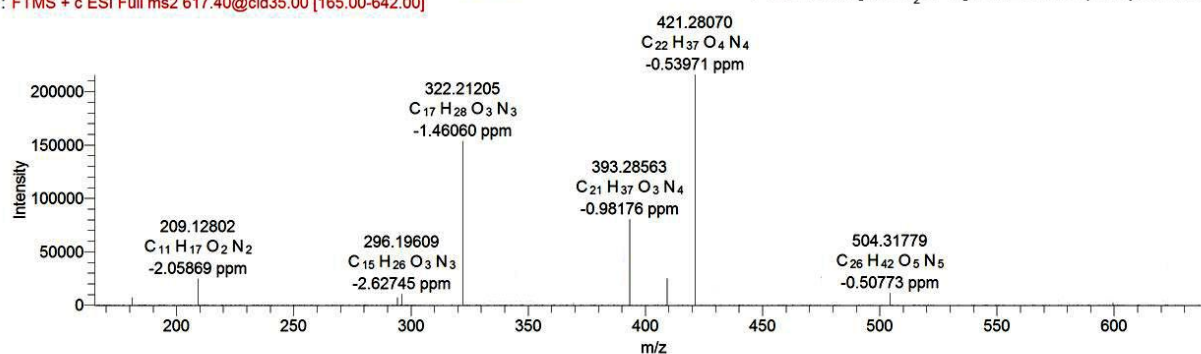
N06-pdb-s-ms2-607 #1461-1467 RT: 13.77-13.83 AV: 7 NL: 4.29E5  
F: FTMS + c ESI Full ms2 607.40@cid35.00 [165.00-642.00]

Parent ion: [M+H]<sup>+</sup>, m/z 607.4 (compound 5)



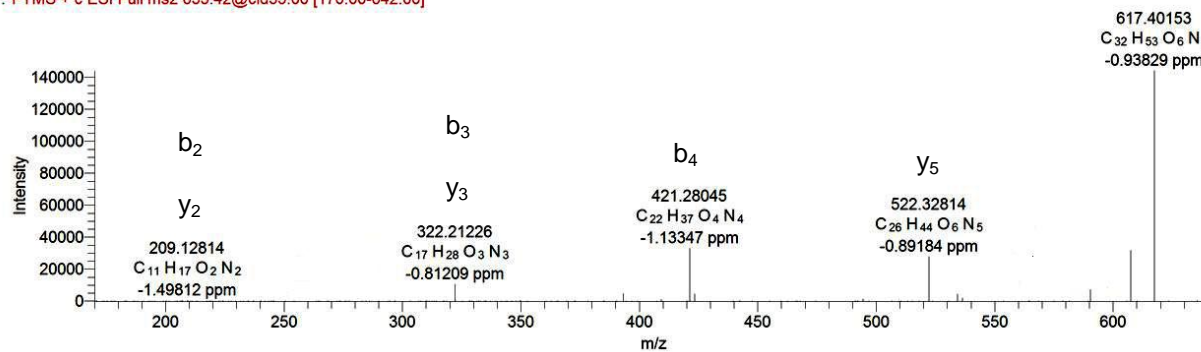
N06-pdb-s-ms2-617 #2038-2081 RT: 19.03-19.43 AV: 44 NL: 2.15E5  
F: FTMS + c ESI Full ms2 617.40@cid35.00 [165.00-642.00]

Parent ion: [M-2H<sub>2</sub>O+H]<sup>+</sup>, m/z 617.4 (compounds 6–8)



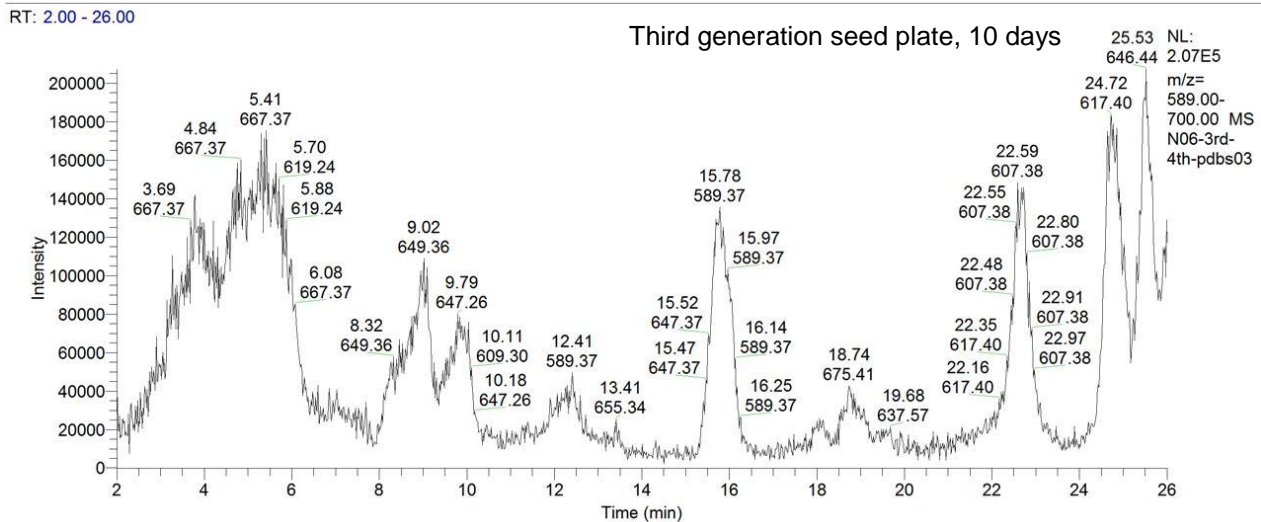
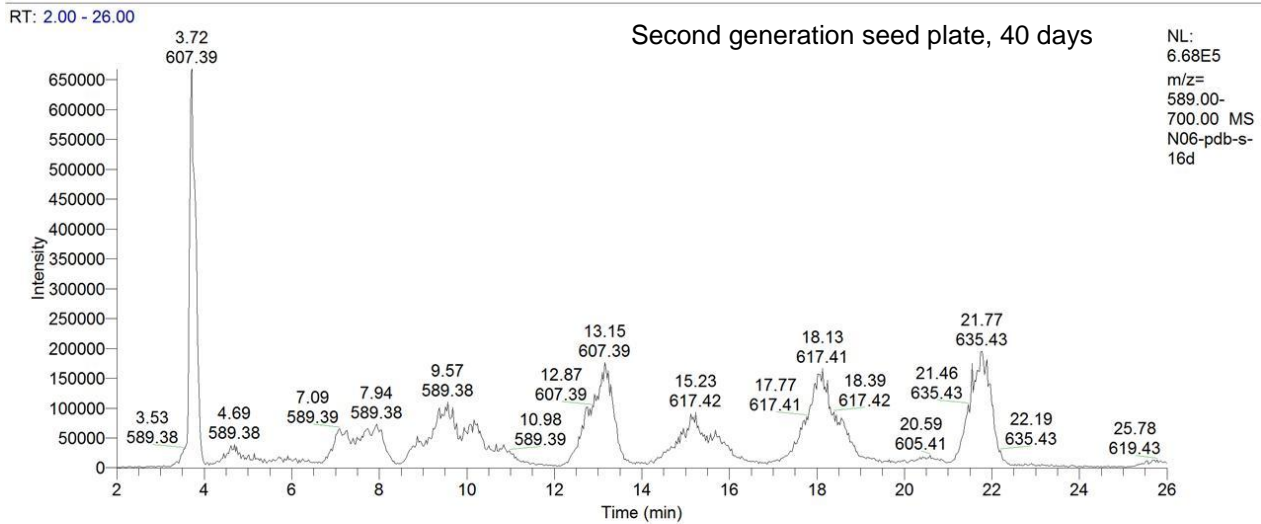
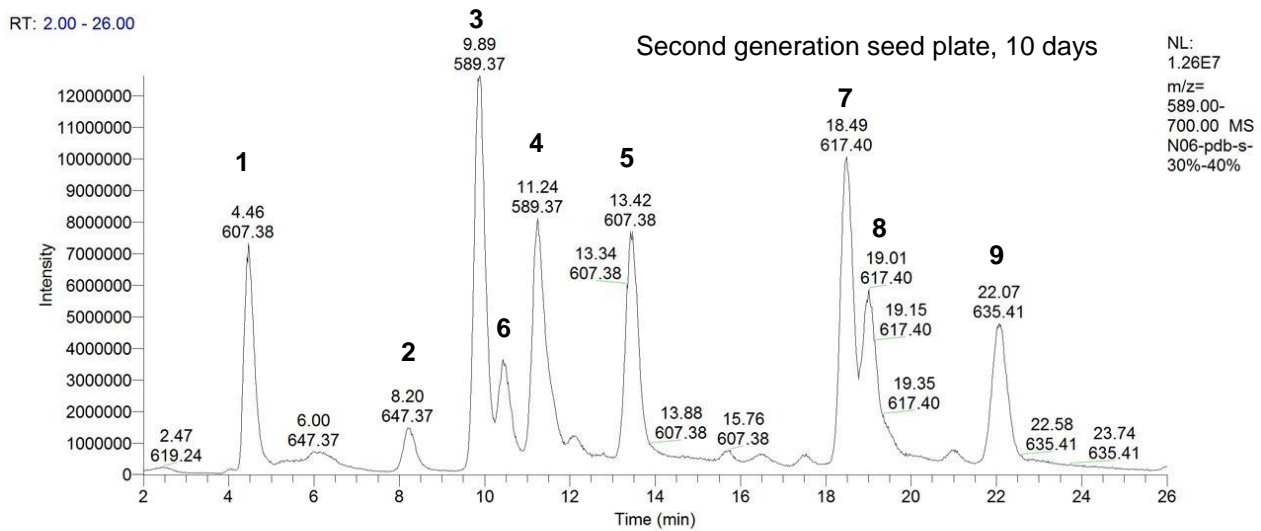
N06-pdb-s-ms2-635 #2377-2396 RT: 22.24-22.42 AV: 20 NL: 1.44E5  
F: FTMS + c ESI Full ms2 635.42@cid35.00 [170.00-642.00]

Parent ion: [M+H]<sup>+</sup>, m/z 635.4 (compound 9)



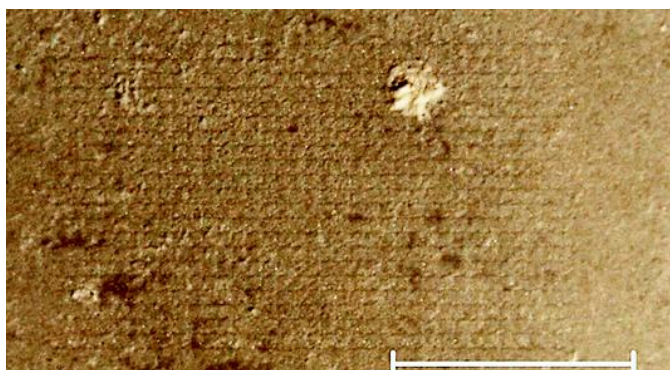
## Chapter 8: Supplemental data

Figure S11 The LC-MS analysis for hexacyclopeptides in fermented static PDB inoculated from different seed plates.

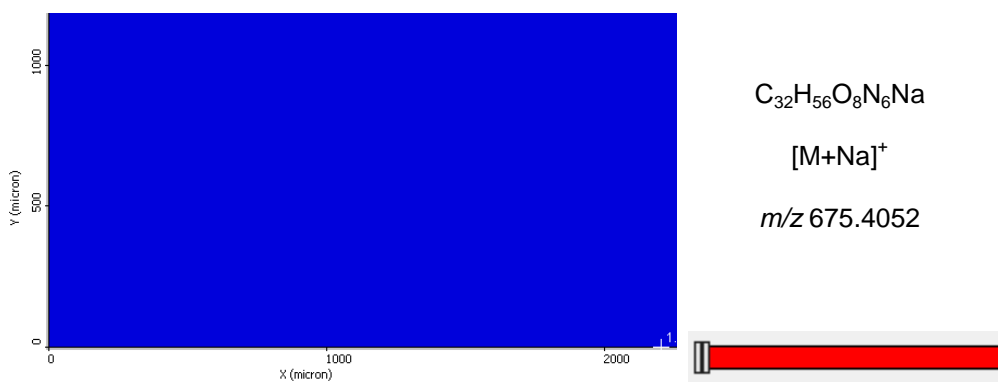
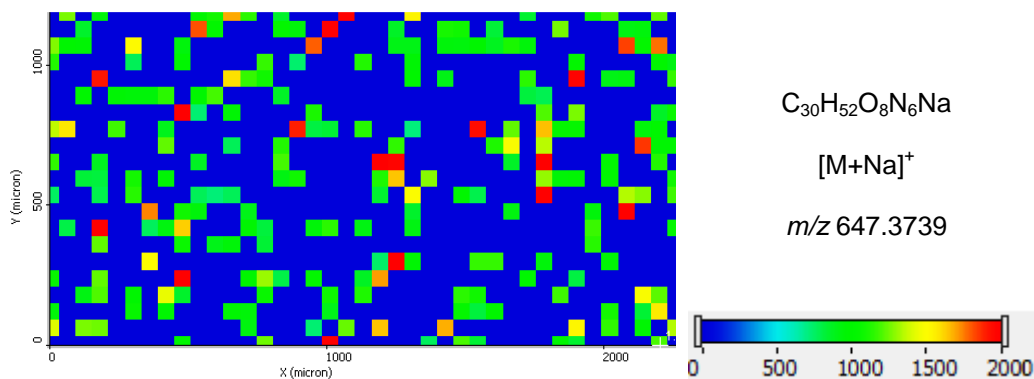


## Chapter 8: Supplemental data

Figure S12 The interferences on blank agar with matrix solution for MALDI-IMS measurement ( $\Delta < 2$  ppm)

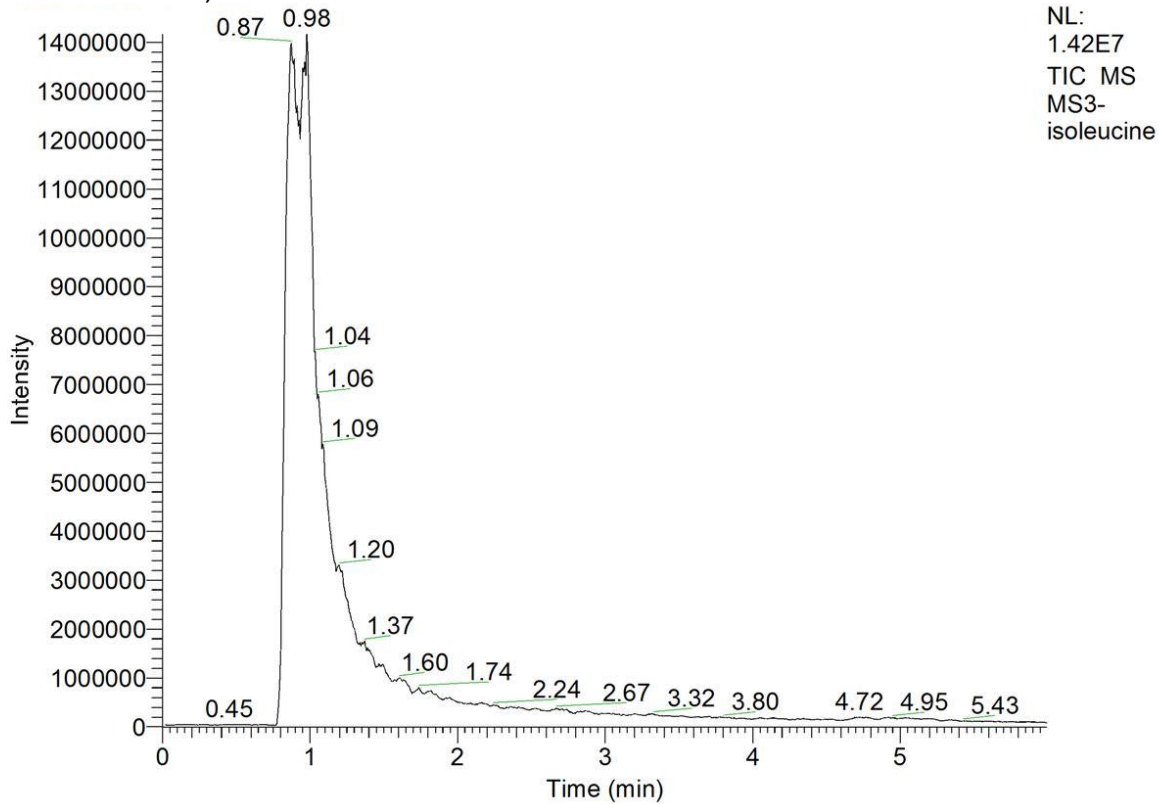


Blank agar with  
sprayed matrix  
(HCCA)

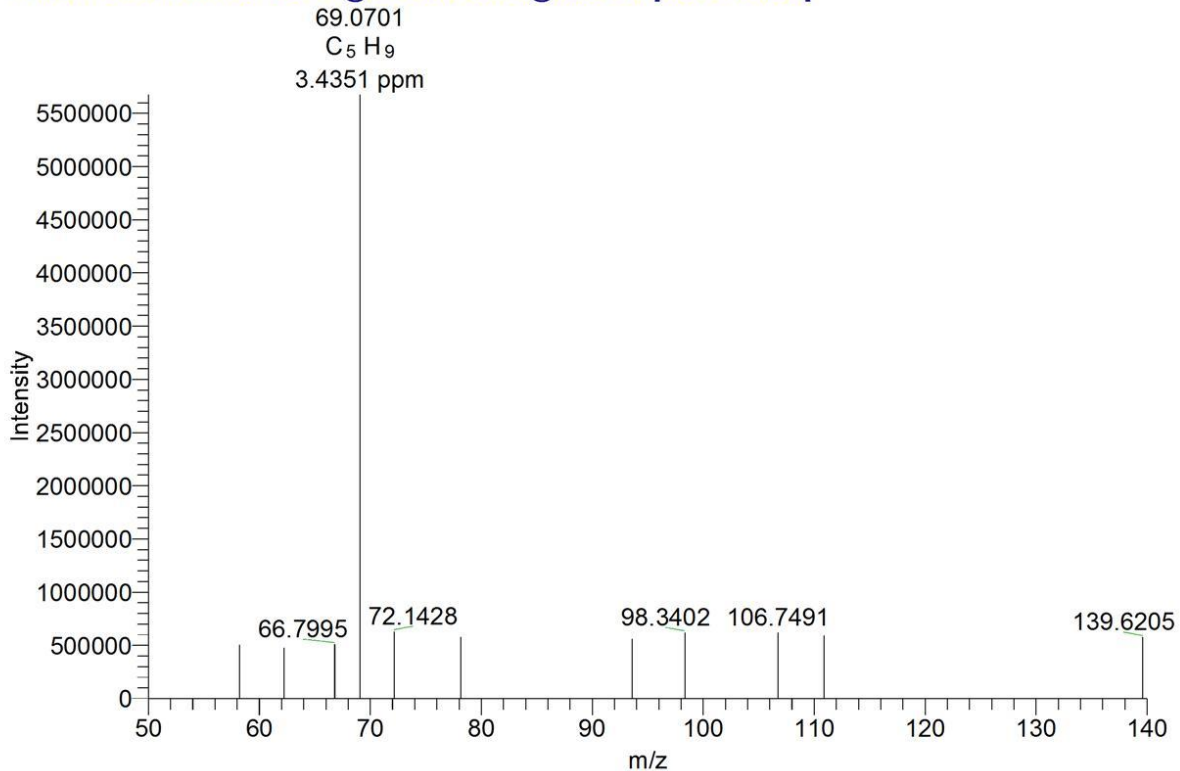


## Chapter 8: Supplemental data

Figure S13 The MS<sup>3</sup> (positive) of isoleucine (C<sub>6</sub>H<sub>13</sub>NO<sub>2</sub>).  
Parent ions: *m/z* 132.1, [M+H]<sup>+</sup> for MS<sup>2</sup> and *m/z* 86.1, [M-HCOOH+H]<sup>+</sup> for MS<sup>3</sup> (isolation width: *m/z* 2 amu).



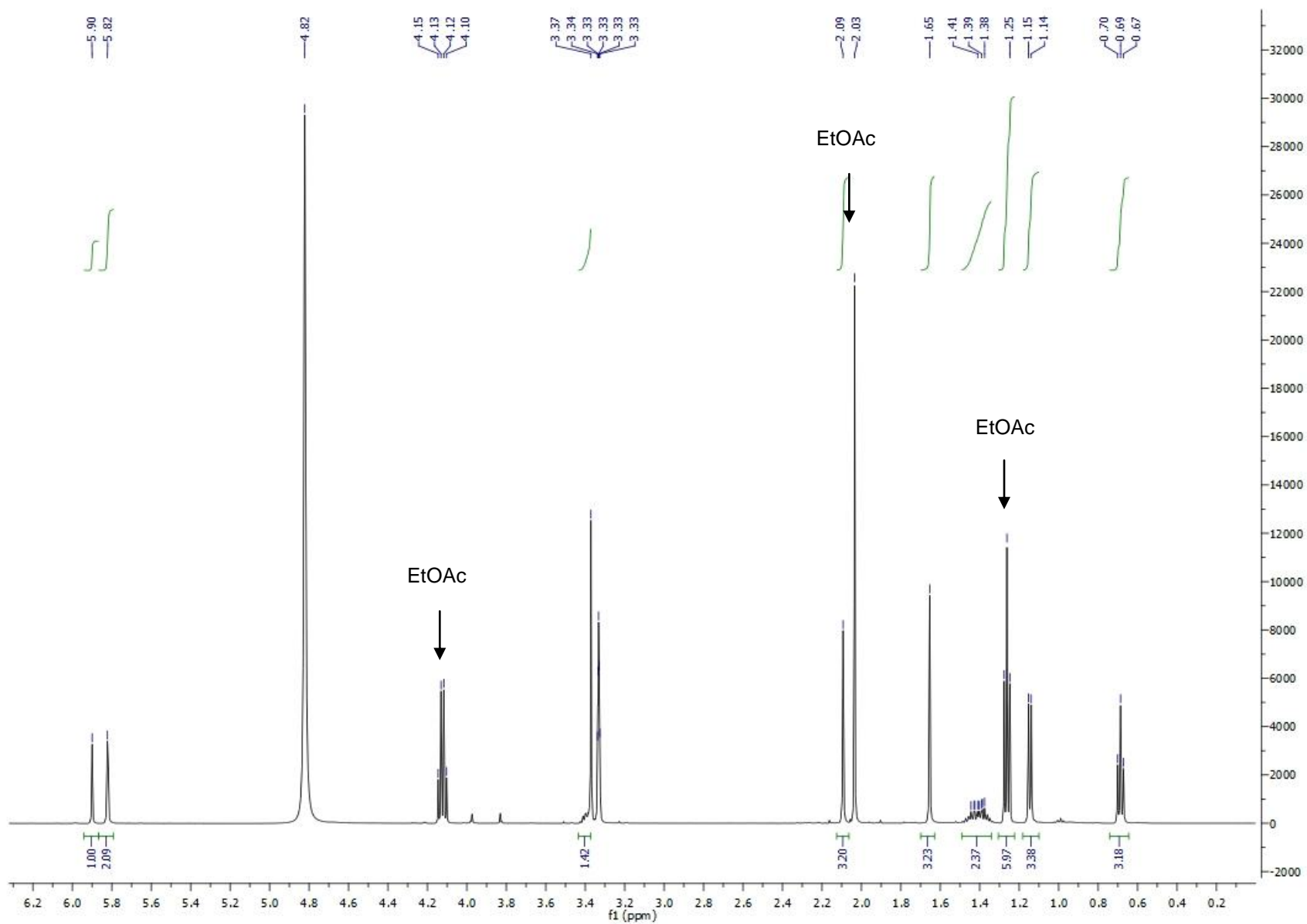
MS3-isoleucine #111 RT: 0.94 AV: 1 NL: 5.67E6  
T: FTMS + c ESI Full ms3 132.17@cid35.00 86.09@cid35.00 [50.00-140.00]





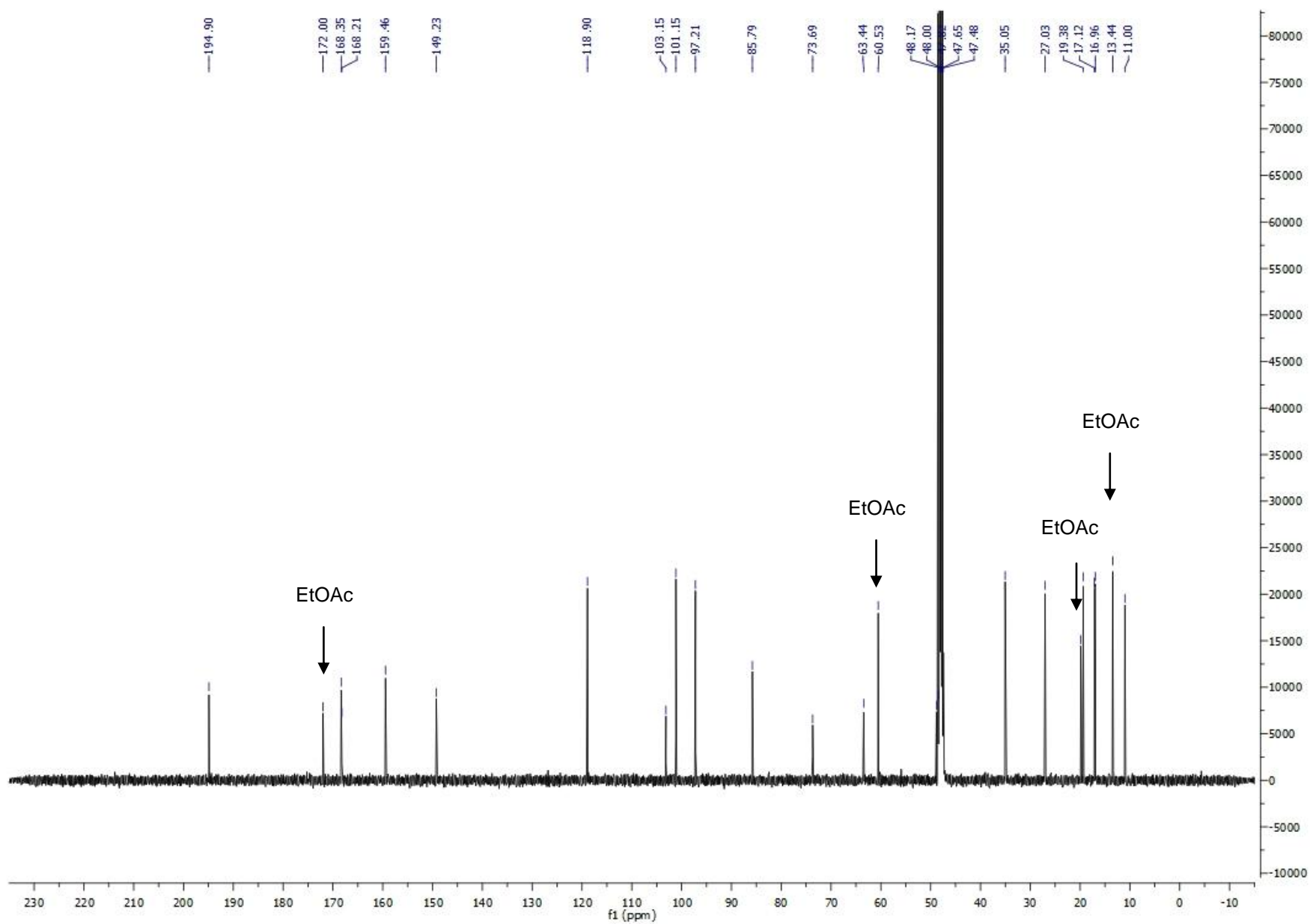
## Chapter 8: Supplemental data

Figure S14 .  $^1\text{H}$  NMR (500 MHz,  $\text{CD}_3\text{OD}$ ) spectrum of colletotrichone A (**10**)



## Chapter 8: Supplemental data

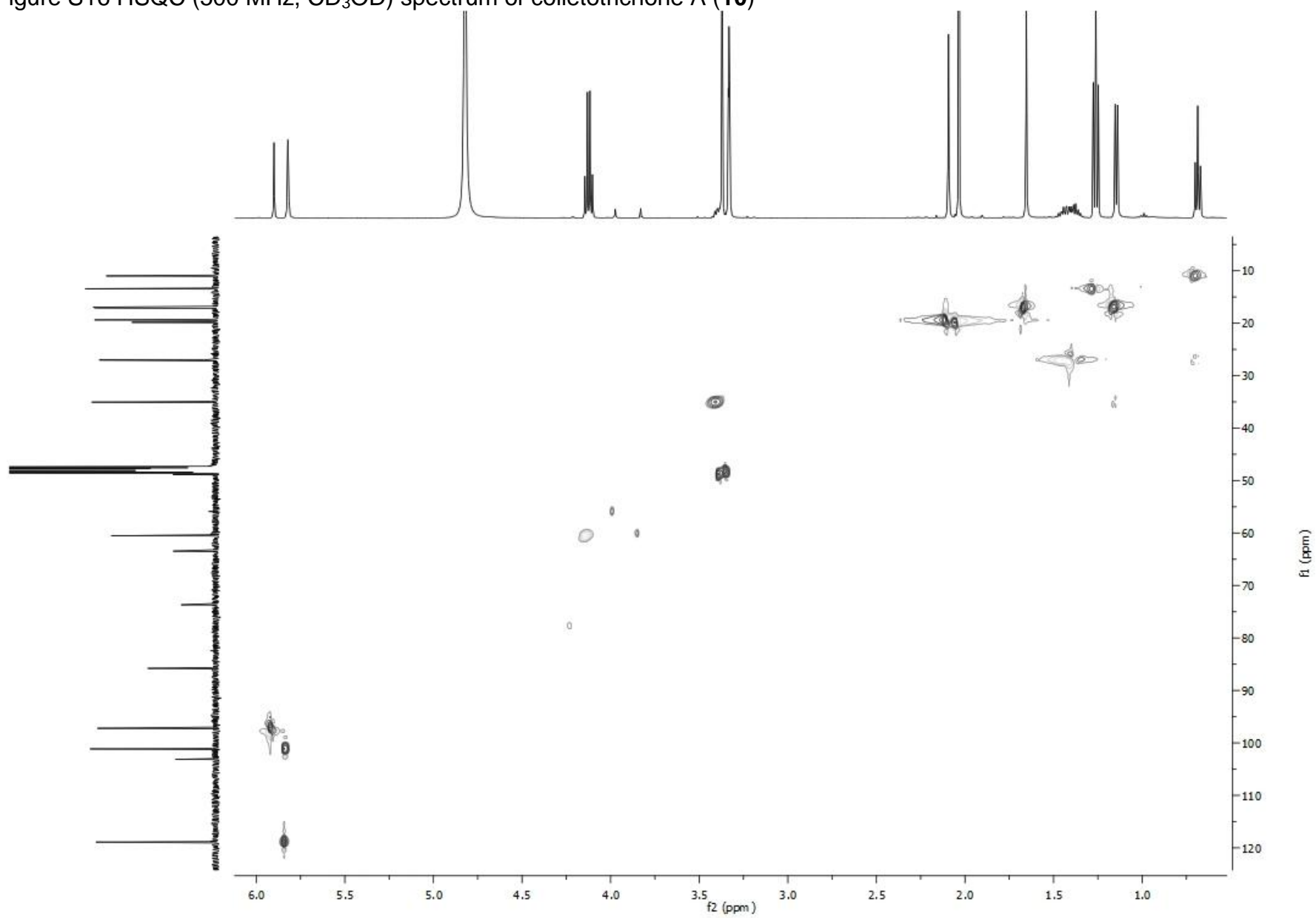
Figure S15  $^{13}\text{C}$  NMR (125 MHz,  $\text{CD}_3\text{OD}$ ) spectrum of colletotrichone A (**10**)





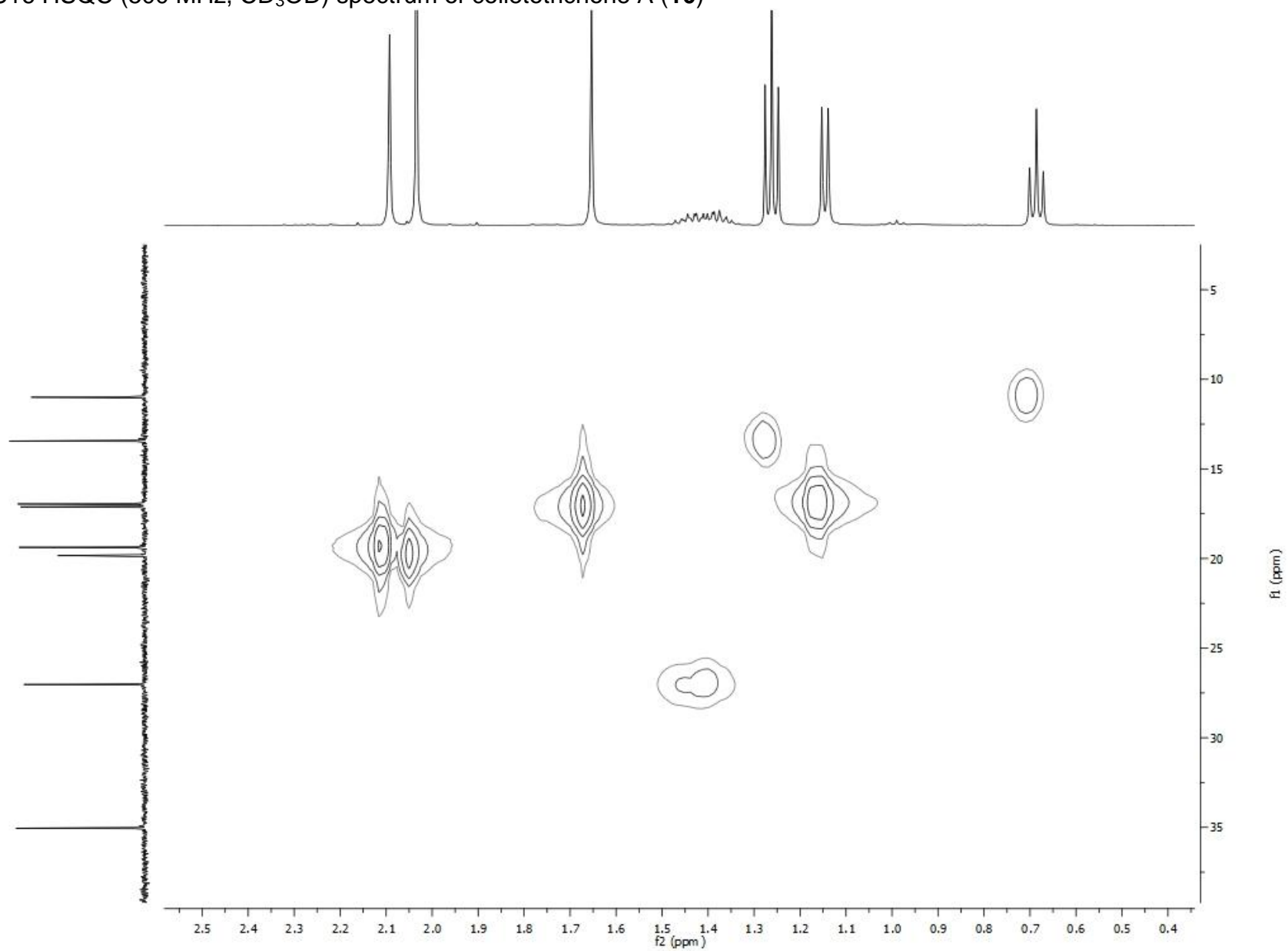
## Chapter 8: Supplemental data

Figure S16 HSQC (500 MHz, CD<sub>3</sub>OD) spectrum of colletotrichone A (**10**)



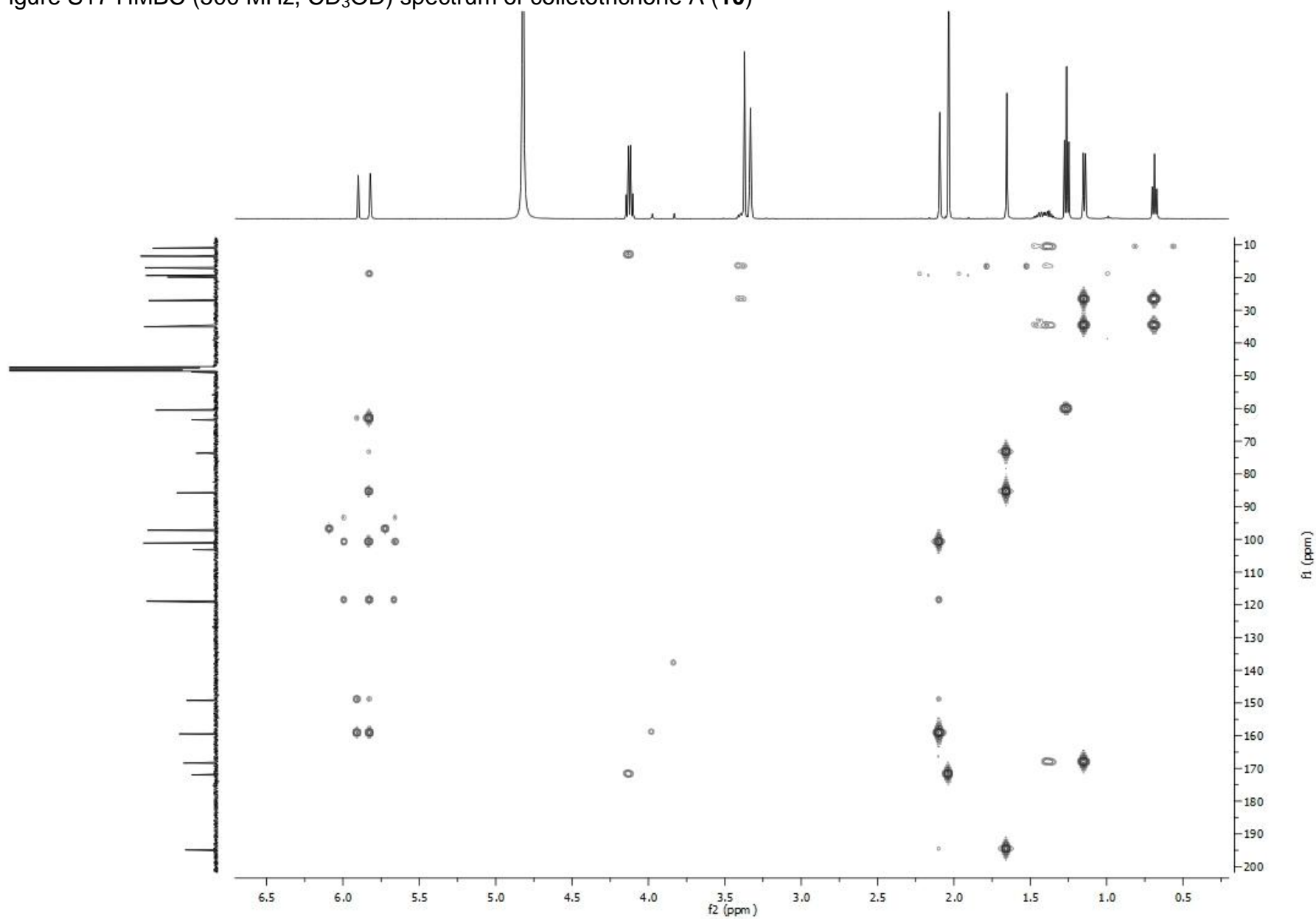
## Chapter 8: Supplemental data

Figure S16 HSQC (500 MHz, CD<sub>3</sub>OD) spectrum of colletotrichone A (**10**)



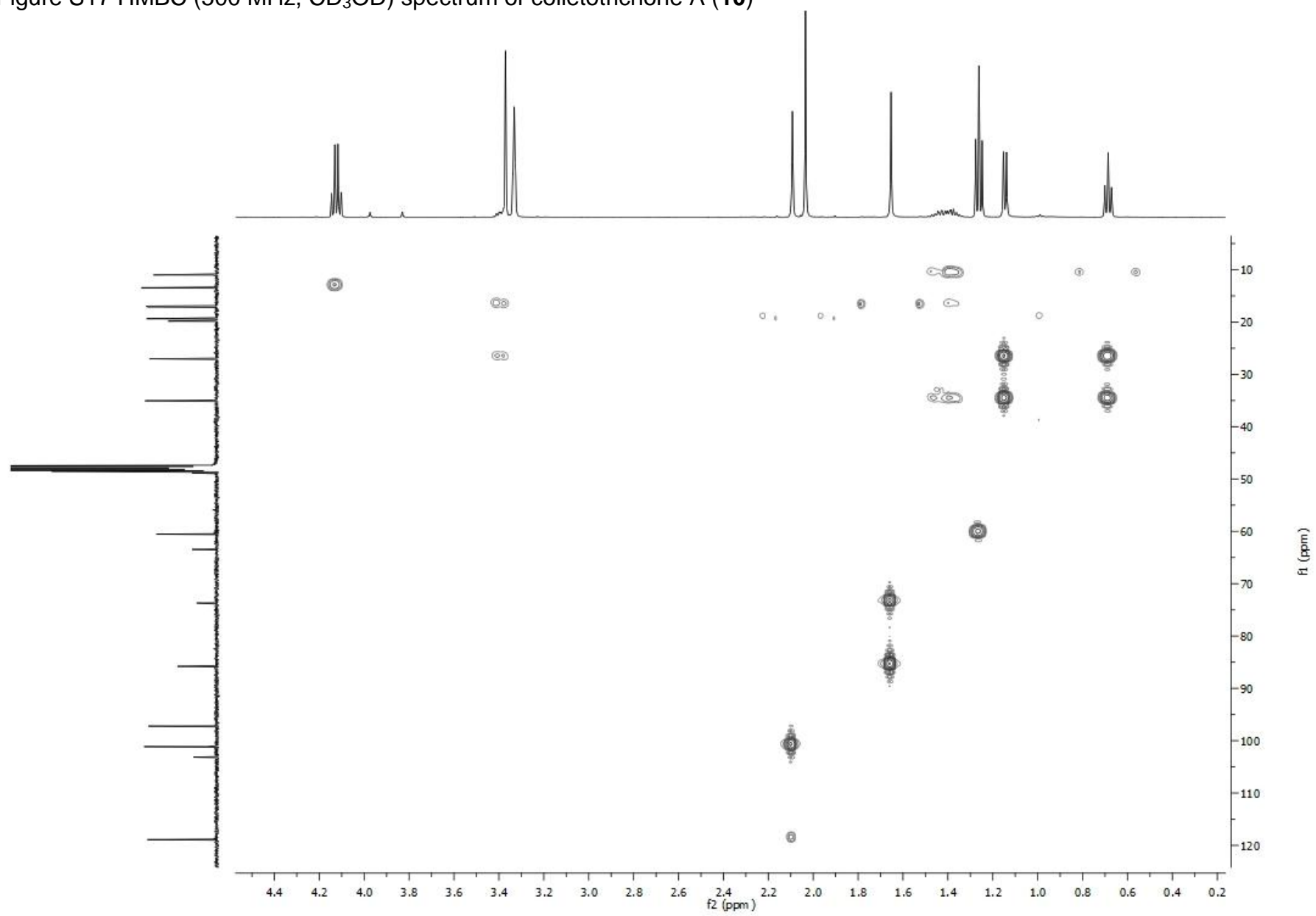
## Chapter 8: Supplemental data

Figure S17 HMBC (500 MHz, CD<sub>3</sub>OD) spectrum of colletotrichone A (**10**)



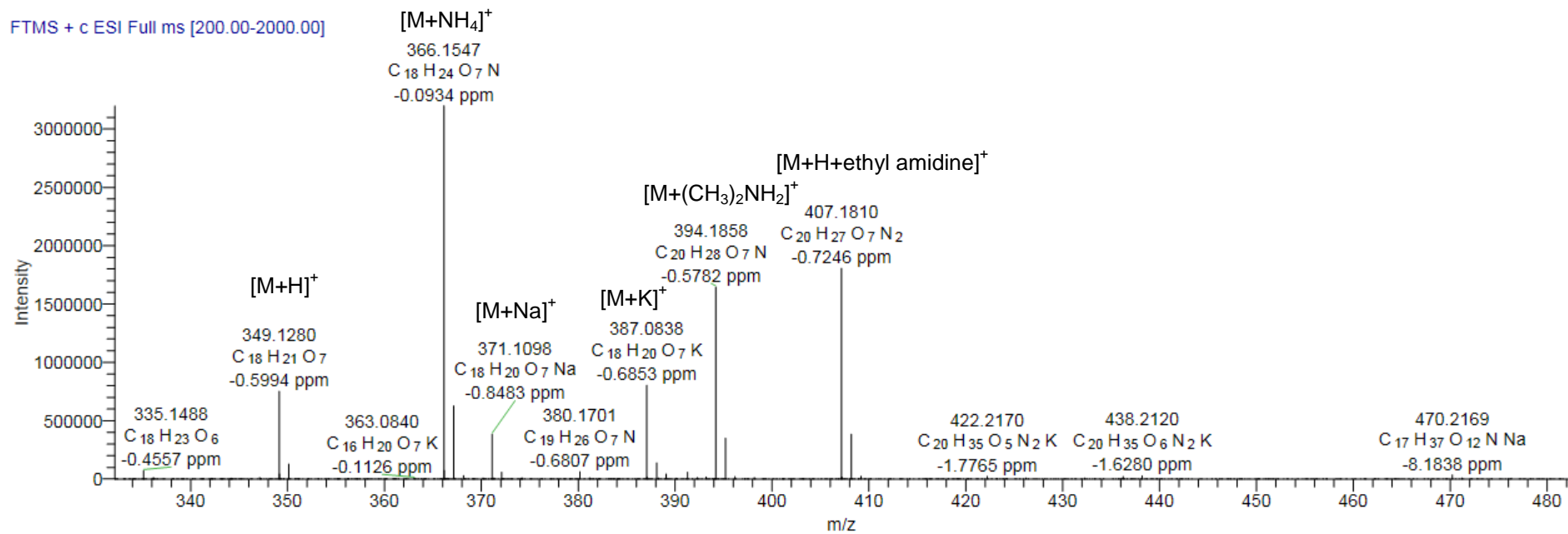
## Chapter 8: Supplemental data

Figure S17 HMBC (500 MHz, CD<sub>3</sub>OD) spectrum of colletotrichone A (**10**)



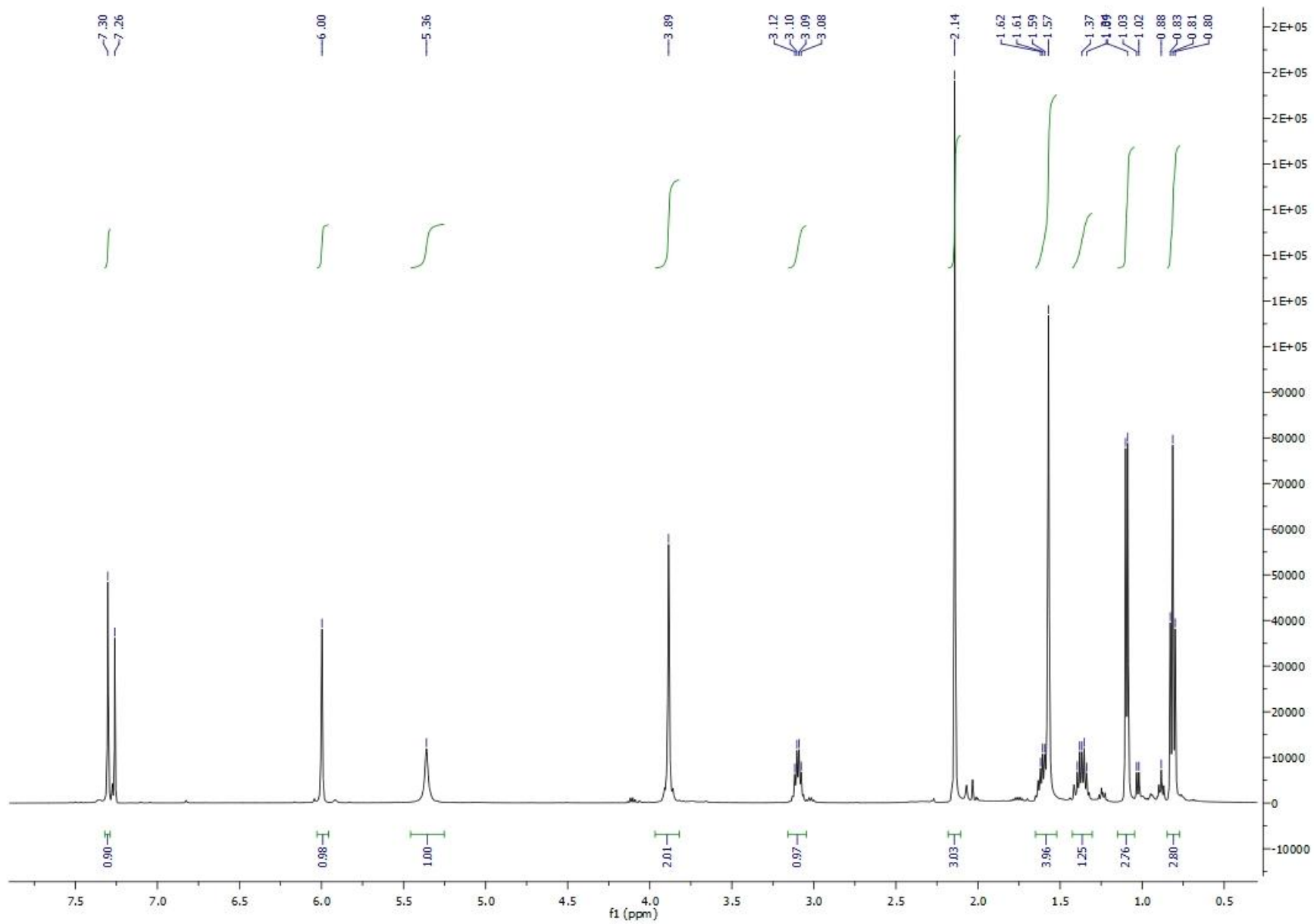
## Chapter 8: Supplemental data

Figure S18 Positive ESIHRMS of colletotrichone A (**10**)



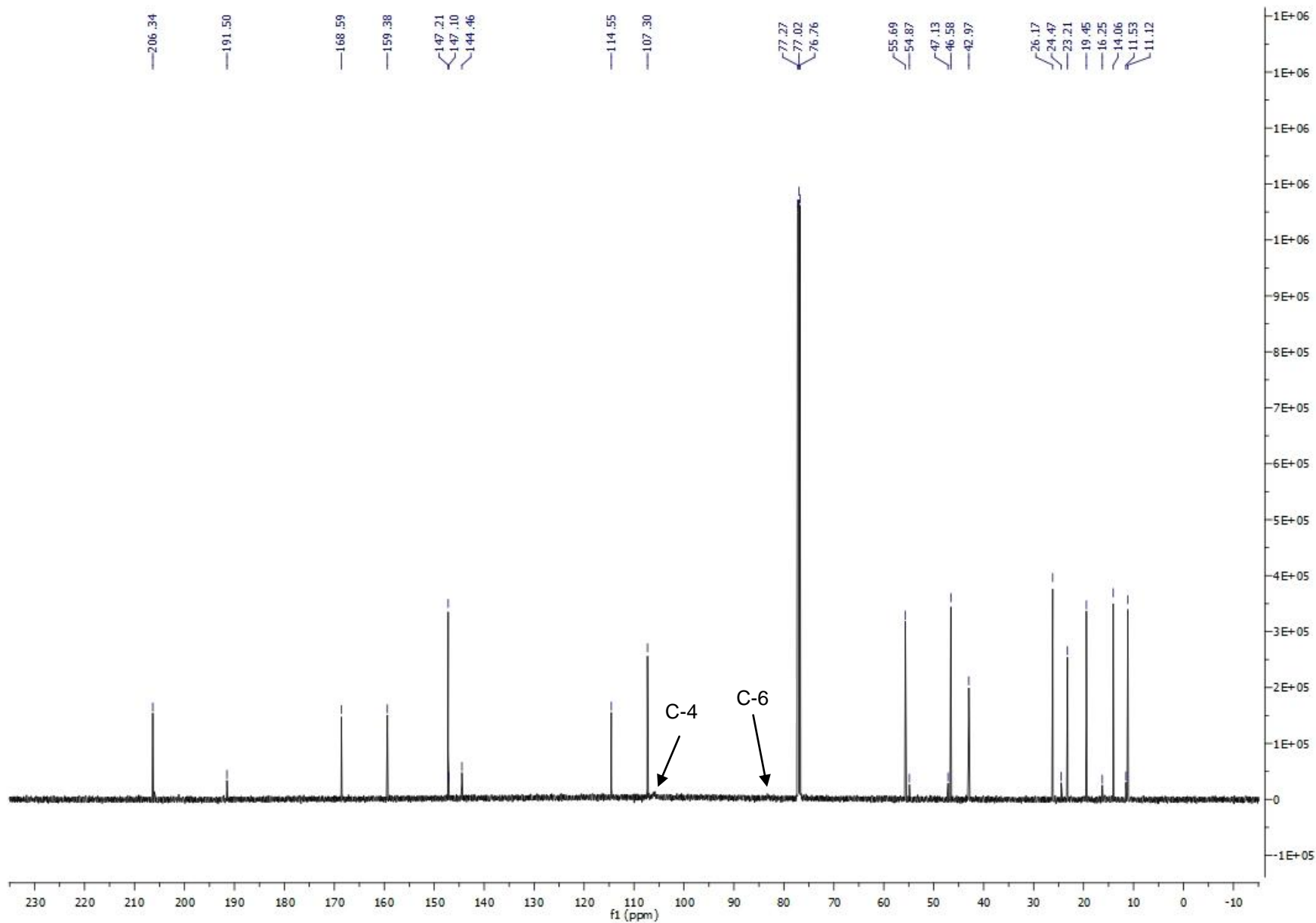
## Chapter 8: Supplemental data

Figure S19  $^1\text{H}$  NMR (500 MHz,  $\text{CDCl}_3$ ) spectrum of colletotrichone B (**11a**)



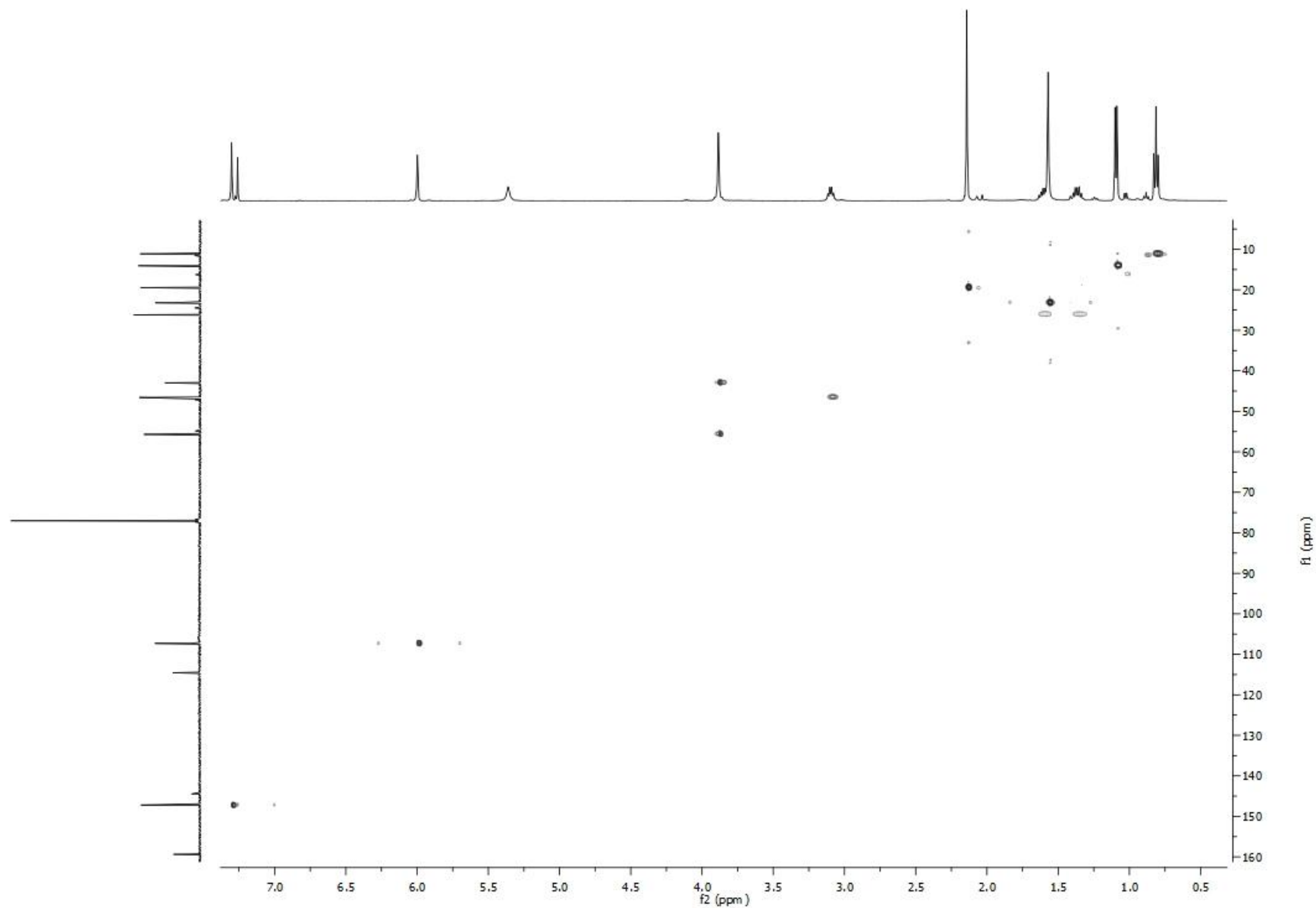
## Chapter 8: Supplemental data

Figure S20  $^{13}\text{C}$  NMR (125 MHz,  $\text{CDCl}_3$ ) spectrum of colletotrichone B (**11a**)



## Chapter 8: Supplemental data

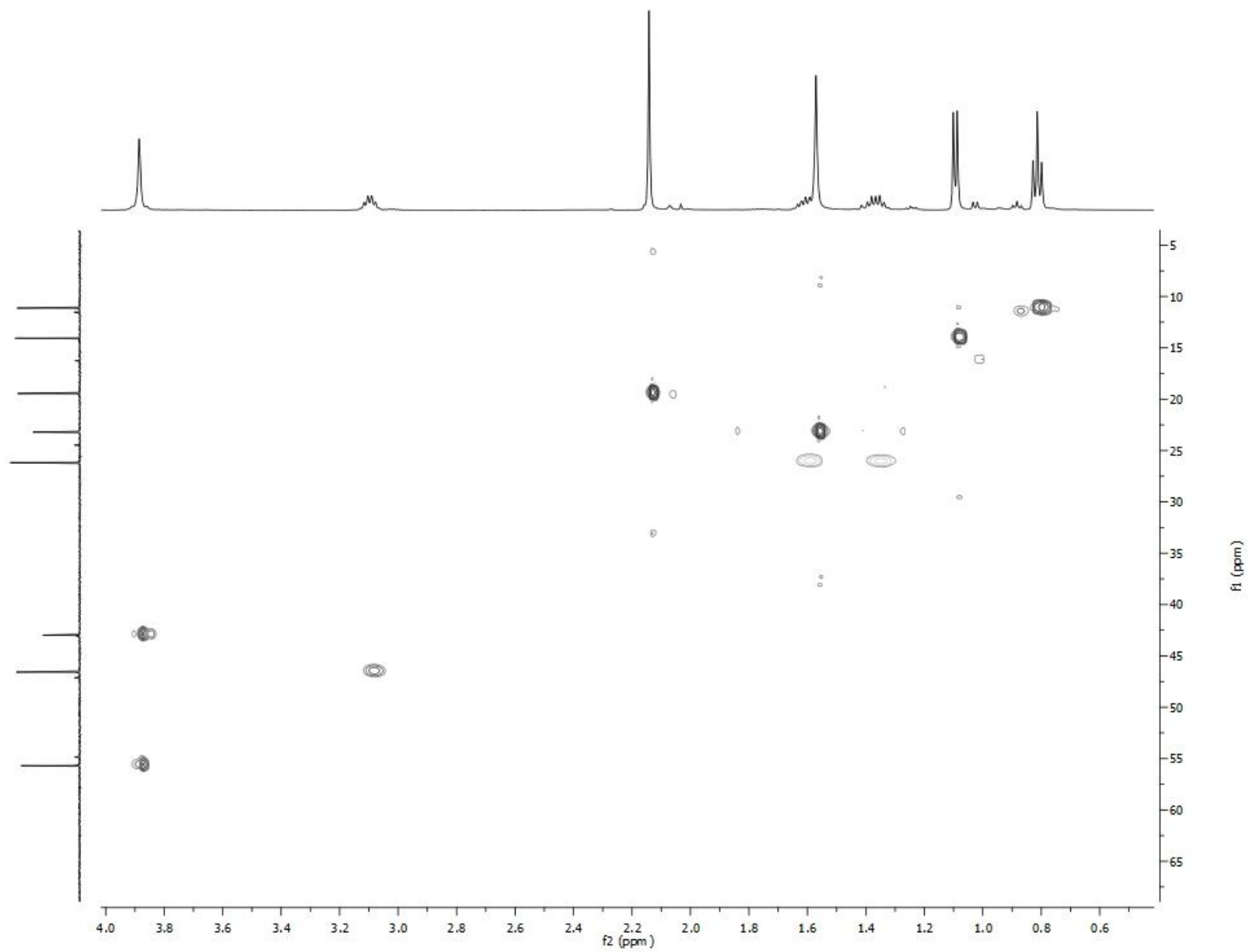
Figure S21 HSQC (500 MHz, CDCl<sub>3</sub>) spectrum of colletotrichone B (**11a**)





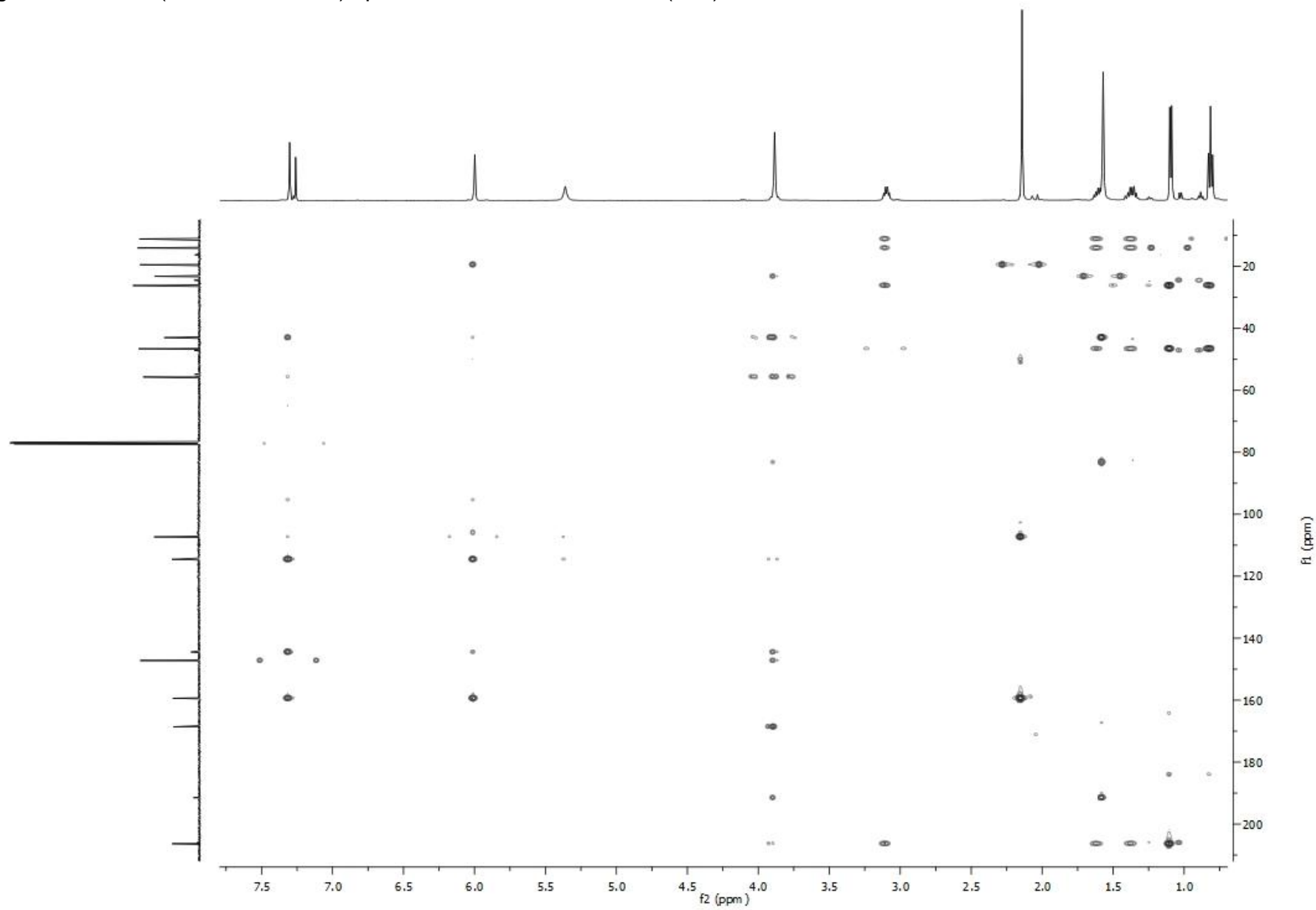
## Chapter 8: Supplemental data

Figure S21 HSQC (500 MHz, CDCl<sub>3</sub>) spectrum of colletotrichone B (**11a**)



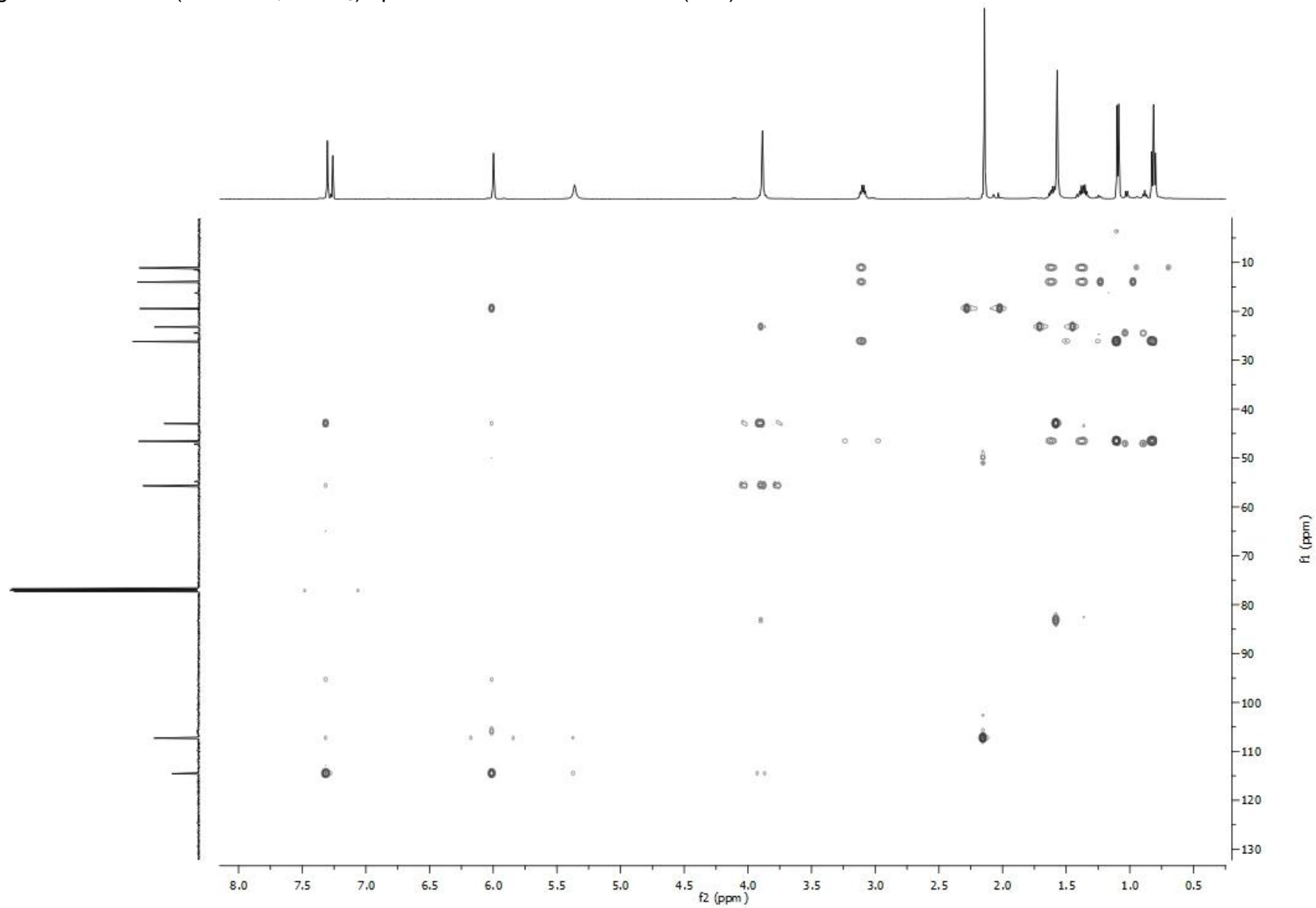
## Chapter 8: Supplemental data

Figure 22 HMBC (500 MHz, CDCl<sub>3</sub>) spectrum of colletotrichone B (**11a**)



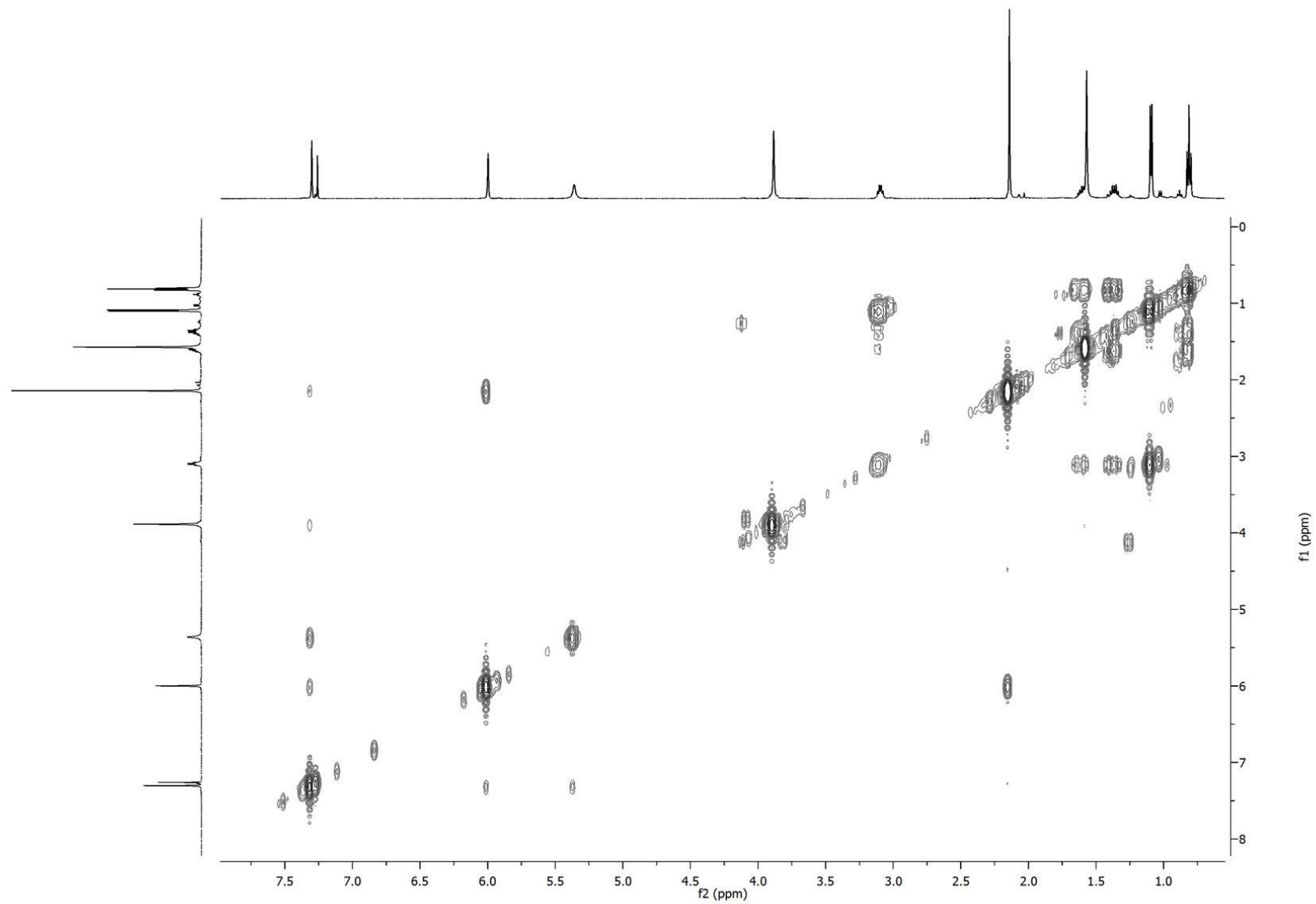
## Chapter 8: Supplemental data

Figure S22 HMBC (500 MHz, CDCl<sub>3</sub>) spectrum of colletotrichone B (**11a**)



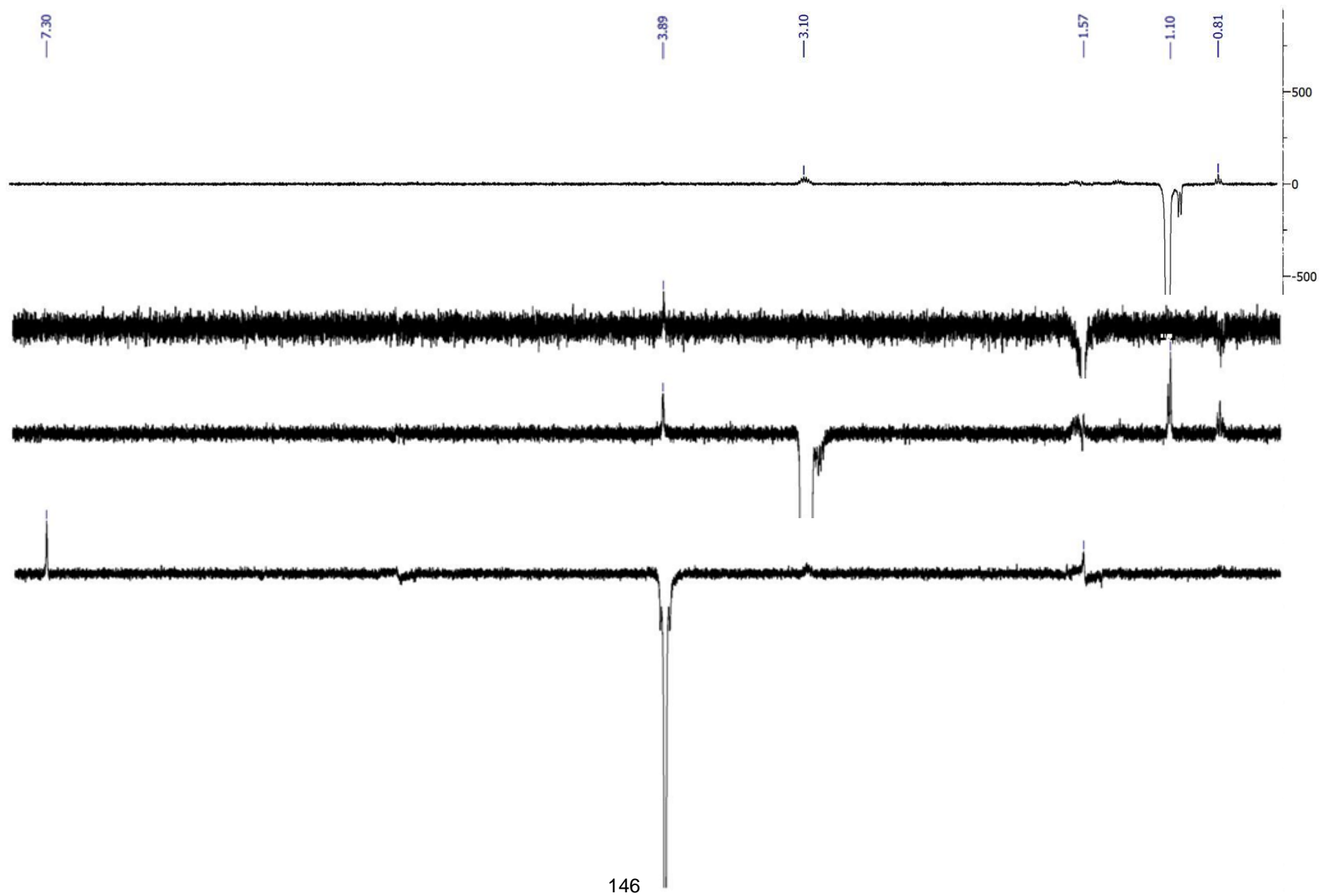
## Chapter 8: Supplemental data

Figure S23  $^1\text{H}$ ,  $^1\text{H}$  COSY (500 MHz,  $\text{CDCl}_3$ ) spectrum of colletotrichone B (**11a**)



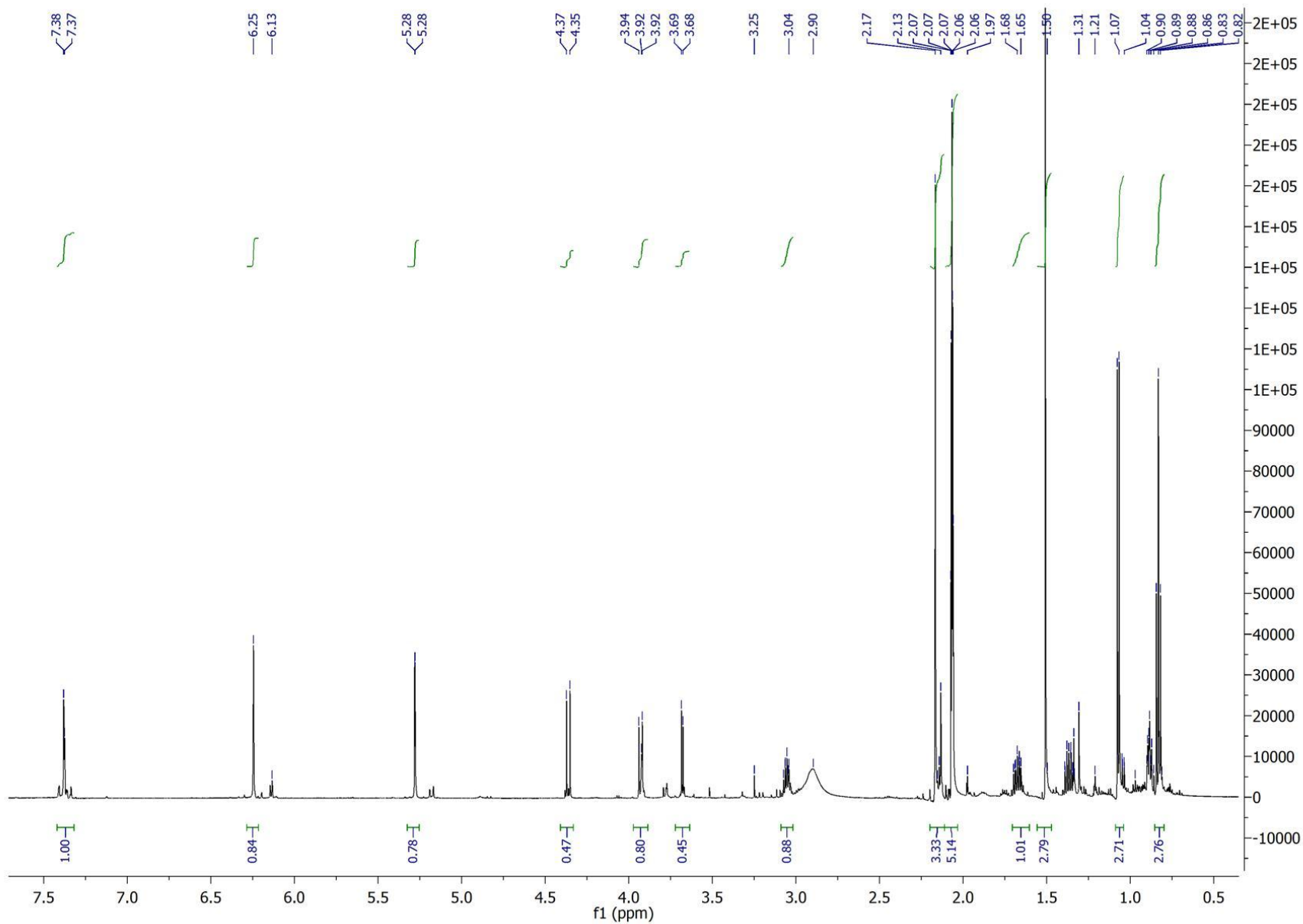
## Chapter 8: Supplemental data

Figure S24 1D NOESY (500 MHz,  $\text{CDCl}_3$ ) spectrum of colletotrichone B (**11a**)



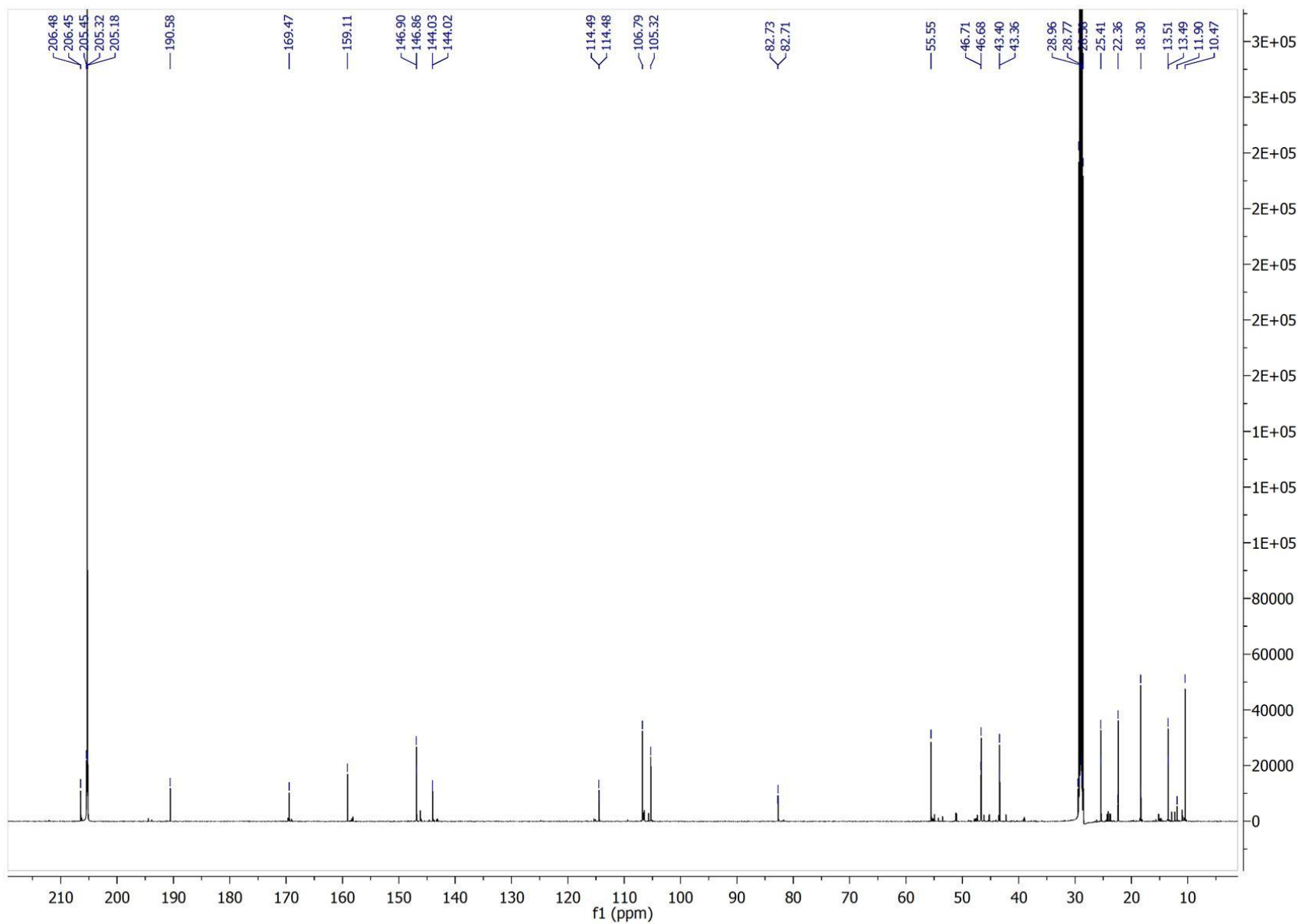
## Chapter 8: Supplemental data

Figure S25  $^1\text{H}$  NMR (500 MHz, acetone- $d_6$ ) spectrum of colletotrichone B (**11a**)



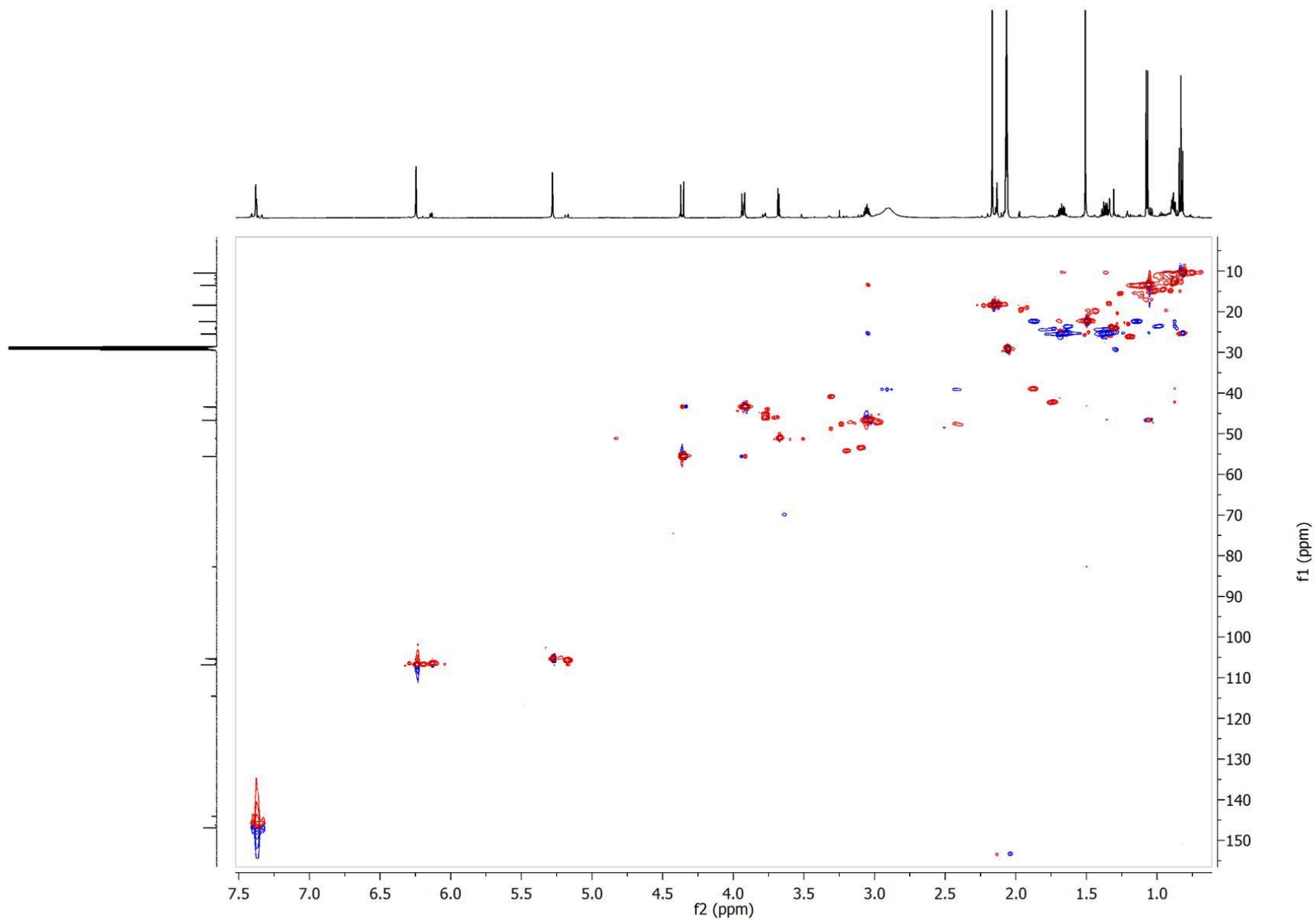
## Chapter 8: Supplemental data

Figure S26  $^{13}\text{C}$  NMR (125 MHz, acetone- $d_6$ ) spectrum of colletotrichone B (**11a**)



## Chapter 8: Supplemental data

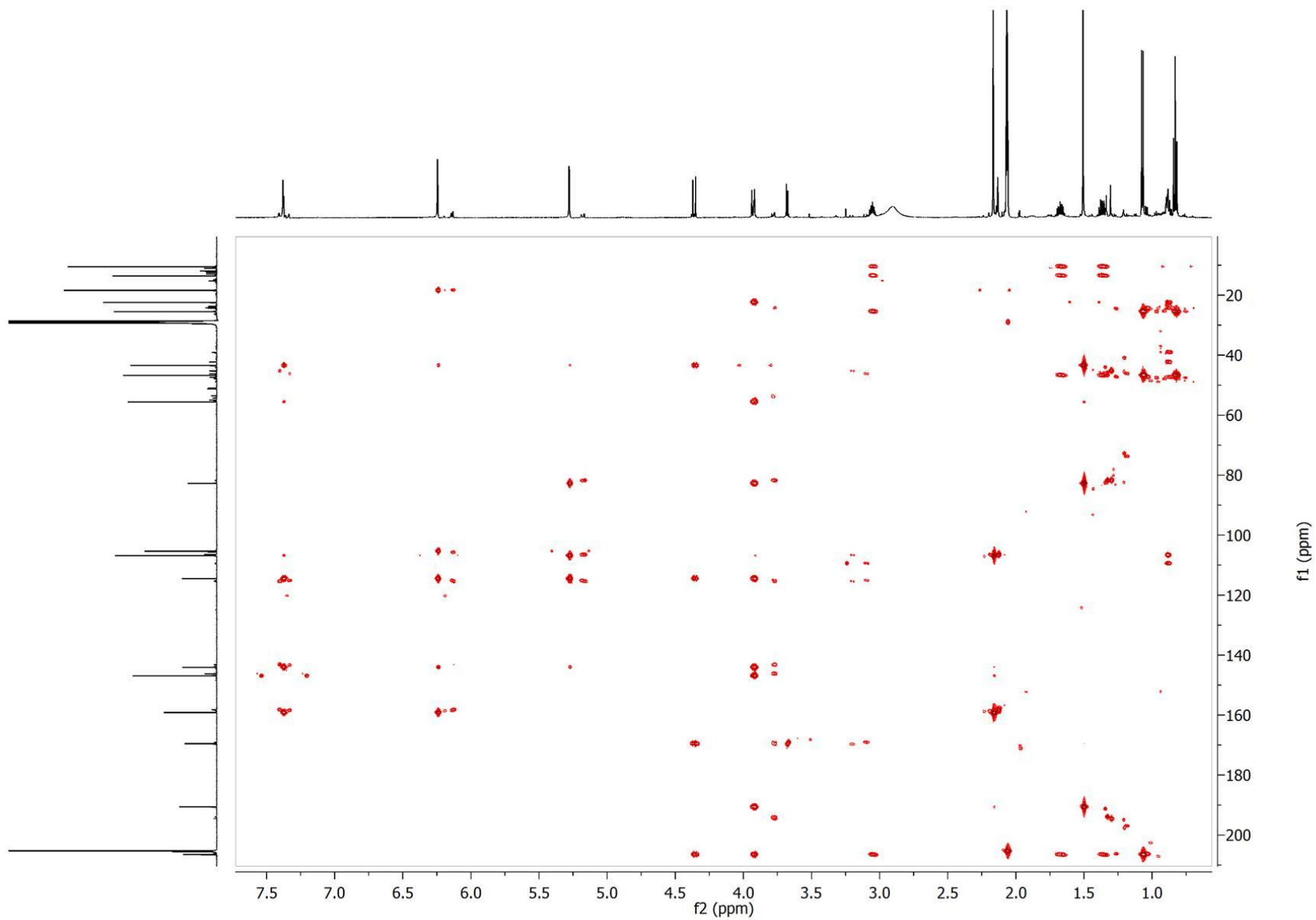
Figure S27 HSQC (500 MHz, acetone- $d_6$ ) spectrum of colletotrichone B (**11a**)





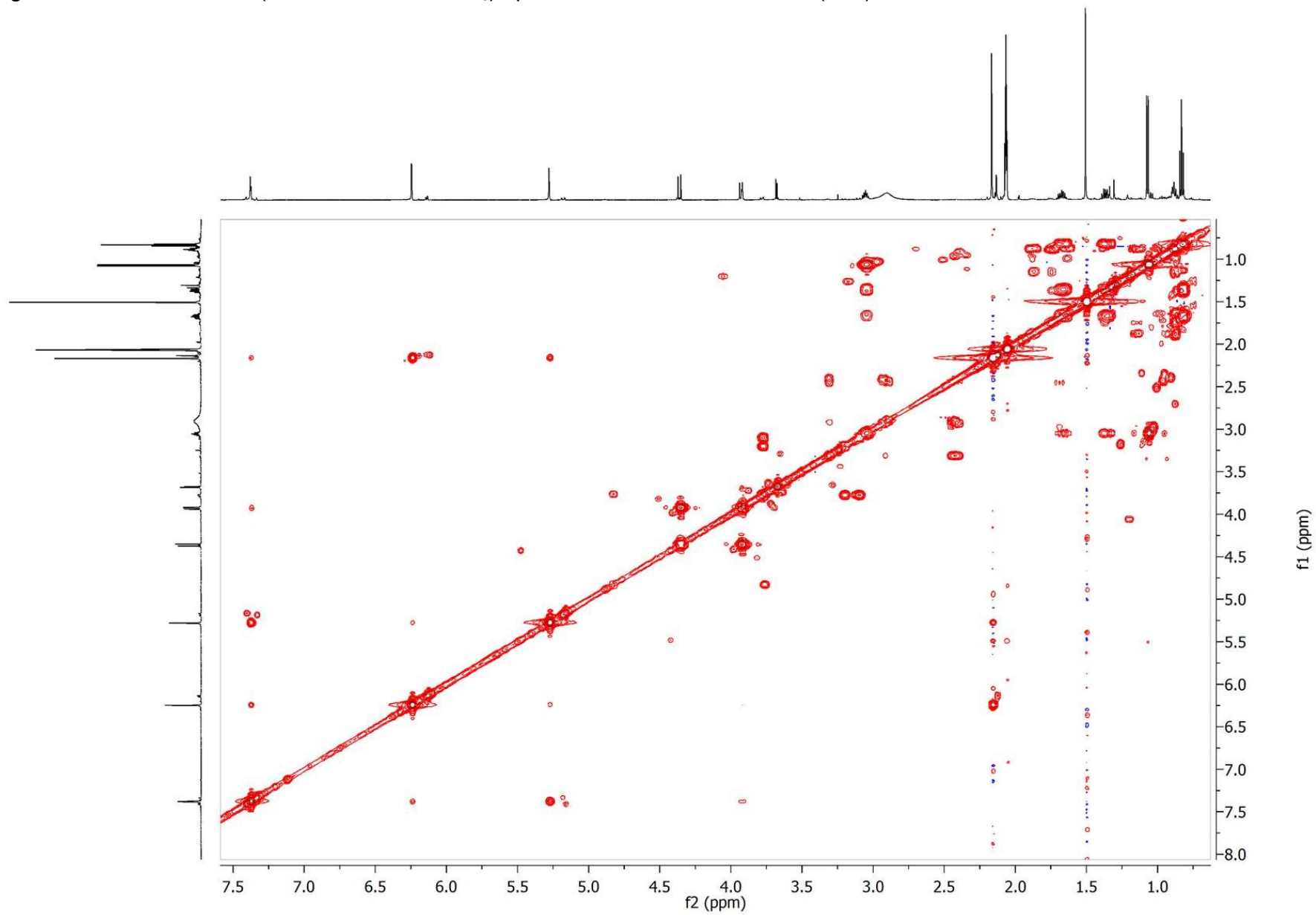
## Chapter 8: Supplemental data

Figure S28 HMBC (500 MHz, acetone- $d_6$ ) spectrum of colletotrichone B (**11a**)



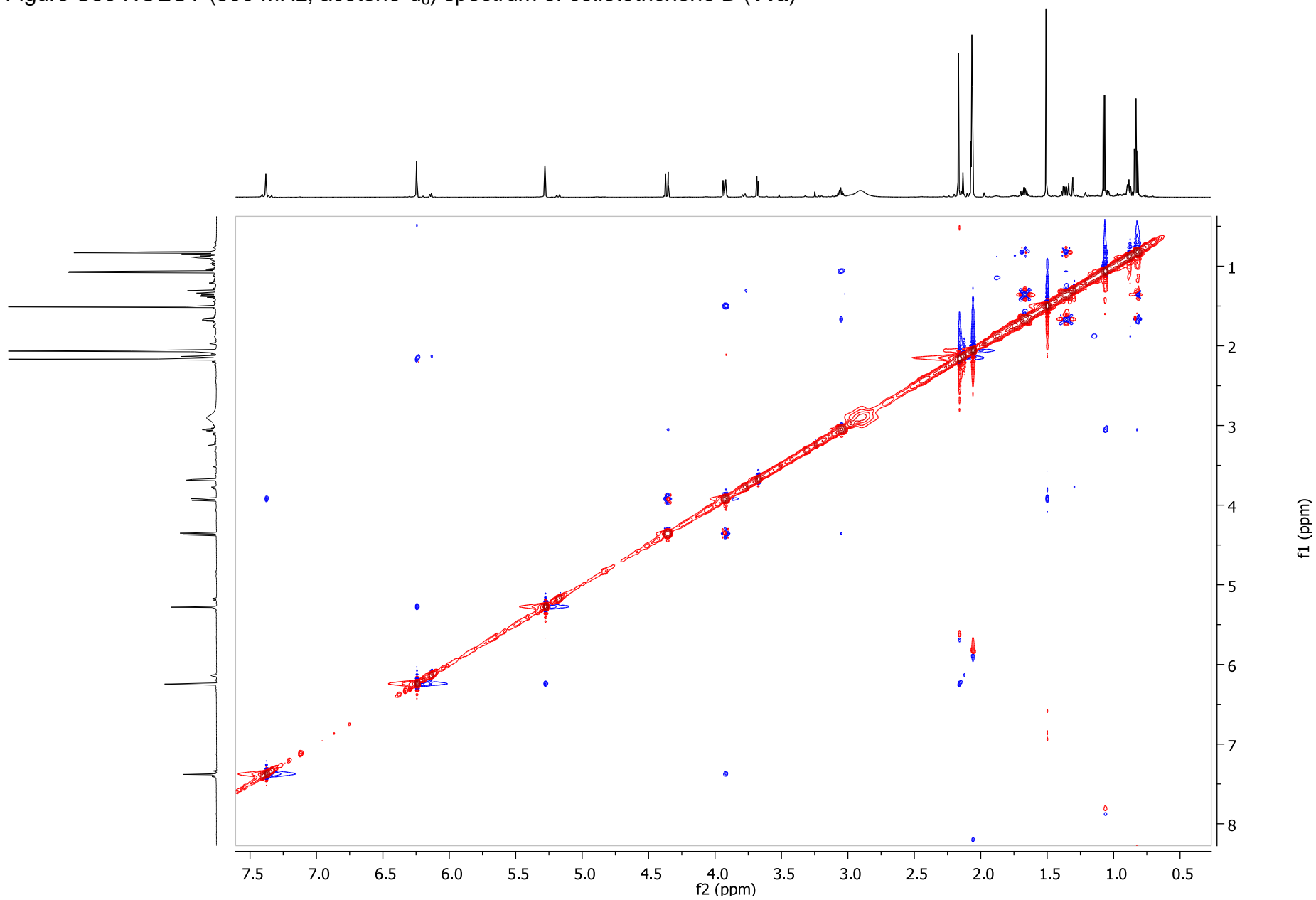
## Chapter 8: Supplemental data

Figure S29  $^1\text{H}$ ,  $^1\text{H}$  COSY (500 MHz, acetone- $d_6$ ) spectrum of colletotrichone B (**11a**)



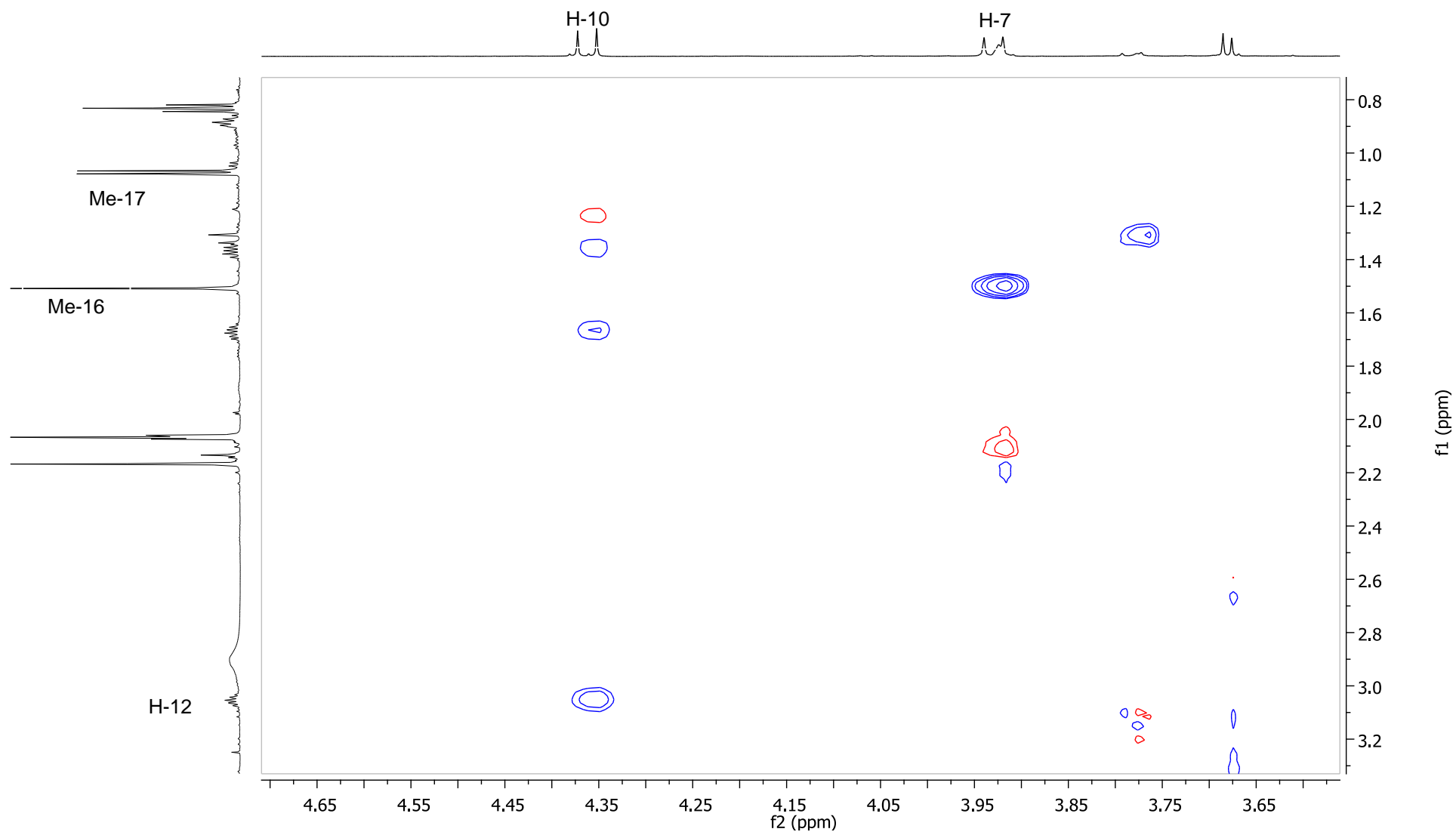
## Chapter 8: Supplemental data

Figure S30 NOESY (500 MHz, acetone- $d_6$ ) spectrum of colletotrichone B (**11a**)



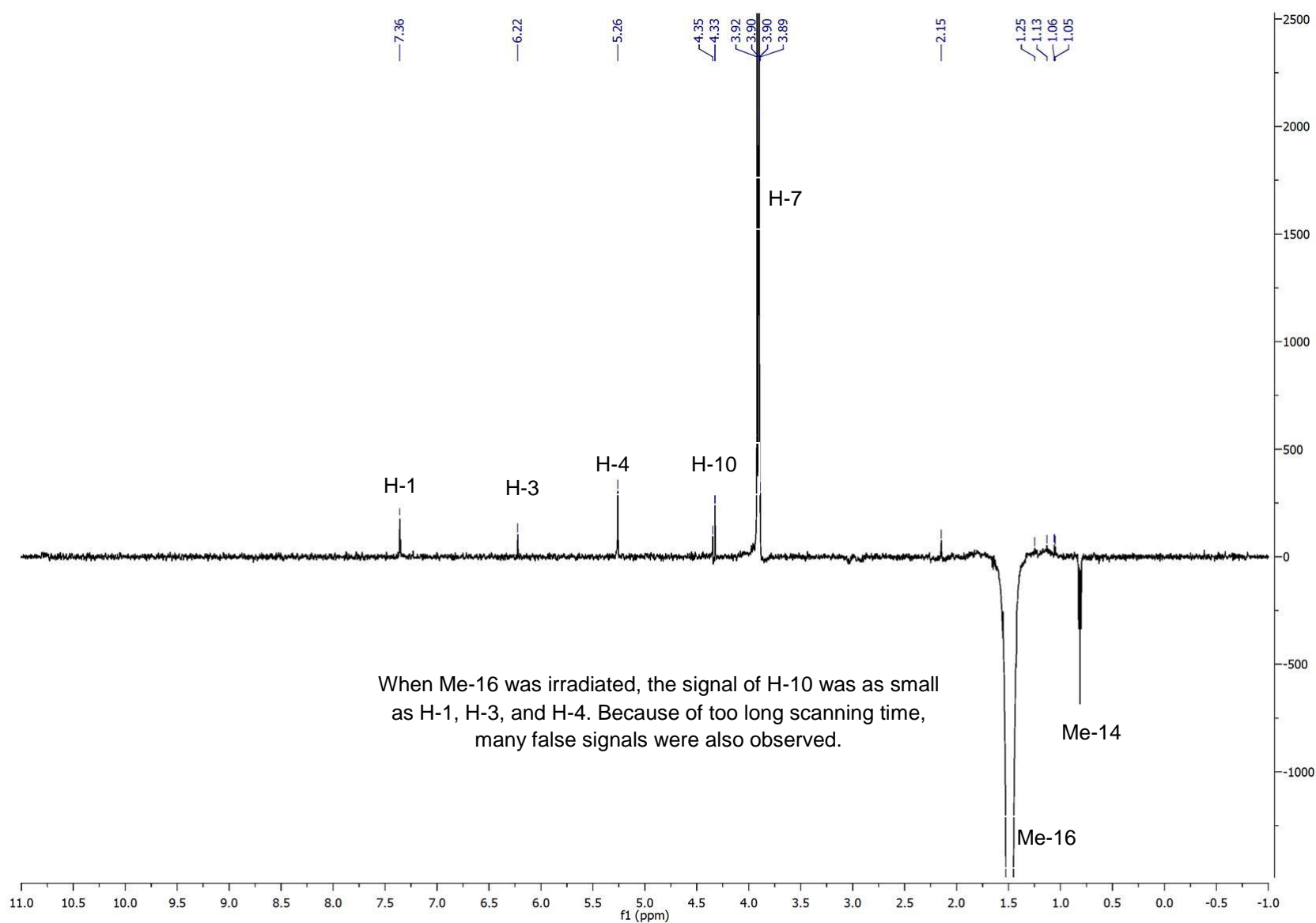
## Chapter 8: Supplemental data

Figure S30 NOESY (500 MHz, acetone- $d_6$ ) spectrum of colletotrichone B (**11a**)



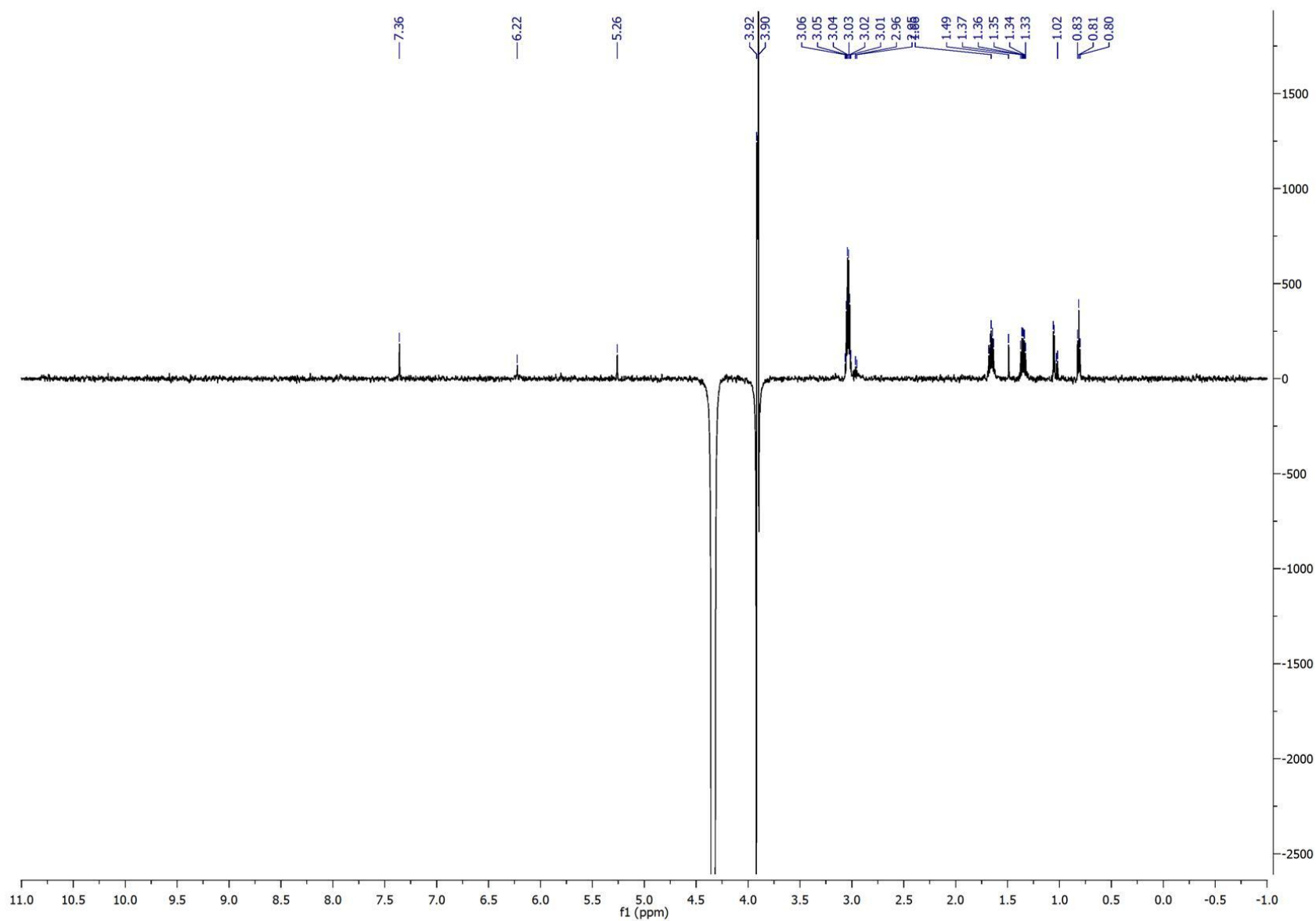
## Chapter 8: Supplemental data

Figure S31 1D NOESY (500 MHz, acetone- $d_6$ ) spectrum of colletotrichone B (**11a**)



## Chapter 8: Supplemental data

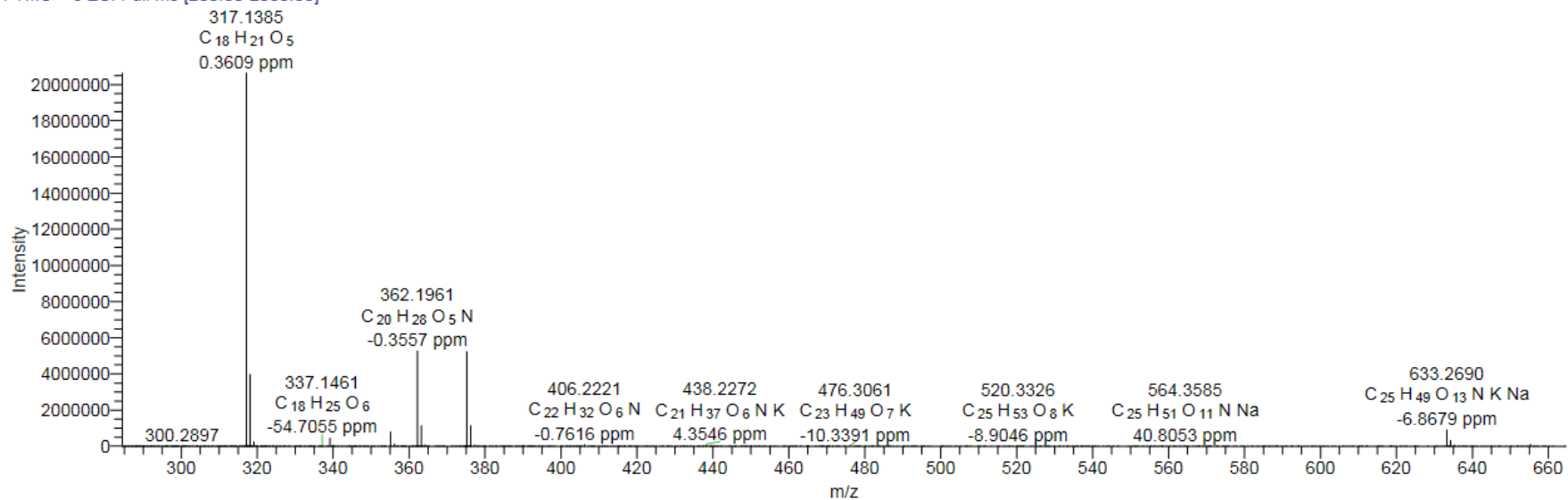
Figure S31 1D NOESY (500 MHz, acetone- $d_6$ ) spectrum of colletotrichone B (**11a**)



## Chapter 8: Supplemental data

Figure S32 Positive ESIHRMS of colletotrichone B (11a)

FTMS + c ESI Full ms [200.00-2000.00]



## Chapter 8: Supplemental data

Table S1. Experimental  $^{13}\text{C}$  NMR data ( $\text{CDCl}_3$ ) of colletotrichone B (**11a**) and calculated  $^{13}\text{C}$  NMR data<sup>a</sup> of compounds **11a/11b/11c/11d**

Atom No.	Exp data of <b>11a</b>	Cacl'd <b>11a</b> (6R,7R,10R,12S)	Abs deviation	Cacl'd <b>11b</b> (6R,7R,10S,12R)	Abs deviation	Cacl'd <b>11c</b> (6R,7R,10R,12R)	Abs deviation	Cacl'd <b>11d</b> (6R,7R,10S,12S)	Abs deviation
1	147.2	146.84	0.36	147.08	0.12	147.15	0.05	147.60	0.40
2	159.4	157.51	1.89	158.25	1.15	157.97	1.43	158.52	0.88
3	107.3	109.37	2.07	110.75	3.45	110.47	3.17	110.68	3.38
4	105.8	107.40	1.60	108.05	2.25	107.06	1.26	108.45	2.65
5	191.5	189.83	1.67	190.62	0.88	189.99	1.51	191.62	0.12
6	83.2	80.72	2.48	81.88	1.32	80.50	2.70	81.81	1.39
7	43.0	42.42	0.58	48.72	5.72	42.27	0.73	48.90	5.90
8	114.6	117.26	2.66	116.72	2.12	118.05	3.45	116.56	1.96
9	144.5	138.69	5.81	142.61	1.89	140.14	4.36	142.55	1.95
10	55.7	56.59	0.89	59.44	3.74	55.48	0.22	59.65	3.95
11	206.3	213.03	6.73	207.09	0.79	212.45	6.15	210.39	4.09
12	46.6	45.67	0.93	47.58	0.98	46.47	0.13	47.48	0.88
13	26.2	29.11	2.91	27.83	1.63	25.09	1.11	27.96	1.76
14	11.1	12.00	0.90	13.31	2.21	12.08	0.98	12.00	0.90
15	19.5	18.18	1.32	19.12	0.38	19.18	0.32	19.12	0.38
16	23.2	22.70	0.50	24.75	1.55	23.82	0.62	24.85	1.65
<b>17</b>	<b>14.1</b>	<b>15.35</b>	<b>1.25</b>	<b>15.77</b>	<b>1.67</b>	<b>16.31</b>	<b>2.21</b>	<b>18.74</b>	<b>4.64</b>
18	168.6	167.58	1.02	170.77	2.17	167.85	0.75	170.61	2.01

<sup>a</sup> The conformer distributions of the molecules in question were searched in a systematic approach with the MMFF routine of Spartan'14 (Wavefunction, Inc.: Irvine, CA, 2014).<sup>8</sup> The geometries of all resulting conformers within an energy range of < 25 kJ/mol above the global minimum were then optimized, first with HF/3-21G and then within < 15 kJ/mol by DFT using the wB97X-D functional and the 6-31G\* basis set. The resulting geometries with preliminary Boltzmann factors > 0.001 were used without further geometry optimization to calculate the NMR spectra with EDF2/6-31G\*; SPARTAN's corrected shifts were used without further solvent corrections (the solvent model is not yet provided in Spartan'14). The final Boltzmann factors were obtained with wB97XD/6-311+G(2df,2p), using Gaussian g09.<sup>9</sup> The NMR shifts of all remaining conformers were averaged with respect to their final Boltzmann factors.

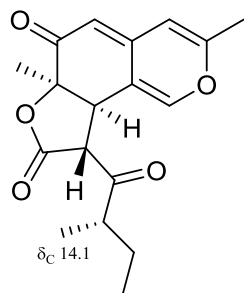


## Chapter 8: Supplemental data

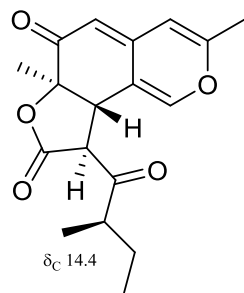
Table S2 Comparison of  $^1\text{H}$  and  $^{13}\text{C}$  NMR spectroscopic data for compounds **11a**, monochaetin (**14b**),<sup>a</sup> **3**, and chermesinone B (**14a**)<sup>a</sup> ( $\text{CDCl}_3$ )

Position	<b>11a</b>		Monochaetin ( <b>14b</b> )		<b>12</b>		Chermesinone B ( <b>14a</b> )	
	$\delta_{\text{C}}$	$\delta_{\text{H}}$ mult. (J in Hz)	$\delta_{\text{C}}$	$\delta_{\text{H}}$ mult. (J in Hz)	$\delta_{\text{C}}$	$\delta_{\text{H}}$ mult. (J in Hz)	$\delta_{\text{C}}$	$\delta_{\text{H}}$ mult. (J in Hz)
1	147.2	7.30, 1H, s	143.3	6.79, dd (1.9, 1.3)	69.0	3.95, 1H, dd (11.5, 5.4) 3.84, 1H, dd (13.5, 11.5)	143.5	6.83, s
2	159.4		158.5		163.9		158.8	
3	107.3	6.00, 1H, s	107.0	6.02, q (< 0.4)	101.1	5.48, 1H, br s	107.3	6.05, s
4	105.8	5.36, 1H, br s	105.7	5.29, d (1.3)	115.0	5.62, 1H, br s	106.1	5.34, d (0.8)
5	191.5		191.8		192.5		192.1	
6	83.2		82.6		83.4		82.8	
7	43.0	3.89, 1H, br s	43.7	3.76, dd (12.8, 1.9)	44.5	3.10, 1H, dd (12.5, 11.5)	43.8	3.81, dd (12.9, 1.9)
8	114.6		116.2		35.6	2.74, 1H, dddd (13.5, 11.5, 5.4, 1.5)	116.5	
9	144.5		145.5		153.0		145.7	
10	55.7	3.89, 1H, br s	52.1	4.05, d (12.8)	52.6	3.93, 1H, d (12.5)	51.7	4.09, d (12.9)
11	206.3		205.9		206.2		206.2	
12	46.6	3.10, 1H, m	46.7	3.19, qdd (6.7, 7.4, 5.4)	47.8	3.07, 1H, m	47.3	3.15, m
13	26.2	1.60, 1H, m 1.37, 1H, m	26.3	1.81, qdd (7.4, 13.0, 5.4) 1.48, qdd (7.4, 13.0, 7.4)	24.5	1.79, 1H, m 1.42, 1H, m	25.1	1.80, m 1.43, m
14	11.1	0.81, 3H, t (7.4)	11.5	0.97, t (7.4)	11.5	0.90, 3H, t (7.5)	11.7	0.90, t (7.4)
15	19.5	2.14, 3H, s	19.5	2.13, d (< 0.4)	20.6	1.95, 3H, s	19.8	2.17, s
16	23.2	1.57, 3H, s	18.9	1.32, s	18.8	1.50, 3H, s	19.1	1.36, s
<b>17</b>	<b>14.1</b>	<b>1.09, 3H, d (6.5)</b>	<b>14.4</b>	<b>1.11, d (6.7)</b>	<b>16.7</b>	<b>1.19, 3H, d (7.2)</b>	<b>17.1</b>	<b>1.24, d (7.1)</b>
18	168.6		169.1		168.8		169.3	

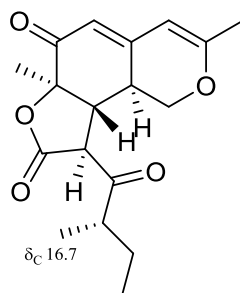
<sup>a</sup> Adapted from the Supporting Information of Huang *et al.* (2011).<sup>7</sup>



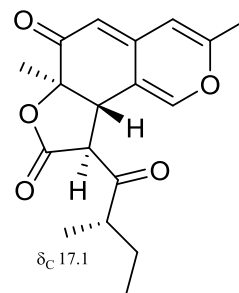
**11a**



Monochaetin **14b**



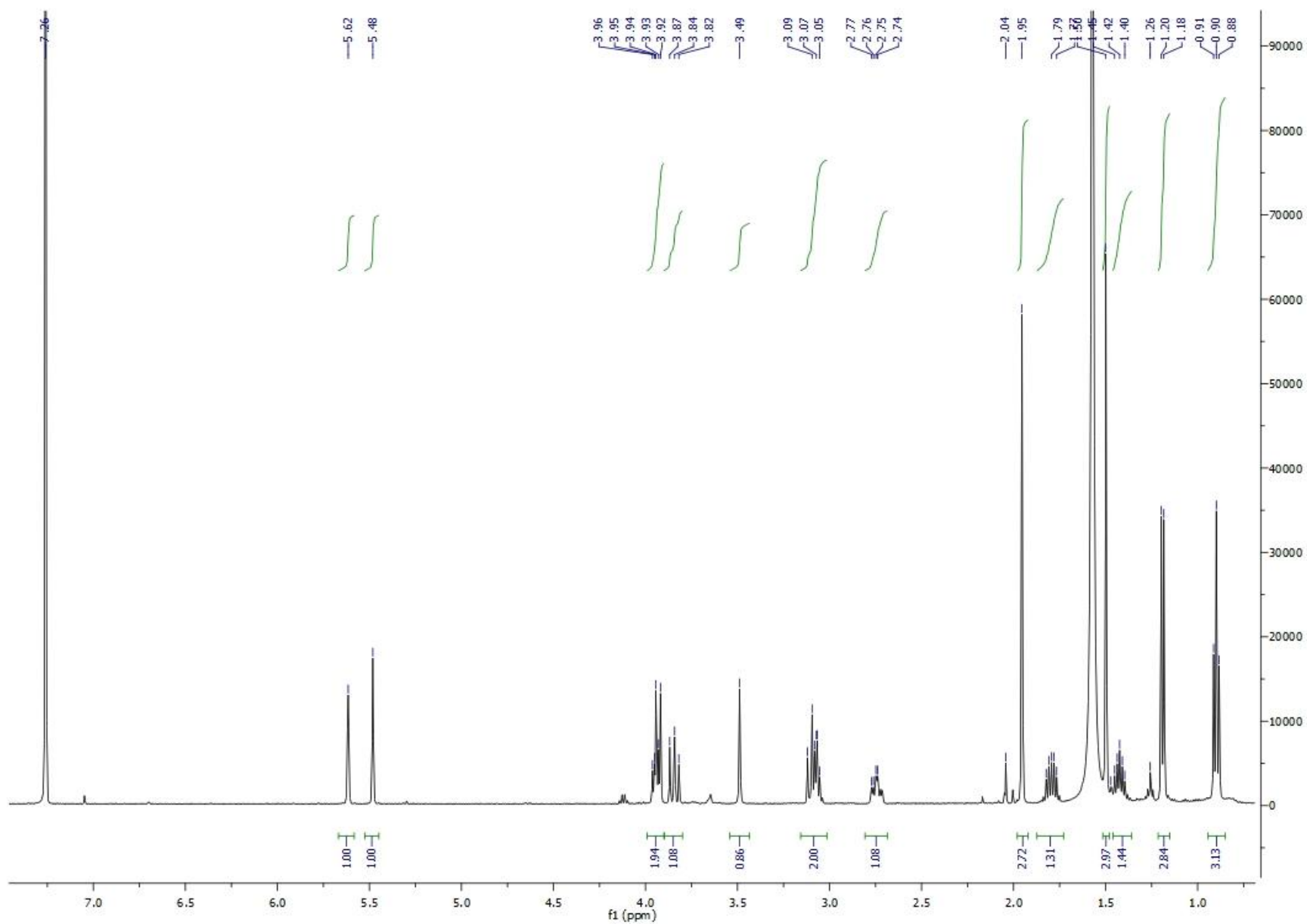
**12**



Chermesinone B **14a**

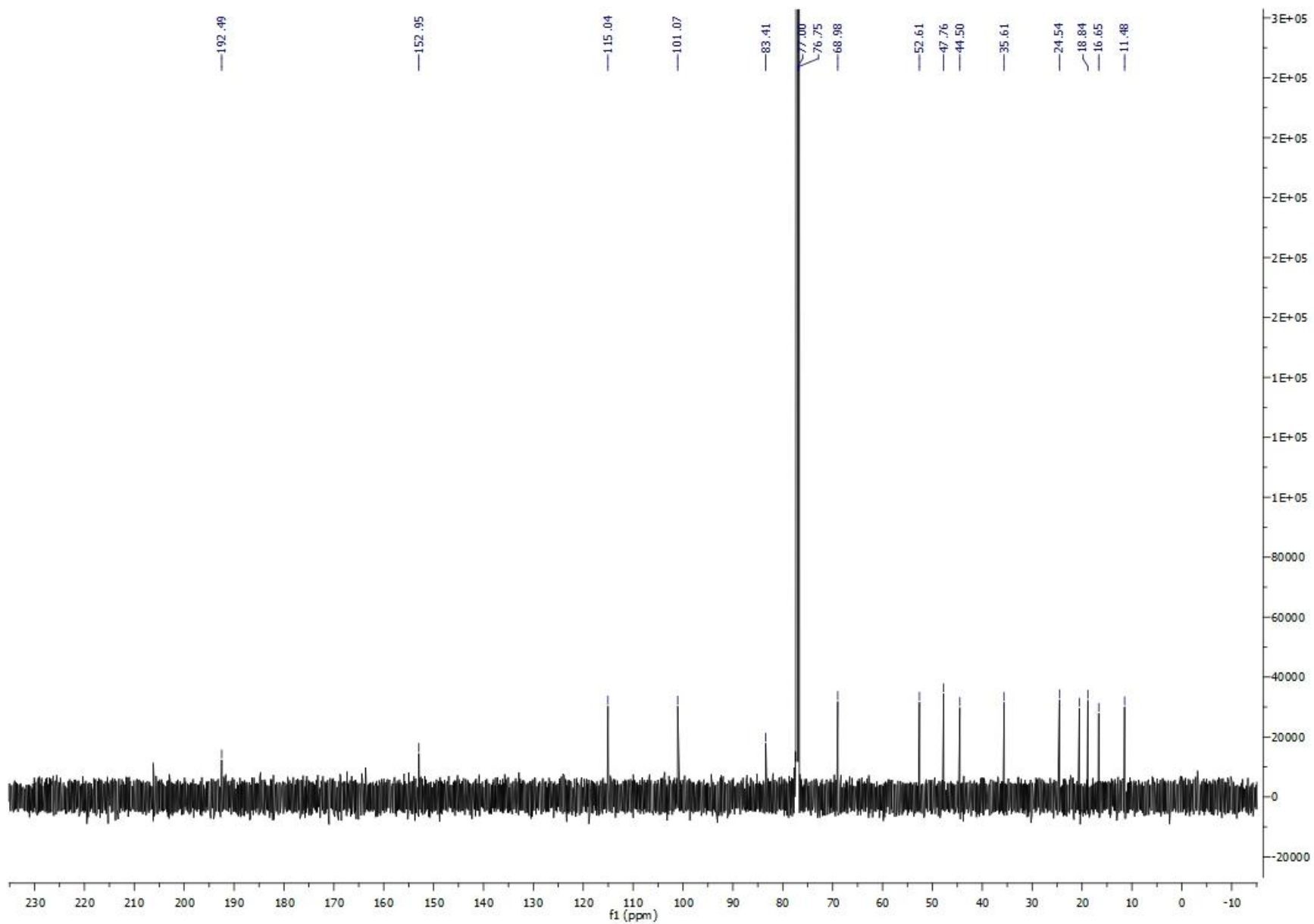
## Chapter 8: Supplemental data

Figure S33  $^1\text{H}$  NMR (500 MHz,  $\text{CDCl}_3$ ) spectrum of colletotrichone C (**12**)



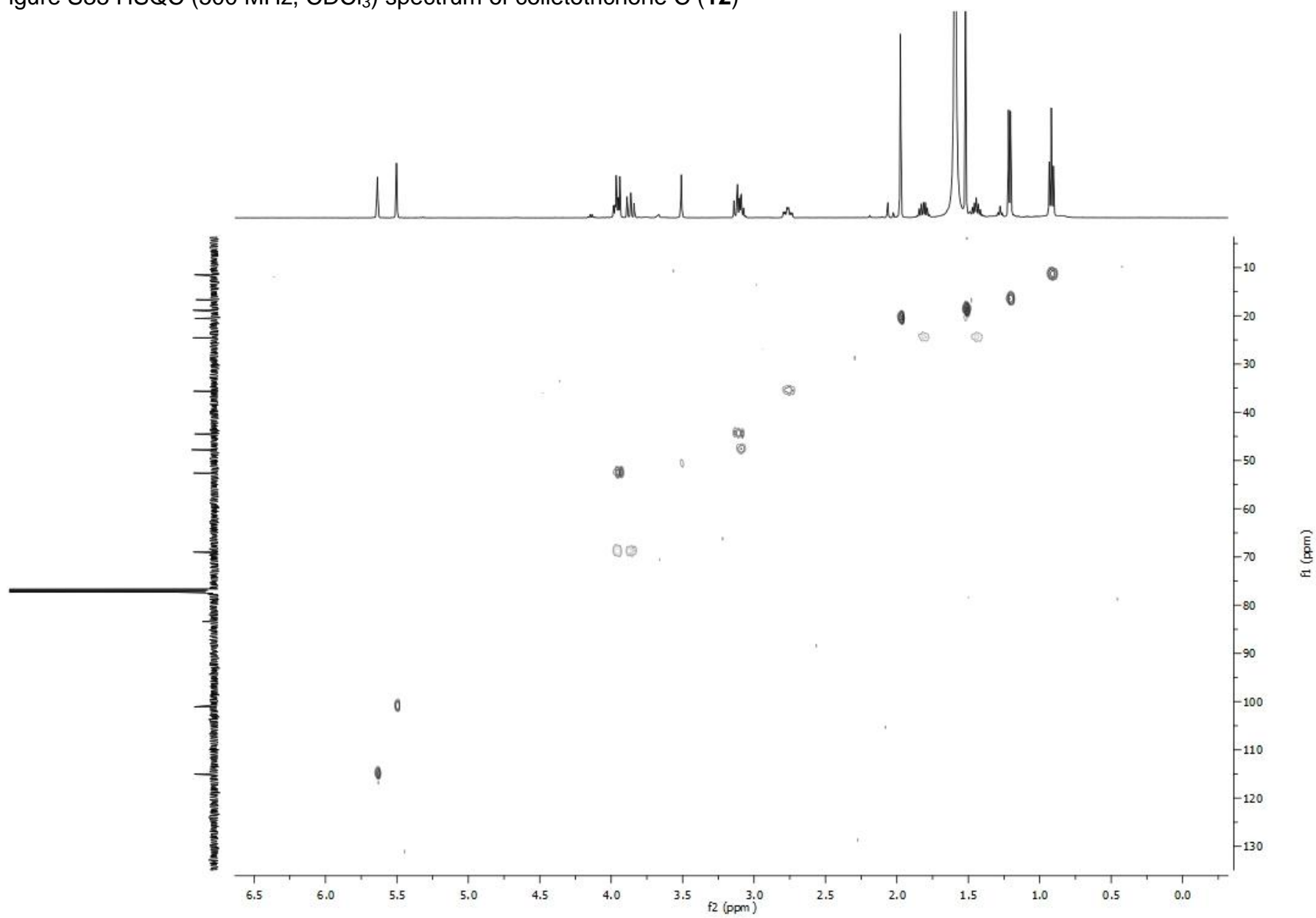
## Chapter 8: Supplemental data

Figure S34  $^{13}\text{C}$  NMR (125 MHz,  $\text{CDCl}_3$ ) spectrum of colletotrichone C (**12**)



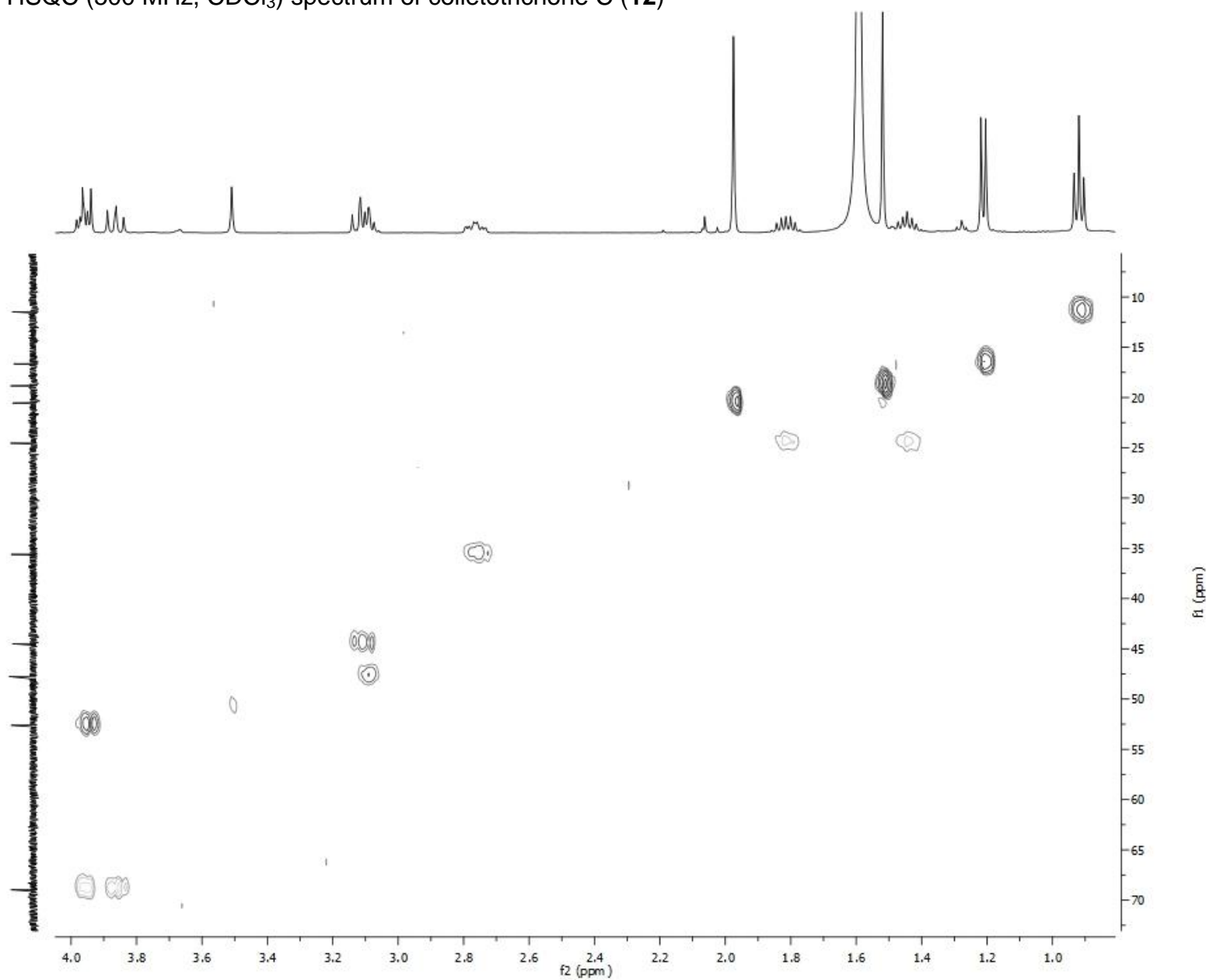
## Chapter 8: Supplemental data

Figure S35 HSQC (500 MHz, CDCl<sub>3</sub>) spectrum of colletotrichone C (**12**)



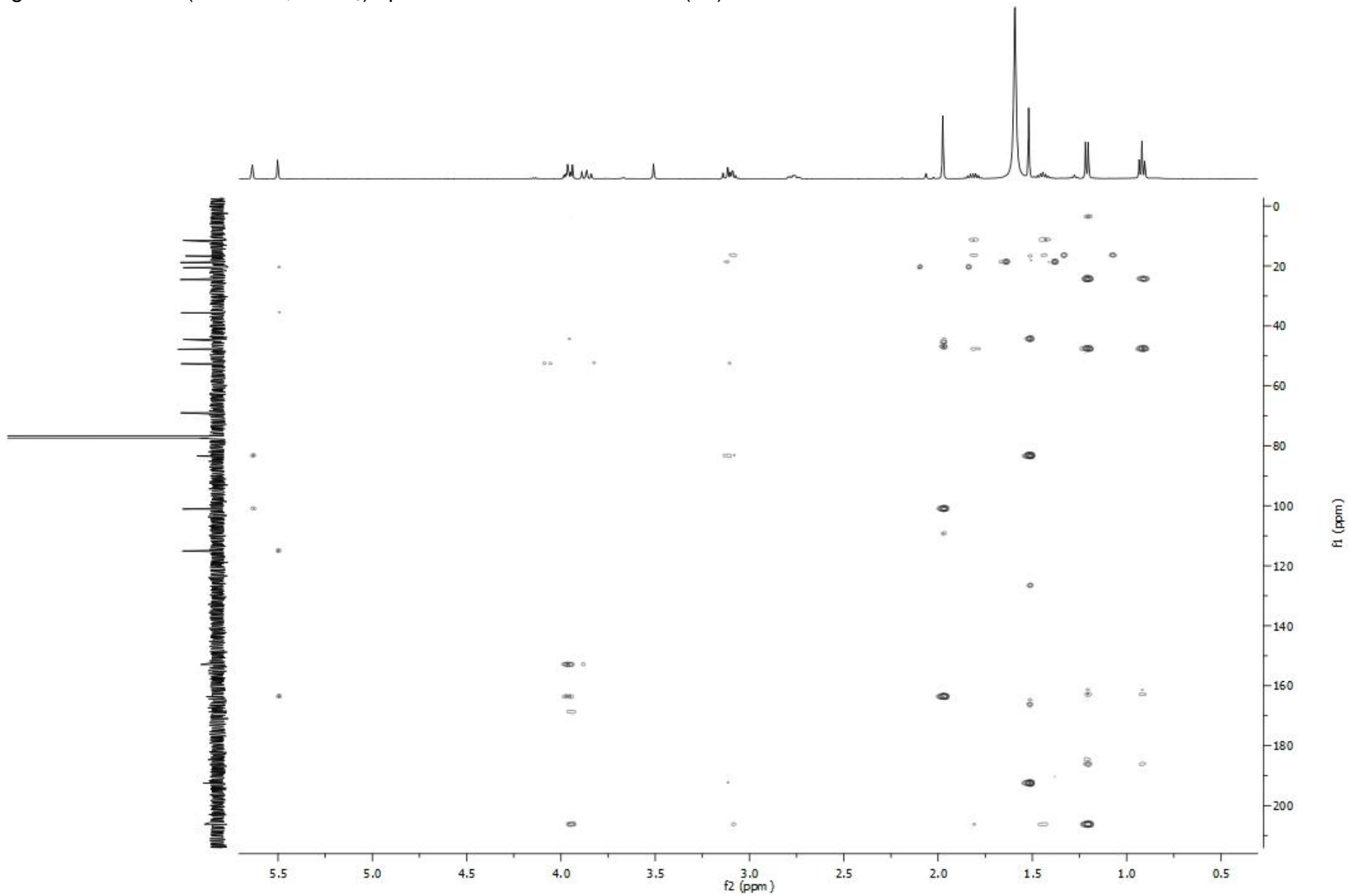
## Chapter 8: Supplemental data

Figure S35 HSQC (500 MHz, CDCl<sub>3</sub>) spectrum of colletotrichone C (**12**)



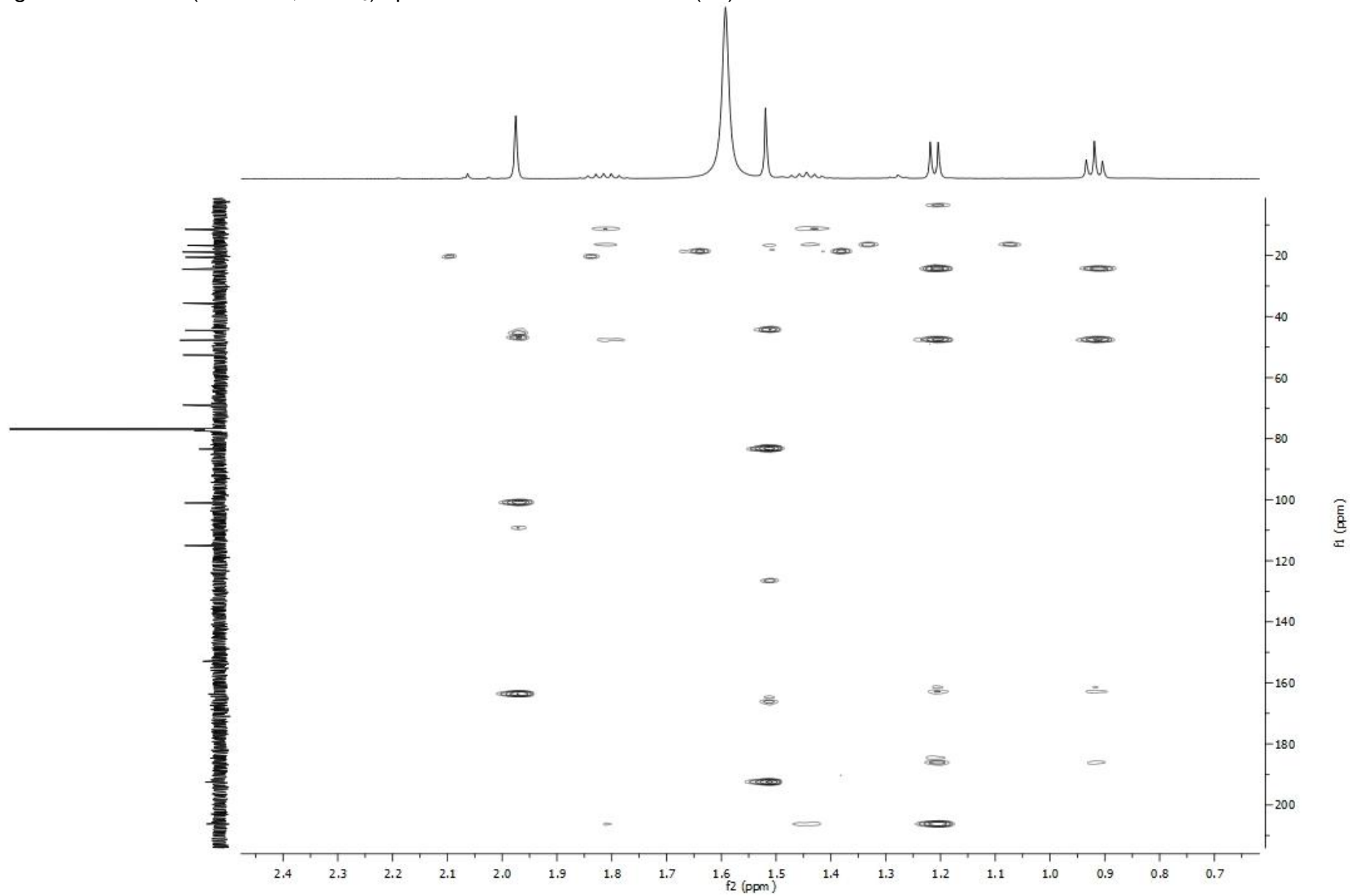
## Chapter 8: Supplemental data

Figure S36 HMBC (500 MHz, CDCl<sub>3</sub>) spectrum of colletotrichone C (**12**)



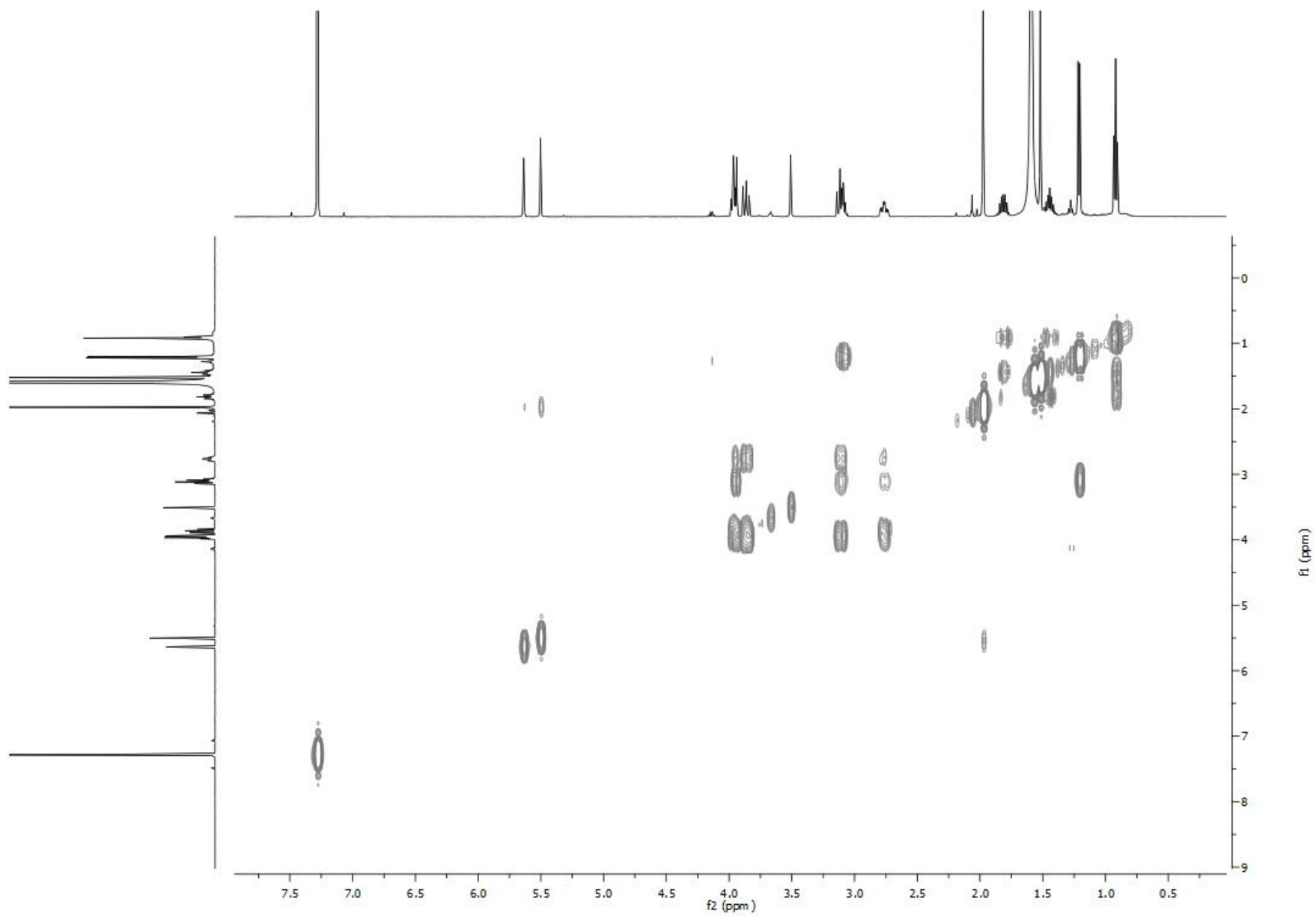
## Chapter 8: Supplemental data

Figure S36 HMBC (500 MHz, CDCl<sub>3</sub>) spectrum of colletotrichone C (**12**)



## Chapter 8: Supplemental data

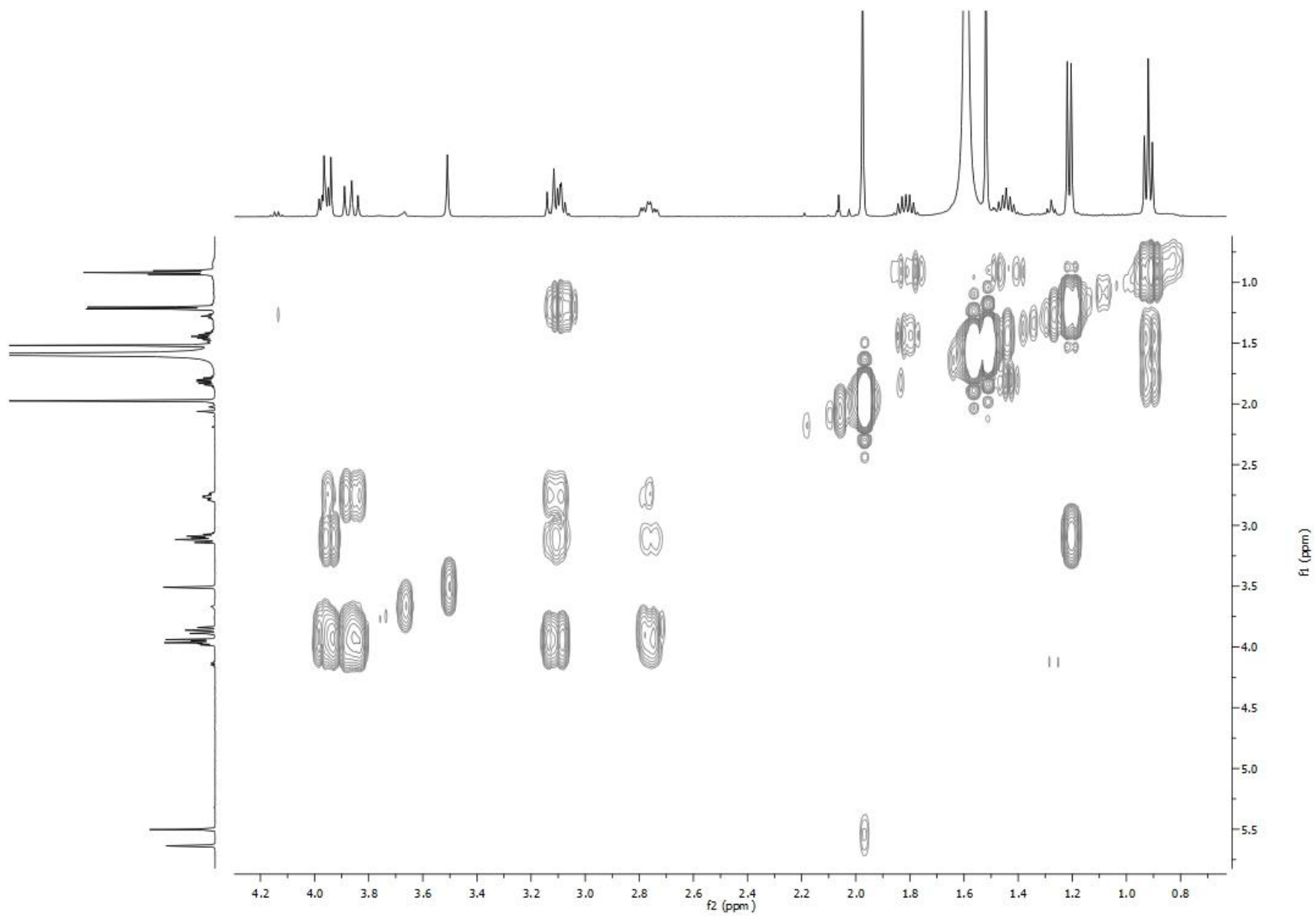
Figure S37  $^1\text{H}$ ,  $^1\text{H}$  COSY (500 MHz,  $\text{CDCl}_3$ ) spectrum of colletotrichone C (**12**)





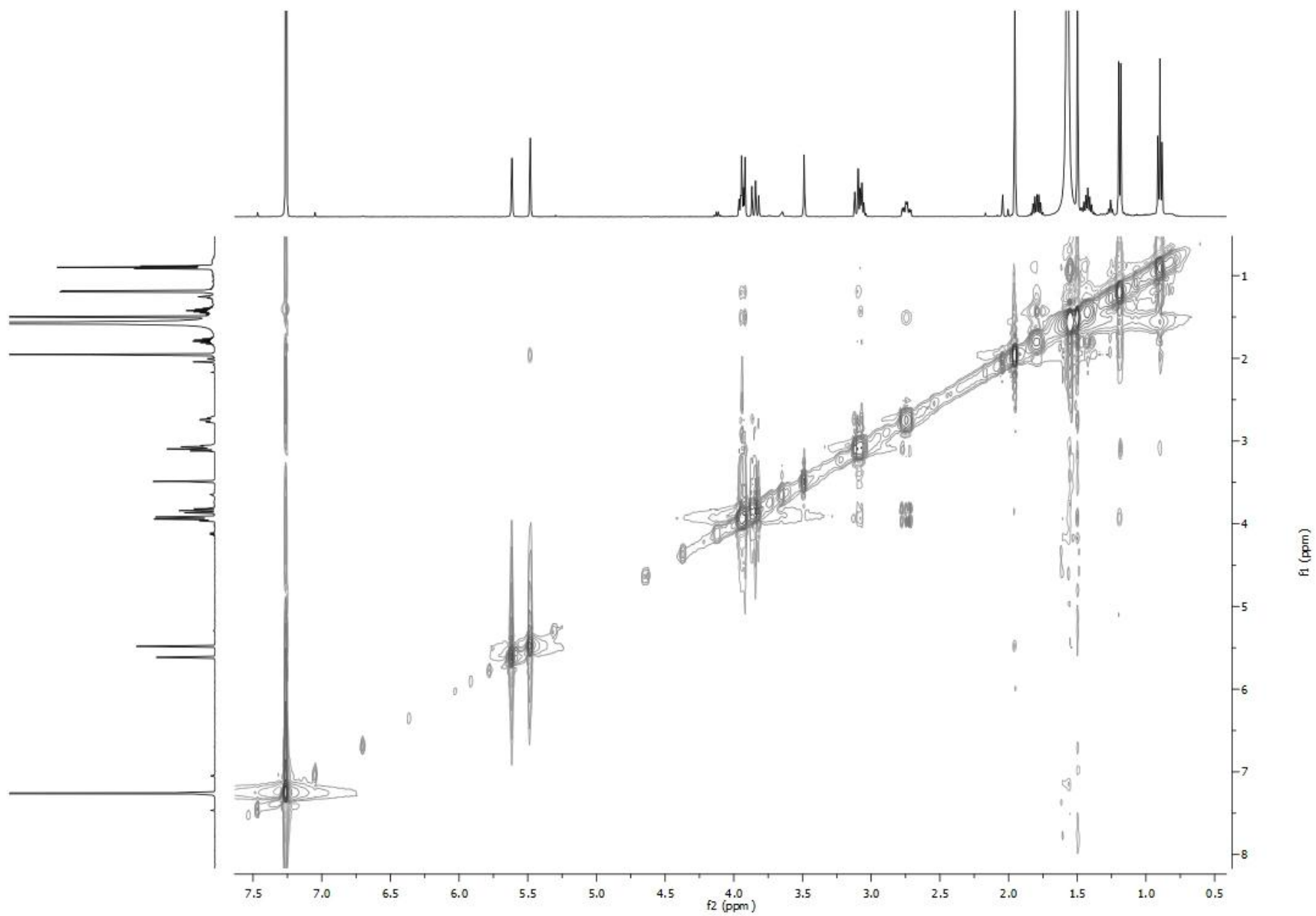
## Chapter 8: Supplemental data

Figure S37  $^1\text{H}$ ,  $^1\text{H}$  COSY (500 MHz,  $\text{CDCl}_3$ ) spectrum of colletotrichone C (**12**)



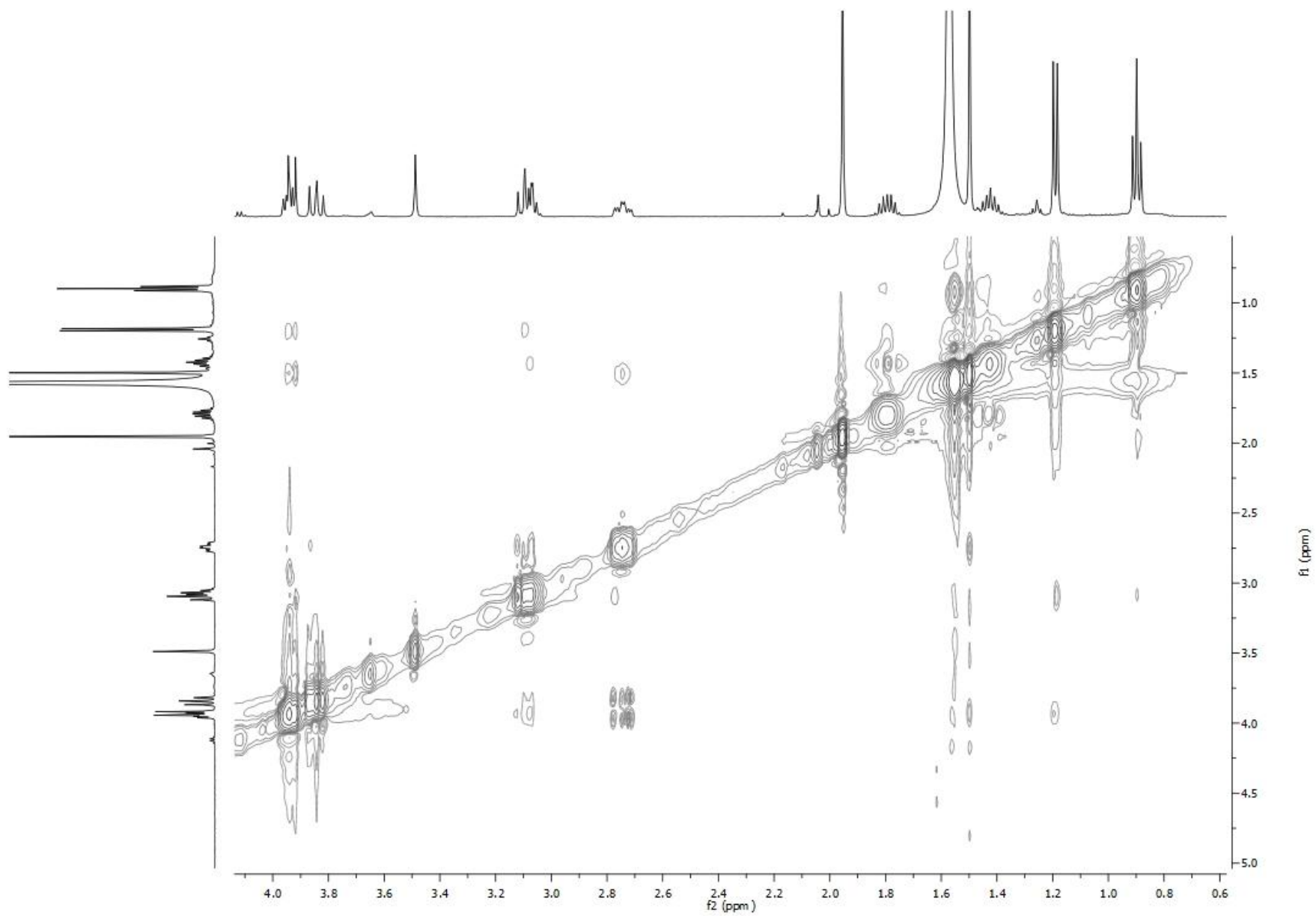
## Chapter 8: Supplemental data

Figure S38 NOESY (500 MHz,  $\text{CDCl}_3$ ) spectrum of colletotrichone C (**12**)



## Chapter 8: Supplemental data

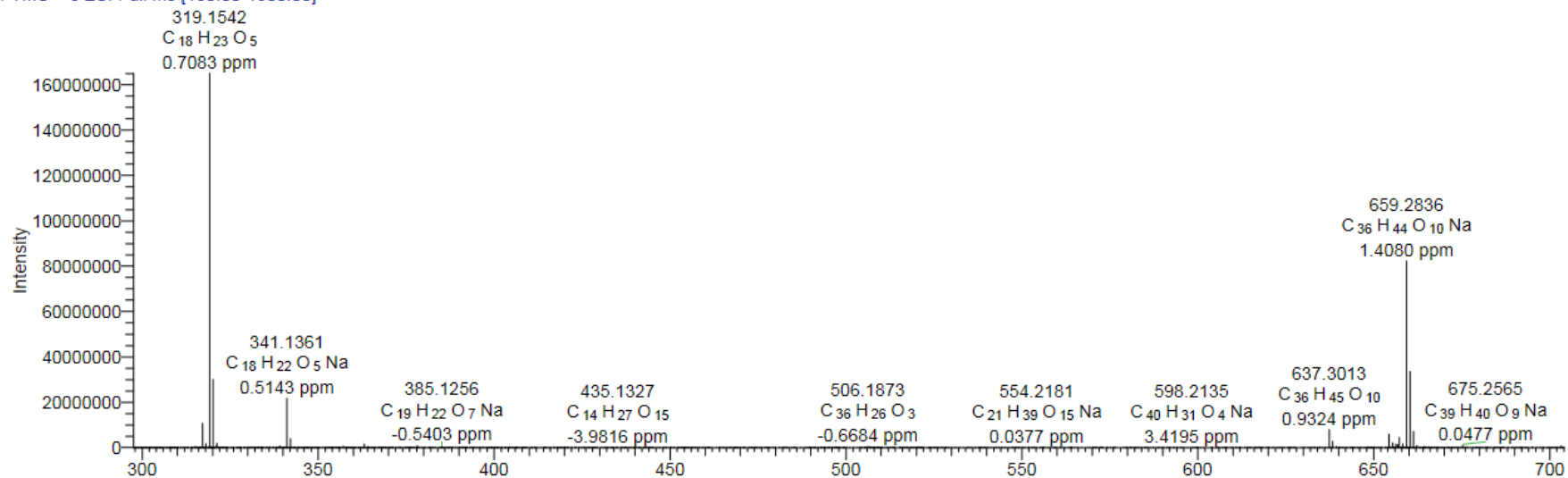
Figure S38 NOESY (500 MHz,  $\text{CDCl}_3$ ) spectrum of colletotrichone C (**12**)



## Chapter 8: Supplemental data

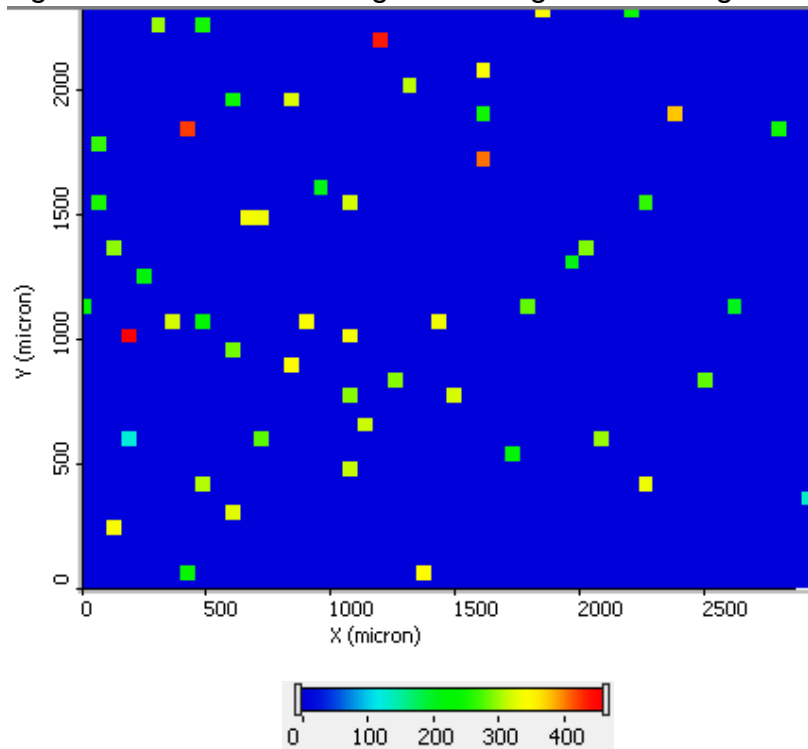
Figure S39 Positive ESIHRMS of colletotrichone C (12)

FTMS + c ESI Full ms [150.00-1500.00]

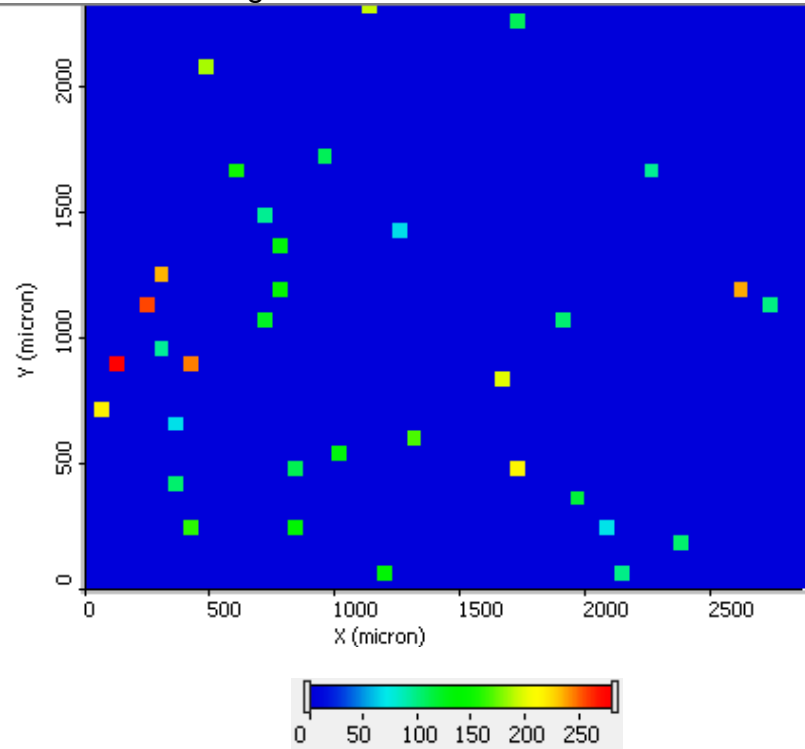


## Chapter 8: Supplemental data

Figure S40 Interference signals of target mass weights on blank control of rice agar



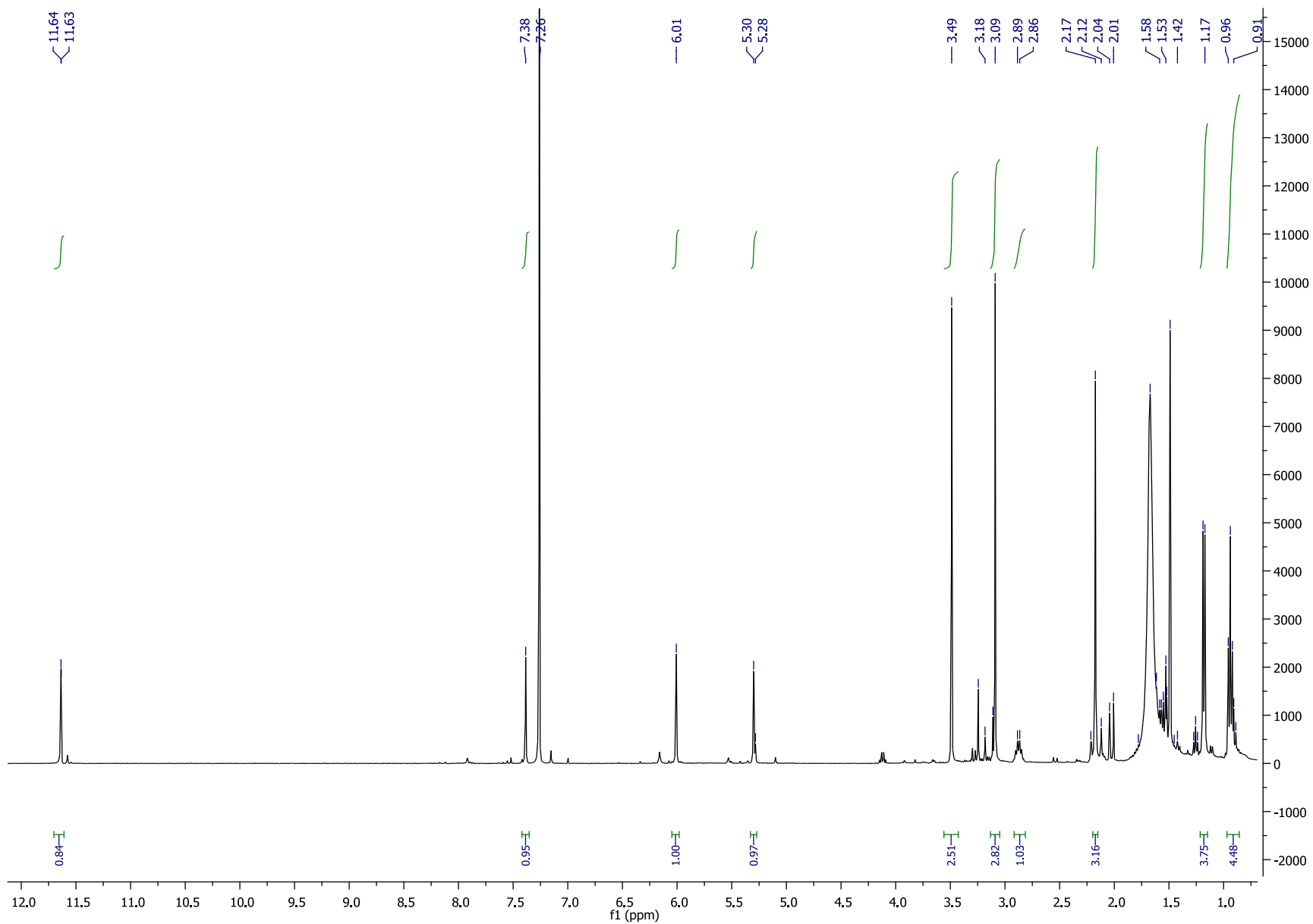
Target mass weight,  $m/z$  387.0840613,  $\Delta = 1$  ppm



Target mass weight,  $m/z$  355.0942321,  $\Delta = 1$  ppm

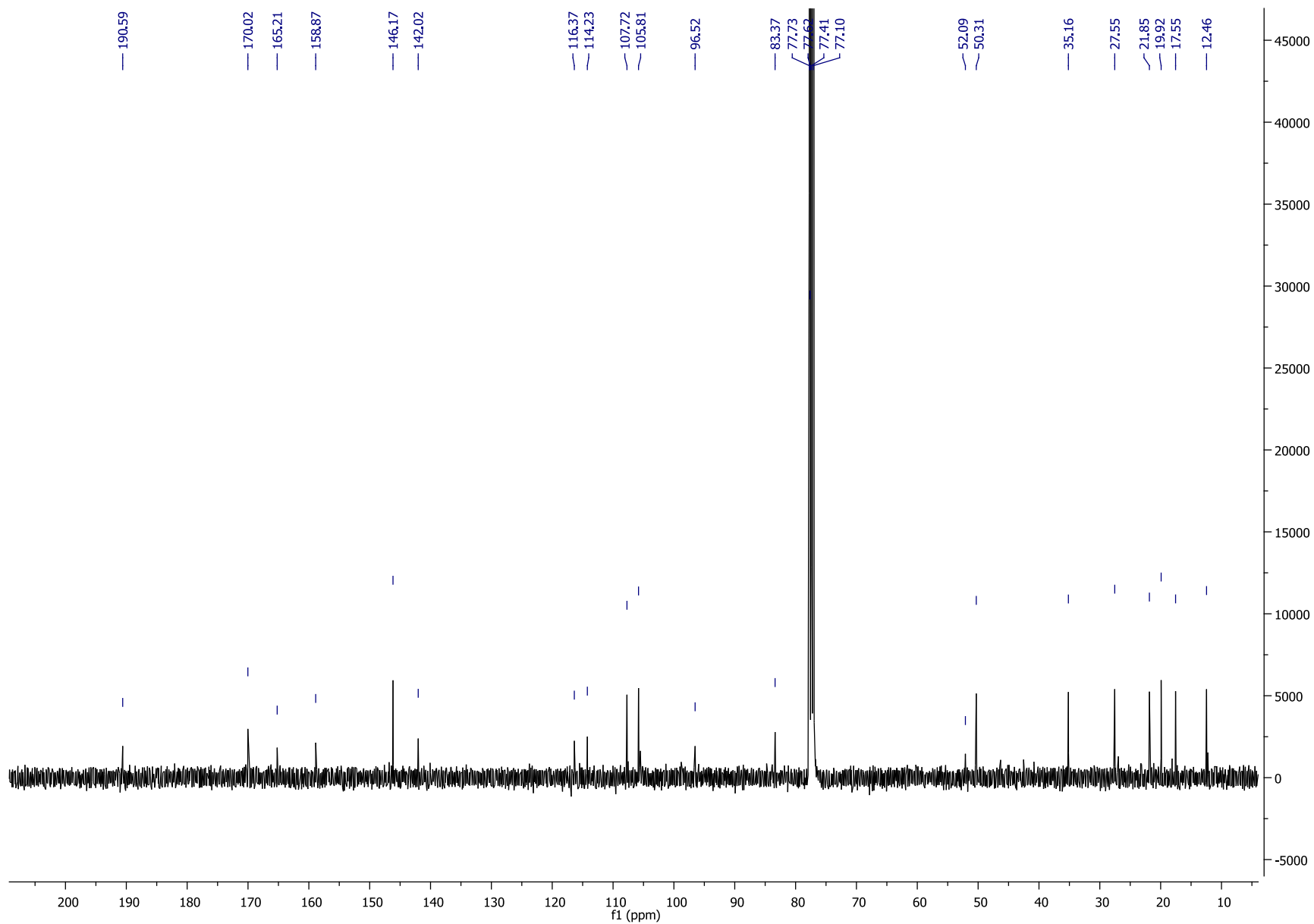
## Chapter 8: Supplemental data

Figure S41  $^1\text{H}$  NMR (500 MHz,  $\text{CDCl}_3$ ) spectrum of colletotrichone D (**13**)



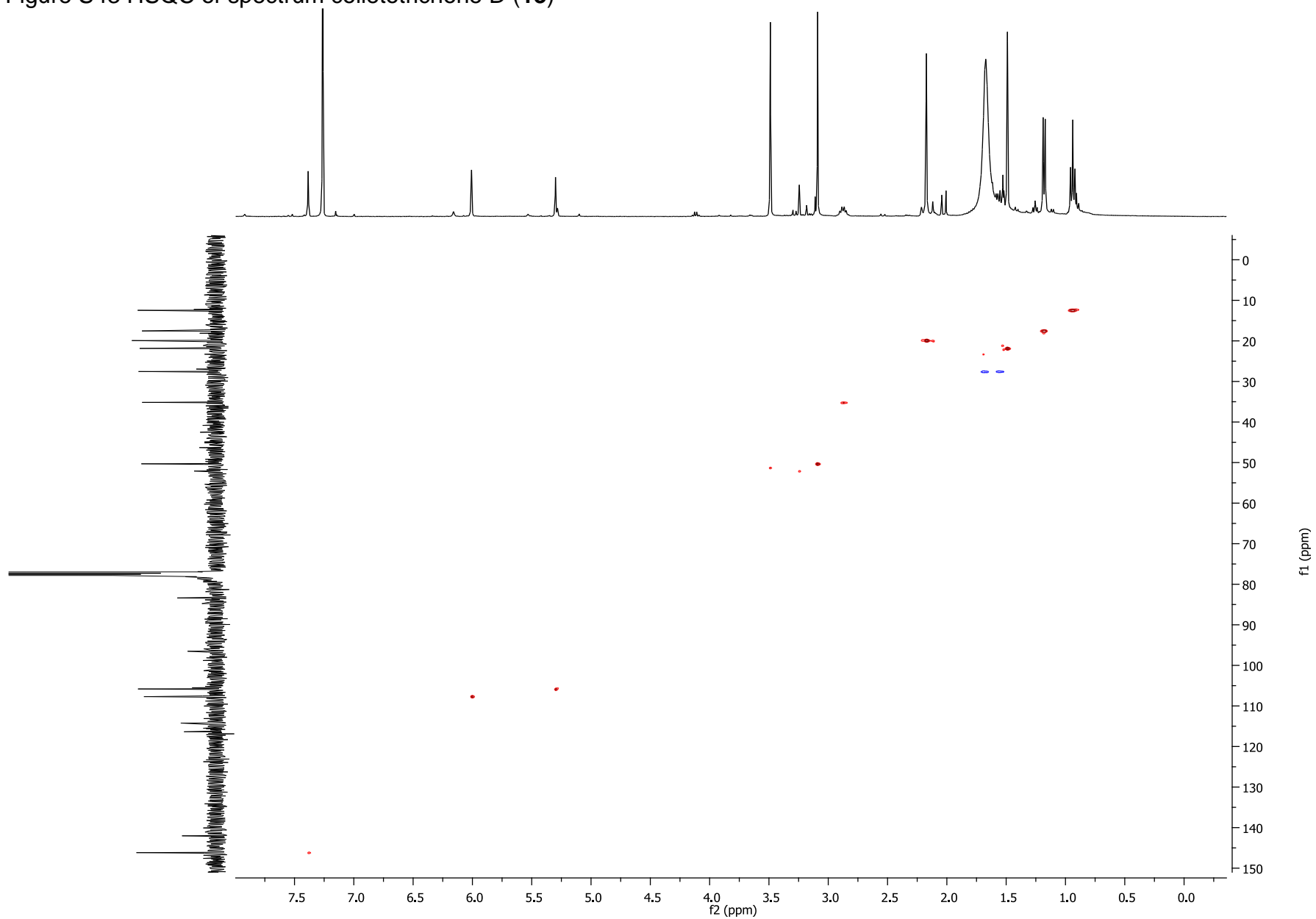
## Chapter 8: Supplemental data

Figure S42  $^{13}\text{C}$  NMR (125 MHz,  $\text{CDCl}_3$ ) spectrum of colletotrichone D (**13**)



## Chapter 8: Supplemental data

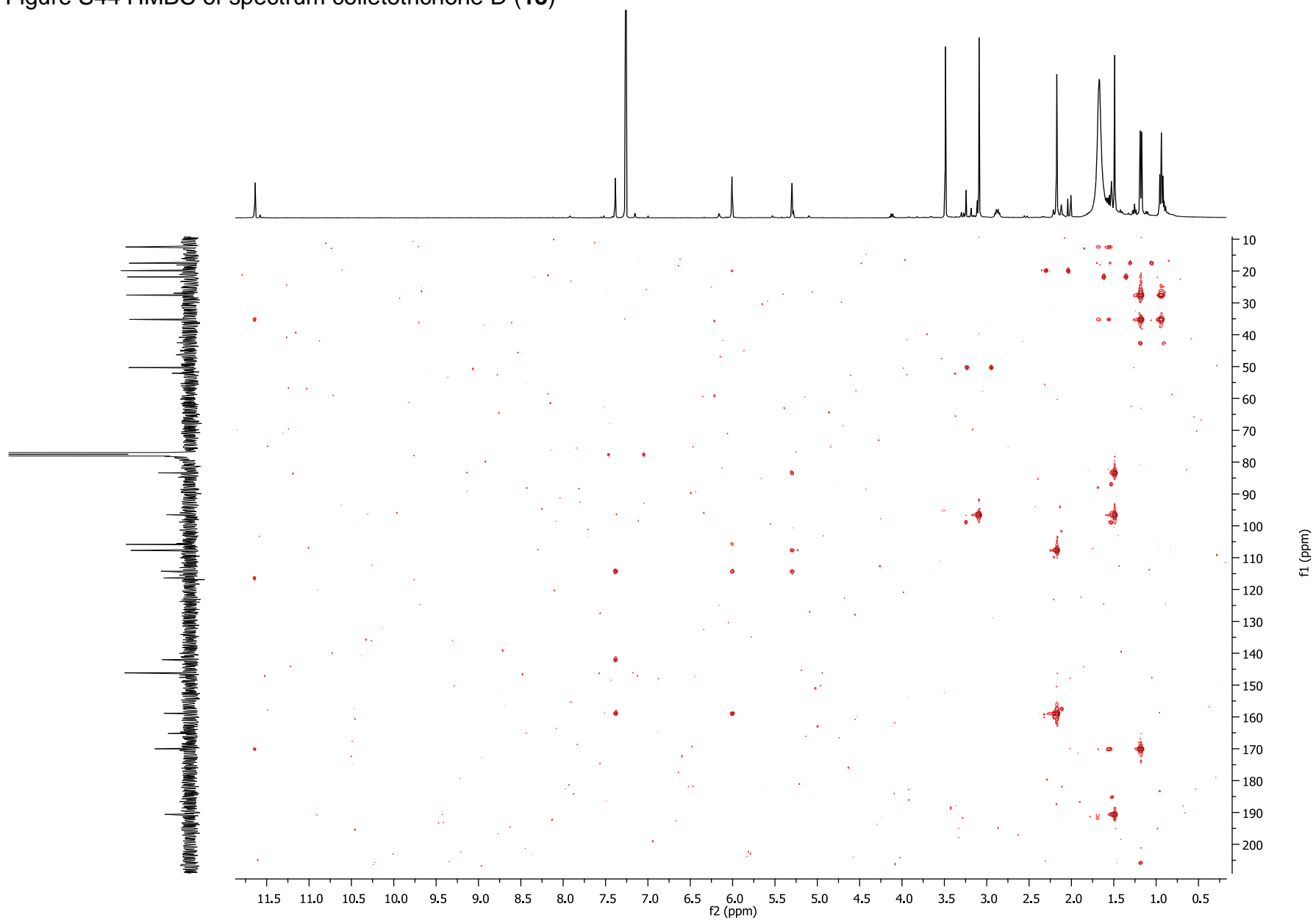
Figure S43 HSQC of spectrum colletotrichone D (13)





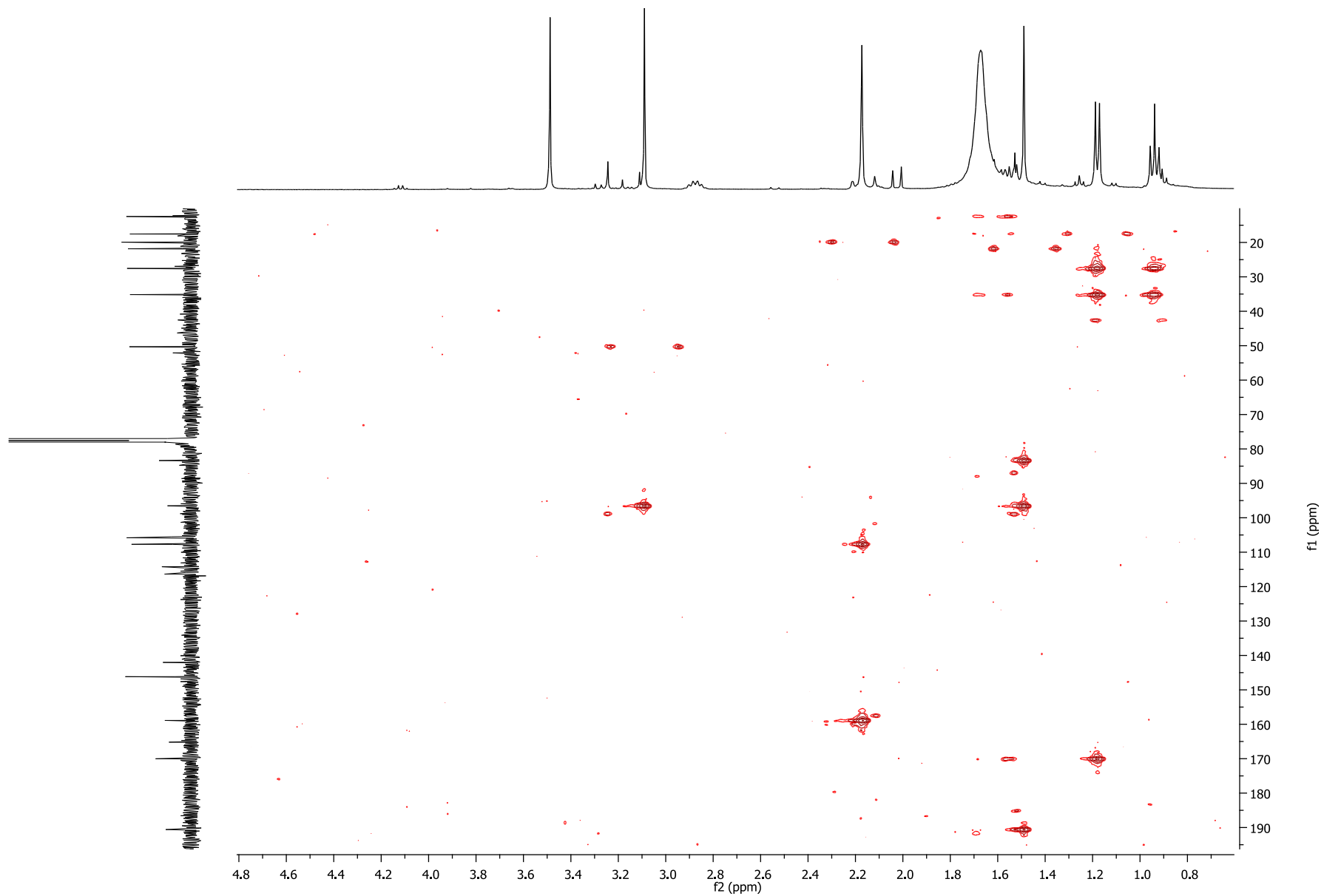
## Chapter 8: Supplemental data

Figure S44 HMBC of spectrum colletotrichone D (**13**)



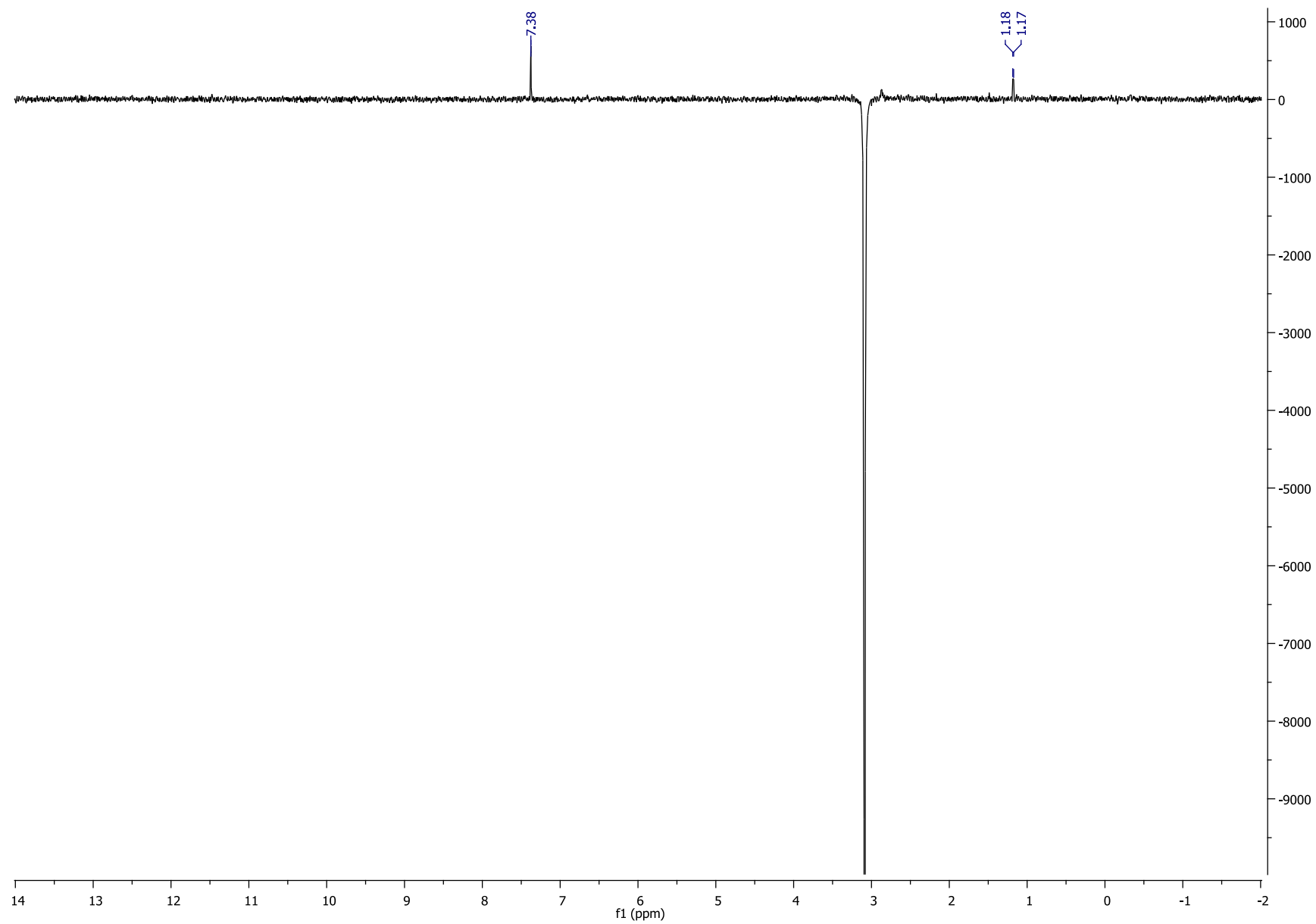
## Chapter 8: Supplemental data

Figure S44 HMBC of spectrum colletotrichone D (**13**)



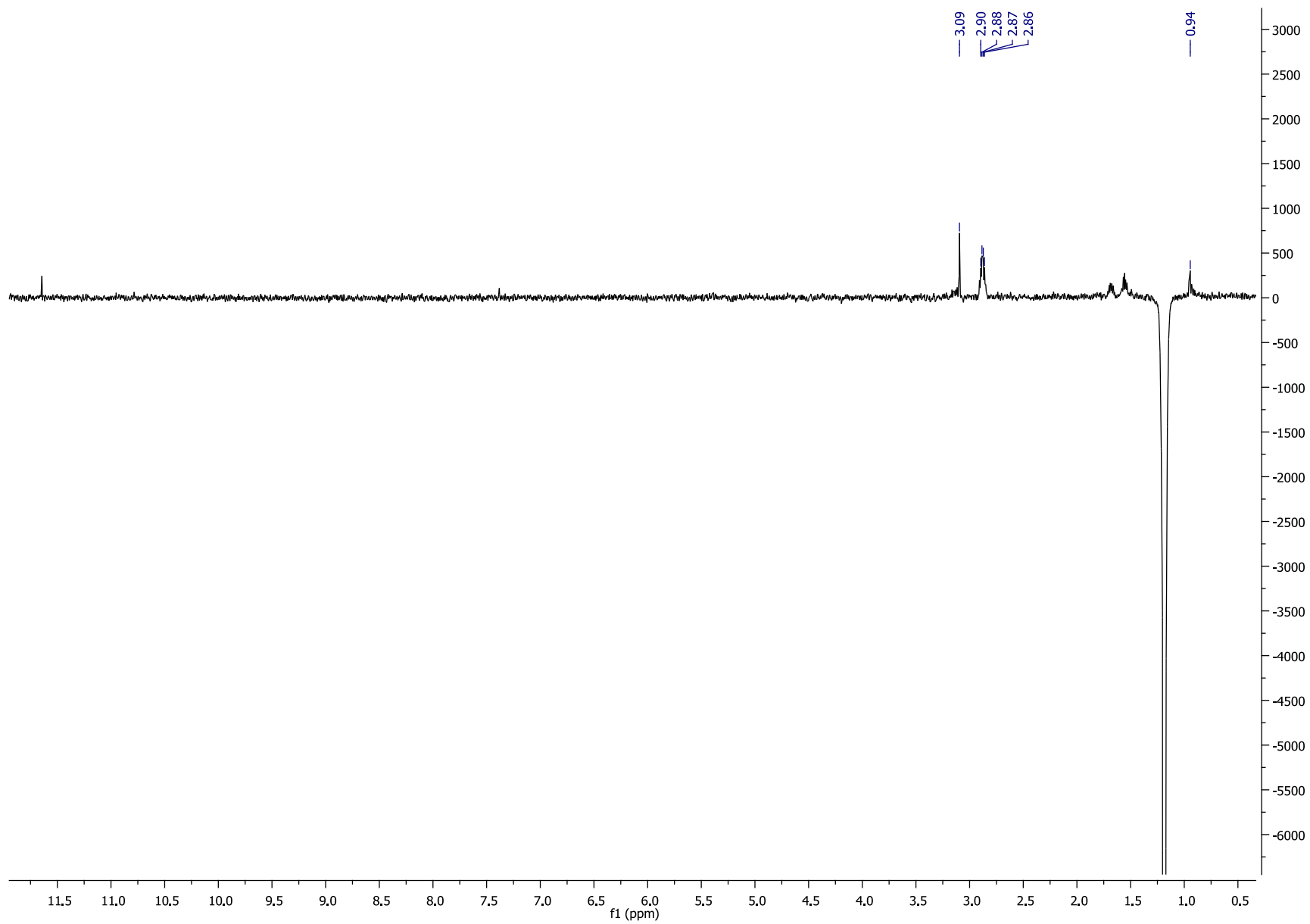
## Chapter 8: Supplemental data

Figure S45 1D NOESY (500 MHz,  $\text{CDCl}_3$ ) spectrum of colletotrichone D (**13**)



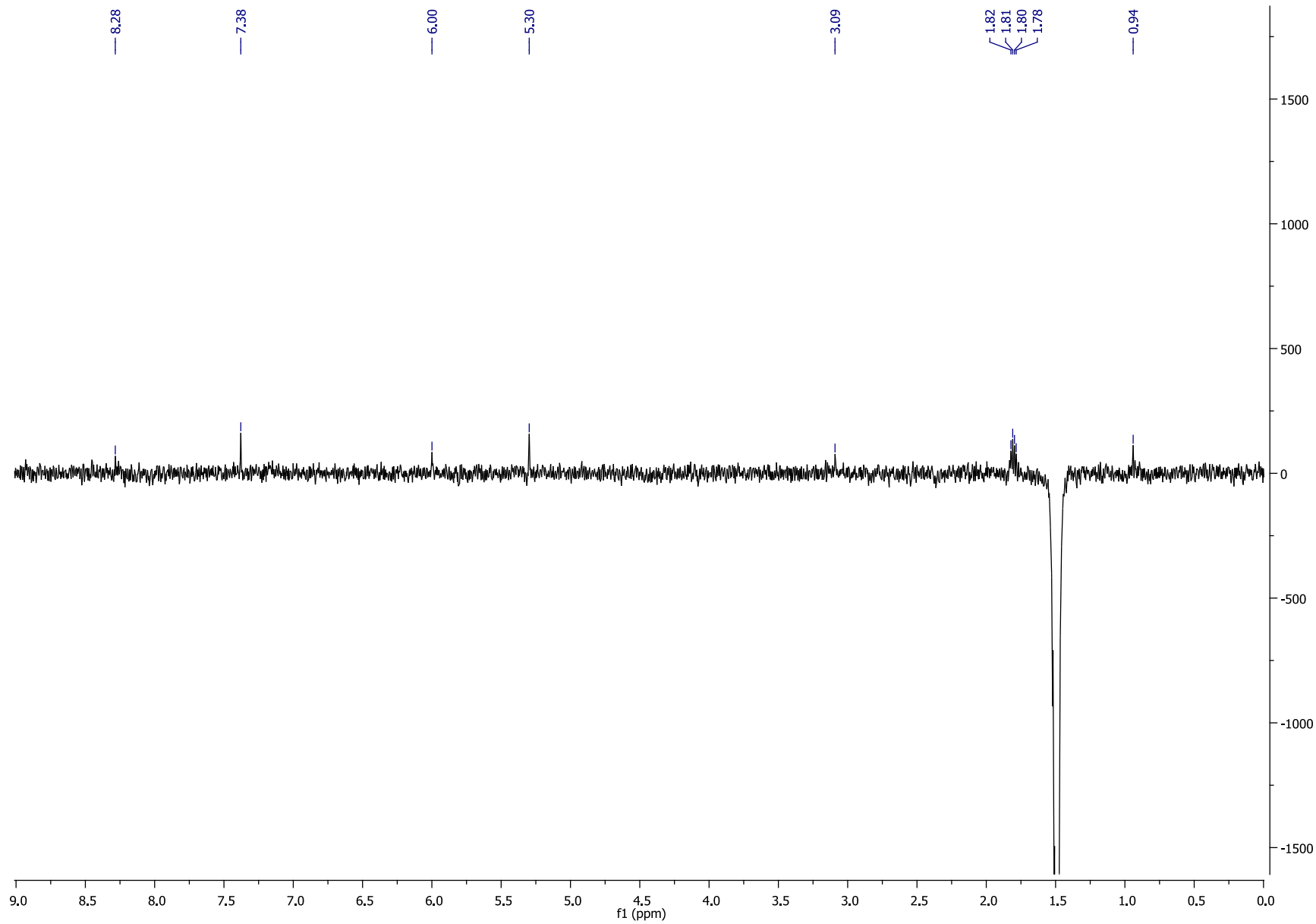
## Chapter 8: Supplemental data

Figure S45 1D NOESY (500 MHz,  $\text{CDCl}_3$ ) spectrum of colletotrichone D (**13**)



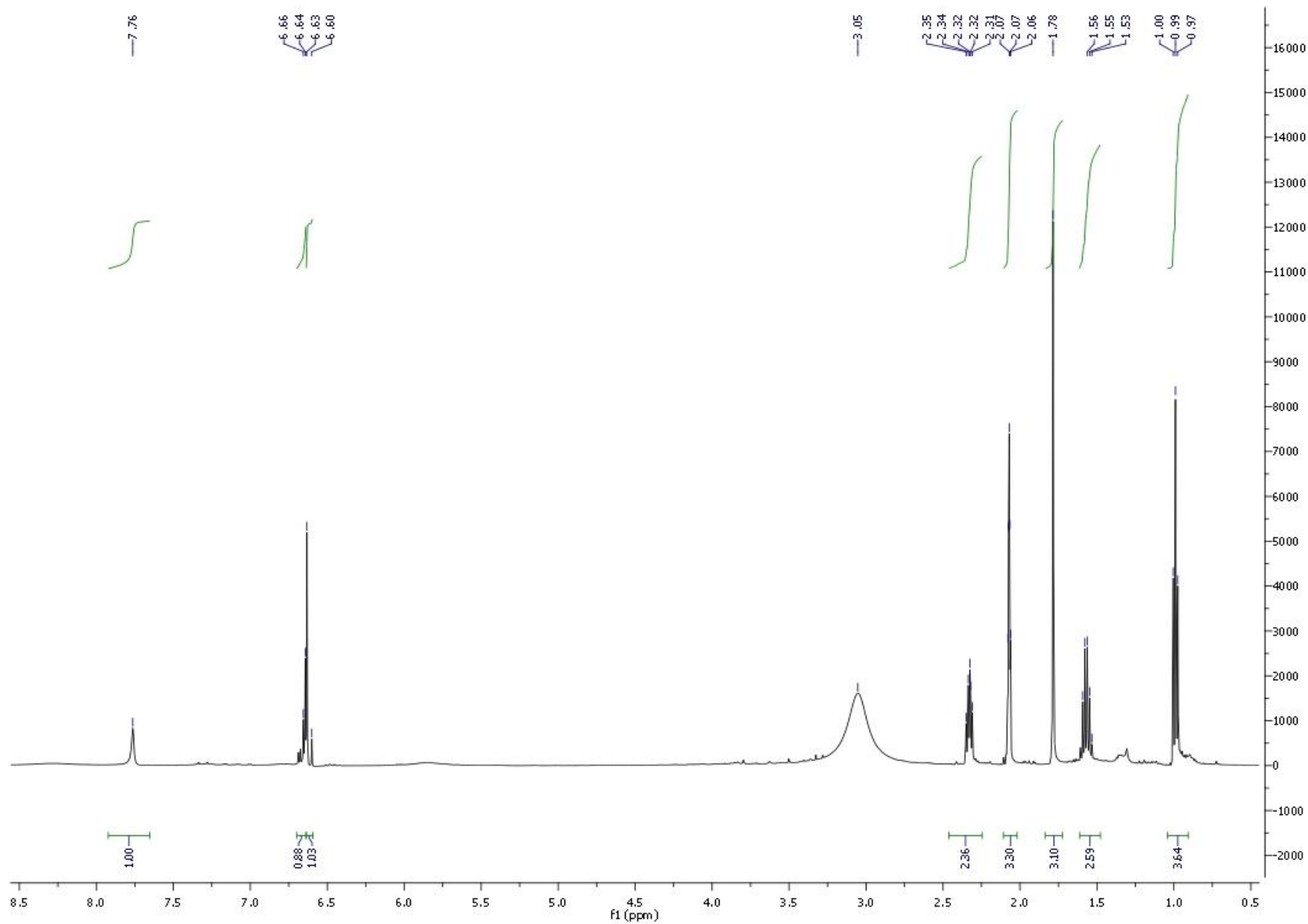
## Chapter 8: Supplemental data

Figure S45 1D NOESY (500 MHz,  $\text{CDCl}_3$ ) spectrum of colletotrichone D (**13**)



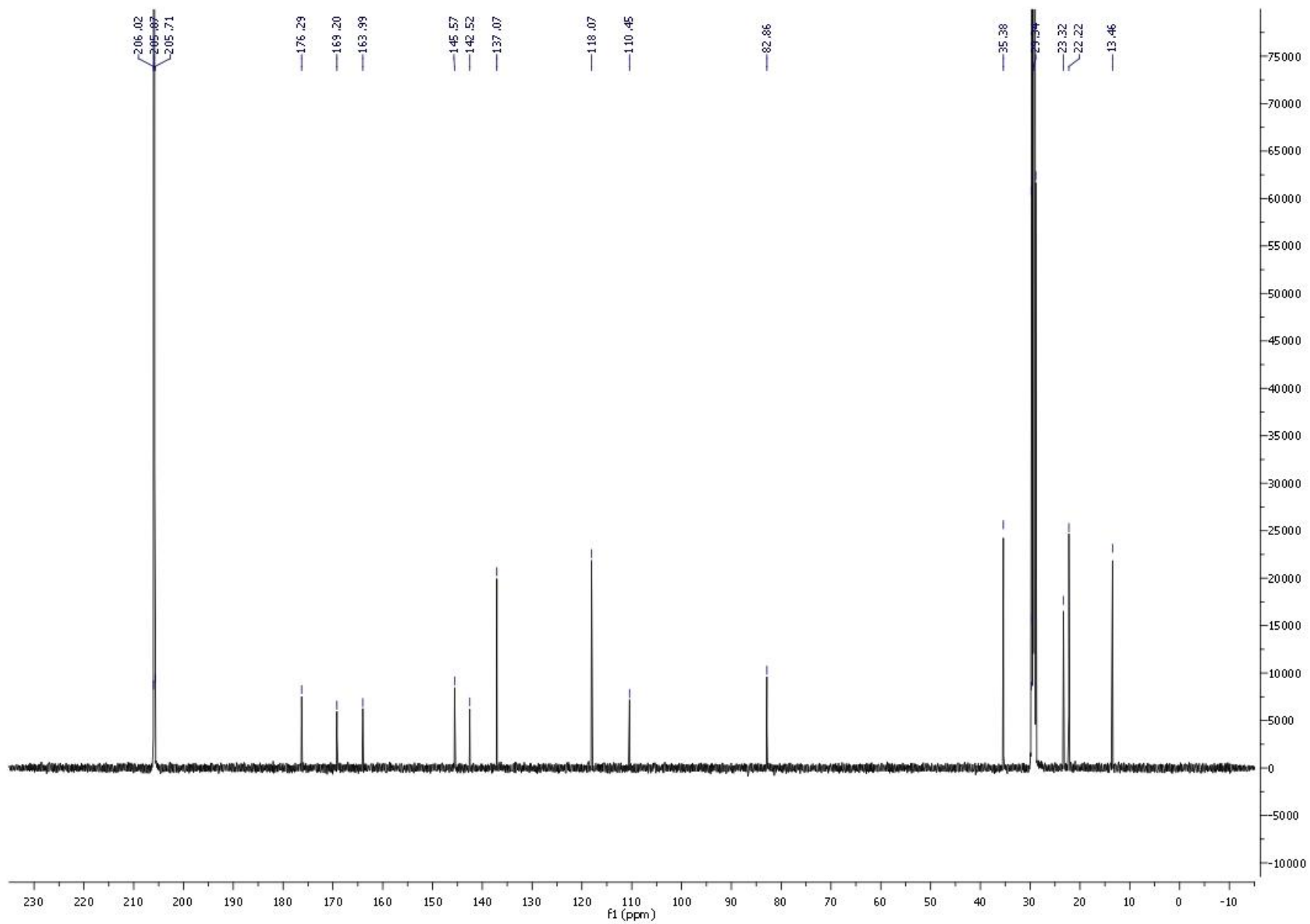
## Chapter 8: Supplemental data

Figure S46  $^1\text{H}$  NMR (500 MHz, acetone- $d_6$ ) spectrum of phyllostictalactam A (**15**)



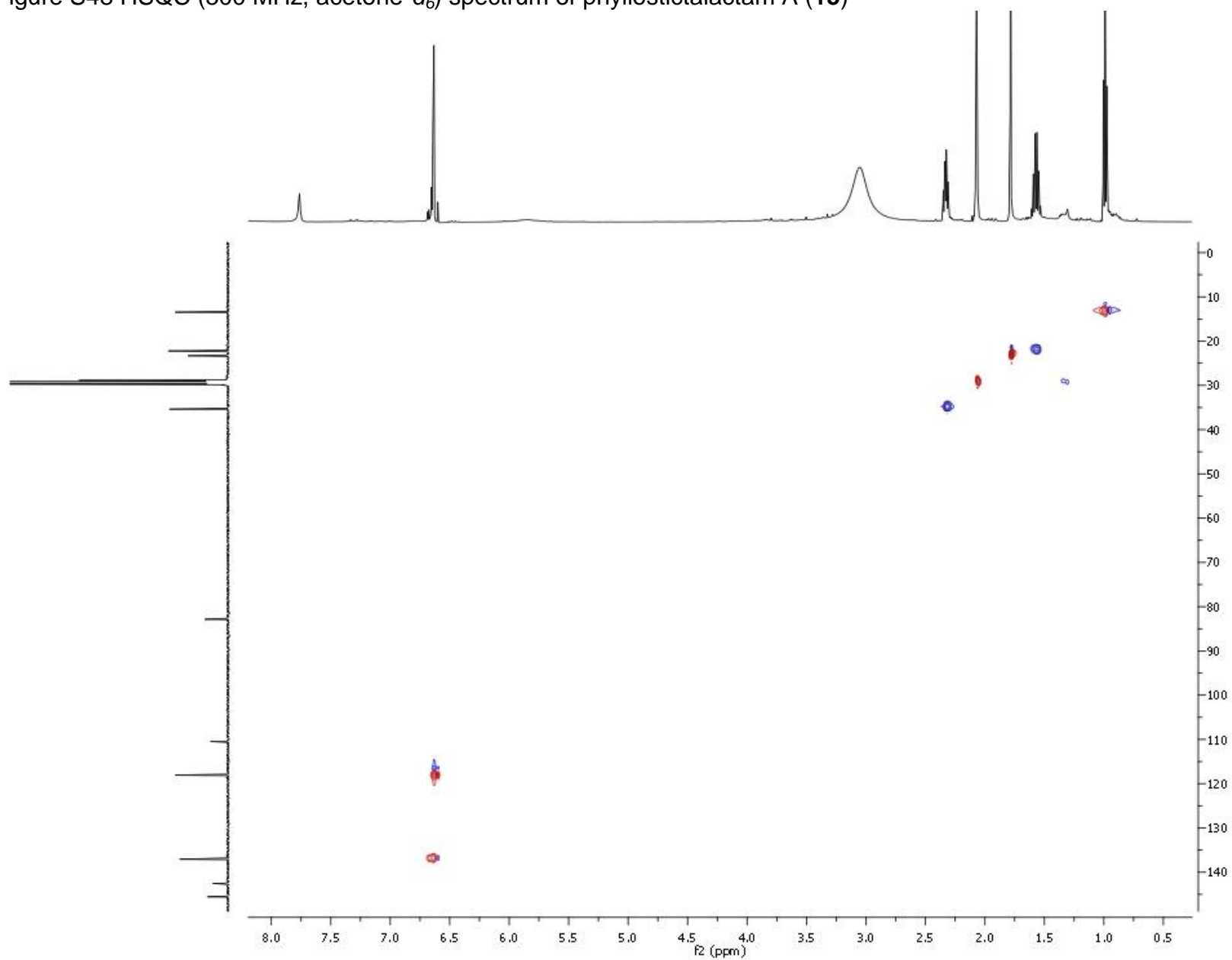
## Chapter 8: Supplemental data

Figure S47.  $^{13}\text{C}$  NMR (125 MHz, acetone- $d_6$ ) spectrum of phyllostictalactam A (**15**)



## Chapter 8: Supplemental data

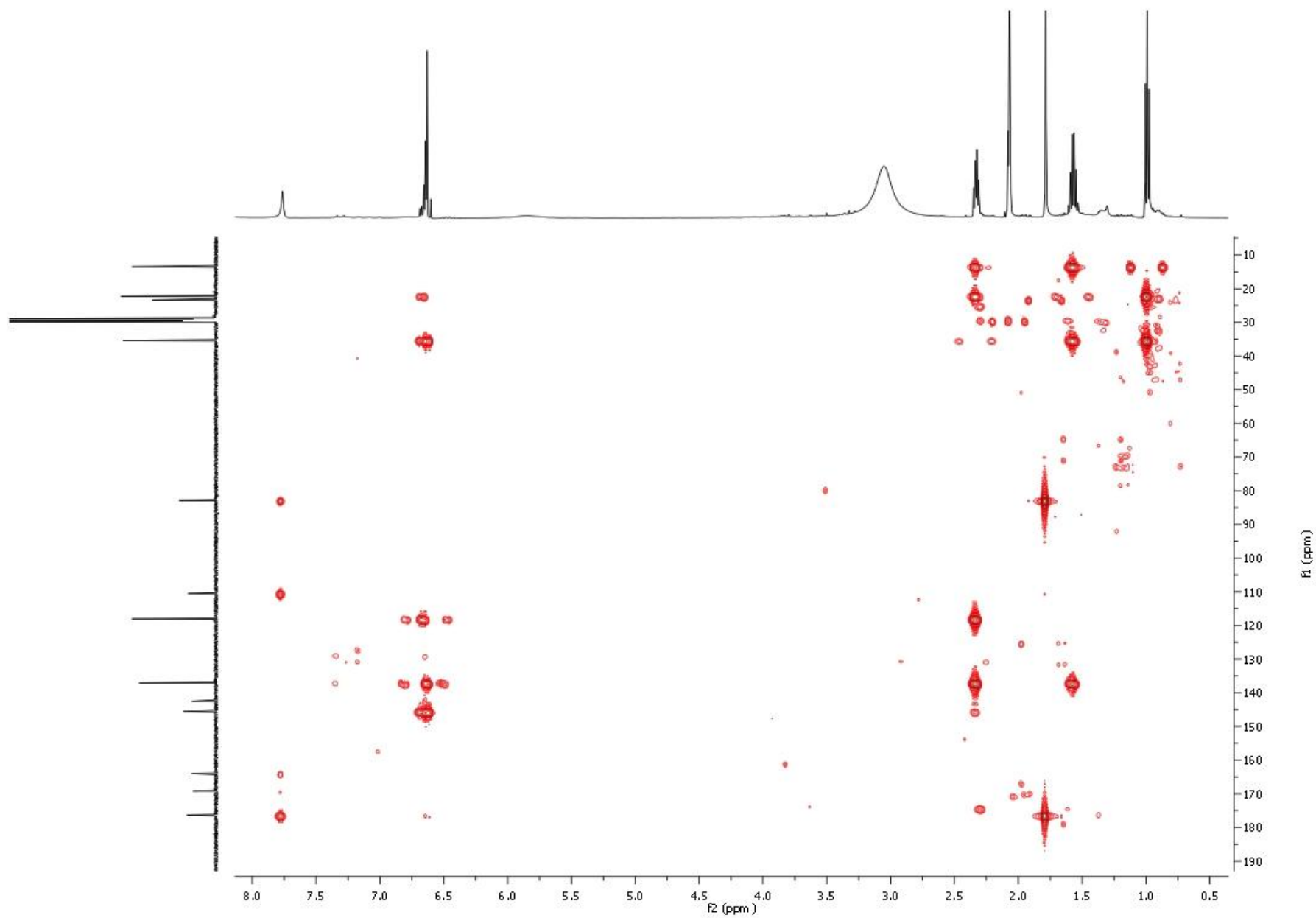
Figure S48 HSQC (500 MHz, acetone- $d_6$ ) spectrum of phyllostictalactam A (15)





## Chapter 8: Supplemental data

Figure S49 HMBC (500 MHz, acetone- $d_6$ ) spectrum of phyllostictalactam A (15)

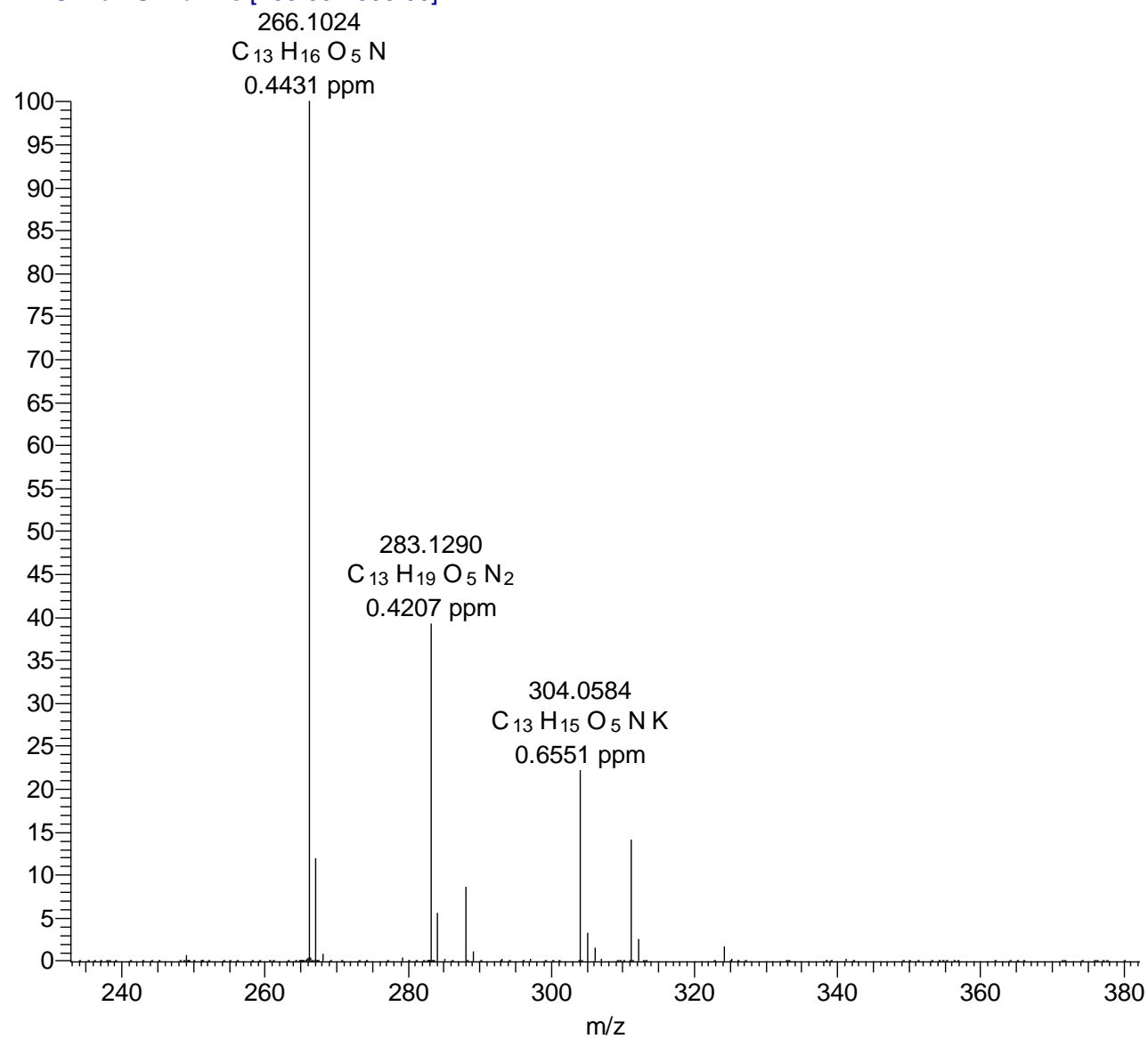


## Chapter 8: Supplemental data

Figure S50 ESI-HRMS of phyllostictalactam A (**15**)

BS53 #226 RT: 5.90 AV: 1 NL: 9.07E6

T: FTMS + c ESI Full ms [200.00-2000.00]



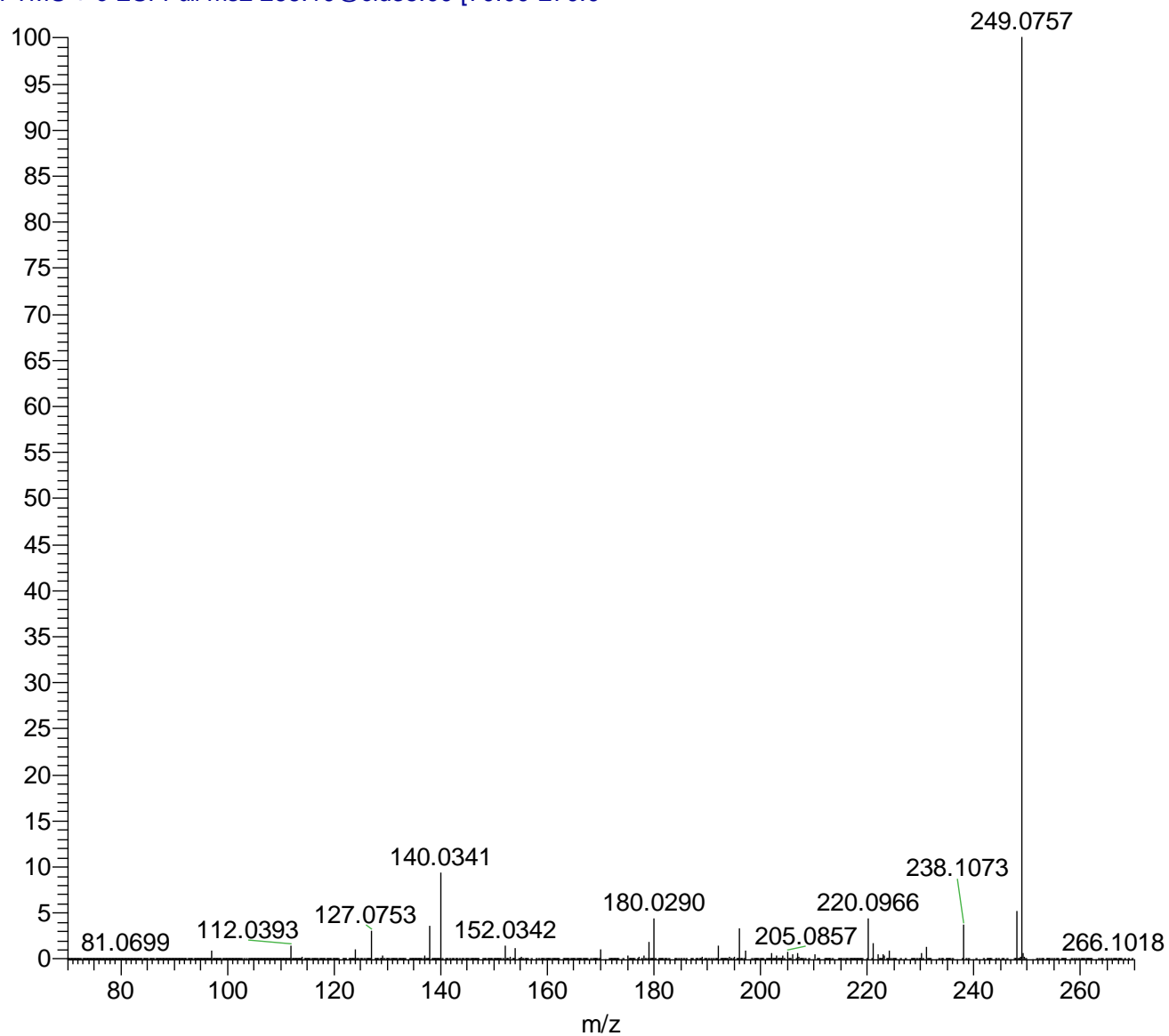
## Chapter 8: Supplemental data

---

Figure S51 MS<sup>2</sup> of phyllostictalactam A (**15**) (parent mass: 266.1024, [M+H]<sup>+</sup>, CID energy: 35 eV)

BS53-MS2 #1609-1714 RT: 13.28-13.98 AV: 106 NL: 2.34E7

T: FTMS + c ESI Full ms2 266.10@cid35.00 [70.00-270.0



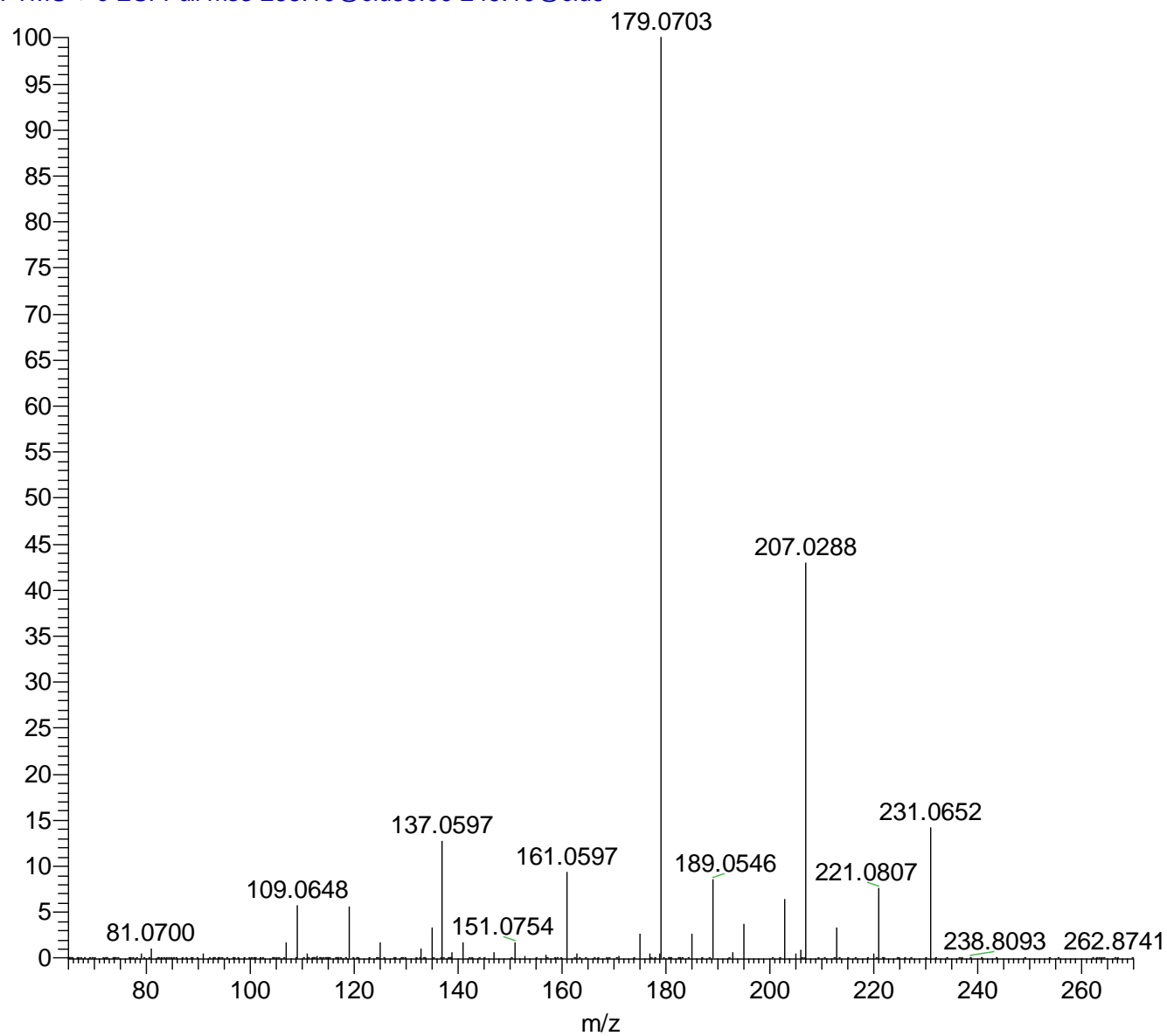
## Chapter 8: Supplemental data

---

Figure S52 MS<sup>3</sup> of phyllostictalactam A (**15**) (parent mass: 249.0757 from MS<sup>2</sup>, CID energy: 35 eV)

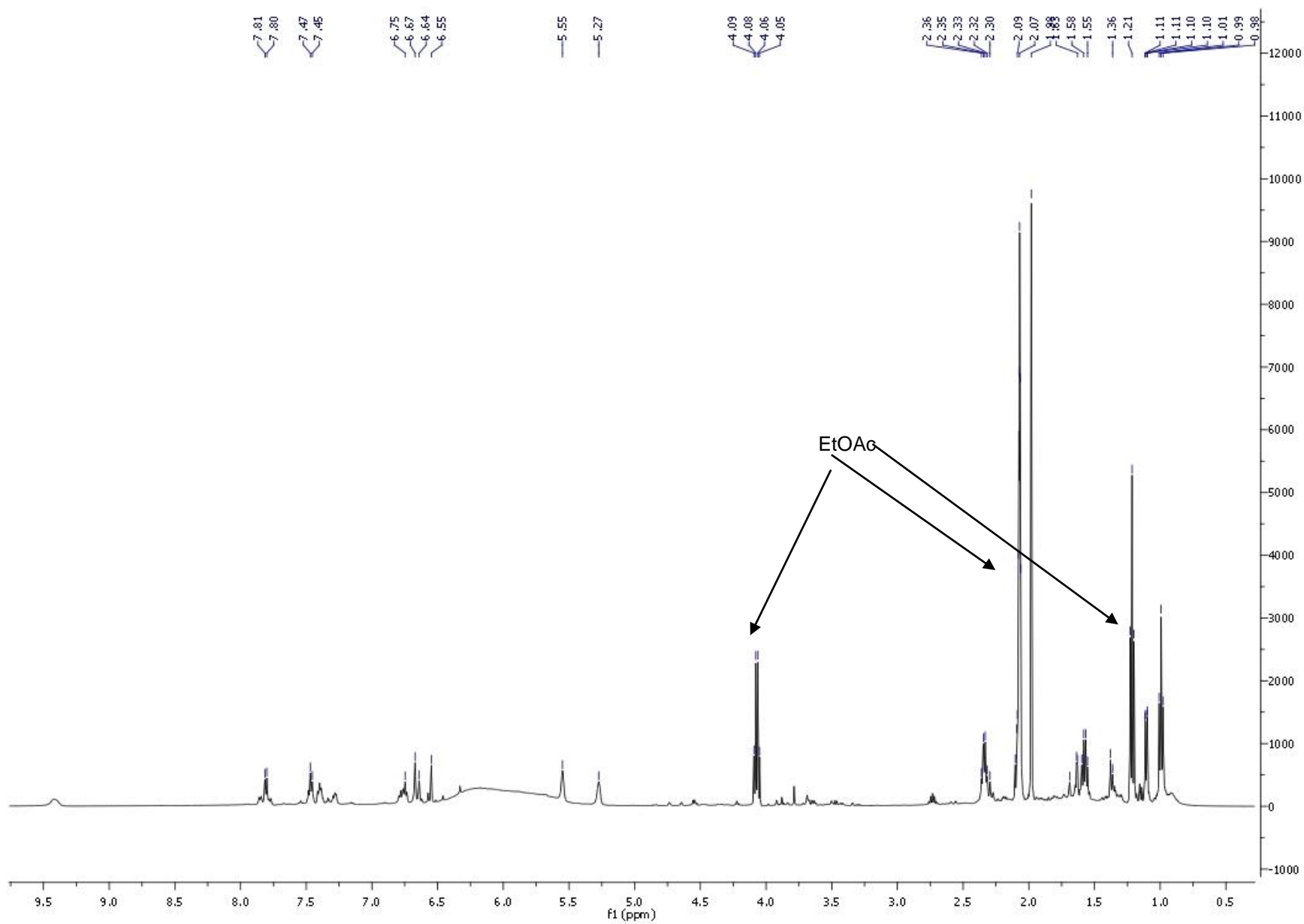
BS53-MS3 #1135-1194 RT: 13.31-13.84 AV: 15 NL: 7.36E6

T: FTMS + c ESI Full ms3 266.10@cid35.00 249.10@cid3



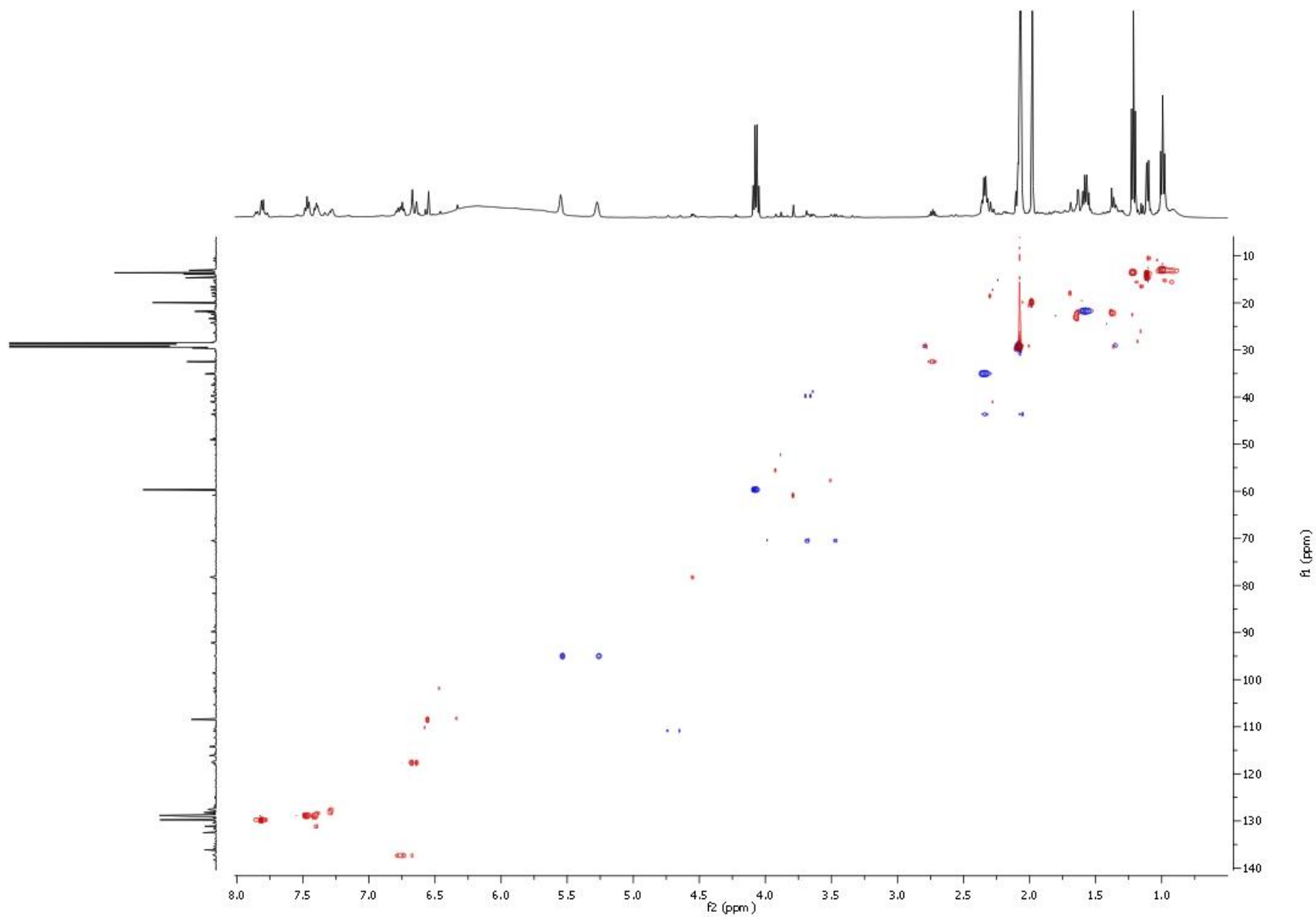
## Chapter 8: Supplemental data

Figure S53.  $^1\text{H}$  NMR (500 MHz, acetone- $d_6$ ) spectrum of phyllostictalactam B (**16**)



## Chapter 8: Supplemental data

Figure S54 HSQC (500 MHz, acetone- $d_6$ ) spectrum of phyllostictalactam B (16)

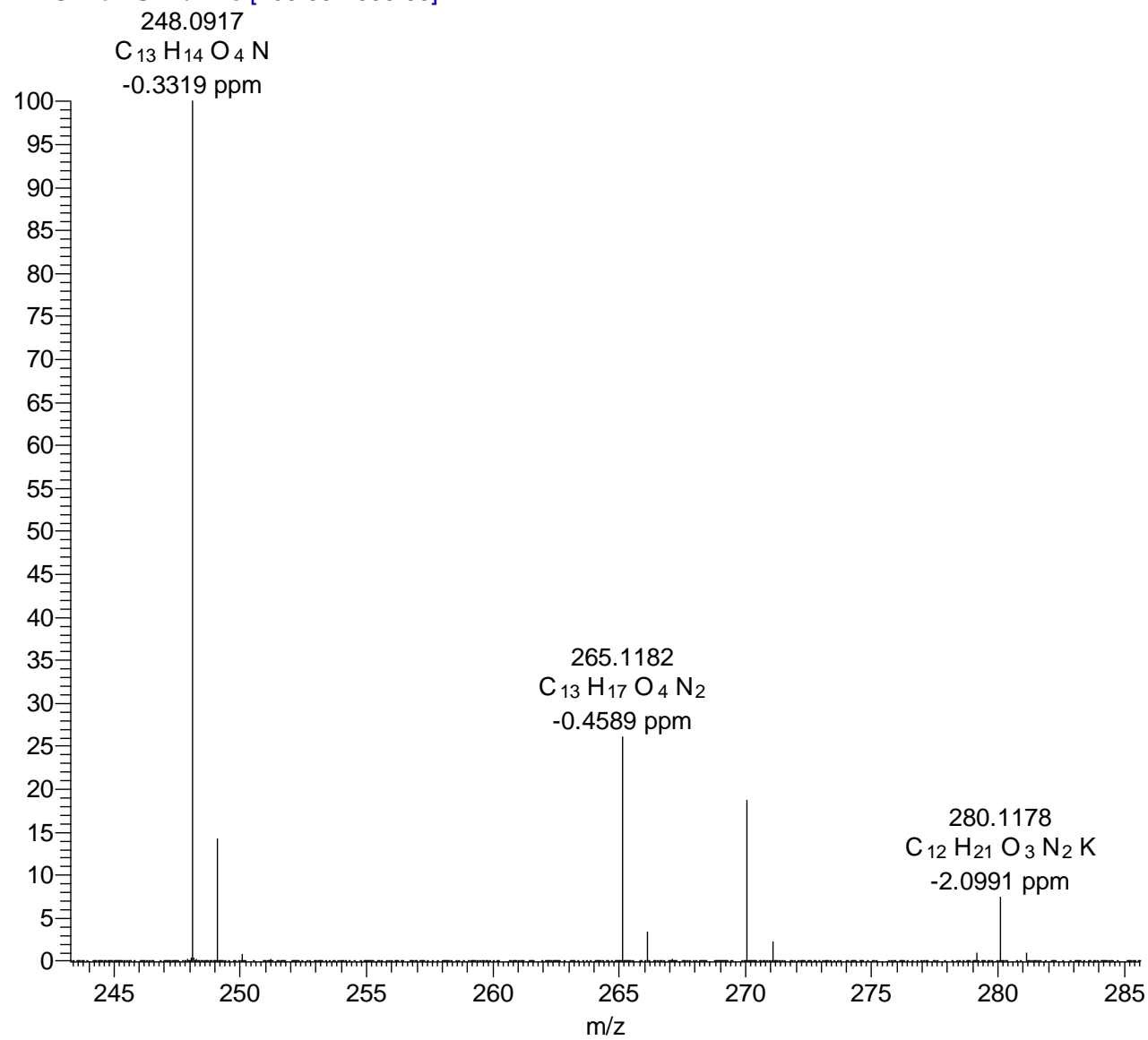


## Chapter 8: Supplemental data

Figure S55 ESIHRMS of phyllostictalactam B (**16**)

BS53-dehydrated2 #983-1030 RT: 16.47-17.19 AV: 48 NL: 9.72E6

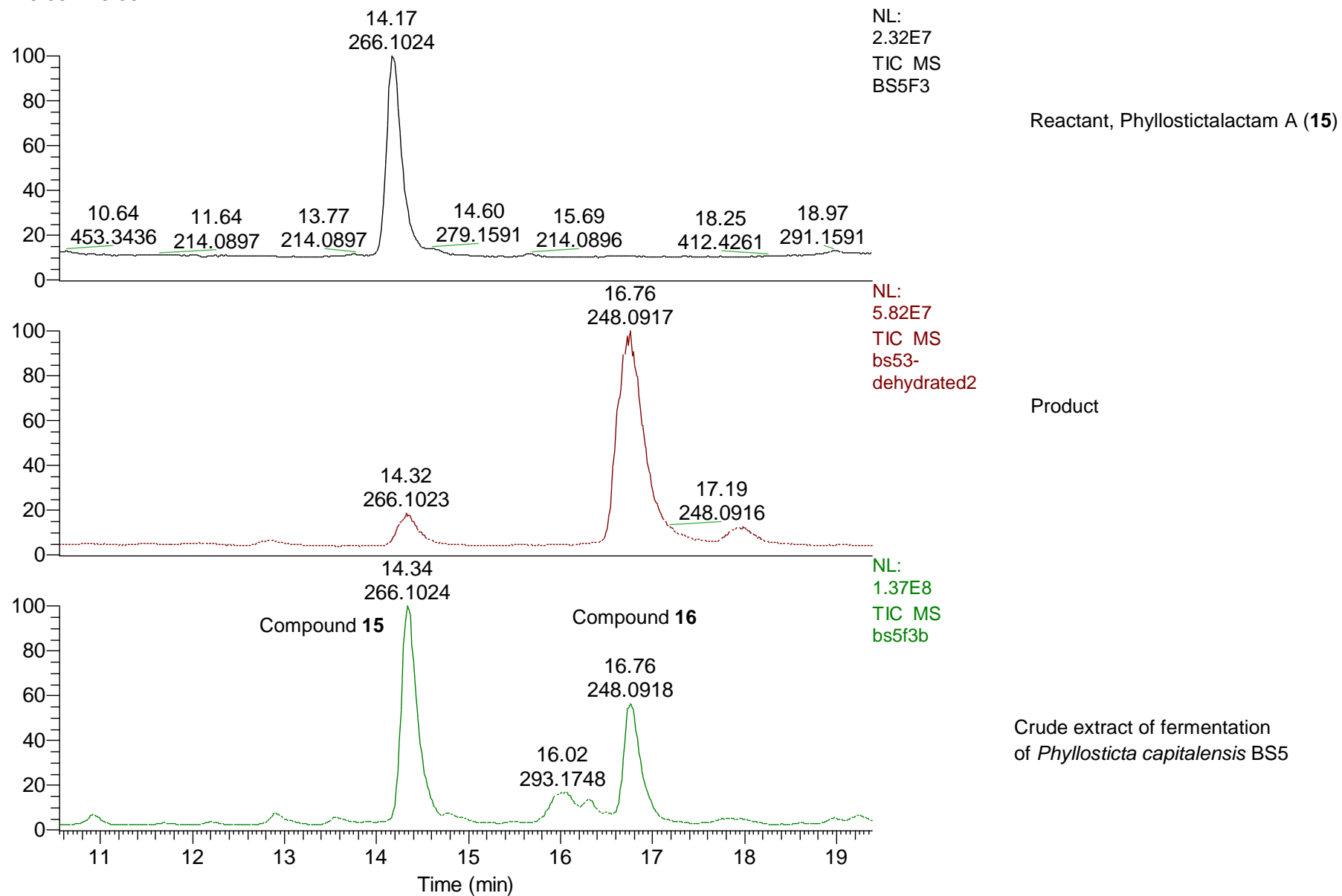
T: FTMS + c ESI Full ms [200.00-1000.00]



## Chapter 8: Supplemental data

Figure S56 LC-MS of synthesized phyllostictalactam B (**16**) and crude extracts

RT: 10.55 - 19.39



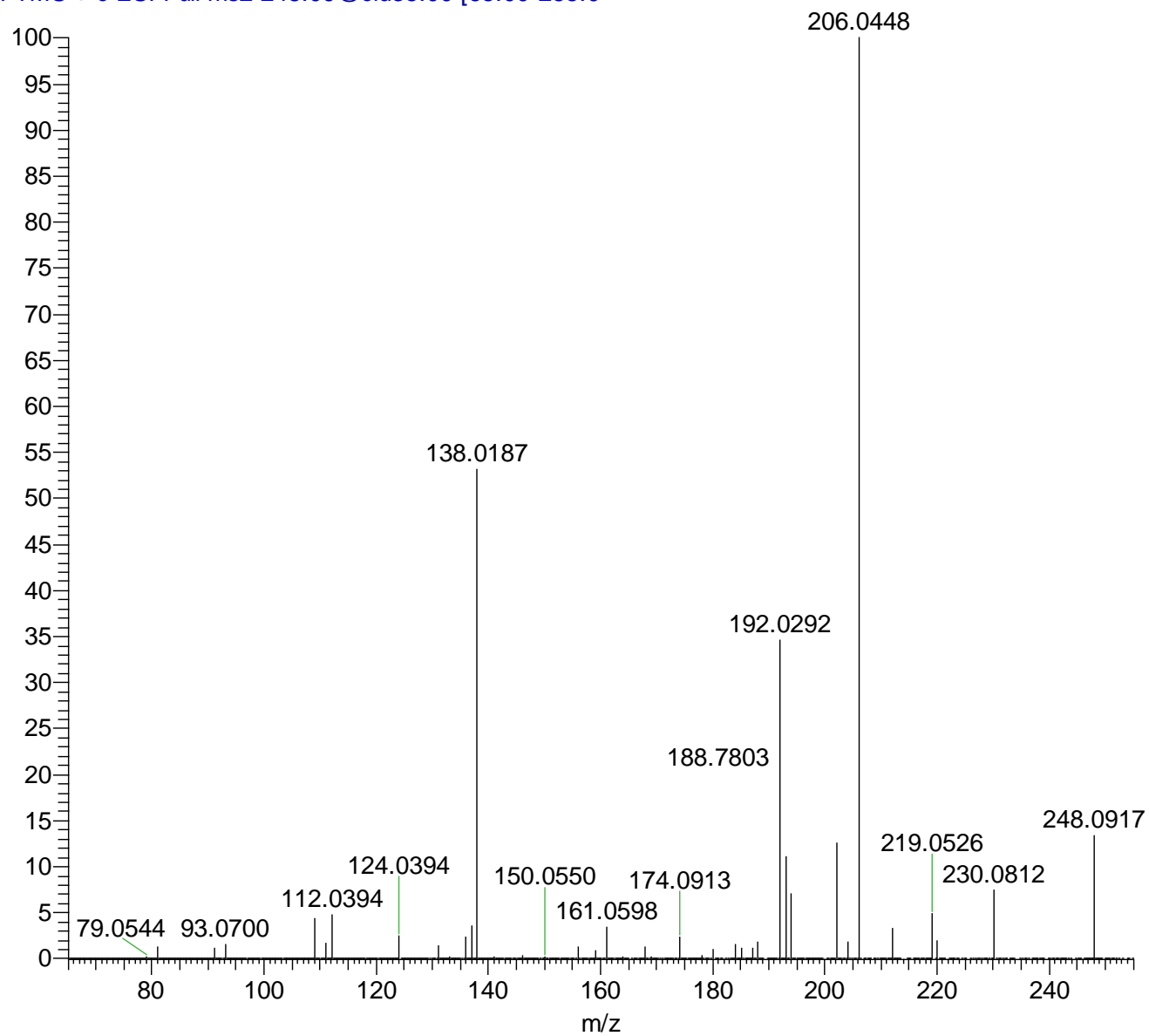


## Chapter 8: Supplemental data

Figure S57 MS<sup>2</sup> spectrum of phyllostictalactam B (**16**) (parent mass: 248.0917, CID energy: 35 eV)

BS53-dehydrated2-MS2 #1218-1259 RT: 16.48-16.96 AV: 42 NL: 2.13E6

T: FTMS + c ESI Full ms2 248.09@cid35.00 [65.00-255.0



**List of abbreviations**

<b>Full name</b>	<b>Abbreviation</b>
BP	Base pairs
Collisionally activated dissociation	CAD
Collisionally-induced dissociation	CID
Double bond equivalent	DBE
Desorption electrospray ionization	DESI
Dilution factor	DF
Density functional theory	DFT
Desorption/ionization on silicon mass spectrometry	DIOS MS
Deoxyribonucleic acid	DNA
Deoxynucleoside triphosphate	dNTP
Ethyl acetate	EtOAc
Formic acid	FA
Fourier transform mass spectrometry	FTMS
Fractional survival	FS
Gauge-including atomic orbitals	GIAO
Imaging mass spectrometry	IMS
$\alpha$ -Cyano-4-hydroxycinnamic acid	HCCA
Liquid chromatography-high resolution mass spectrometry	LC-HRMS
Liquid micro-junction surface sampling probe	LMJ-SSP
Limit of detection	LOD
Mean absolute deviation	MAD
Mean absolute error	MAE
Matrix-assisted laser desorption/ionization	MALDI
Mass spectrometry	MS
Tandem mass spectrometry	MS/MS
Multiple-stage mass spectrometry	MS <sup>n</sup>
Multiple standard method	MTSD
Nutrient agar	NA
Nutrient broth	NB

## Appendix A

---

Nuclear Overhauser effects	NOE
Nuclear Overhauser effect spectroscopy	NOESY
Nonribosomal peptides	NRP
Nonribosomal peptide synthetase	NRPS
One Strain Many Compounds	OSMAC
Phosphate-buffered saline	PBS
Polymerase chain reaction	PCR
Potato dextrose agar	PDA (medium)
Photodiode array detector	PDA (detector)
Potato dextrose broth	PDB
Polyketide synthase	PKS
Plant natural products	PNP
Quorum sensing	QS
Root mean square	RMS
Room temperature	R. t.
Retention time	R. t.
Sabouraud dextrose agar	SDA
Traditional Chinese medicine	TCM
Total ion current	TIC
Trifluoroacetic acid	TFA

### List of figures

**Figure 1.** Representative plant natural products with alternative endophytic sources

**Figure 2.** *N. tazetta* (left) collected from Zhangzhou, Fujian and *B. sinica* (right) collected from Shanghai

**Figure 3.** The chain elongation of NRPS biosynthesis pathway

**Figure 4.** The chain elongation of type I–III PKS biosynthesis pathway

**Figure 5.** Basic azaphilone scaffold

**Figure 6.** Reported lactam-fused 4-pyrones

**Figure 7.** Representative *a*, *b*, *c*, *x*, *y*, and *z* ion pattern of linear peptides

**Figure 8.** The flow chart of MALDI IMS measurement

**Figure 9.** LC-MS positive full scan chromatogram of hexacyclopeptides (**1–9**) from *F. solani* in static PDB medium

**Figure 10.** Distribution visualization of hexacyclopeptides (**1–9**) by MALDI IMS after 48 h. **a** Optical image of *F. solani* N06. **b** TIC (*m/z* 300–800) of detected area. **c** Ion intensity map of  $C_{30}H_{52}O_8N_6Na$ . **d** Ion intensity map of  $C_{32}H_{56}O_8N_6Na$

**Figure 11.** Distribution visualization of hexacyclopeptides detected in MALDI-imaging-HRMS scan of the endophytic fungus *F. solani* and another endophytic bacterium *A. xylosoxidans* isolated from the same plant tissue after 48 h. **a** Optical image of the boundary area between *F. solani* and bacterium *A. xylosoxidans*. **b** TIC (*m/z* 300–800) of detected area. **c** Ion intensity map of  $C_{30}H_{52}O_8N_6Na$ . **d** Ion intensity map of  $C_{32}H_{56}O_8N_6Na$

**Figure 12.** MS<sup>2</sup> fragments of compounds **1–9** with CID (35 eV). **a** MS<sup>2</sup> of  $[M+H-2H_2O]^+$ , *m/z* 589.4 (compounds **1–4**) and  $[M+H-H_2O]^+$ , *m/z* 589.4 (compound **5**). **b** MS<sup>2</sup> of  $[M+H-2H_2O]^+$ , *m/z* 617.4 (compounds **6–8**) and  $[M+H-H_2O]^+$ , *m/z* 617.4 (compound **9**)

## Appendix A

---

**Figure 13.** MS<sup>3</sup> of  $y_5$  ions and  $a_2$  ions of compounds **1–9**. **a**  $y_5$  ion ( $m/z$  476.2) of compounds **1–5**. **b**  $y_5$  ion ( $m/z$  504.2) of compounds **6–9**. **c**  $a_2$  ion ( $m/z$  181.2) of compounds **1–9**

**Figure 14.** Synthesis of 2,4,4,4-tetradeuterium-threonine

**Figure 15.** Synthesis of 4-OH-4-deuterium-proline

**Figure 16.** The MS of labeled hexacyclopeptides in feeding experiment with 2,4,4,4-tetradeuterium-threonine. **a** Labeled compounds **1–4**. **b** Labeled compound **5**. **c** Labeled compounds **6–8**. **d** Labeled compound **9**

**Figure 17.** Structures of compounds **10–14**

**Figure 18.** <sup>1</sup>H, <sup>1</sup>H COSY, key HMBC correlations and X-ray diffraction crystal structure (ORTEP drawing) of colletotrichone A (**10**)

**Figure 19.** Experimental (continuous line) and calculated (dashed curve) ECD spectra (in MeOH) of colletotrichone A (**10**)

**Figure 20.** <sup>1</sup>H, <sup>1</sup>H COSY, key HMBC and NOESY correlations of colletotrichone B (**11a**); 3D structure is the conformer with the lowest energy

**Figure 21.** Experimental CD data in MeOH (black continuous line) and calculated ECD spectra of colletotrichone B (**11a**; red, dashed curve) and 10*S*,12*R*-*epi*-colletotrichone B (**11b**; blue dashed curve)

**Figure 22.** <sup>1</sup>H, <sup>1</sup>H COSY, key HMBC and NOESY correlation of colletotrichone C (**12**)

**Figure 23.** Experimental (continuous line) and calculated (dashed curve) ECD spectra (in MeOH) of colletotrichone C (**12**)

**Figure 24.** Two possible structures of compound **13**

**Figure 25.** Experimental (continuous line) and calculated (dashed curve) ECD spectra (in MeOH) of colletotrichone C (**13**)

**Figure 26.** Proposed biosynthetic pathway of compounds **10–14**

## Appendix A

---

**Figure 27.** *In vitro* cytotoxic assays of compounds **10**, **11a**, **12** and **14a** against THP-1 cells using a resazurin-based assay (to measure metabolic activity) as well as an ATPlite assay (to measure ATP content). Semilogarithmic representation of the fractional survival (FS in %) of THP-1 cells as a function of concentration is provided

**Figure 28.** Spatial distribution of compound **10** and compound **11a/14a** produced by endophytic *Colletotrichum* sp. BS4 on rice agar after 16 days. **a** Optical image of colony and the cross section of agar layer on glass slide. **b** Detected area for MALDI IMS. **c** Spatial distribution of compound **10** ( $[M+K]^+$ ,  $m/z$  387.0841). **d** Spatial distribution of compound **11a** and/or **14a** ( $[M+K]^+$ ,  $m/z$  355.0942)

**Figure 29.** Stained agarose gels of purified PCR products of ITS and 16S rRNA sequences of total genomic DNA of endophytic fungal isolate BS5 harbored in *Buxus sinica*. An approximately 600 bp (sample 2) and 1500 bp (sample 3) band obtained for fungal isolate BS5 and its bacterial endosymbiont

**Figure 30.** The structures of compound **15** and **16**

**Figure 31.** Semi-synthesis of compound **16**

**Figure 32.** Stained agarose gels of purified PCR products of polyketide synthase genes (PKS; spanning around 700 bp) of endophytic isolate BS5 (harboring bacterial endosymbiont). An approximately 700 bp PKS band amplified for isolate BS5 using both bacterial and fungal PKS degenerate primers (sample 3 and 5), although both PKS bands encodes for fungal polyketide. *Aspergillus versicolor* (isolate A12) (sample 2) and *Bacillus subtilis* (DSM 1088) (sample 4) are the positive controls and sterile double distilled water is the negative control (sample 6)

**Figure 33.** Stained agarose gels of purified PCR products of nonribosomal peptide synthetase (NRPS; spanning around 300 bp for fungus and 1000 bp for bacterium) of endophytic isolate BS5 (harboring bacterial endosymbiont). No NRPS band present in fungal isolate BS5 (sample 5), but an approximately 1000 bp NRPS band amplified for bacterial endosymbiont of isolate BS5 (sample 4). *Aspergillus versicolor* (isolate A12) (sample 2) and *Bacillus subtilis* (DSM 1088) (sample 3) are the positive controls and sterile double distilled water is the negative control (sample 6)

## Appendix A

---

**Figure 34.** Stained agarose gels of separating the purified 1000 bp fragment of bacterial NRPS resulting in 1000 bp fragment and 700 bp fragment (similar to fungal PKS)

**Figure 35.** Biosynthesis pathway of compounds **15** and **16**

### List of Tables

**Table 1.** Representative plant natural products with alternative endophytic sources

**Table 2.** Retention time and adducts ion intensity of compounds **1–9** ( $\Delta < 2$  ppm)

**Table 3.**  $^1\text{H}$  NMR Spectroscopic Data of **10–12** at 500 MHz

**Table 4.**  $^{13}\text{C}$  NMR Spectroscopic Data of **10–12** at 125 MHz

**Table 5.**  $^{13}\text{C}$  NMR (125 MHz) and  $^1\text{H}$  NMR (500 MHz) data of compound **11a** in acetone- $d_6$

**Table 6.** Boltzmann averaged distances from H-10 to Me-17 and from H-10 to H-12 of four diastereomers of compound **11a** ( $6R,7R,10R,12R$  (**11c**);  $6R,7R,10R,12S$  (**11a**);  $6R,7R,10S,12S$  (**11d**);  $6R,7R,10S,12R$  (**11b**))<sup>a</sup>, calculated on wB97XD/6-311+G(2df,2p) level of theory

**Table 7.**  $^1\text{H}$  NMR (500 MHz) and  $^{13}\text{C}$  NMR (125 MHz) spectroscopic data for compound **13** at 500 MHz

**Table 8.** Calculated  $^{13}\text{C}$  NMR of structure **13a** and **13b**

**Table 9.** Minimum Inhibitory Concentrations (MIC) of the Compounds **10–14** against Gram-Positive and Gram-Negative Bacteria Compared to Standard References (Streptomycin and Gentamicin)

**Table 10.**  $^1\text{H}$  and experimental  $^{13}\text{C}$  NMR, and HMBC correlations of compound **15** (acetone- $d_6$ )

**Table 11.** Experimental  $^{13}\text{C}$  NMR, calculated  $^{13}\text{C}$  NMR data of global minimum conformer (G. M.), and Boltzmann averaged data of *s-trans*, *s-cis* and all conformers



### Curriculum vitae

**Name:** Wenxuan Wang                      **Gender:** Male                      **Date of birth:** 08/12/2016  
**E-mail:** wen-xuan.wang@tu-dortmund.de                      **Phone:** +49-(0)231-755-8297  
**Nationality:** China

**Education:** 09/2005 ~06/2009 East China University of Science and Technology. Pharmaceutical Engineering  
09/2009 ~ 06/2012 East China Normal University. Chemical biology. Master degree  
11/2012 ~ Now TU-Dortmund. Analytic chemistry. PhD student.

**Publications:**

1. **Wang WX**, Kusari S, Laatsch H, Golz C, Kusari P, Strohmann C, Kayser O, Spiteller M. Antibacterial azaphilones from an endophytic fungus *Colletotrichum* sp. BS4. *Journal of Natural products*, **2016**, doi: 10.1021/acs.jnatprod.5b00436.
2. **Wang WX**, Kusari S, Sezgin S, Lamshöft M, Kusari P, Kayser O, Spiteller, M. Hexacyclopeptides secreted by an endophytic fungus *Fusarium solani* N06 act as crosstalk molecules in *Narcissus tazetta*, *Applied Microbiology and Biotechnology*, **2015**, 99, 7651–7662.
3. **Wang WX**, Xiong J, Tang Y, Zhu JJ, Li M, Zhao Y, Yang, GX, Xia G, Hu, JF. Rearranged abietane diterpenoids from the roots of *Clerodendrum trichotomum* and their cytotoxicities against human tumor cells, *Phytochemistry*, **2013**, 89, 89–95.
4. **Wang WX**, Zhu JJ, Zou Y, Hong ZL, Liu ST, Li M, Huang Y, Xiong J, Zhao Y, Yang GX, Xia G, Hu JF. Trichotomone, a new cytotoxic dimeric abietane-derived diterpene from *Clerodendrum trichotomum*, *Tetrahedron Letters*, **2013**, 54, 2549–2552.
5. **Wang WX**, Cao L, Xiong J, Xia G, Hu JF. Constituents from *Chimonanthus praecox* (wintersweet). *Phytochemistry Letters*, **2011**, 4, 271–274.

**Fellowship:** CSC 2012 fellowship for Ph. D. students

**Work experiment:** Wissenschaftliche Hilfskraft (WHK), 11.2015 ~ 04.2016, TU-Dortmund

**Skills:**

1. The isolation, culture, and fermentation of microbes, as well as antimicrobial bio-assay
2. Analytic technologies of LC-MS, GC-MS, MALDI-imaging-MS
3. Chromatographic purification of bioactive compounds, and structural elucidation of unknown organic compounds via extensive spectroscopic methods and chemical reactions.
4. Property *ab initio* calculations of small organic compounds including ECD, optical rotation, NMR calculations.